242
7-9-79

DR. 285 D

MASTER

DOE/JPL/954698-1A

MODULE/ARRAY INTERFACE STUDY

Final Report

August 1978

Work Performed Under Contract No. NAS-7-100-954698

Research and Engineering Operation
Bechtel National, Incorporated
San Francisco, California

U.S. Department of Energy

DISTRIBUTION OF THIS DOCUMENT IS UNLIMITED

Solar Energy

DISCLAIMER

This report was prepared as an account of work sponsored by an agency of the United States Government. Neither the United States Government nor any agency Thereof, nor any of their employees, makes any warranty, express or implied, or assumes any legal liability or responsibility for the accuracy, completeness, or usefulness of any information, apparatus, product, or process disclosed, or represents that its use would not infringe privately owned rights. Reference herein to any specific commercial product, process, or service by trade name, trademark, manufacturer, or otherwise does not necessarily constitute or imply its endorsement, recommendation, or favoring by the United States Government or any agency thereof. The views and opinions of authors expressed herein do not necessarily state or reflect those of the United States Government or any agency thereof.

DISCLAIMER

Portions of this document may be illegible in electronic image products. Images are produced from the best available original document.

NOTICE

This report was prepared as an account of work sponsored by the United States Government. Neither the United States nor the United States Department of Energy, nor any of their employees, nor any of their contractors, subcontractors, or their employees, makes any warranty, express or implied, or assumes any legal liability or responsibility for the accuracy, completeness or usefulness of any information, apparatus, product or process disclosed, or represents that its use would not infringe privately owned rights.

This report has been reproduced directly from the best available copy.

Available from the National Technical Information Service, U. S. Department of Commerce, Springfield, Virginia 22161.

Price: Paper Copy $9.50
Microfiche $3.00

DOE/JPL/954698-1A
Distribution Category UC-63b

MODULE/ARRAY INTERFACE STUDY

Final Report

August 1978

Work performed under
Jet Propulsion Laboratory Contract No. 954698
for the
Engineering Area of the Low-Cost Solar Array Project

Prepared By

Bechtel National, Inc.
Research and Engineering Operation
50 Beale Street
P.O. Box 3965
San Francisco, California 94119

NOTICE

This report was prepared as an account of work sponsored by the United States Government. Neither the United States nor the United States Department of Energy, nor any of their employees, nor any of their contractors, subcontractors, or their employees, makes any warranty, express or implied, or assumes any legal liability or responsibility for the accuracy, completeness or usefulness of any information, apparatus, product or process disclosed, or represents that its use would not infringe privately owned rights.

The JPL Low-Cost Solar Array Project is sponsored by the U.S. Department of Energy and forms part of the Solar Photovoltaic Conversion Program to initiate a major effort toward the development of low-cost solar arrays. This work was performed for the Jet Propulsion Laboratory, California Institute of Technology by agreement between NASA and DOE.

DISTRIBUTION OF THIS DOCUMENT IS UNLIMITED

ACKNOWLEDGMENTS

This study was conducted as a team effort by members of Bechtel National, Inc., Research and Engineering Operation. Overall management responsibility rested with T.E. Walsh, Manager of the Power Technology Group. W.J. Stolte served as the Project Manager.

ABSTRACT

Bechtel National, Inc. has conducted a study of alternate module, panel, and array designs for use in large scale applications such as central station photovoltaic power plants. The objective of the study is to identify design features that will lead to minimum plant costs.

Several aspects of module design are evaluated, including glass superstrate and metal substrate module configurations, the potential for hail damage, light absorption in glass superstrates, the economics of glass selection, and electrical design. Also, three alternate glass superstrate module configurations are evaluated by means of finite element computer analyses. Two panel sizes, 1.2 by 2.4 m (4 by 8 ft) and 2.4 by 4.8 m (8 by 16 ft), are used to support three module sizes, 0.6 by 1.2 m (2 by 4 ft), 1.2 by 1.2 m (4 by 4 ft), and 1.2 by 2.4 m (4 by 8 ft), for design loadings of ±1.7 kPa (35 psf), ±2.4 kPa (50 psf), and ±3.6 kPa (75 psf). Designs and cost estimates are presented for twenty panel types and nine array configurations at each of the three design loadings. Structural cost sensitivities of combined array configurations and panel cases are presented.

THIS PAGE

WAS INTENTIONALLY

LEFT BLANK

CONTENTS

Section		Page
1	SUMMARY	1
2	INTRODUCTION	7
2.1	Report Format	8
2.2	Cost Bases	8
2.3	Units	9
3	BASELINE PLANT DESCRIPTION	11
3.1	Terminology	11
3.2	Baseline Plant Features	11
4	MODULE DESIGN	17
4.1	Module Configurations	18
	4.1.1 Glass Superstrate Modules	19
	4.1.2 Metal Substrate Modules	27
4.2	Hail	32
	4.2.1 Data Sources	32
	4.2.2 General Discussion	33
	4.2.3 Review of Data	33
	4.2.4 Application	38
4.3	Light Absorption	41
	4.3.1 Glass Superstrate	41
	4.3.2 Curved Glass Superstrate	47
	4.3.3 Other Aspects	49
4.4	Electrical	50
	4.4.1 Module Electrical Insulation Requirements	51

CONTENTS (Continued)

Section			Page
	4.4.2	Insulation Thickness Versus System Voltage	61
	4.4.3	Module Leakage Current	66
4.5	Module/Panel Computer Analyses		71
	4.5.1	Preliminary Calculations	74
	4.5.2	Case I - Picture Frame Concept	75
	4.5.3	Case II - Clip-Supported Concept	78
	4.5.4	Case III - Clip-Supported Curved Plate Concept	79
5	PANEL DESIGN		83
5.1	Design Bases		84
5.2	1.2 by 2.4 Meter (4 by 8 Foot) Panels		85
5.3	2.4 by 4.8 Meter (8 by 16 Foot) Panels		93
5.4	Case 9 Panel		101
5.5	Panel Comparisons		102
5.6	Curved Glass Superstrate Panel		109
6	ARRAY STRUCTURE AND FOUNDATION DESIGN		113
6.1	Design Bases		113
	6.1.1	Requirements	113
	6.1.2	Assumptions and Conventions	115
	6.1.3	Cost Bases	116
6.2	Array Configurations		116
	6.2.1	Case 1 Design	117
	6.2.2	Case 2 Design	120
	6.2.3	Case 3 Design	123
	6.2.4	Case 4 Design	125

CONTENTS (Continued)

Section			Page
	6.2.5	Case 5 Design	127
	6.2.6	Case 6 Design	129
	6.2.7	Case 7 Design	131
	6.2.8	Case 8 Design	133
	6.2.9	Case 9 Design	135
6.3	Array Comparisons		138
	6.3.1	Cost Comparisons	138
	6.3.2	Array Tilt Angle	141
	6.3.3	Array Structure and Foundation Design Summary	143
7	ARRAY DESIGN SUMMARY		153
7.1	Total Array Costs		153
7.2	Combined Array and Panel Structure Comparisons		155
	7.2.1	Beam Versus Post Support	157
	7.2.2	Best Beam Support	159
	7.2.3	Best Girder Support	161
	7.2.4	Best Beam Support Versus Best Girder Support	164
	7.2.5	Best Slant Height	164
	7.2.6	Comparison Summary	166
7.3	Wind Forces		167
8	CONCLUSIONS		173
8.1	Major Cost Drivers		173
8.2	Modules		174
8.3	Panels		176
8.4	Array Structures and Foundations		177

CONTENTS (Continued)

Section		Page
8.5	Combined Array and Panel	178
9	RECOMMENDATIONS	179
10	NEW TECHNOLOGY	183
Appendix		
A	COMPUTER ANALYSES OF GLASS PLATES	185
References		211

ILLUSTRATIONS

Figure		Page
3-1	Delineation of Terminology	12
4-1	Glass Thickness Versus Area	21
4-2	Thickness Versus Area for Annealed Glass	22
4-3	Thickness Versus Area for Tempered Glass	23
4-4	Thickness Versus Area for Steel Substrate Modules	24
4-5	Thickness Versus Area for Aluminum Substrate Modules	29
4-6	Hail Size Distribution	36
4-7	Reported Occurrences of Hail 19 Millimeter (3/4 Inch) and Larger	39
4-8	Cell Output Versus Glass Thickness	43
4-9	Glass Cost Data	44
4-10	Glass Selection Economics	46
4-11	System Voltage Versus Solar Cell Temperature	52
4-12	Breakdown Measurements on HMPE - Insulated Wires	56
4-13	Maximum Allowable Electrical Stress for Cable Insulation	57
4-14	Voltage Gradient and Stress Distribution for Glass Superstrate Module Design	59
4-15	Encapsulant System I - Sylgard 184 and Mylar	62
4-16	Encapsulant System II - Sylgard 184 and Tedlar	62
4-17	Encapsulant System III - Sylgard 184 and Tedlar	64
4-18	Module Encapsulant Partial Cost Versus Voltage	65
4-19	Model for Leakage Current Calculations	69
4-20	Module Leakage Current	70
4-21	Glass Superstrate Module Concepts	73

ILLUSTRATIONS (Continued)

Figure		Page
4-22	Case I Tensile Stress Versus Loading	76
4-23	Case I Displacement Versus Loading	77
4-24	Case III Tensile Stress Versus Loading	81
4-25	Case III Displacement Versus Loading	82
5-1	1.2 by 2.4 Meter (4 by 8 Foot) Panel Types	86
5-2	2.4 by 4.8 Meter (8 by 16 Foot) Panel Types	94
5-3	Panel Cost Versus Module Size	104
6-1	Case 1 Array Configuration	118
6-2	Case 1 Array Cost Versus Loading	118
6-3	Case 2 Array Configuration	121
6-4	Case 2 Array Cost Versus Loading	121
6-5	Case 3 Array Configuration	124
6-6	Case 3 Array Cost Versus Loading	124
6-7	Case 4 Array Configuration	126
6-8	Case 4 Array Cost Versus Loading	126
6-9	Case 5 Array Configuration	128
6-10	Case 5 Array Cost Versus Loading	128
6-11	Case 6 Array Configuration	130
6-12	Case 6 Array Cost Versus Loading	130
6-13	Case 7 Array Configuration	132
6-14	Case 7 Array Cost Versus Loading	132
6-15	Case 8 Array Configuration	134
6-16	Case 8 Array Cost Versus Loading	134
6-17	Case 9 Array Configuration	136
6-18	Case 9 Array Cost Versus Loading	136

ILLUSTRATIONS (Continued)

Figure		Page
6-19	Array Structure and Foundation Cost Versus Loading	140
6-20	Cost Impact Of Sharing Foundations	146
7-1	Array Cost Versus Loading	156
7-2	Cost Comparison Of Post Versus Beam Support	157
7-3	Cost Comparison Of Beam Support, Intermediate Versus End Support	159
7-4	Cost Comparison of Girder Span	162
7-5	Cost Comparison Of Girder Support	163
7-6	Cost Comparison Of Beam Versus Best Girder Support	165
7-7	Cost Comparison Of Slant Heights	165
7-8	Wind Loading Versus Height Above Grade	169
A-1	Glass Superstrate Module Concepts	186
A-2	Finite Element Layout for Case I	190
A-3	Case I - Tensile Stress Versus Loading	191
A-4	Case I - Displacement Versus Loading	192
A-5	Case I - Minimum Principal Stress, Top of Plate	194
A-6	Case I - Maximum Principal Stress, Top of Plate	195
A-7	Case I - Minimum Principal Stress, Bottom of Plate	196
A-8	Case I - Maximum Principal Stress, Bottom of Plate	197
A-9	Case I - Perpendicular Displacement	198
A-10	Case II - Principal Stresses at 0.48 kPa (10 psf)	200
A-11	Finite Element Layout for Case III	202
A-12	Case III - Tensile Stress Versus Loading	203

ILLUSTRATIONS (Continued)

Figure		Page
A-13	Case III - Displacement Versus Loading	204
A-14	Case III - Minimum Principal Stress, Top of Plate	205
A-15	Case III - Maximum Principal Stress, Top of Plate	206
A-16	Case III - Minimum Principal Stress, Bottom of Plate	207
A-17	Case III - Maximum Principal Stress, Bottom of Plate	208
A-18	Case III - Radial Displacement	209

TABLES

Table		Page
2-1	Conversion Of Dimensional Units	10
4-1	Electrical Properties of Modules Evaluated in This Study	18
4-2	Glass Superstrate Module Cost Estimate	26
4-3	Metal Substrate Module Cost Estimate	31
4-4	Terminal Velocity Of Large Hailstones	34
4-5	Terminal Velocity Of Small Hailstones	35
4-6	Frequency Distribution Of Maximum Hail Size	35
4-7	Number of Hail Reports	37
4-8	Restivities Of Candidate Module Encapsulating Materials (@ 25°C)	68
4-9	Typical Module Configurations	70
5-1	Panel Type, Class, and Associated Array Configuration	85
5-2	Type A Panel Cost Estimate	88
5-3	Type B Panel Cost Estimate	88
5-4	Type C Panel Cost Estimate	89
5-5	Type D Panel Cost Estimate	89
5-6	Type E Panel Cost Estimate	90
5-7	Type F Panel Cost Estimate	90
5-8	Type Q Panel Cost Estimate	91
5-9	Type R Panel Cost Estimate	91
5-10	Panel Type, Class, and Associated Array Configuration	95
5-11	Type G Panel Cost Estimate	96
5-12	Type H Panel Cost Estimate	96
5-13	Type I Panel Cost Estimate	97

TABLES (Continued)

Table		Page
5-14	Type J Panel Cost Estimate	97
5-15	Type K Panel Cost Estimate	98
5-16	Type L Panel Cost Estimate	98
5-17	Type M Panel Cost Estimate	99
5-18	Type N Panel Cost Estimate	99
5-19	Type O Panel Cost Estimate	100
5-20	Type P Panel Cost Estimate	100
5-21	Case 9 Panel/Array Structure Cost Estimate	102
5-22	Panel Structural Cost Estimate Summary	103
5-23	Curved Glass Panel Cost Estimate	111
6-1	Array Structure and Foundation Cost Estimate Summary	139
7-1	Array Cost Estimate Summary	154

Section 1

SUMMARY

This report presents the results of an engineering study conducted by the Research and Engineering Operation of Bechtel National, Inc. The objective of the study was to determine design features that lead to low cost solar photovoltaic arrays. The approach used was to parametrically evaluate module, panel, and array structural designs, estimate their costs, and determine cost sensitivities.

The study emphasized large scale applications, such as central station photovoltaic power plants. The general design approach and purchase quantities reflected what would be needed for a 200 MW (peak) plant. For study purposes, the plant was located at a 35° latitude, with the array tilt fixed at the latitude angle. An encapsulated cell efficiency of 15 percent, an NOCT efficiency of 92 percent, and a module packing efficiency of 0.92 were provided by JPL, thereby setting the module surface area required for the plant at 1.58×10^6 m^2. Estimated costs (in 1975 dollars) are presented in terms of dollars per square meter of total module surface area. Costs in terms of other bases (e.g., dollars per watt) or costs for other efficiencies can easily be estimated from the data presented (see Section 2).

Several aspects of module design were evaluated including glass superstrate and metal substrate module configurations, the

potential for hail damage, light absorption in module cover sheets, and electrical insulation design. Also, three alternate glass superstrate module configurations were evaluated by means of a nonlinear structural analysis computer program.

In this study, panels consist of lightweight steel frameworks needed to support the modules and are designed to be used with the array structure and foundation configurations evaluated to form complete arrays. Two panel sizes, 1.2 by 2.4 m (4 by 8 ft) and 2.4 by 4.8 m (8 by 16 ft), were designed with both end- and intermediate-support point versions. Three module sizes, 0.6 by 1.2 m (2 by 4 ft), 1.2 by1.2 m (4 by 4 ft), and 1.2 by 2.4 m (4 by 8 ft), were used. In order to identify cost drivers, designs were performed for uniform loadings of ±1.7 kPa (35 psf), ±2.4 kPa (50 psf), and ±3.6 kPa (75 psf). Nine array configurations, each consisting of foundation and primary support structure, were selected to determine structural cost sensitivities of various structural support parameters such as slant height, foundation sharing, etc. With the variations in panel and array configurations, module and panel sizes, and loading, a total of 57 panels and 27 arrays were designed and their costs estimated.

For the designs evaluated, the glass superstrate modules were found to be slightly less expensive than the metal substrate configuration. However, determining the configuration of a minimum cost module warrants further detailed studies (such as

those being conducted as a part of the Automated Array Assembly Task in JPL's LSA Project).

Several methods were evaluated for calculating the structurally required thicknesses for glass superstrates. However, for reasons of resistance to hail damage and the size of commercially available tempered glass, the glass superstrate was constrained to be thicker than 3.2 millimeters (0.125 inch). Because of this, the estimated cost of the module remained virtually constant at $60/m² for the ±1.7 kPa (35 psf), ±2.4 kPa (50 psf), and ±3.6 kPa (75 psf) loadings evaluated in this study, although approximately two-thirds of this cost is for the solar cells. An evaluation of light absorption in glass superstrate showed 0.05 percent iron, tempered glass to be the most economic with the JPL-provided future cell cost estimate. However, with the present cost of cells, 0.01 percent iron, tempered glass is more economic.

Based on experience in the cable industry, it was found that some module encapsulating materials may have to be thicker than required for weatherability in order to provide long-term (e.g., 20 years) electrical insulation at the dc system voltages envisaged for central station power plants. Present module encapsulant designs should be adequate for the voltage levels in current applications.

The estimated costs for the panel designs evaluated were found to be strongly dependent on design loading. Also, the estimated cost of panels supported at intermediate points along their long edge was found to be lower than equivalent panels supported at their ends. However, further analysis is required to assure that this relationship still holds true when the effects of reverse bending on glass thickness selection, the movement of the support location with applied loading, and nonuniform loading are considered.

For the most part, the 1.2 by 2.4 m (4 by 8 ft) panels were found to have a lower cost ($/m^2) than the 2.4 by 4.8 m (8 by 16 ft) panels. When the cost of suitably designed array structure is added to the panel costs, the total cost of array configurations using the 1.2 by 2.4 m (4 by 8 ft) panels is slightly lower than for the studied array configurations using the 2.4 by 4.8 m (8 by 16 ft) panel.

In all designs evaluated, the lowest cost panels utilized 1.2 by 2.4 m (4 by 8 ft) modules. Smaller module sizes lead to higher panel costs because of the larger amount of framing material required. Whereas, larger module sizes require thicker glass which results in more light absorption and thereby leads to higher total cost for a fixed power output.

Preliminary evaluation of a panel based on a curved glass superstrate module indicates that its structural cost excluding

the cost of the module would be on the order of one-half to one-third the cost of the conventional panel structure evaluated in detail during the study, due to a reduction in the amount of panel steel required. It is recommended that a suitable array configuration be designed and costed for the curved glass module to determine its economic viability when compared to the installed cost of flat-plate modules presented in this report.

As with the panel costs, the array structure and foundation costs were found to be strong functions of design loading. However, among the designs evaluated, there was little difference in the combined cost of the array structure and foundation.

For most of the array configurations evaluated, the foundation costs are approximately double the cost of the array structure. It is expected that the foundation costs could be lowered if the uniform loadings were resolved into components (e.g., dead, live, etc.), the specified two foot minimum array height above grade were lowered, and wind forces for the structures were more accurately known.

In summary, the study described herein has produced alternative designs and cost estimates for several of the components and design features needed in assembling solar cells into a photovoltaic power system in order to identify structural cost drivers and, as a result, has shown that:

- array costs do not vary greatly among the designs evaluated
- panel and array costs are strongly dependent on design loading
- the best support configuration is load dependent, and
- the curved glass superstrate module has the potential to significantly reduce panel structural costs although installed costs have yet to be determined.

Additional details and conclusions are presented in the remainder of this report.

Section 2

INTRODUCTION

This final report documents an engineering study of photovoltaic module, panel, and array design. The study was performed by the Research and Engineering Operation of Bechtel National, Inc. for the Engineering Area of the Jet Propulsion Laboratory's Low-Cost Solar Array Project under Contract Number 954698 as a part of the U.S. Department of Energy's Solar Photovoltaic Conversion Program.

The primary emphasis of the study was on the structural aspects of design for large-scale applications such as photovoltaic central station power plants. The study was conducted with the viewpoint of an architect/engineering firm engaged to design such plants.

The direct objectives in the study were to identify module, panel, and array design features that govern component costs, to determine their interaction and the relative magnitudes of the cost elements, and to determine structural cost sensitivities. Thus, the results of the study facilitate accomplishing the overall project objective of evolving designs that minimize total plant life-cycle cost.

The approach used in accomplishing these objectives was to design and cost a large number of module, panel, and array

configurations and compare the resultant estimated costs. The results of that effort are presented in this report.

2.1 REPORT FORMAT

This report has been prepared in accordance with the format specified by JPL Document Number 1030-26, Rev. B.

A brief description of a conceptual plant design is presented in Section 3 in order to put ensuing discussions of its components into perspective. Section 4 addresses several aspects of module design. Panel designs are discussed in Section 5, and Section 6 presents a discussion of the array configurations studied. A summary comparison of the costs of these three components is presented in Section 7. Major conclusions and recommendations resulting from the conduct of this study are presented in Sections 8 and 9, respectively. Section 10 is a statement on new technology identified by this study. Details of a finite element computer analysis of glass superstrate modules are presented in the appendix.

2.2 COST BASES

In order to be consistent with current practice in the LSA Project, all costs in this report are in 1975 dollars. Cost estimates were derived in first-quarter 1978 dollars and reduced

to constant 1975 dollars by using a factor of 1.17 from the LSA Price Deflator Table supplied by JPL, Reference 2-1.

Cost data are normalized to terms of dollars per square meter ($/m²). The cost data can be translated to other bases by dividing by appropriate conversion factors (e.g., $/W = $/m² ÷ W/m² or $/ft² = $/m² ÷ 10.764 ft²/m²), etc. Also, costs for encapsulated cell, NOCT, and packing efficiencies other than the 15 and 92 percents given, can be obtained by dividing the costs in $/m² by the desired value of watts per square meter.

During the course of the study, efforts were made to uniformly apply design criteria and design and cost estimating procedures so as to produce unbiased results. The accuracy of the cost estimates presented herein are consistent with the level of detail in an engineering study.

2.3 UNITS

For the most part, English units were used in performing the study. These units were subsequently converted to SI units for presentation in this report. An exception was made for the computer generated plots presented in Appendix A where English units are retained for values of stress and displacement. The SI units were rounded to correspond to nominal values currently being used by the Engineering Area of JPL's LSA Project, as

typified by the conversion of panel and array dimensions shown in Table 2-1.

TABLE 2-1

CONVERSION OF DIMENSIONAL UNITS

English Units (feet)	SI Units Precise (meters)	SI Units Nominal (meters)
2	0.6096	0.6
4	1.2192	1.2
8	2.4384	2.4
16	4.8768	4.8
32	9.7536	9.8

Section 3

BASELINE PLANT DESCRIPTION

This section presents a brief description of the postulated baseline plant in order to put ensuing discussions of its components into perspective.

3.1 TERMINOLOGY

At present, several institutions are working to establish a consistent set of terms and a hierarchy to describe the components and systems that comprise a photovoltaic power plant. Attempts are being made to have these terms be consistent, as far as possible, for both flat-plate and concentrator array designs.

Figure 3-1 delineates the meanings given to such terms within this report. The definitions shown in the figure are consistent with those being used in the Engineering Area of JPL's LSA Program at the time this report was written. Primary emphasis in the study described herein is on the structural aspects of module, panel, and array design. However, for completeness, all terms relevant to a photovoltaic power plant are presented.

3.2 BASELINE PLANT FEATURES

The general design approach and purchase quantities used in this study reflect what would be needed for a 200 MWp central station

SOLAR CELL – The basic photovoltaic device which generates electricity when exposed to sunlight.

MODULE – The smallest complete, environmentally protected assembly of solar cells and other components (including electrical connectors) designed to generate dc power when under unconcentrated terrestrial sunlight.

PANEL – A collection of one or more modules fastened together, factory preassembled and wired, forming a field installable unit.

ARRAY – A mechanically integrated assembly of panels together with support structure (including foundations) and other components, as required, to form a free-standing field installed unit that produces dc power.

BRANCH CIRCUIT – A group of modules or paralleled modules connected in series to provide dc power at the dc voltage level of the power conditioning unit (PCU). A branch circuit may involve the interconnection of modules located in several arrays.

ARRAY SUBFIELD – A group of solar photovoltaic arrays associated by the collection of branch circuits that achieves the rated dc power level of the power conditioning unit.

ARRAY FIELD – The aggregate of all array subfields that generate power within the photovoltaic central power station.

PHOTOVOLTAIC CENTRAL POWER STATION – The array field together with auxiliary systems (power conditioning, wiring, switchyard, protection, control) and facilities required to convert terrestrial sunlight into ac electrical energy suitable for connection to an electric power grid.

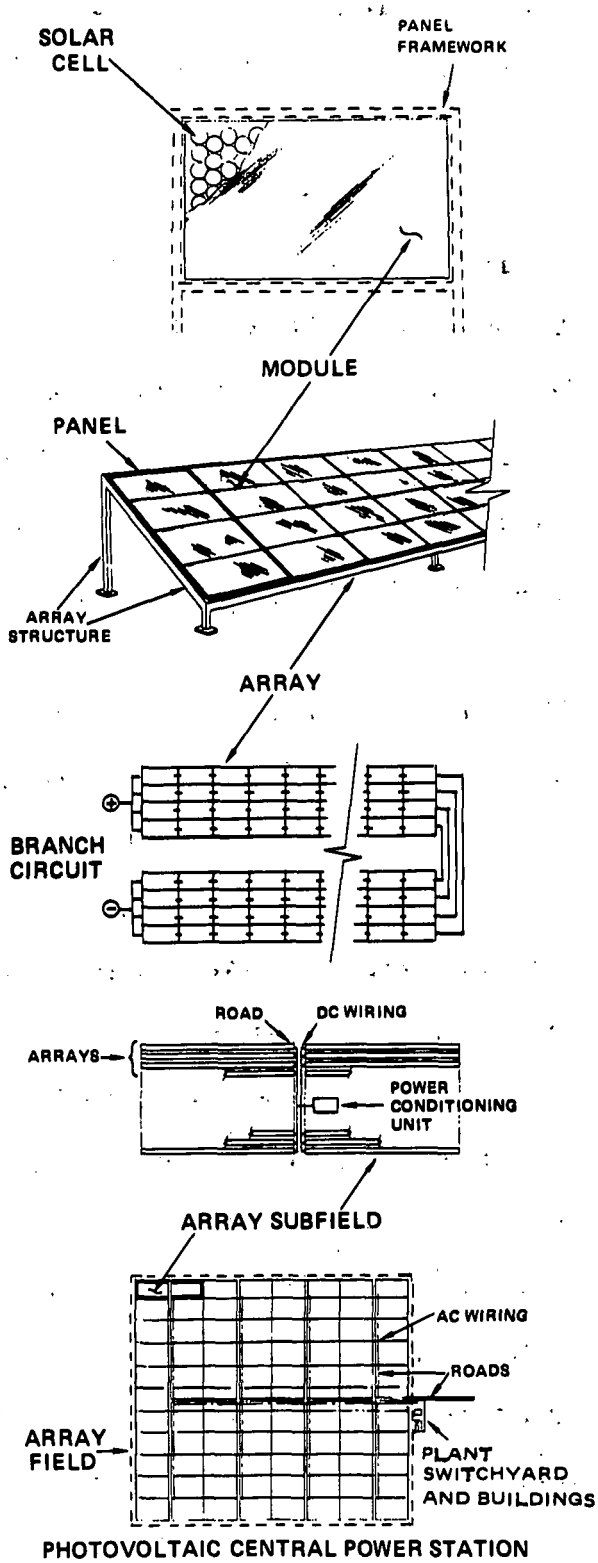

Figure 3-1 DELINEATION OF TERMINOLOGY

photovoltaic power plant or similar large-scale applications. The postulated baseline plant concepts are those developed in previous studies by Bechtel (Refs. 3-1, 3-2, and 3-3).

For purposes of this study, the plant is located at a 35° latitude, with the array tilt fixed at the latitude angle. An encapsulated cell efficiency of 15 percent, an NOCT efficiency of 92 percent, and a module packing efficiency of 0.92 are assumed, thereby setting the module surface area required for the plant at 1.58×10^6 m^2. Estimated costs are presented in terms of dollars per square meter.

The unit shipped to the site for installation is a panel and consists of a frame supporting one or more modules. The modules, in turn, support and encapsulate the solar cells. The panels are field installed on array structures at the plant site to form an array. Array slant heights of 2.4 m (8 ft) and 4.8 m (16 ft) are evaluated in this study. The arrays are approximately 152 meters (500 feet) long, with adjacent arrays separated by 1.5 times the vertical height of the array (i.e., 2.8 m (9.18 ft) interarray separation for 4.8 m (16 ft) slant heights and 1.4 m (4.59 ft) for 2.4 m (8 ft) slant heights). Additionally, maintenance roads (running parallel to the arrays) separate groups of arrays at spacings of approximately 18 meters (60 feet). Main plant roads, perpendicular to the arrays, connect the maintenance roads.

Modules on two adjacent arrays are wired in series to form a branch circuit with a nominal operating voltage of 1500 volts dc. Several adjacent branch circuits are wired in parallel to obtain a current of approximately 300 amps. These 300 ampere dc feeder cables are brought to a power conditioning unit (pcu) within the array subfield. The dc feeder cables are direct buried and run alongside the main plant roads.

Each one of 36 power conditioning units is rated at approximately 6 MW at 1500 Vdc and includes all components (e.g., converter, harmonic filters, control circuitry, etc.) necessary to convert the dc output of the arrays into a 34 kV, 60 hertz waveform compatible with electric utility standards.

The filtered outputs of the power conditioning units in the array field are then collected at 34 kV and brought to the plant switchyard by direct buried cables running parallel to the main plant roads. At the switchyard, the voltage is stepped up to 230 kV for connection to the utility transmission line.

The control and data acquisition system consists of microcomputers located within the power conditioning units and connected by a serial data link to a central computer located in the central control room. The system monitors converter and array operating parameters and controls the converters to track the arrays' maximum power point with variations in insolation and temperature.

The plant design also includes switchgear, protective relaying, grounding and lightning protection systems, and other auxiliary systems required for proper plant operation and protection. Shops, warehouses, and other maintenance facilities are provided as required.

THIS PAGE

WAS INTENTIONALLY

LEFT BLANK

Section 4

MODULE DESIGN

This section presents a discussion of several aspects of module design including evaluations of glass superstrate and metal substrate module configurations, hail damage, light absorption in the module's cover sheet, electrical design, and a summary of finite element computer analyses of three alternate glass superstrate module configurations.

For purposes of this study, a module is defined as a series-parallel interconnected set of solar cells terminating in two power leads (plus and minus) brought out through an encapsulant system. The solar cells are protected from the environment by the encapsulation system. Although the module is easily handleable as a unit, it is not capable of being installed directly on an array. One or more modules are assembled into a frame to form a panel, which is the unit shipped from the manufacturer for installation in the field.

Module sizes evaluated in this study were 0.6 by 1.2 m (2 by 4 ft), 1.2 by 1.2 m (4 by 4 ft), and 1.2 by 2.4 m (4 by 8 ft). Table 4-1 provides a comparison of electrial properties typical of such modules.

TABLE 4-1

ELECTRICAL PROPERTIES OF MODULES EVALUATED IN STUDY

Module Size m	Module Size ft	Module Power (Maximum)[1] watts	Module Voltage volts	Module Current amps
0.6x1.2	2x4	91	6.3	14.6
1.2x1.2	4x4	183	6.3	29.3
1.2x2.4	4x8	366	12.5	29.3

[1] At NOCT and 15 percent encapsulated cell efficiency, 92 percent NOCT efficiency, and 92 percent packing efficiency.

4.1 MODULE CONFIGURATIONS

Current module configurations may be divided into two broad categories by the position of the structural support element with respect to the cells. With a superstrate configuration, support for the cells is mainly provided by a transparent cover sheet (e.g., glass) in front of the illuminated side of the cells. A substrate configuration derives its structural support from a structural element behind the cells. Many substrate materials are in use or proposed, including metals, printed circuit board material, plastics, wood, etc.

Two module configurations, a glass superstrate and a metal substrate were structurally evaluated in this study.

4.1.1 Glass Superstrate Modules

Typically, a glass superstrate module consists of a flat glass sheet structure with interconnected cells fastened to it by an adhesive, such as PVB (polyvinyl butyral). A silicone rubber pottant and a polyester film back cover sheet complete the encapsulant system.

Glass Thickness. Determining the thickness of the glass is a complex problem influenced by several factors. As discussed in Section 4.3, it is desirable to have the glass as thin as possible so as not to reduce module efficiency by the absorption of light within the glass. Counter to this, is a need to provide some degree of hail resistance for many areas of the country (as discussed in Section 4.2). Also, the glass must be capable of withstanding structural loads imposed by wind or snow. Hail by itself does not produce a structural load in the usual sense, although it does produce an impact load.

Several methods are available to calculate the thickness of glass required to resist uniform structural loading. Linear methods generally result in overspecifying the required thickness, whereas nonlinear computer analyses result in thinner minimum glass thicknesses. A third method is to rely on glazing industry experience. Unfortunately, all of these methods, even those based on industry experience, yield different answers. This point is illustrated by Figure 4-1 which compares the results of

several methods of determining the required thickness of annealed glass as a function of area.

For purposes of this study, the thickness of glass required to resist structural loads is determined using the results of a third quarter 1977 informal working document prepared by JPL. Curves in that draft report were the result of a study utilizing a nonlinear computer analysis. This analysis accounts for the in-plane membrane forces that develop and provide significant increases in strength as deflections increase beyond about half the thickness of the plate. It was necessary to extrapolate the graphed data for use with tempered glass. Additionally, the JPL document gave a mean breaking strength of 276 MPa (40,000 psi) for tempered glass and 69 MPa (10,000 psi) for annealed glass. These values were reduced by a factor of four to yield a maximum working stress of 69 MPa (10,000 psi) for tempered glass and 17 MPa (2,500 psi) for annealed glass in accordance with the JPL document. Calculation results are presented in Figures 4-2 and 4-3, for annealed and tempered glass sheets, respectively, with aspect ratios (i.e., ratio of module length to width) of 2:1 and 1:1. The curves are for glass sheets simply supported on four sides in a picture frame configuration.

These curves and other data are used in Section 4.3 to evaluate the impact of light absorption in glass cover sheets. Consideration of light absorption effects in conjunction with minimizing the cost of energy produced by a photovoltaic plant

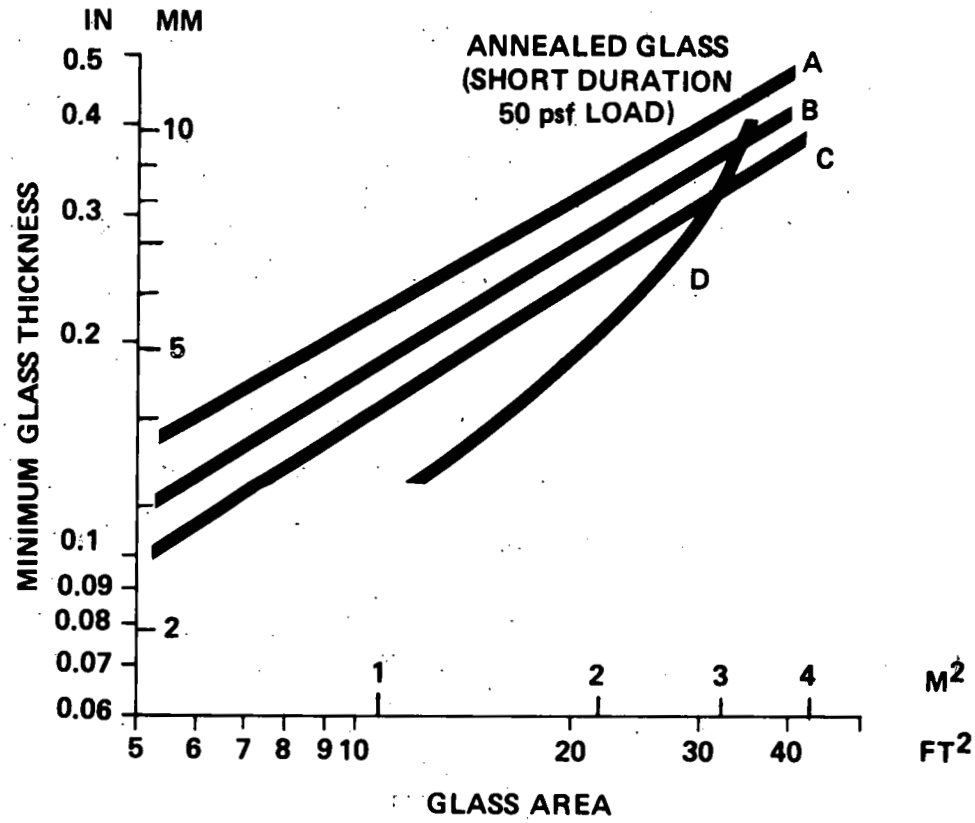

CURVE: A – FLAT PLATE, LINEAR THEORY, ASPECT RATIO 1.59, SIMPLY SUPPORTED ON 4 SIDES.

B – FLAT PLATE, LARGE DEFLECTION (JPL, MOORE) ASPECT RATIO 3, SIMPLY SUPPORTED ON 4 SIDES.

C – FLAT PLATE, ASG & LOF, ASPECT RATIO<5, SIMPLY SUPPORTED ON 4 SIDES.

D – FLAT PLATE, PPG, ASPECT RATIO<3, SIMPLY SUPPORTED ON 4 SIDES.

Figure 4-1 GLASS THICKNESS VERSUS AREA

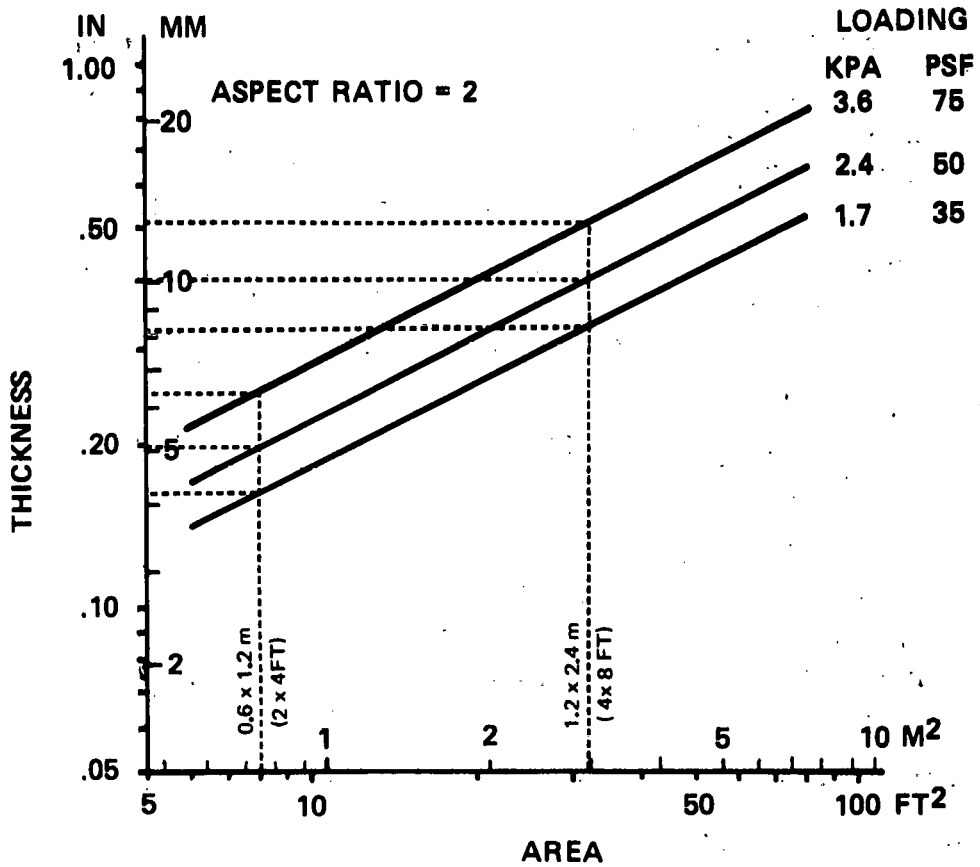

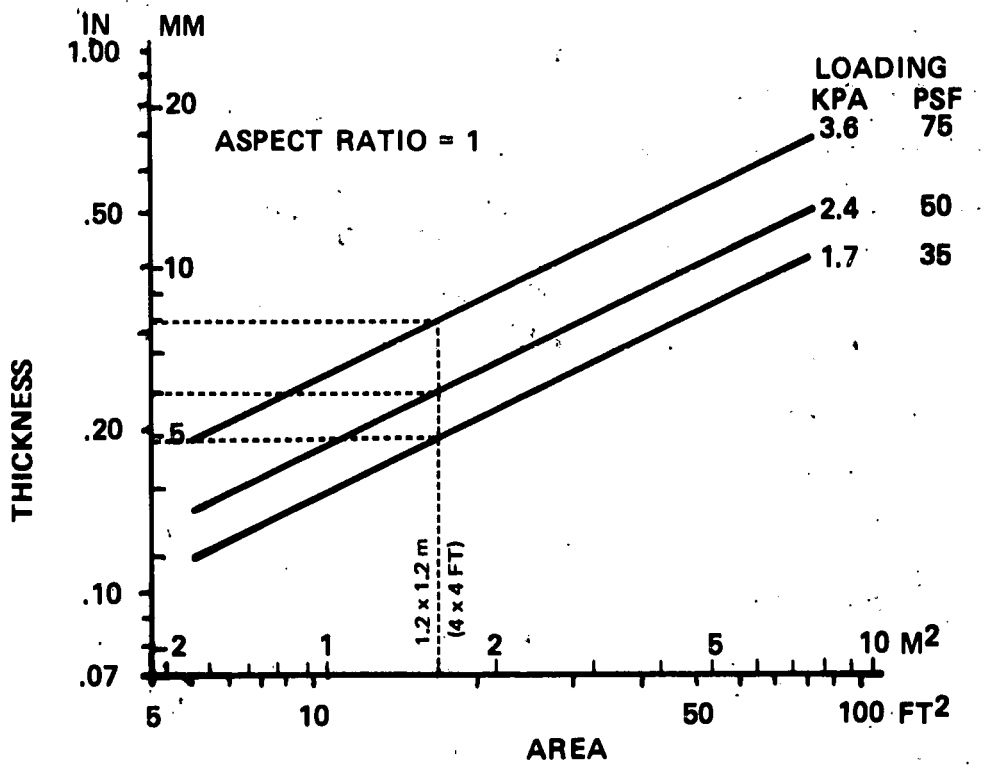

Figure 4-2 THICKNESS VERSUS AREA FOR ANNEALED GLASS

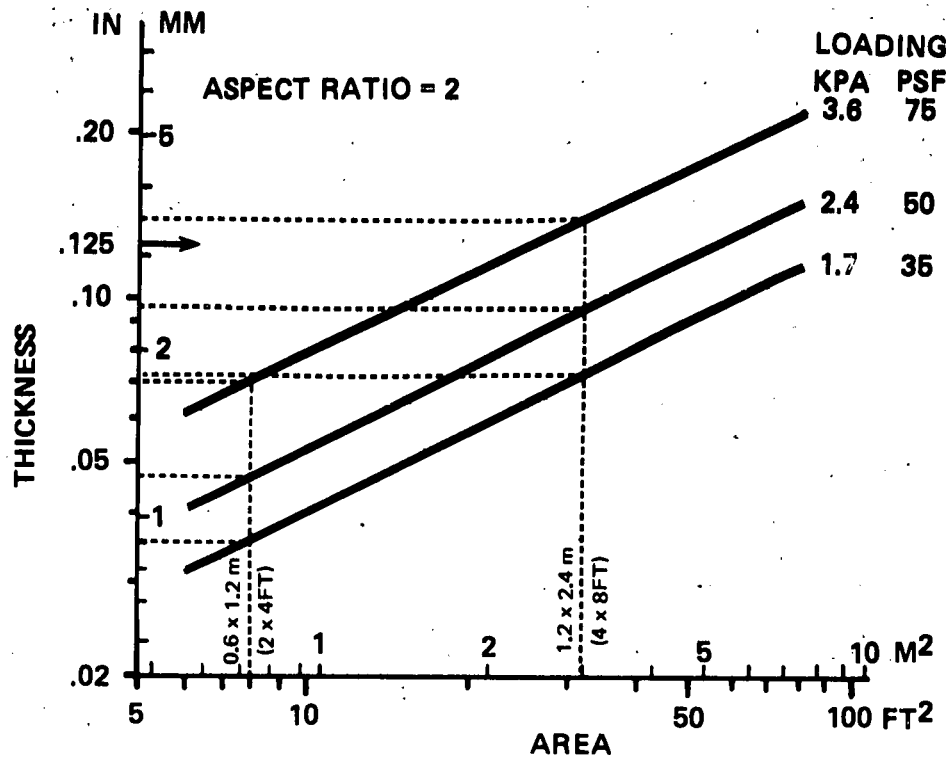

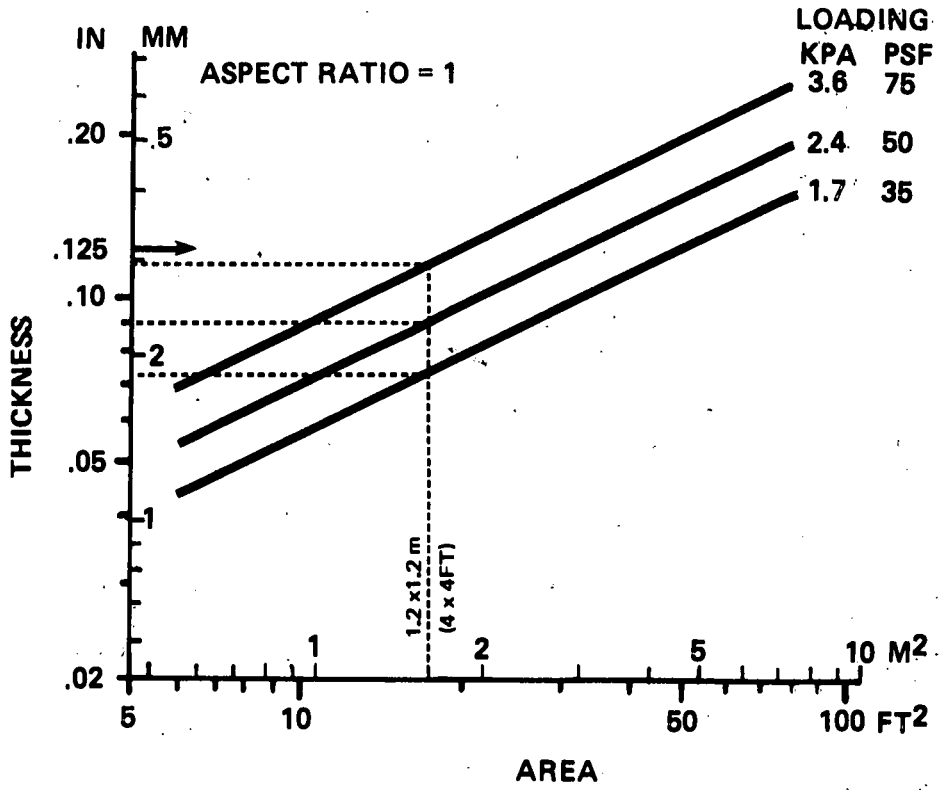

Figure 4-3 THICKNESS VERSUS AREA FOR TEMPERED GLASS

led to selection of tempered glass with a 0.05 percent iron content for the glass superstrate design (see Section 4.3.1). For reasons of hail resistance (see Section 4.2) and manufacturability (see Section 4.3.1), the thickness of the glass is constrained to be greater than 3.2 millimeters (0.125 inch) (arrows on Figure 4-3) despite the fact that calculations show that for loads less than 3.6 kPa (75 psf) thinner glass would suffice if structural loading alone were considered. This constraint is judgmental. Thinner glass could be selected for areas of the country where large hail is not prevalent and if current manufacturing processes were refined to enable production of thinner tempered glass.

Adhesive/Pottant. Although adhesives, pottants, and cells have negligible contributions to structural strength, they significantly contribute to module cost. Accordingly, an adhesive and pottant are included in the postulated module design. The configuration selected is a 0.76 millimeter (0.030 inch) layer of PVB (polyvinyl butyral) in which the cells are embedded. Other configurations are possible and are discussed further in conjunction with electrical aspects in Section 4.4.

PVB is available in several grades. The grade selected for purposes of this study is aircraft grade (e.g., Saflex) with a cost of $9.32 per square meter per millimeter of thickness ($0.022 per square foot per mil) (1975 $). Although

architectural grades are about one-half to one-third this cost, and automotive grades cost less yet, several module manufacturers are currently utilizing the aircraft grade PVB in their module designs. Additional work is needed to determine the acceptability of the lower cost grades of PVB.

Back Cover. PVB is unsuitable for use as the back cover because of its susceptability to moisture and its low dielectric strength. Consideration of electrical insulation requirements, discussed in in Section 4.4.2, led to selection of a 0.19 millimeter (0.0075 inch) thick polyester sheet for the back cover material. Additionally, the polyester sheet is mechanically strong, both holding and protecting the PVB.

Electrical Connectors. As mentioned, the definition of a module as used in this study includes a mated pair of electrical connectors. Based on the results of a previous Bechtel study (Ref. 3-1), a molded-rubber, quick-disconnect connector was selected. The assembled cost of a 100 ampere connector pair (for the 1.2 by 2.4 m (4 by 8 ft) module) and a short length of wire, 0.15 m (6 inch), is estimated to be $3.45 (1975 $) in the quantities required; this cost translates to $1.16/m². For the 1.2 by 1.2 m (4 by 4 ft) module, the cost of the connector pair is essentially the same in terms of dollars per square meter. The behavior of connector cost versus ampere rating (Ref. 3-1) is such that the connector cost for the 0.6 by 1.2 m (2 by 4 ft) module is $0.65/m².

Module Cost. The costs of the components and module described above (1.2 by 2.4 m (4 by 8 ft)) are presented in Table 4-2 in terms of 1975 dollars per square meter. The costs of the interconnected assembly of solar cells and labor to assemble the module are provided by JPL.

TABLE 4-2

GLASS SUPERSTRATE MODULE COST ESTIMATE
(1.2 by 2.4 m (4 by 8 ft) module)

Component	Cost			
	1.7	2.4	3.6	kPa
	35	50	75	psf
Cell Assembly[1]	40.00	40.00	40.00	
PVB (0.76 mm, 0.030")	7.12	7.12	7.12	
Glass (3.2 mm, 0.125", 0.05% iron)	4.20	4.20	4.51[2]	
Mylar (0.19 mm, 0.0075")	0.79	0.79	0.79	
Connectors	1.16	1.16	1.16	
Assembly Labor[1]	7.00	7.00	7.00	
MODULE COST	60.27	60.27	60.58	

[1] provided by JPL
[2] 3.6 mm (0.141") glass

These module costs are used in other areas of the study. However, the glass cost component changes with loading in accordance with Figure 4-3 (2:1 aspect ratio), the 3.2 millimeter (0.125 inch) minimum thickness constraint, and glass cost data in Figure 4-9, Section 4.3. Also, the cost of the electrical connectors causes the module cost to vary with size as previously discussed.

4.1.2 Metal Substrate Modules

Various configurations for metal substrate modules have been proposed and are currently being used. Generally, these modules consist of a cover sheet and/or pottant, an embedded assembly of cells, an insulating medium, and a substrate.

Substrate. Recent results of field tests indicate that metal substrate modules can have cell cracking problems if the metal is nonplanar, i.e., has stamped grooves to increase the rigidity of the substrate. The cracking, attributed to differential thermal expansion of pottant material in grooved areas under the cells, has resulted in alternate designs in which the cells are mounted on a flat substrate. Thus, for purposes of this study, a flat metal sheet substrate is considered.

Figures 4-4 and 4-5 show the required thickness for steel and aluminum substrates as a function of size with loading and aspect ratio as parameters. These curves were derived from the JPL informal working document discussed in Section 4.1.1 and are therefore consistent with the methods used to derive required glass thicknesses. Both the steel and aluminum are assumed to have a working stress of 138 MPa (20,000 psi) as typical of mild steel and high-alloy aluminum.

From Figure 4-4, the calculated thickness of a 1.2 by 2.4 m (4 by 8 ft) steel sheet is 1.55 millimeters at 2.4 kPa

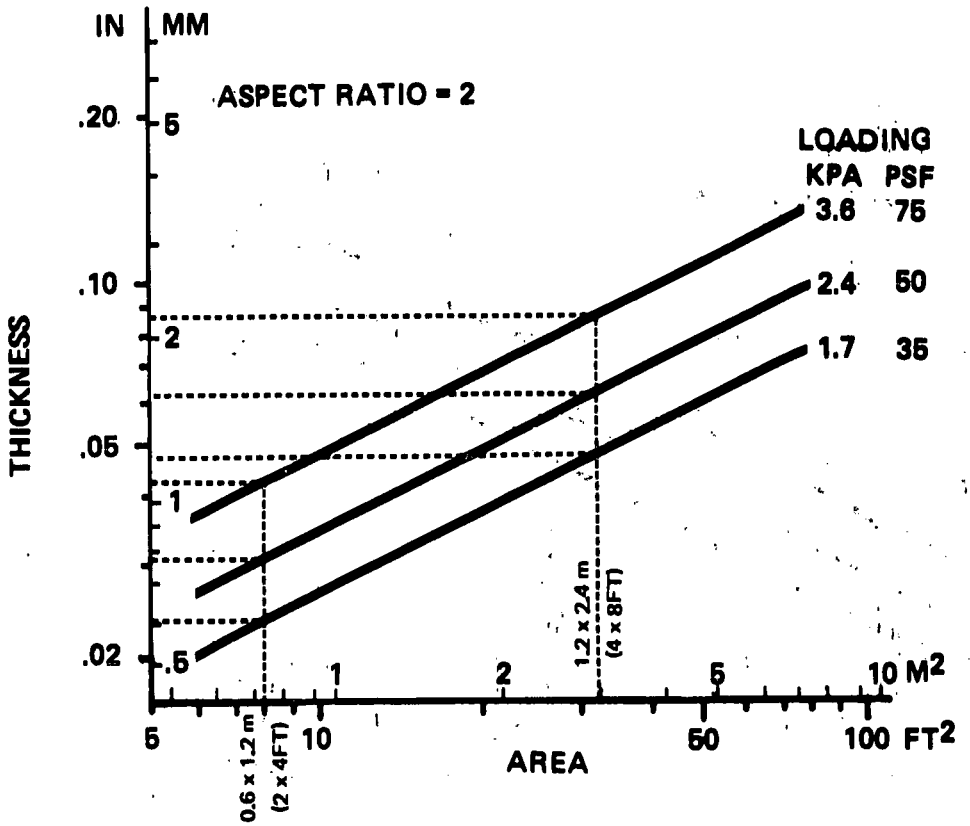

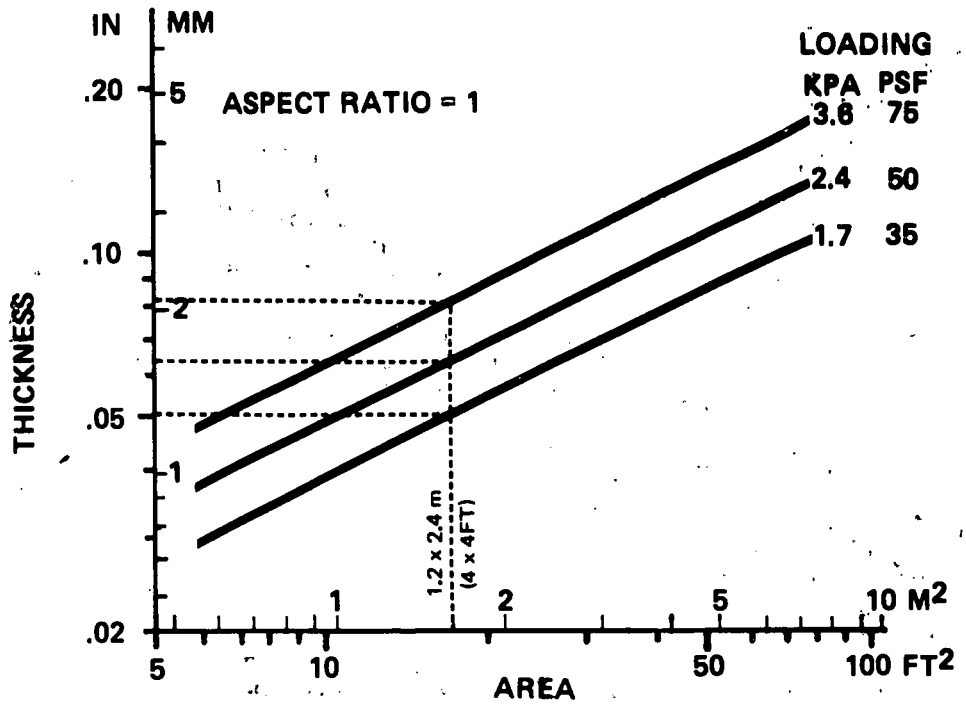

Figure 4-4 THICKNESS VERSUS AREA FOR STEEL SUBSTRATE MODULES

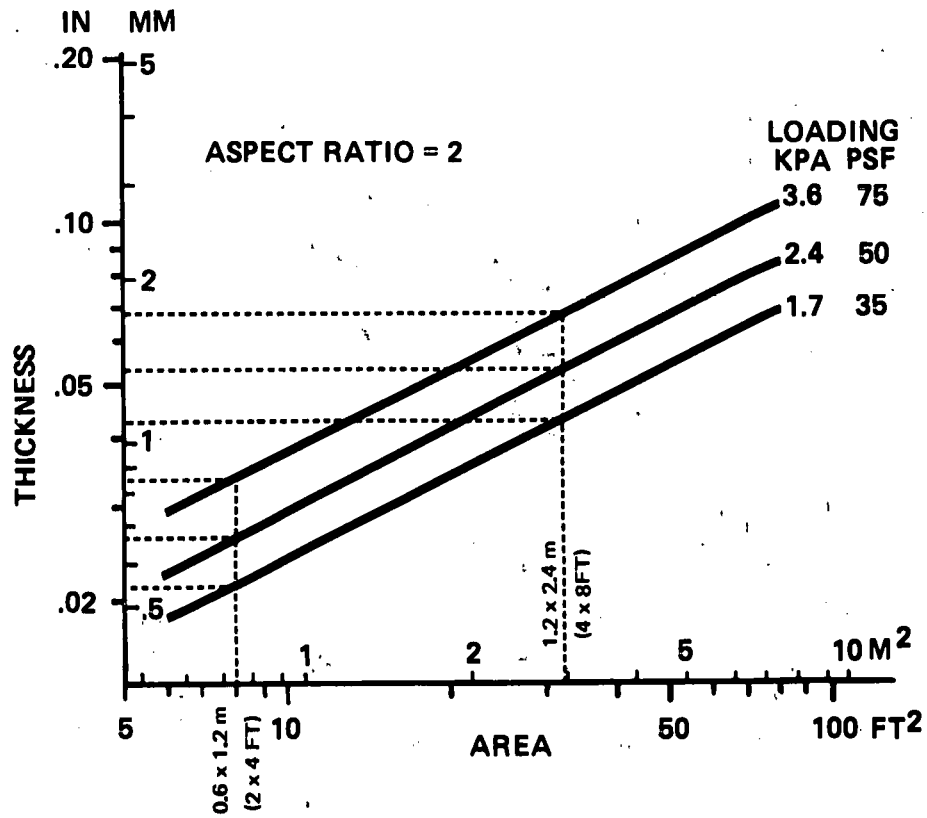

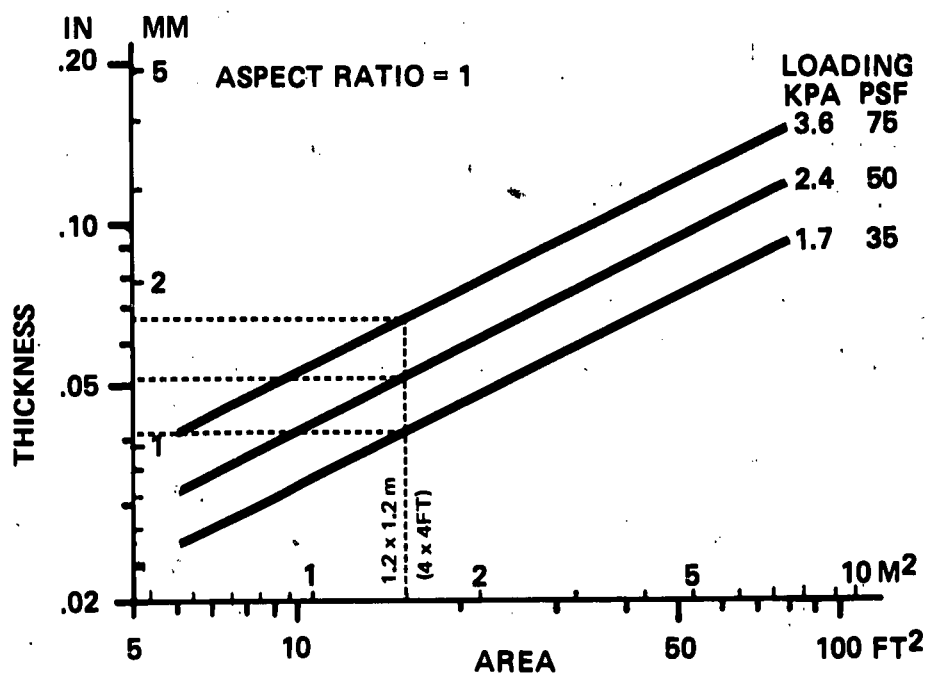

Figure 4-5 THICKNESS VERSUS AREA FOR ALUMINUM SUBSTRATE MODULES

(0.061 inch at 50 psf). Translating present day steel prices to 1975 dollars, the cost of this steel is $4.48/m². From Figure 4-5, the thickness of an aluminum sheet is 1.3 millimeters (0.053 inch) and is estimated to cost $6.29/m² (1975 $). Therefore, steel was selected as the substrate material.

Adhesive/Pottant. For purposes of this study, the same 0.030 inch thick PVB configuration postulated for the glass superstrate module is also used for the metal substrate module design. However, a 0.19 millimeter (0.0075 inch) sheet of Mylar is added to insulate the cells from the metal substrate. Less expensive means of providing insulation may exist, however.

Front Cover. In this design, the front cover serves two functions. It protects the cells from the environment, and it provides electrical insulation. Tedlar is selected as the front cover because of its weatherability and electrical insulating properties. Tedlar is currently available in sheets up to 0.1 millimeter (0.004 inch) thick. Thicker sheets are obtained by laminating. A 0.2 millimeter (0.008 inch) sheet is selected for reasons of electrical insulation (Section 4.4.2 discusses the selection methodology) although a thinner sheet would suffice from a weatherability point of view or if the system voltage was lower.

Electrical Connectors. The connectors postulated for the glass substrate module are also used for the metal substrate configuration.

Module Cost. The estimated cost of the 1.2 by 2.4 m (4 by 8 ft) metal substrate module described is presented in Table 4-3.

TABLE 4-3

METAL SUBSTRATE MODULE COST ESTIMATE
(1.2 by 2.4 m (4 by 8 ft) module)

Component	Cost ($/m²) 2.4 kPa 50 psf
Cell Assembly(1)	40.00
PVB (0.76 mm, 0.030")	7.12
Mylar (0.19 mm, 0.0075")	0.79
Tedlar (0.2 mm, 0.008")	3.61
Steel (1.55 mm, 0.061")	4.48
Connectors	1.16
Assembly Labor(1)	7.00
MODULE COST	64.16

(1) provided by JPL

By comparison with Table 4-2, it can be seen that the postulated metal substrate module is slightly more expensive than the glass superstrate configuration. Thus, its costs were not estimated at other loadings. However, the cost difference resulting from the preceding evaluations is not great, and the subject warrants further detailed analyses, such as those being carried out by several contractors for JPL's Automated Array Assembly Task.

4.2 HAIL

Tests conducted by JPL indicate that the present module designs can be damaged by hailstone impact. Some of the designs survived impacts by a 38 millimeter (1.5 inch) diameter simulated hailstone falling at its terminal velocity. However, many of the designs were damaged or destroyed by 38 millimeter (1.5 inch) or smaller hailstones. Therefore, the question of vulnerability of the modules to damage by hail storms is important. This problem is reviewed here in general terms.

4.2.1 Data Sources

There are numerous references concerning the occurrence of hail in the United States (Ref. 4-1). Perhaps the most important data resource is the operational log of severe local storm occurrences, maintained since 1954 by the National Severe Storms Forecast Center, NOAA, Kansas City, Missouri. This log includes reports of hail 19 millimeters (0.75 inch) in diameter and greater. Other sources include the remarks section of airport hourly weather data (WBAN-10), the military teletypewriter network, newspaper clippings, and special reports (e.g., Ref. 4-2).

It should be noted that not all hail storms are observed; all of those observed are not reported; and some which are reported are incorrectly classified. This problem was more pronounced in

earlier years, but with increasing interest and improved methods and effort, this problem is now less pronounced than in the past.

4.2.2 General Discussion

Reports of hail can be summarized in terms of hail days or number of hail events reported (Ref. 4-3). For purposes of the present work, the number of hail events reported provides the most useful information. However, this type of information is more difficult to obtain.

Hail that is larger than 5.3 millimeters (0.21 inch) in diameter, true hail, falls almost exclusively in violent thunderstorms, but never when surface air temperature is below freezing. Hail generally occurs during two weather conditions, either during instability showers in a single air mass or during frontal activity between two or more air masses. The highest contribution to annual hail occurrence is made by the spring season frontal activity. Occurrences of hail diminish gradually as convective-type summer storms take over.

4.2.3 Review of Data

The theoretical maximum hailstone is about 3.31 kg (1.5 pounds) with a diameter of approximately 132 millimeters (5.2 inches) (Ref. 4-3), although slightly larger hailstones have been reported (Ref. 4-4). The terminal velocity of falling hail

depends upon the force of gravity, the drag coefficient, the Reynolds number, the density of the hailstone and the air, and the kinematic viscosity of the air. Large hailstones with complex surfaces may reach the critical Reynolds number and attain a sudden and large increase in terminal velocity.

The calculated terminal velocity of hailstones (Ref. 4-3) for an assumed specific gravity of 0.6 is given in Table 4-4.

TABLE 4-4

TERMINAL VELOCITY OF LARGE HAILSTONES

Formation Altitude		Hailstone Weight		Hailstone Diameter		Terminal Velocity	
(m)	(ft)	(kg)	(lb)	(mm)	(in)	(m/s)	(mph)
0	0	.45	1.0	114	4.50	43	96
1219	4,000	.52	1.15	118	4.65	46	104
3049	10,000	.58	1.28	123	4.83	51	114
4573	15,000	.64	1.41	127	5.00	56	126
6098	20,000	.72	1.58	132	5.20	62	139

Terminal velocities for smaller hailstones are given in Table 4-5 (Ref. 4-7).

TABLE 4-5

TERMINAL VELOCITY OF SMALL HAILSTONES

Hailstone Weight (kg)	Hailstone Weight (lb)	Hailstone Diameter (mm)	Hailstone Diameter (in)	Terminal Velocity (m/s)	Terminal Velocity (mph)
0.001	0.002	13	0.5	15.2	34
0.007	0.016	25	1.0	21.9	49
0.026	0.057	38	1.5	27.4	61
0.062	0.14	51	2.0	32.0	72
0.12	0.27	64	2.5	36.0	81
0.21	0.46	76	3.0	39.6	89
0.33	0.73	89	3.5	42.7	96
0.50	1.10	102	4.0	45.4	102

The size frequency distribution of hailstones for the Denver area was studied by United Air Lines for the period 1949 through 1955 (Ref. 4-3). Data from that study are shown in Table 4-6 and as a graph in Figure 4-6.

TABLE 4-6

FREQUENCY DISTRIBUTION OF MAXIMUM HAIL SIZE
DENVER, 1949-1955

Number of Reported Occurrences	Approximate Diameter (mm)	Approximate Diameter (in)	General Size Description
12	<6.4	<1/4	Grain
125	6.4	1/4	Currant
290	12.7	1/2	Pea
151	19	3/4	Grape
40	25-32	1 - 1-1/4	Walnut
28	45-51	1-3/4 - 2	Golf Ball
5	64-76	2-1/2 - 3	Tennis Ball

The amount of damage caused by hailstones of various sizes depends on the nature and condition of the target. For example,

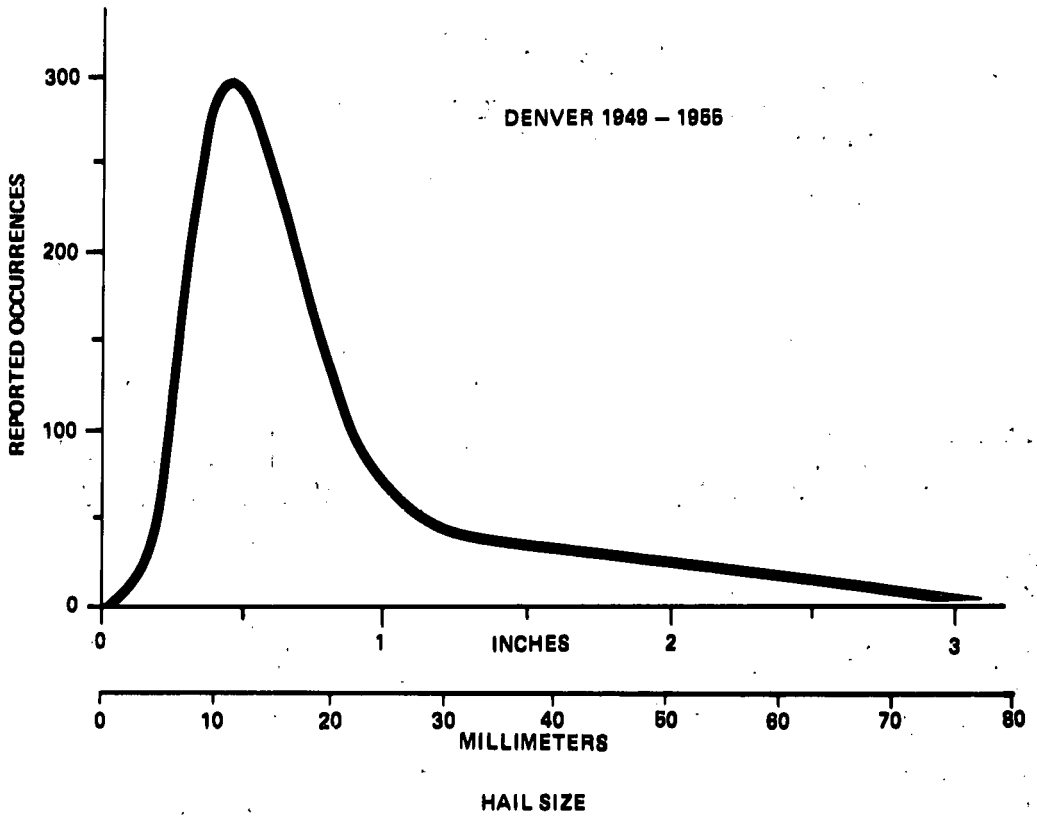

Figure 4-6 HAIL SIZE DISTRIBUTION

stones of equal size will exert a diversity of damage on various crops and their various maturity levels. Reports of hail damage to crops are complicated by the fact that the crops are also susceptible to damage by wind and hard rain. Generally, of course, the larger the stone, the greater the damage. Table 4-7 (Ref. 4-1) presents a summary of reports for hail of 19 millimeter (0.75 inch) diameter or greater for the years 1955 through 1967, for each state. This information is useful for site screening purposes and estimating relative insurance costs. Table 4-7 shows that the states of Texas, Oklahoma, Kansas,

TABLE 4-7

NUMBER OF HAIL REPORTS
(Total for Years 1955 through 1967)

State	Diameter 19-38mm .75-1.5in	Diameter >38mm >1.5in	State	Diameter 19-38mm .75-1.5in	Diameter >38mm >1.5in
AL	50	54	NE	295	301
AZ	12	9	NV	7	0
AR	113	82	NH	13	3
CA	13	6	NJ	6	2
CO	130	107	NM	85	46
CN	22	7	NY	28	21
DE	0	0	NC	40	30
FL	84	32	ND	53	67
GA	46	28	OH	73	40
ID	46	6	OK	575	443
IL	143	86	OR	16	3
IN	61	57	PA	37	20
IO	153	123	RI	1	2
KA	388	444	SC	42	31
KY	42	24	SD	107	160
LA	60	54	TE	71	47
ME	21	8	TX	530	676
MD	24	10	UT	23	1
MA	34	17	VT	15	9
MI	88	40	VA	56	26
MN	133	124	WA	4	4
MS	56	37	WV	19	11
MO	266	212	WI	122	46
MT	177	87	WY	44	15

Nebraska, and Missouri account for over half (51.1%) of the total large diameter hail reports.

4.2.4 Application

The foregoing information, while helpful, can only be used to establish hail probability on a general basis for large areas. For example, Table 4-7 indicates that Oklahoma had 1018 reports of hail 19 millimeter (0.75 inch) diameter and greater during the 13 year period 1955-1967. These data indicate an average number of occurrences of 1018/13 or 78.3/year for the state. This leaves unanswered the question of the probability of a certain target within the state of Oklahoma receiving one of the average 78.3 hailstorms annually.

The information can be refined somewhat by using Figure 4-7 (Ref. 4-1). This figure shows the total number of reported occurrences for hail 19 millimeter (0.75 inch) and greater in 1° squares across the United States. Unfortunately it does not indicate the size classification given in Table 4-5. Figure 4-7 shows that the 1° square area (approximately 10^{10} square meters (3890 square miles) at 35° latitude) containing Oklahoma City listed 104 reports of hail 19 millimeter (0.75 inch) and greater. These data indicate an average of eight occurrences per year in the 10^{10} square meters (3890 square mile) area around Oklahoma City.

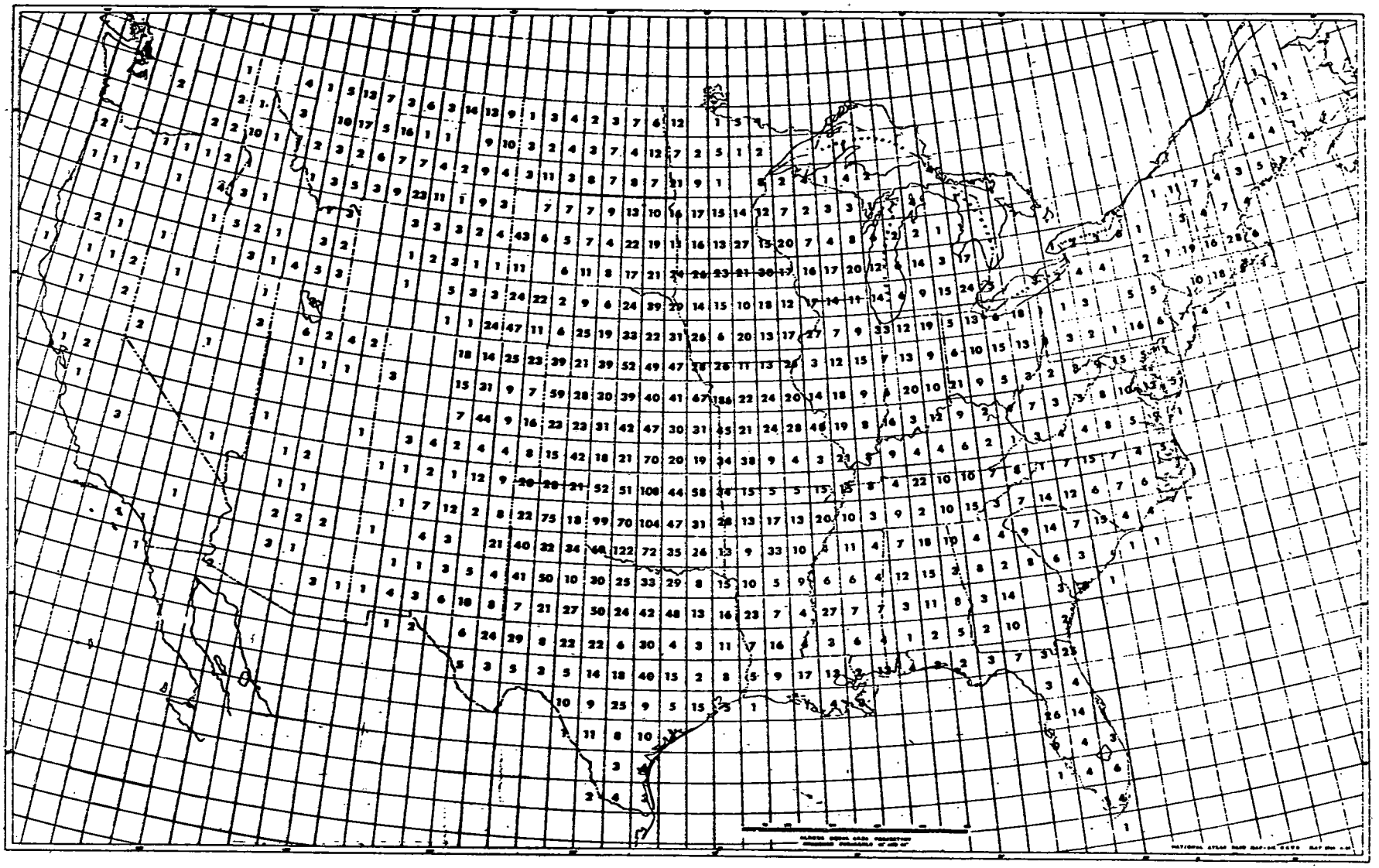

Figure 4-7 REPORTED OCCURRENCES OF HAIL 3/4 INCH AND LARGER, 1955 - 1967

This type of information is still of an approximate nature, since, for example, the area of a hailstorm swath has not been taken into account. For a specific application, a site study and investigation could develop the required data base to prepare a detailed evaluation.

One related consideration is the cost of insurance. During the conduct of another Bechtel study for JPL (Ref. 3-2), it was found that the annual premiums for hail insurance for photovoltaic power systems would be approximately equal to twice the expected cost to repair the damage divided by the recurrence interval in years (i.e., one over the probability) for such damage causing hailstorms. The present worth of 30 years of hail insurance premiums is on the order of 3¢/watt for severe storm areas (e.g., portions of Oklahoma) and, of course, is zero for areas of the country not subject to damaging hailstorms.

Further risk, module design analyses, and insurance cost evaluation will require data on how well modules survive a hailstone impact. Results from tests conducted by JPL indicate that 3.2 millimeters (0.125 inch) thick tempered glass will survive the impact of a 32 millimeter (1.25 inch) hailstone traveling at its terminal velocity. In order to design modules to resist hail damage, it will be necessary to know the thickness of glass required to resist various hailstone diameters. Factors that should be considered in obtaining this data include glass state of temper, edge treatment of the glass (e.g., chamfered or

not), changes in glass characteristics with age and temperature, support method (completely framed, segmentally supported, or segmentally supported and curved), and impacts at high velocity (i.e., wind-driven hail).

A more detailed analysis of the risk of hail occurrences can be found in a JPL published report, Reference 4-7.

4.3 LIGHT ABSORPTION

4.3.1 Glass Superstrate

A study was made to determine the cost sensitivity of modules to light absorption in a glass sheet used as a structural support and front cover encapsulant for solar cells in glass superstrate module designs.

The amount of light energy absorbed in a glass sheet is an exponential function of its thickness and absorption coefficient. Tempering the glass allows the use of thinner sheets, thereby decreasing absorption losses. (The thickness of glass required for several module configurations is discussed in Section 4.1.1.) The absorption coefficient is a function of the chemical makeup of the glass. Reducing the iron content of soda-lime glass is the principal means of reducing absorption in glass sheet used for solar applications.

For purposes of this study, only absorption in the glass is considered; it is assumed that reflections remain unchanged as the iron content and thickness of the glass vary. Factors affecting reflection losses (e.g., cells, antireflection coatings, adhesives, glass surface, and assembly techniques) are held constant. Changes in reflection due to changes in glass index of refraction and bifringence are assumed to be negligible. Except for optical uses, glass is seldom manufactured and sold in large quantities with a controlled index of refraction. More commonly, glass is coated to control reflections.

Glasses with several iron contents were evaluated by considering their light absorption properties in the 0.4 to 1.1 micron range of silicon solar cell sensitivity. A weighted absorption factor was determined by convoluting the relative response of a silicon cell (Ref. 4-8) with the absorption coefficient of the glasses (Ref. 4-9) for several thicknesses of glass. Since most transmission data on glass includes the loss from two surface reflections. This loss was removed in determining the absorption coefficients of the glasses. Additionally, only normal incidence was considered. The results of the evaluation are presented in Figure 4-8, which shows the relative power output from a cell versus glass thickness with iron content in the glass as a parameter.

Estimates of glass costs were obtained from a manufacturer for several thicknesses, iron contents, and state of temper. Figure

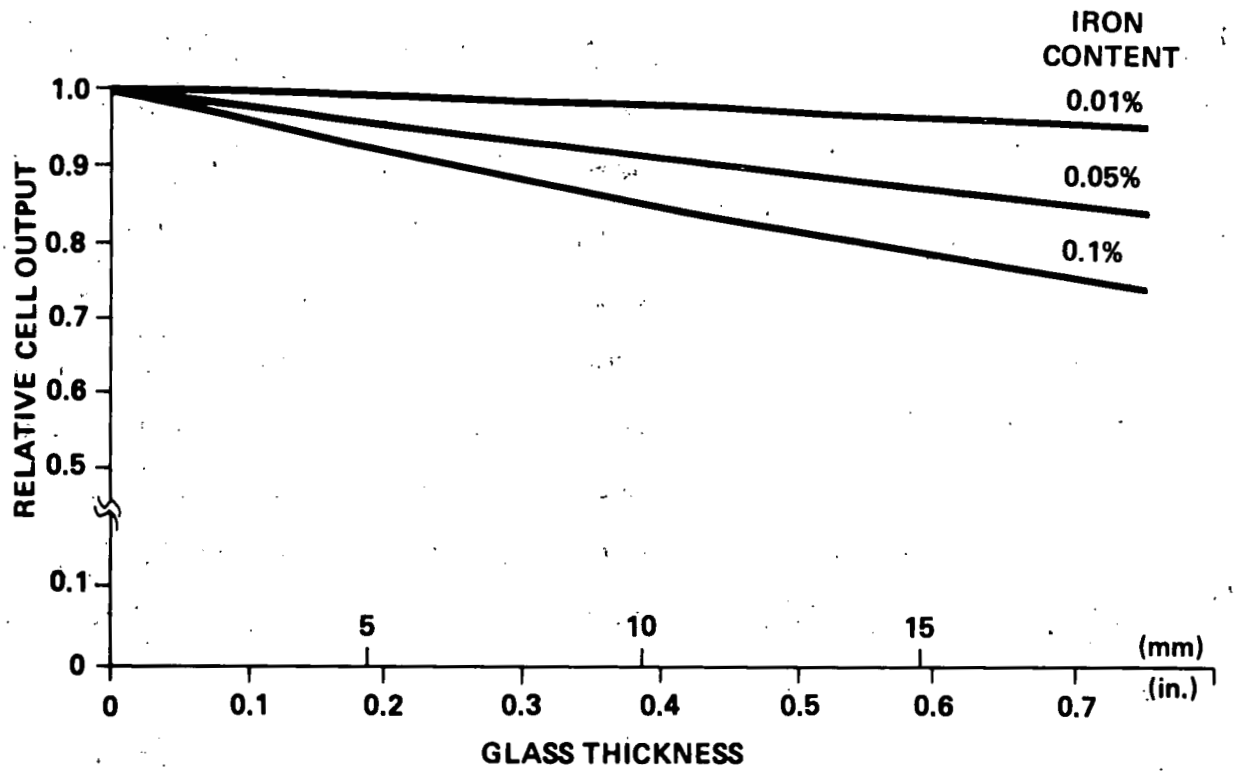

Figure 4-8 CELL OUTPUT VERSUS GLASS THICKNESS

4-9 presents the data normalized to dollars per square meter. The price and availability of these types of glass are influenced by many factors, such as purchase volume, unused industry capacity, tolerances, etc.

The data on glass cost (Figure 4-9) and relative cell output (Figure 4-8) as functions of required glass thickness (Figures 4-2 and 4-3) were combined to determine the optimum material. Doing this requires that some value be placed on the energy cost to light absorption in the glass cover. For the present evaluation, this is done by keeping plant output constant and adding modules, arrays, and balance of plant equipment to make up

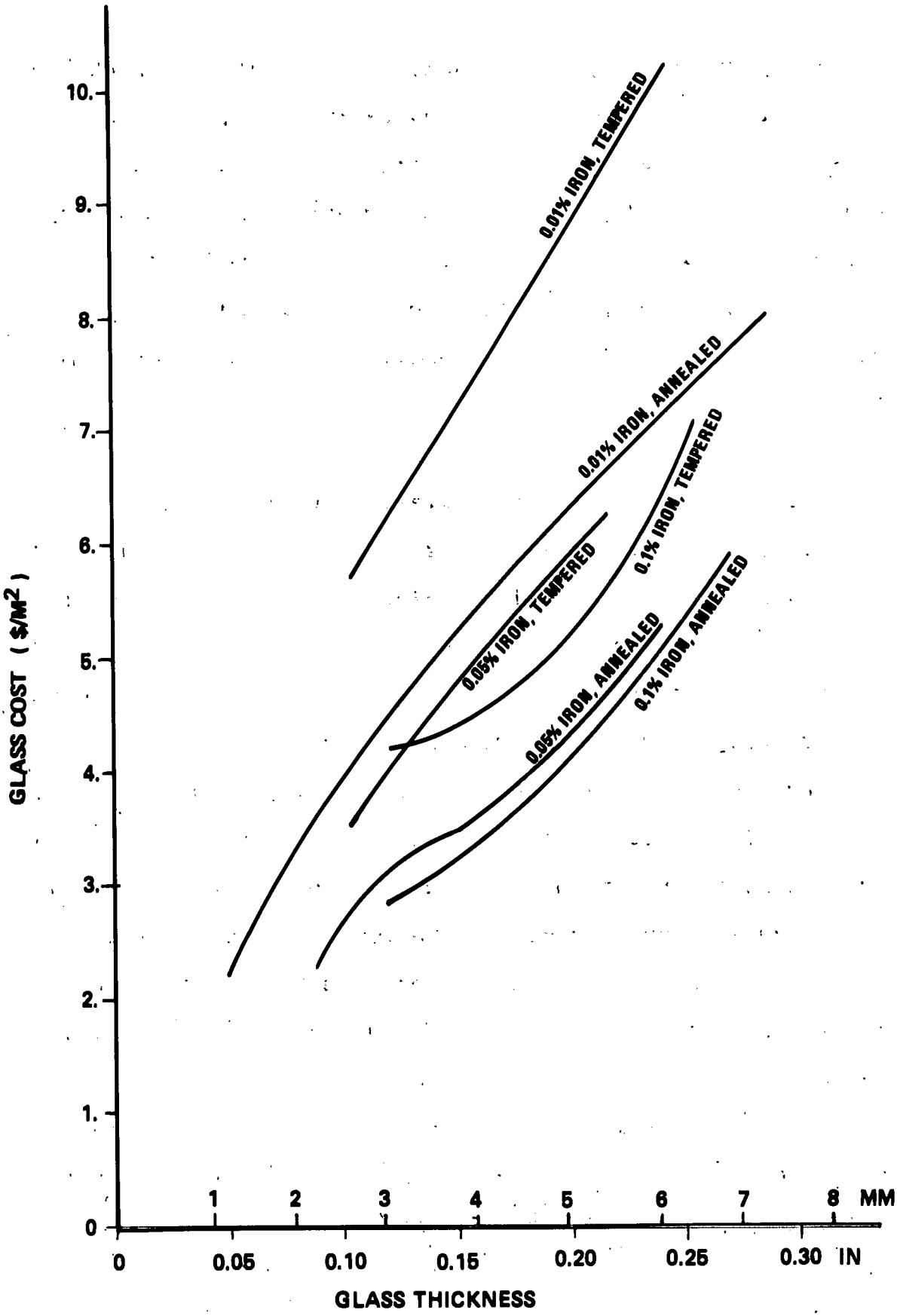

Figure 4-9 GLASS COST DATA

for the power lost by absorption. (Costs for a plant of this type were estimated in a study by Bechtel (Ref. 3-2).) With a constant power level, certain plant costs will not increase with added panels and arrays (e.g., converters, switchyard, etc.). Using data from Reference 3-2, it was determined that those portions of the plant that would be added to keep the output constant would cost approximately $103 per square meter of module.

The thickness of the tempered glass superstrate is constrained to be greater than 3.2 millimeters (0.125 inch) for reasons of hail resistance (as discussed in Section 4.2) and manufacturability. With existing technology, there is rapid heat transfer from the surface of glass sheet which, in turn, limits the thickness of commercially available sheets of thermally tempered glass. Thinner sheets of glass can be chemically tempered, but this results in a product that is sensitive to surface scratches and is therefore not considered further. The thickness of annealed glass versus resistance to hailstones of various sizes is not known. Therefore, in the light absorption calculations the thicknesses of annealed glass required for various module sizes was based only on structural considerations determined from Figure 4-2. As will be shown, this does not affect the selection of material. In all cases, a glass thickness capable of resisting 2.4 kPa (50 psf) loading is used.

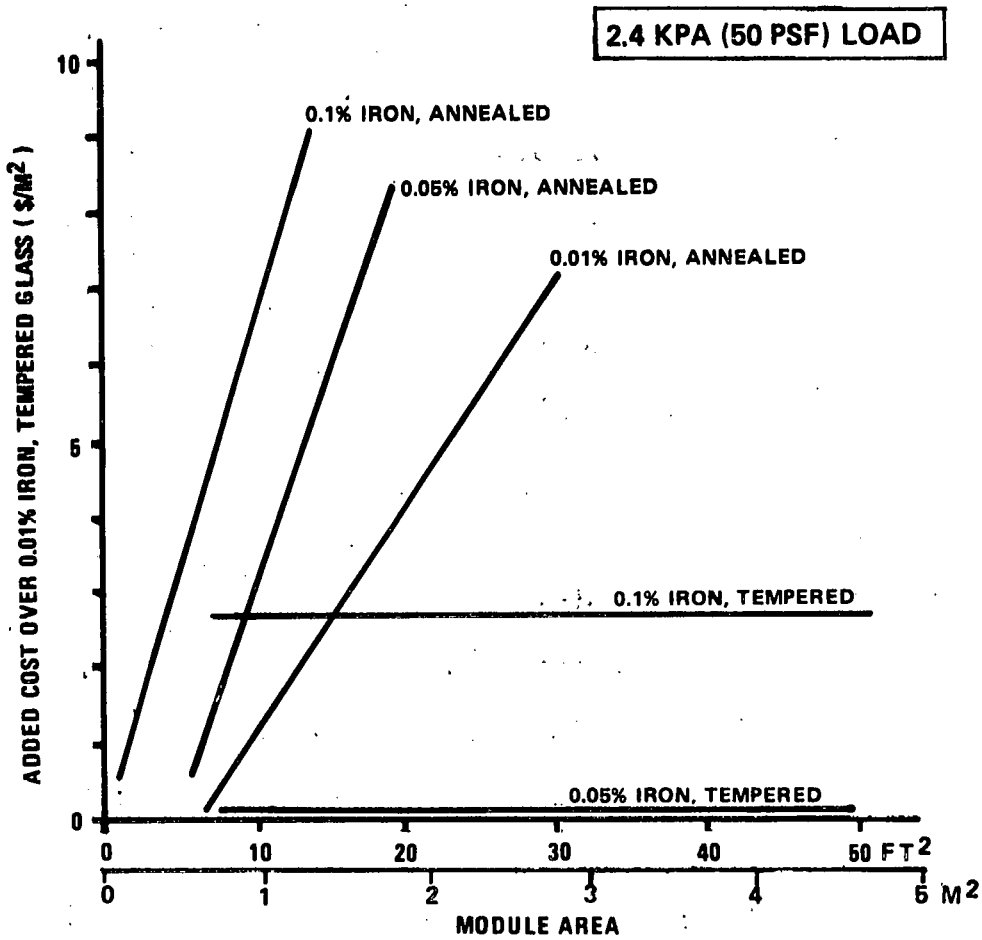

Figure 4-10 GLASS SELECTION ECONOMICS

Figure 4-10 shows the cost penalty incurred by using glass other than the 0.01 percent iron, tempered glass used as a baseline. Figure 4-10 shows that thinner tempered glass results in lower total plant costs than annealed glass for modules larger than 0.6 by 1.2 m (2 by 4 ft) (i.e., 0.74 square meters, 8 square feet). Similarly, the use of tempered, 0.1 percent iron glass leads to higher plant cost. The difference in plant cost between using the tempered, 0.05 and 0.01 percent iron cases is relatively small and this difference would be zero if the costs of plant equipment added to maintain constant power were reduced by 3 percent (i.e., from $103/m² to $100/m²). The plant costs

from Reference 3-2 are such that it is felt that at least a 3 percent reduction in balance-of-plant costs will be required to make photovoltaic central station power plants economically viable. On this basis, selection of the tempered, 0.05 percent iron glass will result in the lowest total plant cost. Thus, this type of glass is used in Section 4.1.1.

The major reason for the low cost of the 0.05 percent iron glass is that it is produced by a drawing process. At present, the 0.01 percent iron is a rolled glass. If warranted, a new factory could be built to draw the 0.01 percent iron glass and lower its cost. However, this would require a large, predictable and constant market. Such a market does not now exist, but future demand due to solar thermal and photovoltaic installations together might cause its creation.

4.3.2 Curved Glass Superstrate

Light absorption in a curved glass superstrate was compared to that in a more conventional flat glass superstrate module configuration in order to assure that structural advantages inherent in the curved plate were not offset by any decrease in energy output.

The configurations compared are the flat glass module discussed in Section 4.1.1 and the curved glass module discussed in Section 4.5. Both are evaluated for a tilt angle of 35° at a 35°

latitude site; the curved module's cylindrical axis is inclined at 35°. Other bases for the evaluation include the following.

- It is assumed that the additional encapsulant or adhesive material between a flat solar cell and the curved glass will not significantly reduce the energy output. This additional thickness is less than 0.025 millimeter (0.001 inch) at the center of a 76 millimeter (3 inch) cell for the 2.4 meter (8 foot) radius of curvature and 1.2 meter (4 foot) span used.
- Electrical energy was calculated on an hourly basis for 12 hours of insolation on March 21 at 35° north latitude.
- The incident insolation was derived from Reference 4-10.
- The evaluation includes the diffuse component of insolation.
- The Fresnel equation was used to calculate front surface reflections, and Snell's equation was used to relate the angle of incidence to the angle of refraction.
- A refraction index of 1.5 was used for the glass.
- A light absorption coefficient of 0.022/cm was used. This is derived from work described in Section 4.3.1 and is representative of 0.05 percent iron glass in the 600 to 800 nanometer wavelength range. Calculations were performed for only one wavelength of light.
- The thickness of flat glass was 8.6 millimeters (0.34 inch). (Figure 4-2 for annealed glass at 1.7 kPa (35 psf) loading). The thickness of the curved glass is 4.7 millimeters (0.187 inch) (that analyzed in Section 4.5.4).
- The curved plate was approximated by seven flat facets.

The results of the calculations show the energy output of the curved glass superstrate module is 0.9997 times that of the flat glass superstrate module. Although this value should not be considered as accurate as indicated by the four significant

figures, it does however, support the conclusion that electrical energy output is not significantly altered by curving the module.

4.3.3 Other Aspects

Two other methods of optically improving a module's performance were briefly evaluated. One method of improving a module's performance would be by the formation of a hot mirror (i.e., infrared reflecting surface) on the glass surface. This would increase module performance by lowering its temperature. Existing thin-film technology can be used to reflect energy that is outside of the 0.4 to 1.1 micron band in which silicon cells are sensitive. It is estimated that this would lower a module's temperature by approximately 5°C (9°F), which in turn would increase conversion efficiency by a quarter of a percentage point. Considering modules costing $0.5/watt and relevant portions of the balance of plant translates the worth of this improvement to about $1.15/m². However, present thin film coatings cost on the order of $20 to $100/m² in limited production. Thus, it appears that this technique is not economically suited for flat-plate arrays. However, it may be applicable in concentrator arrays where the area to be coated is significantly less. Also, such coatings will perform better with concentrator arrays where the light tends to be normally incident on the cell for the entire day. In such evaluations, it must be remembered that a hot mirror's in-band transmission is not 100 percent.

A second method to improve module performance is to reduce the reflection at the first surface of the glass. Experimental data for solar thermal collectors indicate that an etch antireflection "coating" can reduce the first surface reflection from about 4 percent to less than 1 percent in the 0.4 to 1.1 micron range (Ref. 4-11). This improvement would have to cost less than $5/m². It is estimated that such processing would cost on the order of $1 to $5/m². Thus, it appears such techniques should be evaluated further. Also, the performance of this type of coating improves with increasing angles of incidence. However, the durability (e.g., resistance to continued leaching of the glass surface), and the moisture and dirt resistance of antireflection coatings produced by this process may preclude its use unless improvements can be made.

Improvements in cell antireflection coatings and design of the glass-adhesive-cell optical interface are considered beyond the scope of the present study.

4.4 ELECTRICAL

Several electrical aspects of module design are discussed in this section. Included are evaluations of insulation and leakage current. Other reports by Bechtel contain further data on connectors, wiring, voltage transients, and selection of dc system voltage (Refs. 3-1 and 3-2).

4.4.1 Module Electrical Insulation Requirements

The materials employed in the fabrication of terrestrial photovoltaic solar cell modules must exhibit acceptable electrical insulating properties throughout the module's useful life in addition to providing the required structural support and/or environmental protection. Module encapsulants are stressed by electric fields resulting from normal dc operating voltages and, from time to time, by transient overvoltages originating either within the system (e.g., converter generated) or from outside the system (e.g., lightning induced).

Normal dc system voltage is determined by the voltage of each solar cell and the number of solar cells connected in series. The following solar cell voltage characteristics were supplied by JPL for use in this study and are used to determine array voltage conditions:

- The open circuit voltage is 0.58 volt/cell for a 28°C cell temperature.
- The open circuit voltage decreases by 0.0038 volt/volt per °C increase in cell operating temperature.
- The nominal operating cell temperature (NOCT) is 44°C.
- The maximum power point voltage is 0.15 volt/cell less than the open circuit voltage.

Based on the above parameters, Figure 4-11 illustrates the variations of system peak-power point and open circuit voltages with solar cell operating temperature for the baseline plant

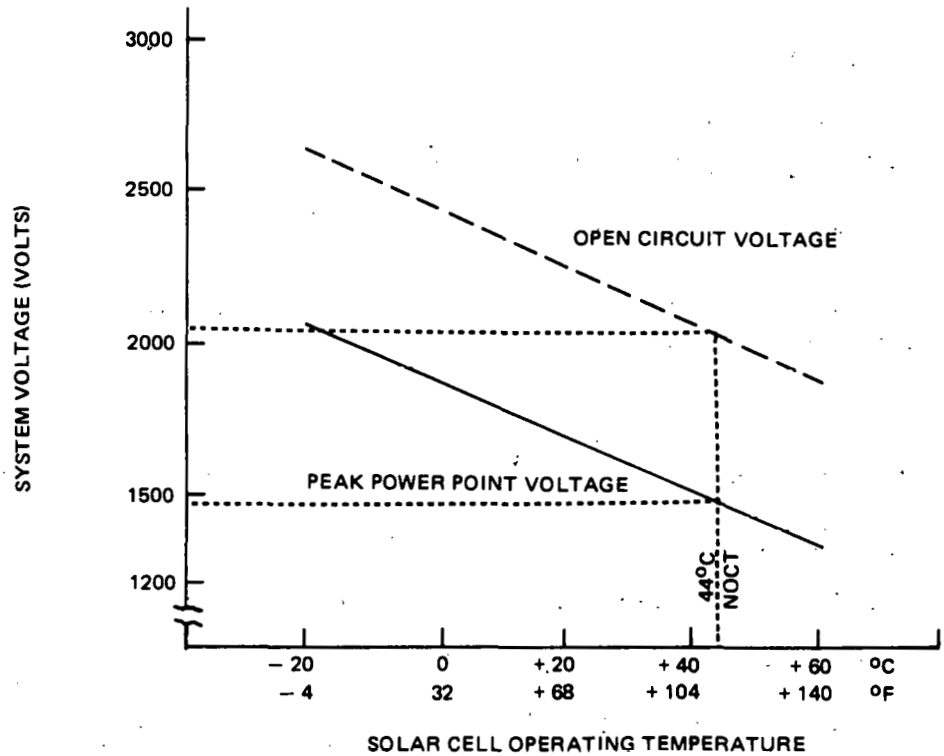

Figure 4-11 SYSTEM VOLTAGE VERSUS SOLAR CELL TEMPERATURE

design discussed in Section 3. This system has a peak-power point operating voltage of 1500 volts at an insolation level of 1 kW/m² and a nominal operating cell temperature (NOCT) of 44°C. It can be seen from Figure 4-11 that "normal" system voltage, and therefore insulation stress, will vary over a wide range during system operation.

Transient voltage levels are somewhat more difficult to predict, especially at this early stage of design, due to the absence of detailed site and system design characteristics. As reported in an earlier Bechtel study (Ref. 3-1), transient voltage levels depend on such system characteristics as:

- Converter design
- Dc system impedance
- Site isokeraunic level
- Soil resistance
- Type and characteristics of the lightning protection scheme and other auxiliary protective devices

Based on a consideration of these and other factors, it is estimated that expected values of transient voltages will be on the order of 2.5 to 3 times the dc system voltage. However, it is more likely that long-term performance requirements under normal system voltages, rather than transient voltage levels, will determine insulation requirements. The reasons for this conclusion are discussed in this section.

The ability of a material to act as an insulator depends on its ability to inhibit the acceleration of electrons within the material. The maximum uniform electric field to which a homogeneous substance can be subjected without breakdown is referred to as the intrinsic dielectric strength of the material (Ref. 4-12). Dielectric strength is usually presented in terms of volts per mil (i.e., volts per 0.001 inch). For example, the intrinsic dielectric strength of polyethylene, a solid dielectric commonly used in cable insulation, is reported to be about 650,000 volts per millimeter (16,500 volts per mil) of insulation thickness (Ref. 4-12). Unfortunately, in actual practice many factors intercede to prevent the attainment of dielectric strengths that come anywhere near the intrinsic values. Factors

that have been identified as contributing to this reduction in dielectric strength include:

- Material imperfections in the form of holes, bubbles, and foreign particles
- Stress concentrations introduced by the presence of sharp edges or points on conducting surfaces
- Oxidation and ion bombardment resulting from corona discharge

Material imperfections result in localized distortion of the electric field within the insulation. For example, if a conducting particle is entrapped in the insulation, the voltage gradient across the particle will be negligible, thereby forcing a local increase in the voltage gradient appearing across the surrounding insulation. Such imperfections can be introduced during the manufacturing process. Similar effects result from holes and bubbles that may form during manufacture or as the result of thermal cycling.

Sharp edges on conductor surfaces, such as those on solar cell edges and interconnect edges, result in local field intensifications on the order of two to three times that which would exist between parallel flat electrodes.

The presence of corona discharge, located either at the conductor-insulation interface or in voids within the insulation, produces a slow but steady degradation of insulator properties which can, in time, lead to failure. Although corona degradation

is more prominent with ac voltages, it can be a contributing factor to failure in dc applications.

For possible module insulation systems in dc fields, where the voltage is distributed across a series combination of two or more different insulating materials, the ratio of the field strengths in the materials varies directly with the ratio of their resistivities. In such cases, the dielectric strength of the insulating system can be less (and therefore, cost more) than would be acceptable if either material was used solely.

The dielectric strength of insulating materials varies inversely with the length of time under stress. This is demonstrated by the data presented in Figure 4-12 (Ref. 4-13), which presents breakdown levels on a #14 AWG copper wire insulated with 50 mils of high molecular-weight polyethylene (HMPE). Along with the observed decrease in dielectric strength with time, the higher dielectric strength possible with dc voltages is also apparent.

The successful long-life design of any insulation system therefore requires that stress levels be kept sufficiently below measured levels that have caused dielectric breakdown over periods of time less than or equal to the design life of the insulation system.

Much information on long-term insulation performance has been collected by the insulated power cable industry. Figure 4-13

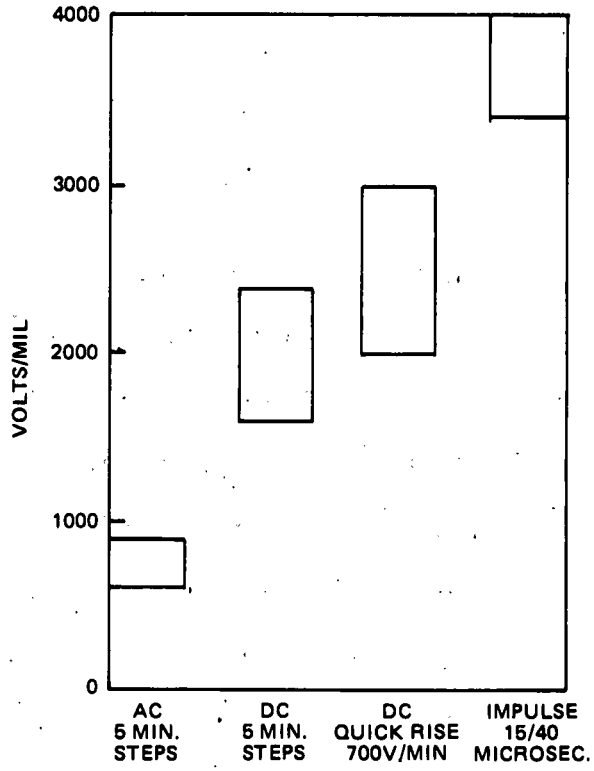

Figure 4-12 BREAKDOWN MEASUREMENTS ON HMPE–INSULATED WIRES

presents maximum permissible stress levels versus applied voltage for two common insulating materials based on standards published by the Insulated Power Cable Engineers Association (IPCEA) for the manufacture of wire and cable. The stress levels presented in Figure 4-13 are based on required insulation thickness and maximum permissible voltage. This voltage was converted to the equivalent, peak phase-to-ground voltage for the RMS alternating current phase-to-phase voltages listed in the standards. The indicated stress levels for the lower voltage levels probably result from the minimum thicknesses dictated by mechanical considerations. From the data in Figure 4-13, it appears that maximum acceptable electrical stress levels for operation in ac fields are about 1770 and 3350 volts per millimeter (45 and

85 volts/mil) for rubber and cross-linked polyethylene, respectively.

There is no universal industry agreement as to the acceptable stress level for insulation in dc fields. One estimate is that dc stress levels of three to seven times those used for ac designs may be used (Ref. 4-14). Because acceptable stress levels for module insulation will be identified only after long-term performance data have been obtained for modules operating under actual system conditions (e.g., voltage profile and weather conditions), initial designs should carefully consider stress levels for the selected module insulation materials.

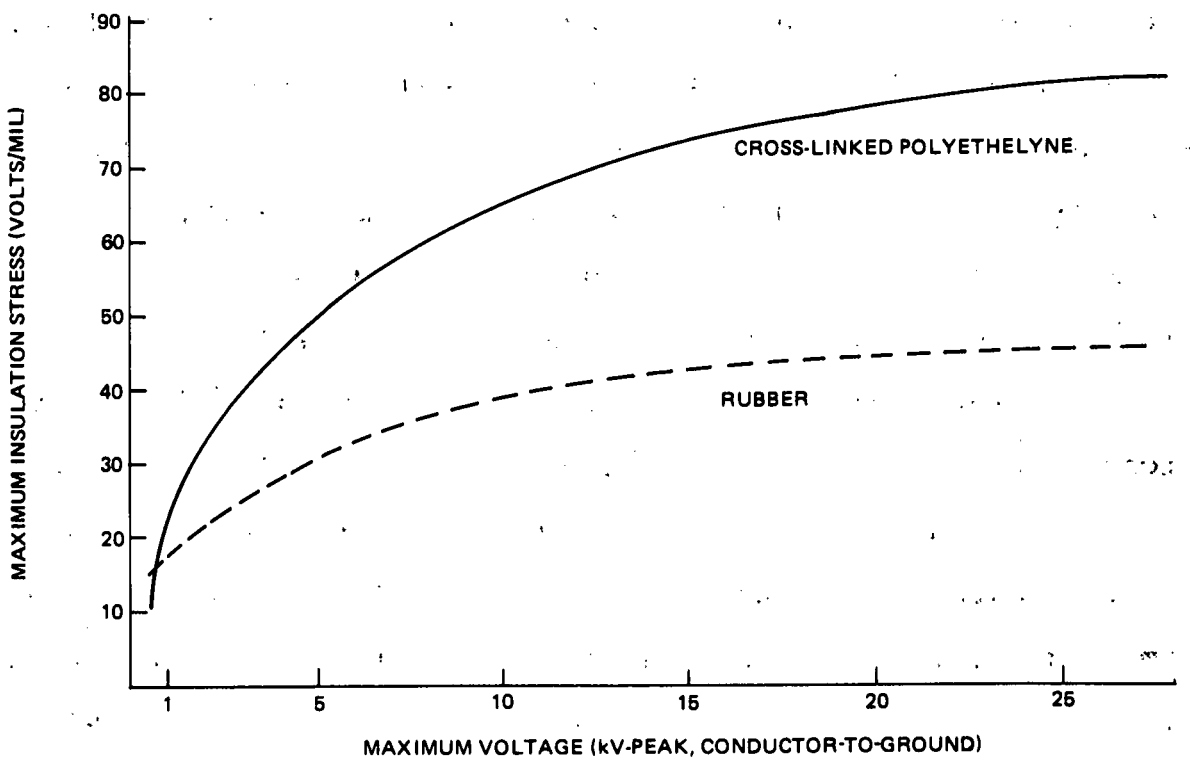

Figure 4-13 MAXIMUM ALLOWABLE AC ELECTRICAL STRESS FOR CABLE INSULATION

Based on the above discussion, a maximum operating stress of 7870 volts per millimeter (200 volts/mil) in a uniform dc field was selected for this study. Comparing this value to the data contained in Figure 4-12, it can be seen that the short-time (transient) rating of the insulation will be many times the value of its nominal long-time rating. Thus, the long-term rating tends to govern insulation requirements.

At present many candidate encapsulating materials and module configurations are under investigation (e.g., Refs. 4-15 and 4-16), however no firm designs have been established. Therefore, a module design was selected for illustrative purposes. This design consists of a soda-lime glass superstrate, 0.25 millimeter (0.01 inch) thick silicon solar cells, Sylgard 184 adhesive/encapsulant, and a Mylar sealant film (back cover). The module cross section is presented in Figure 4-14, along with the expected voltage gradient and stress distribution for a module operating at 1000 volts dc with respect to ground.

It is assumed that the entire outside surface of the Mylar film is at ground potential. This assumption is based on the fact that, once installed, any part of the module's back surface can come into contact with ground due to the presence of moisture, pollutants, or other low resistance paths. The following evaluation is therefore also valid for a module design employing a metal substrate.

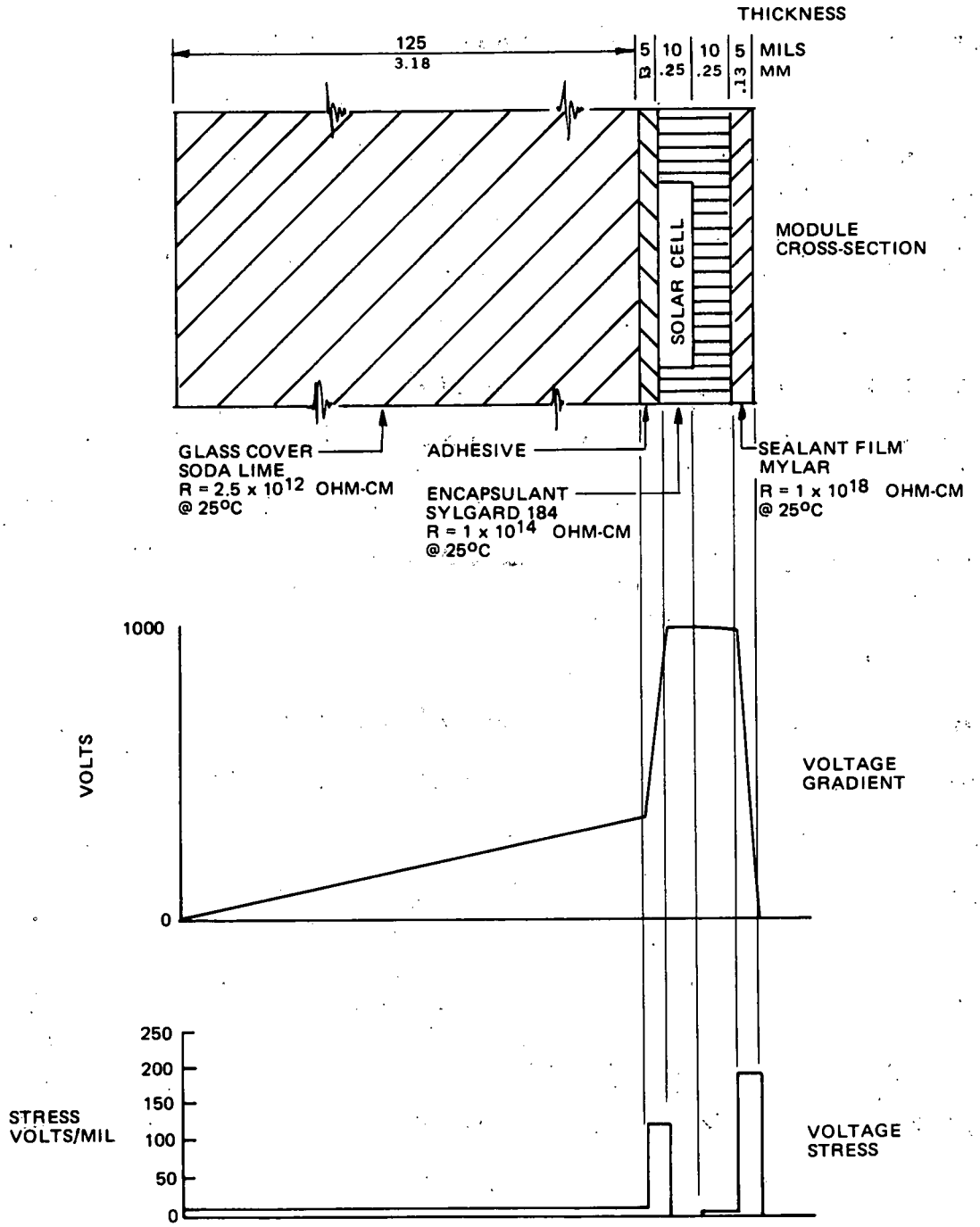

NOTE: MAXIMUM PERMISSIBLE VOLTAGE STRESS, IN A UNIFORM FIELD, SET AT 200 VOLTS/MIL

Figure 4-14 VOLTAGE GRADIENT AND STRESS DISTRIBUTION FOR GLASS SUPERSTRATE MODULE DESIGN

It can be seen from Figure 4-14 that, for this encapsulation system, the maximum voltage stress would appear across the Mylar cover film. This is because the Mylar film has a resistivity four orders of magnitude higher than that of the Sylgard adhesive/encapsulant. When field intensifications due to solar cell and interconnect edges are considered, equivalent stress in the Mylar would be in the range of 15,750 to 23,600 volts per millimeter (400 to 600 volts/mil). It is likely, therefore, that insulation failures would initiate in the Mylar film. The presence of bubbles or moisture (introduced during manufacture or during operation) would tend to further contribute to insulation failure, especially if located at the Mylar-Sylgard interface. It should also be recognized that the maximum electrical stress to which any particular module will be subjected depends on the module's electrical location (i.e., voltage between the module and panel frame) in the branch circuit, particularly for center- or one-pole-grounded systems.

Since actual performance data will be a large factor in the ultimate determination of module insulation requirements, performance tests should be initiated as soon as possible. To accomplish this, one or more modules (either existing or special designs) could be mounted outdoors, biased to about 1000 volts dc with respect to ground, and operated to simulate the actual conditions to which full scale power plant modules will be subjected. Periodic injection of transient overvoltage pulses, followed by measurement of insulation resistance and other

significant parameters, would provide valuable data as to the long-term performance of module insulation systems under central station photovoltaic power plant conditions.

4.4.2 Insulation Thickness Versus System Voltage

The economics of the balance-of-plant system design indicate the desirability of operating central station power plant arrays at relatively high dc system voltage levels. Consideration of converter costs, dc wiring costs, and I^2R losses indicate that optimum dc system voltage is in the range of 1000 to 5000 volts. When encapsulation costs are also considered, the optimum voltage is toward the low end or middle of this range, depending on the cost of encapsulation as a function of voltage (Ref. 3-2).

The module encapsulating system will be required to have sufficient material thickness (depending on the specific configuration and materials) to maintain electrical stress levels at or below the acceptable maximum. Additional material required for operation at higher voltage levels will affect encapsulation costs, and, to some extent, the module's heat transfer characteristics. To illustrate the effect of system voltage on the module encapsulating system, material thicknesses for the back side of the module configuration shown in Figure 4-14 were calculated as a function of voltage level and are presented in Figure 4-15.

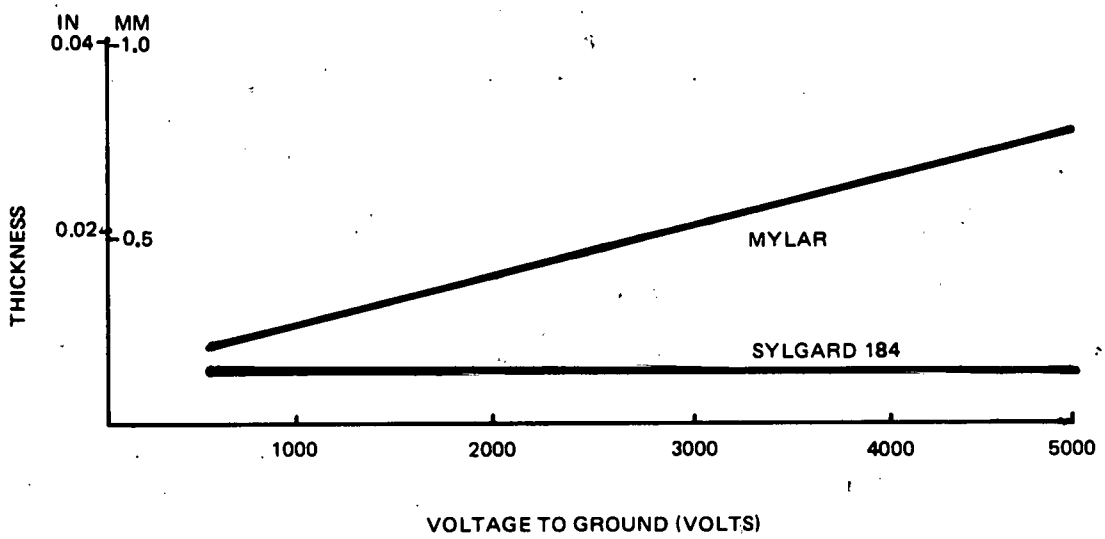

Figure 4-15 ENCAPSULANT SYSTEM I – SYLGARD 184 AND MYLAR

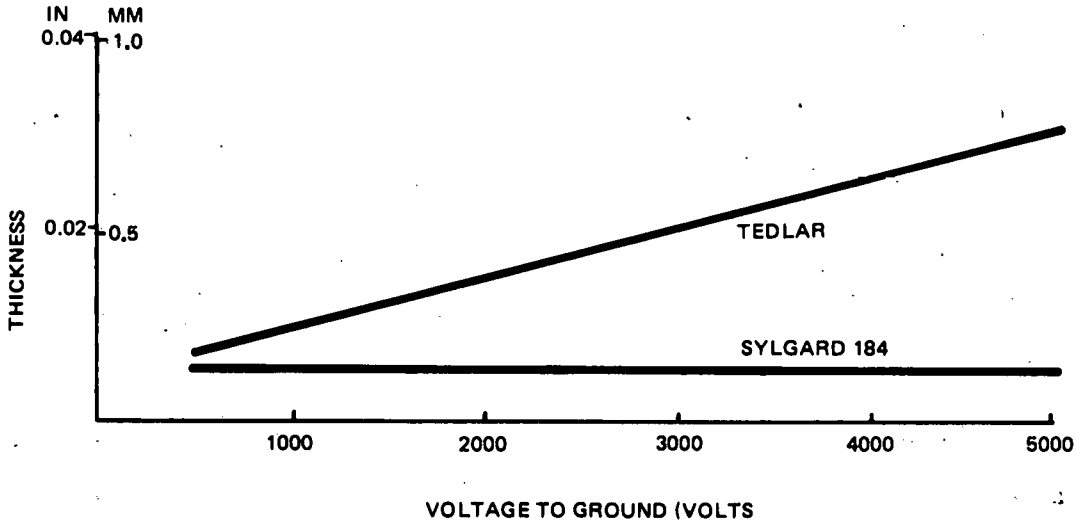

Figure 4-16 ENCAPSULANT SYSTEM II – SYLGARD 184 AND TEDLAR

Since the voltage stress divides in direct proportion to the material resistances, and the resistance (at 25°C (77°F)) of Mylar is about four orders of magnitude higher than Sylgard, virtually all of the stress occurs in the Mylar. It therefore becomes necessary, with increasing system voltage, to increase the Mylar thickness (keeping the Sylgard thickness fixed) in order to maintain an acceptable stress level (7870 volts per millimeter (200 volts/mil)) in this case.

Figure 4-16 presents the required thicknesses if Tedlar film is used instead of Mylar. Tedlar has a resistivity about four times that of Sylgard at 25°C (77°F). This ratio changes with temperature. The majority of the stress occurs in the Tedlar (7870 volts per millimeter (200 volts/mil)) in the Tedlar and 1140 volts per millimeter (29 volts/mil) in the Sylgard), so that increasing the thickness of the Tedlar, rather than the thickness of the Sylgard, provides the required insulation performance with a minimum of material. Although the same insulation performance could be provided by increasing the thickness of the Sylgard, significantly more material would be required. This is illustrated in Figure 4-17, which presents required material thicknesses versus voltage for a Tedlar thickness of 0.1 millimeter (0.004 inch) (the maximum thickness presently available without laminating). It can be seen that large thicknesses of Sylgard become necessary in order to maintain the stress in the Tedlar at no more than 7870 volts per millimeter (200 volts/mil).

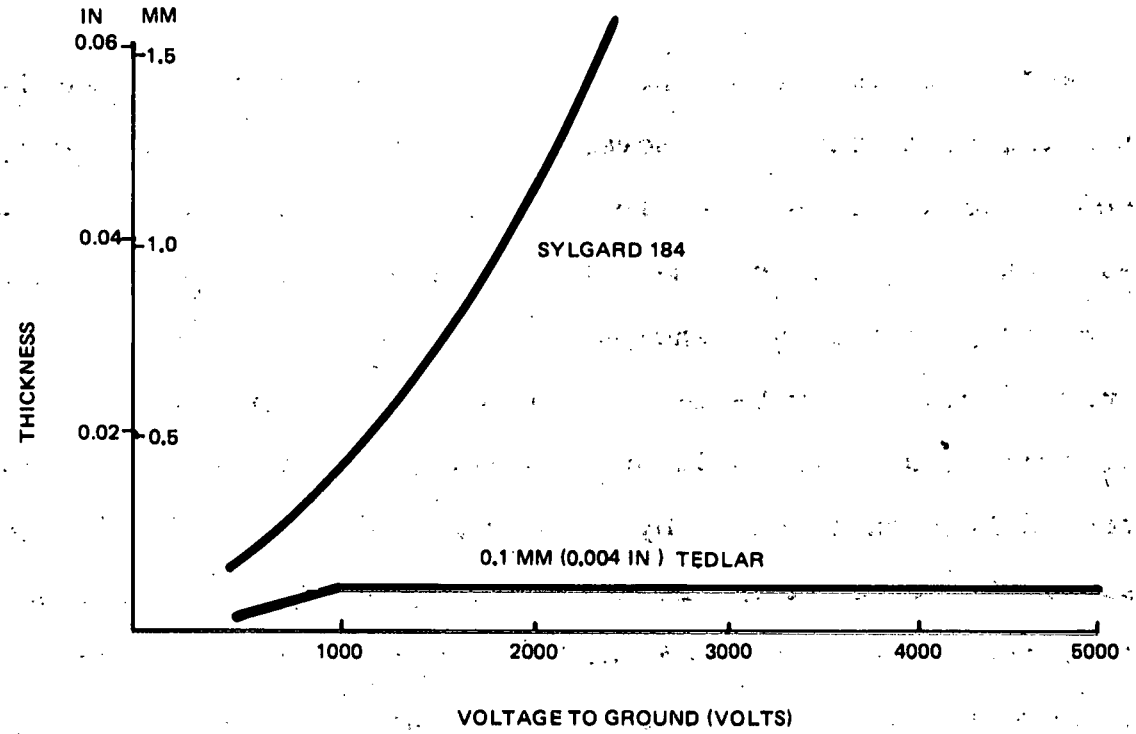

Figure 4-17 ENCAPSULANT SYSTEM III – SYLGARD 184 AND TEDLAR

Other module configurations and encapsulating materials will require individual analysis to determine their particular characteristics and requirements. For example, a configuration receiving recent consideration consists of a glass superstrate, polyvinyl butyral (PVB) adhesive/encapsulant, and some kind of sealant film, as yet unspecified. Since the resistivity of PVB is on the order of 5×10^{10} ohm-cm, virtually all of the voltage stress would appear in the sealant film, if either Mylar or Tedlar were used. If PVB and Mylar were used, material thicknesses would be the same as for the Sylgard and Mylar case since the volume resistivity of the Mylar is several orders of magnitude greater than either PVB or Sylgard.

Figure 4-18 illustrates the affect of voltage on module encapsulating costs for the several configurations previously discussed. Costs presented in Figure 4-18 represent only the material located in back of the solar cells and do not include front covers, adhesive, encapsulant between the cells, or fabrication costs. Material prices were obtained from manufacturers and Ref. 4-16 and are normalized to 1975 dollars using cost deflators supplied by JPL (see Section 2.2). The material costs noted in Figure 4-18 are representative averages, typical of the thicknesses used and are offered as a guide. There is some variation in normalized cost with thickness.

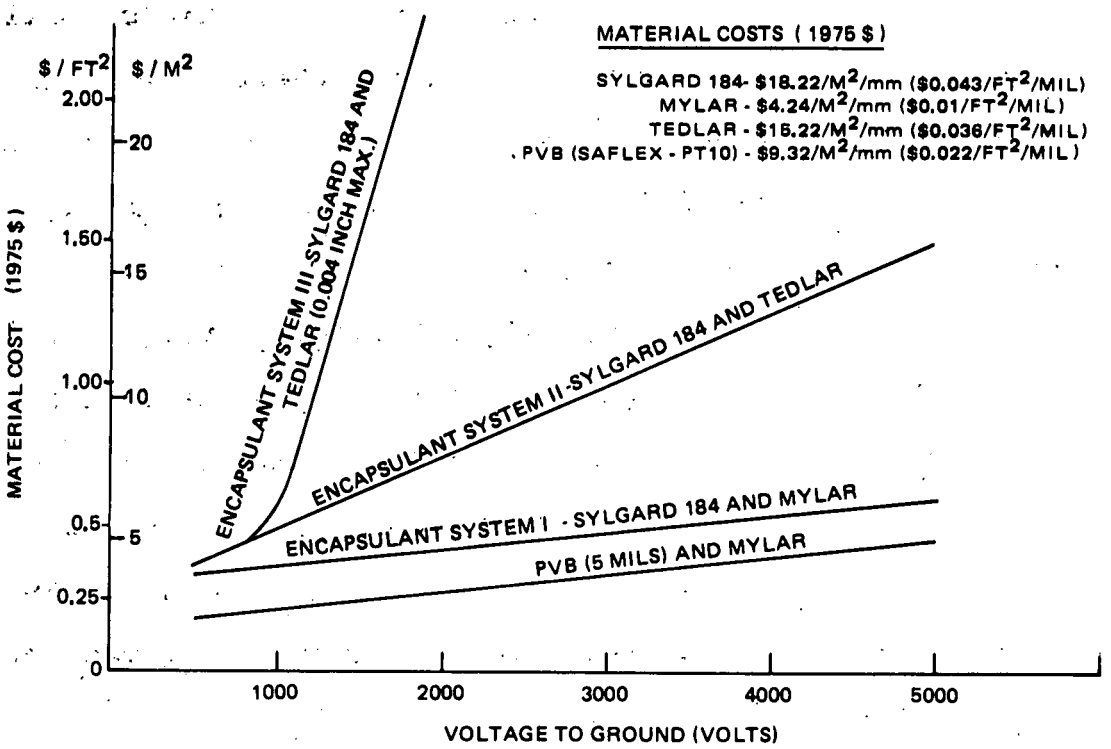

Figure 4-18 MODULE ENCAPSULANT PARTIAL COST VERSUS VOLTAGE

As is seen from Figure 4-18, the cost and feasibility of constructing modules for operation at higher system voltages is dependent on the materials and configuration used. When alternative or new encapsulation systems are proposed, it is recommended that the design and/or evaluation procedures include the consideration of voltage gradients as illustrated in Sections 4.4.1 and 4.4.2.

Based on the foregoing evaluations, an insulating system consisting of PVB and 0.19 mm (0.0075 inch) thick Mylar is used for the back cover of the glass superstrate module described in Section 4.1.1. The insulation selected for the metal substrate module is 0.2 mm (0.008 inch) Tedlar for the front cover (which is exposed to weather) and 0.19 mm (0.0075 inch) Mylar to insulate the cells from the metal.

4.4.3 Module Leakage Current

The use of a material as an electrical insulator necessarily implies that the material has a low electrical conductivity (i.e., high volume and surface resistivities). However, even materials that are good insulators have a finite resistivity and will therefore allow a finite current flow between electric conductors at different potentials. Good insulators typically have resistivities on the order of 10^{15} to 10^{18} ohm-cm. It is therefore assumed that a leakage current will flow through the

module insulation whenever a voltage exists between the solar cells and ground.

Effects of photovoltaic solar cell module leakage currents include:

- Corrosion of metal components of the array at array soil interfaces or at junctions between dissimilar metals, especially in the presence of moisture
- I^2R heating of the insulation material, contributing to thermal aging and possible failure
- Complication of ground fault detection
- Safety hazard to plant personnel

The value of module dc leakage current will depend primarily on the thicknesses and resistivities of the encapsulants and the module's voltage with respect to ground. Conduction in insulators is thought to be due to mobile ions located in or on the insulator material. With the presence of moisture, a material's resistivity is reduced, sometimes by several orders of magnitude. This is true of both the volume resistivity and the surface resistivity. Most organic insulators, such as those commonly used in module construction, also have a negative temperature coefficient of resistivity. Volume and surface resistivities of several candidate module encapsulating materials are presented in Table 4-8.

TABLE 4-8

RESISTIVITIES OF CANDIDATE MODULE ENCAPSULATING MATERIALS (@25°C)

Name	Use	Volume Resistivity (ohm-cm)	Surface Resistivity (ohm-cm)	Rel. Humidity (%)
Soda-Lime Glass	cover sheet	2.5×10^{12}	5×10^{12}	≤40
Soda-Lime Glass	cover sheet	2.5×10^{12}	1×10^{10}	70
Soda-Lime Glass	cover sheet	2.5×10^{12}	8×10^{7}	≥90
Plexiglass (VB11)	cover sheet	6×10^{17}	6×10^{18}	dry
Scotchweld 2216/B/A	adhesive	1.9×10^{12}	5.5×10^{16}	dry
Korad A	sealant film	1×10^{16}	2×10^{14}	dry
Mylar	sealant film	1×10^{18}	1×10^{16}	dry
Tedlar	sealant film	7×10^{14}	-	-
RTV 615	adhesive/ encapsulant	1×10^{15}	-	-
Sylgard 184	adhesive/ encapsulant	2×10^{14}	-	-
PVB	adhesive/ encapsulant	5×10^{10}	-	dry

Since many different encapsulating systems and module configurations are under consideration, calculations were made to determine order of magnitude leakage currents for several possible configurations.

These calculations were based on the simple model presented in Figure 4-19. Although this model neglects lateral conduction in the encapsulant volume, this is not believed to cause significant error because the volumetric resistances of candidate cover materials are typically much greater than their surface resistances.

Total module leakage current was obtained by summing the individual leakage currents calculated for each cell in the

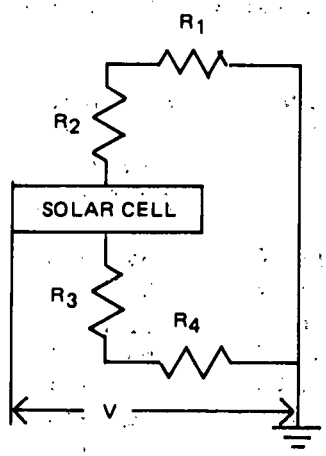

R_1 = SUPERSTRATE SURFACE RESISTANCE
R_2 = SUPERSTRATE VOLUME RESISTANCE
R_3 = SUBSTRATE VOLUME RESISTANCE
R_4 = SUBSTRATE SURFACE RESISTANCE
(R_4 = 0 FOR METAL SUBSTRATE)
V = VOLTAGE OF MODULE CONDUCTORS TO GROUND

$$\text{LEAKAGE CURRENT} = \frac{V}{(R_1 + R_2)} + \frac{V}{(R_3 + R_4)}$$

Figure 4-19 MODEL FOR LEAKAGE CURRENT CALCULATIONS

module. Leakage currents for several module configurations, described in Table 4-9, are presented in Figure 4-20. The calculated values of leakage current are presented as a function of relative ambient humidity for a 1.2 by 2.4 m (4 by 8 ft) module operating at 1000 volts dc with respect to ground. For purposes of illustration, glass and plexi-glass were selected as representative front cover materials.

The results indicate a wide range in expected leakage current, depending on module construction. This is because the total leakage current is determined by the equivalent parallel resistance of the superstrate and substrate materials, as shown in Figure 4-19. If the superstrate and substrate resistances differ greatly, the magnitude of the leakage current is determined by the lower of the two values. In addition, if

TABLE 4–9

TYPICAL MODULE CONFIGURATIONS

CASE	COVER		ADHESIVE		ENCAPSULANT		SEALANT FILM		SUBSTRATE
NO.	TYPE	THICKNESS	TYPE	THICKNESS	TYPE	THICKNESS	TYPE	THICKNESS	TYPE
1	GLASS	63 MILS	–	–	SYLGARD	5 MILS	–	–	–
2	GLASS	125 MILS	–	–	SYLGARD	5 MILS	–	–	–
3	GLASS	125 MILS	SYLGARD	5 MIL		5 MILS	–	–	–
4	GLASS	125 MILS				5 MILS	MYLAR	5 MILS	–
5	PLEXI-GLASS	20 MILS				5 MILS	–	–	METAL
6	PLEXI-GLASS	100 MILS				5 MILS	–	–	METAL
7	PLEXI-GLASS	20 MILS				20 MILS	–	–	METAL
8	PLEXI-GLASS	20 MILS				5 MILS	MYLAR	1 MIL	METAL
9	PLEXI-GLASS	20 MILS				5 MILS	MYLAR	5 MILS	METAL

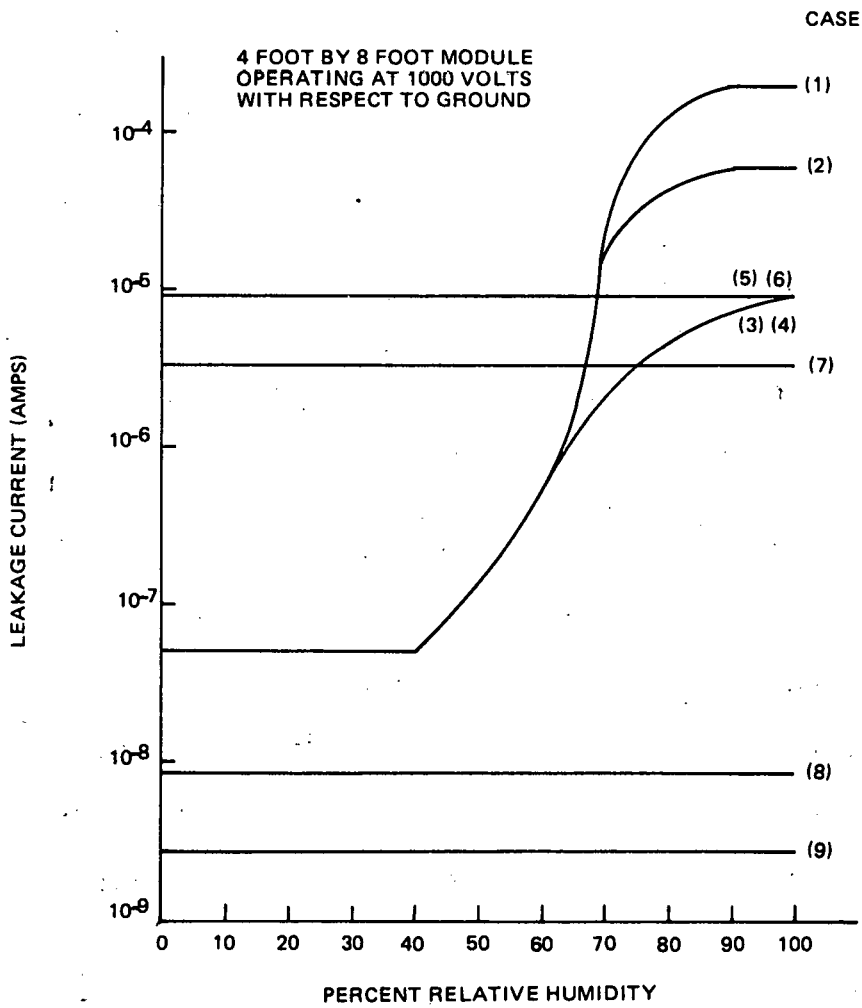

Figure 4-20 MODULE LEAKAGE CURRENT

either the superstrate or substrate is composed of two or more different materials electrically in series, its resistance is determined by the material with the highest resistivity.

For example, from Figure 4-20 it can be seen that for modules with glass covers, it is the glass superstrate leakage current that dominates, as indicated by the increase in current magnitude with increasing humidity (and hence decreasing glass surface resistance). Conversely, for metal substrates and plastic covers (substrate surface resistance equals zero) it is the substrate leakage current which dominates. This is clearly indicated by the reduction in leakage current that results with the inclusion of a thin layer of high resistivity (Mylar) material in the substrate.

Of course, it must be remembered that leakage current is also determined by module voltage to ground, so that, for an ungrounded dc system, the leakage current of any given module will be proportional to its electrical location in the array branch circuit. For a grounded dc system, leakage current will be proportional to the module's electrical location with respect to the ground point.

4.5 MODULE/PANEL COMPUTER ANALYSES

During this study, it was realized that lower cost panels might result from a reduction in the amount of frame material used. To

this end, three generic glass-superstrate module/panel concepts were evaluated by means of a nonlinear structural analysis. Since the analysis mostly concerns the behavior of a glass sheet (subject to boundary conditions imposed by the panel frame), a summary of the analyses is presented in this section on modules. Detailed information is presented in Appendix A.

Three basic module concepts are analyzed. Case I is a flat module supported continuously along its edges like a picture frame. Case II is also a flat module but is supported at four points by edge clips. Case III has the same supports as Case II but the glass module is curved into an arch between the support points. These three concepts are illustrated in Figure 4-21.

Classical, closed form analytical solutions exist for Case I, but not for Cases II and III. However, the true behaviors of all three cases involve large deflections and therefore require nonlinear analyses. Thus, finite element computer analyses were performed to predict the results of this behavior at 1.7 kPa (35 psf), 2.4 kPa (50 psf), and 3.6 kPa (75 psf) uniform loadings. Several computer codes to perform this type of analysis are commercially available, and ANSYS, a computer program developed and maintained by Swanson Analysis Systems, was selected for use in this study because of its nonlinear capability. Further details of this computer code are presented in Appendix A and in References 4-17 and 4-18.

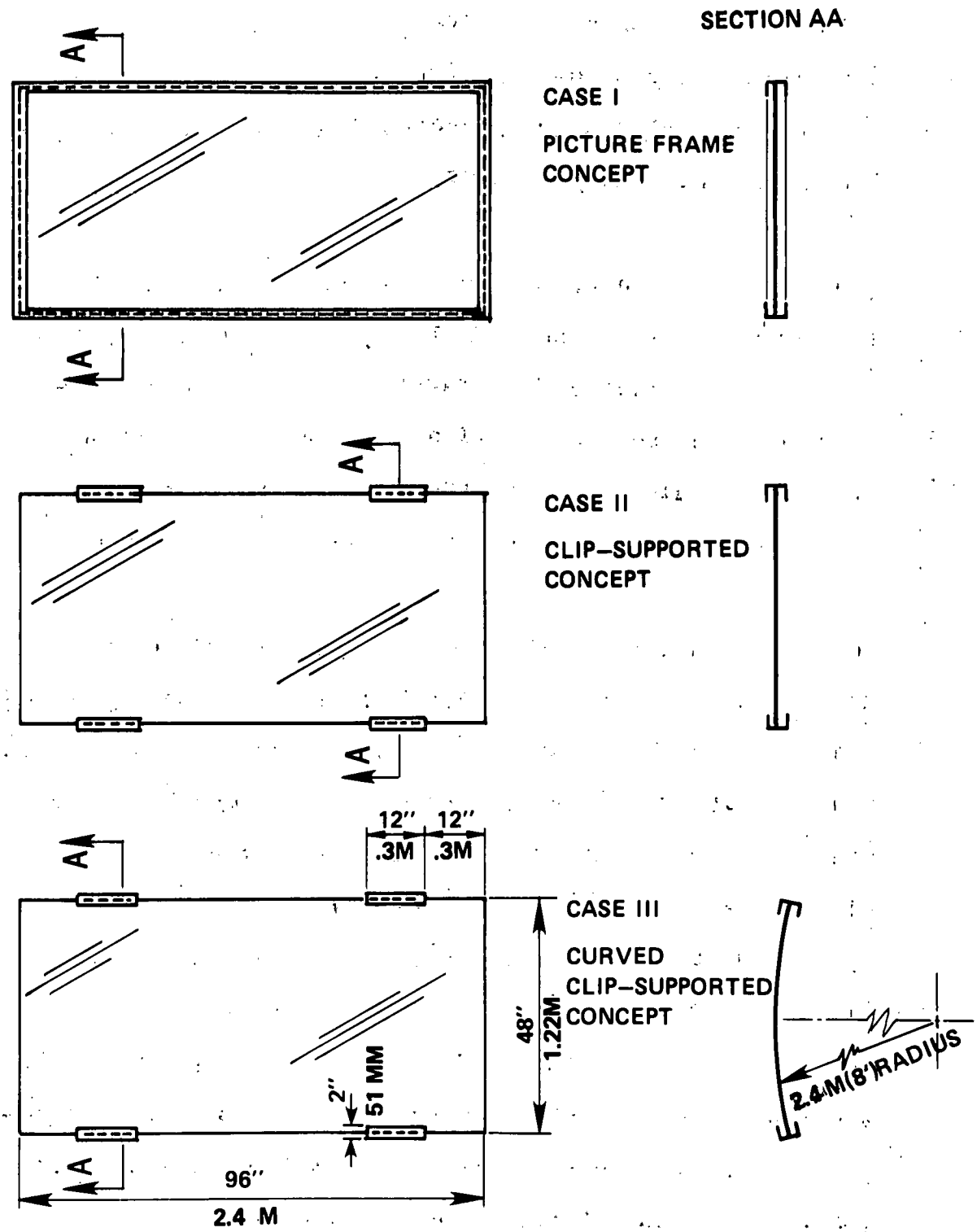

Figure 4-21 GLASS SUPERSTRATE MODULE CONCEPTS

4.5.1 Preliminary Calculations

Before initiating elaborate computer calculations, a series of manual calculations were made using several simplifying assumptions. For Case I, the calculations were based on work done by Levy (Ref. 4-19) and classical formulae, such as those tabulated in Roark (Ref. 4-20). For Case II, formulae for fixed end and simply supported beams (Ref. 4-20) were used. Timoshenko's work for cylindrical archs (Ref. 4-21) was used for Case III. In addition, approximate numerical solutions were obtained for Case III by using a programmable calculator.

For Case I, calculations based on Levy's work indicated that a thinner plate could be used than that predicted by classical linear theory. Therefore, it was concluded that a detailed computer analysis was warranted.

Results of the calculations for Case II indicated that unless significant membrane action developed at very low loads (e.g., below 0.96 kPa (20 psf)), this design would not be viable. The decision was made to compare the results of the nonlinear computer analyses at 0.48 kPa (10 psf) with a linear analysis at 0.48 kPa (10 psf) and see if further work was warranted.

Preliminary numerical calculations for Case III indicated that this concept was viable and that the glass plate should be as thin as possible in order to minimize bending stresses.

4.5.2 Case I - Picture Frame Concept

A literature search was conducted for work related to the effort described herein. Reference 4-22 provided experimental data against which the finite element analysis results could be compared. This was an important step before proceeding with nonlinear analyses. One of the authors (Mr. Stewart of PPG) provided additional experimental deflection data not reported in Reference 4-22. The size of the glass plate in PPG's experimental work was 1.2 by 2.4 m (4 by 8 ft), the same as the baseline module size evaluated herein. The experimental data were for 4.8 millimeter (0.187 inch) thick, annealed glass. This thickness and state of temper were selected for the computer analysis models to allow comparison with the experimental results. This provided a means to verify the analytical approach and computer model.

Figure 4-22 shows calculated and experimental stress levels as a function of load. As can be seen from the figure, there is very good correspondence between the classical theory and the computer linear analysis. More important, however, is the good agreement shown between the experimental data and the nonlinear computer analysis.

Figure 4-23 shows displacement of the center of the plate as a function of load. Again there is good agreement between these computer results and the experimental data.

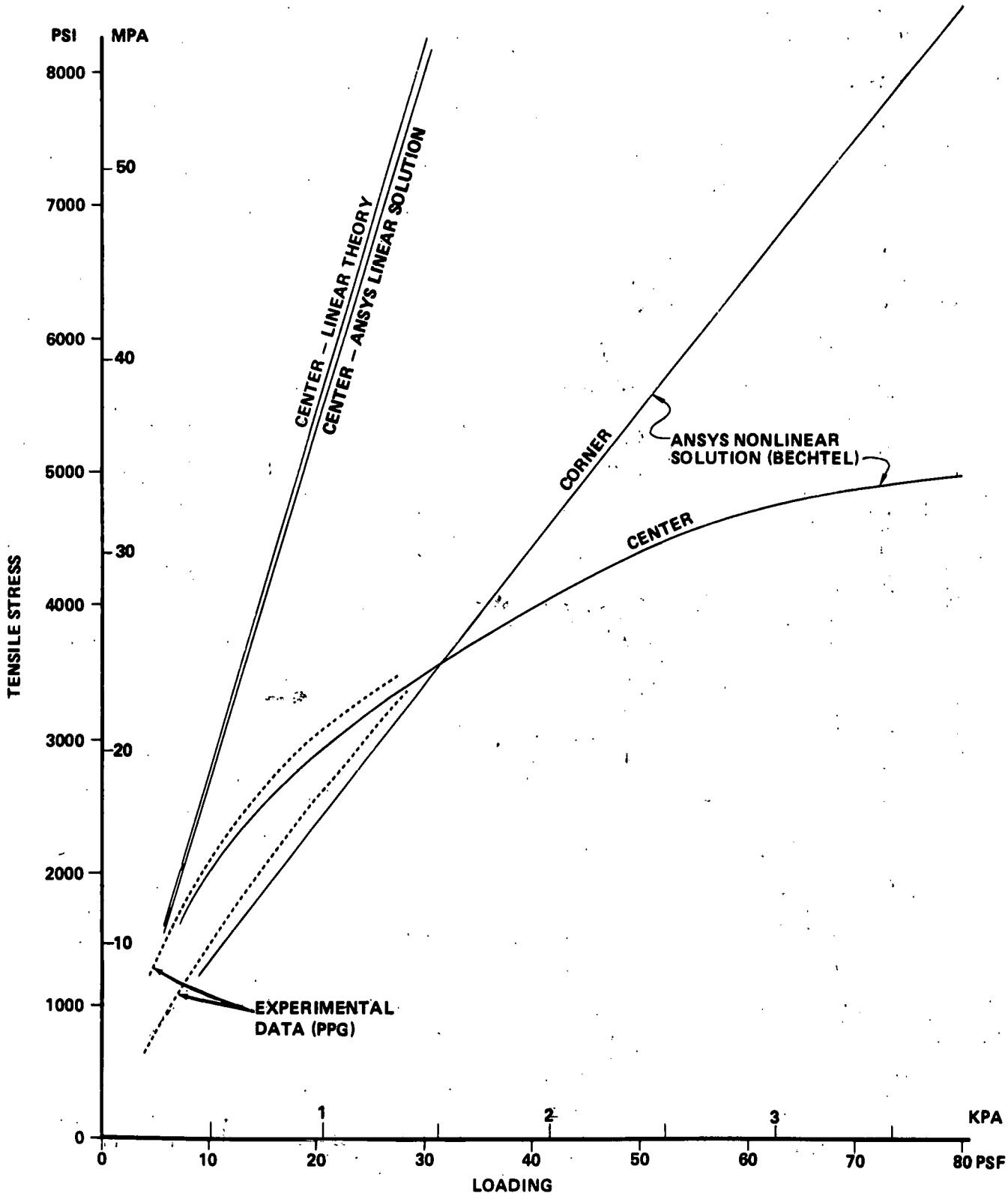

Figure 4-22 CASE I TENSILE STRESS VERSUS LOADING

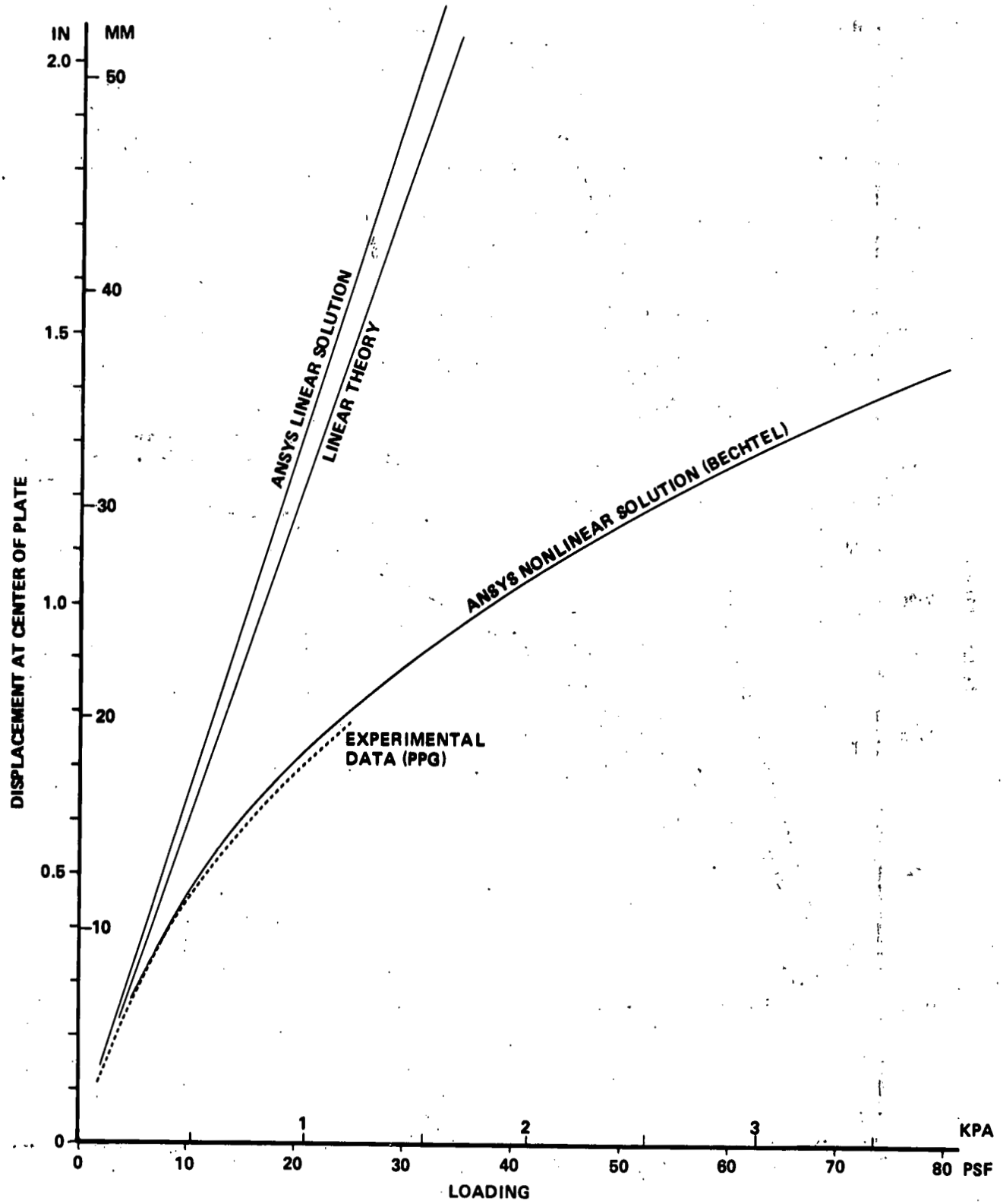

Figure 4-23 CASE I DISPLACEMENT VERSUS LOADING

The conclusions are that the computer model accurately represents actual behavior and that the Case I picture frame support concept using 4.8 millimeter (0.187 inch) annealed glass performs adequately under uniform loads up to 3.6 kPa (75 psf).

4.5.3 Case II - Clip-Supported Concept

The clip-supported module concept consists of a flat glass superstrate plate supported by clips at four points. As shown in Figure 4-21, the 1.2 by 2.4 m (4 by 8 ft) baseline case analyzed used 0.3 meter (12 inch) long clips located on the 2.4 meter (8 foot) edges and spaced 0.3 meter (12 inches) in from the 1.2 meter (4 foot) edges. Actual support clips would likely consists of metal channels with a resilient gasket material. This would allow the glass to deflect elastically in the vertical direction as well as translate elastically. Consequently the clips were represented by springs in the computer model.

The computer model for Case I was modified to represent the boundary conditions imposed by the four clips. As for Case I, 4.7 millimeter (0.187 inch) thick annealed glass was used in the model.

Based on the assumption that the plate acts as a beam between the clips, preliminary calculations were made using appropriate formulas from Reference 4-20. A linear analysis by the ANSYS program verified that the plate behaves in this same manner. A

nonlinear analysis was then performed for a 0.48 kPa (10 psf) uniform loading and compared to the results of the linear analysis. High stresses were present near the clips and at center of the plate. Extrapolation of data indicated that the flat-plate, clip-supported module design would not survive much higher loading. Therefore, it was decided to discontinue the analysis of this concept.

4.5.4 Case III - Clip-Supported Curved Plate Concept

As shown by Figure 4-21, the clip-supported curved plate module is similar to the Case II concept. However, for Case III the plate is a cylindrical section with the axis of the cylinder parallel to the long edge of the plate and a radius of curvature equal to twice the narrow dimension of the plate. The location of the clips is the same as for Case II.

Preliminary calculations based on formulae for cylindrical arches (Ref. 4-20) indicated that the curved plate module concept could use thinner glass than the picture frame concept. For consistency, however, the model was based on the 0.187 inch thick annealed glass used for the other analyses. The element mesh layout was modified in order to improve the behavior of the elements in the three dimensional model of the curved plate module.

After verifying the performance of the model, nonlinear computer analyses were run for uniform loadings of 0.48, 0.96, 1.7, 2.4 and 3.6 kPa (10, 20, 35, 50, and 75 psf). The resulting maximum tensile stress levels are plotted in Figure 4-24. As can be seen the stresses for the clip-supported curved plate are significantly lower than for the Case 1 picture-frame concept. Deflections for the Case III design are shown in Figure 4-25 and are significantly lower than for the picture-frame concept. However, for Case III, the maximum deflection occurs along the edge of the module.

The estimated cost of a panel based on the Case III module is presented in Section 5.6.

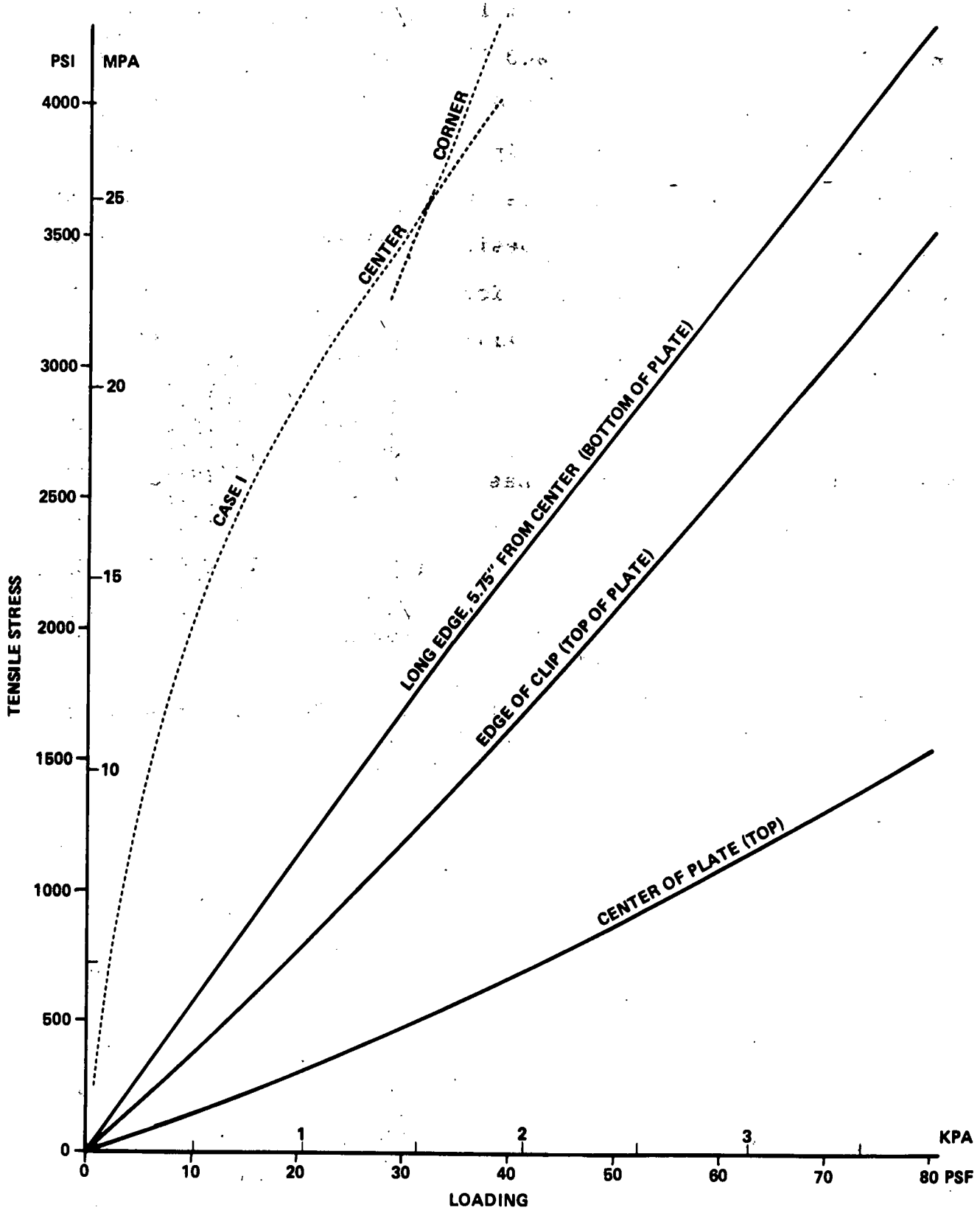

Figure 4-24 CASE III TENSILE STRESS VERSUS LOADING

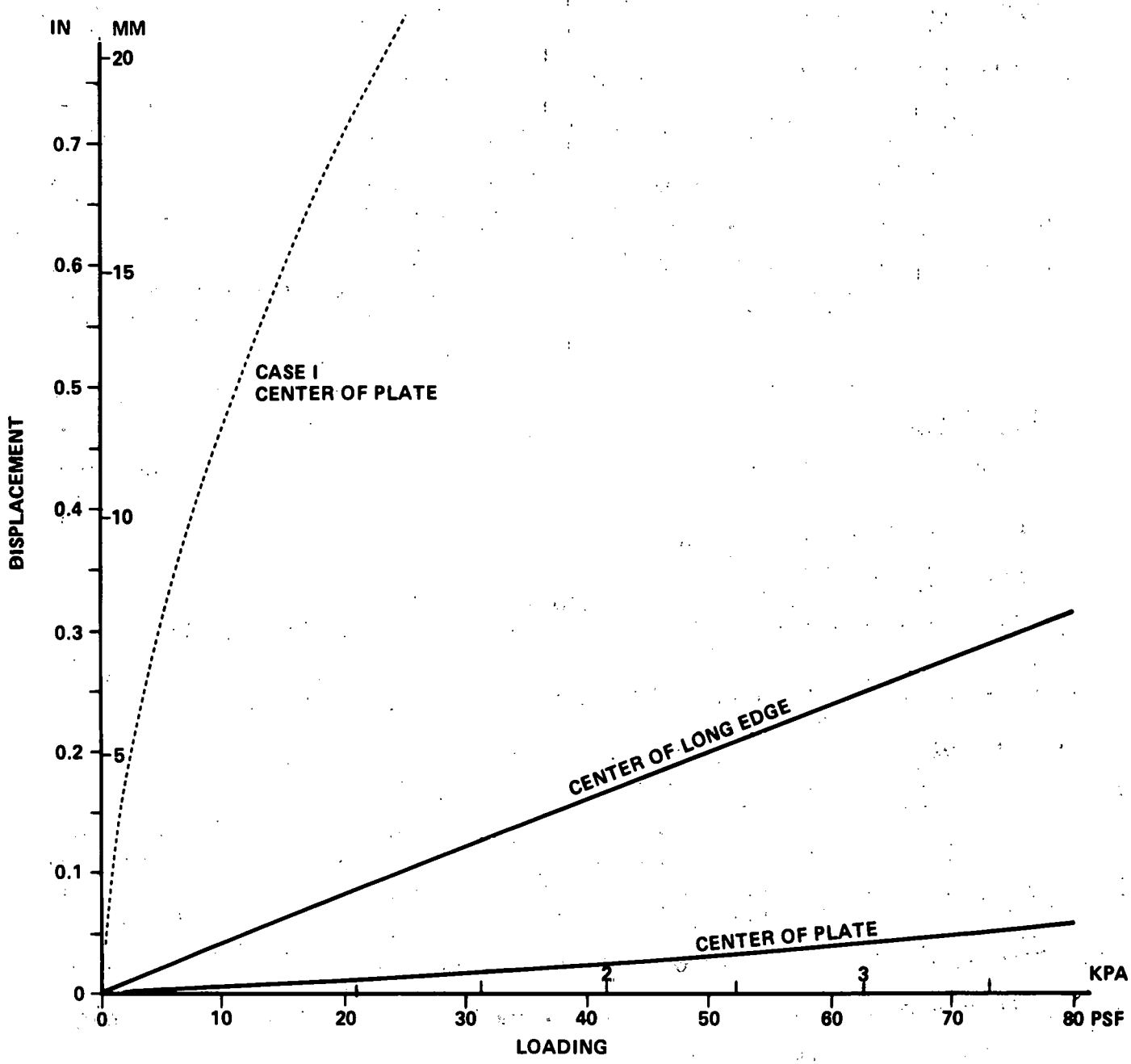

Figure 4-25 CASE III DISPLACEMENT VERSUS LOADING

Section 5

PANEL DESIGN

This section presents a discussion of panel design. The panels consist of the framework needed to support the modules discussed in Section 4 and are used with the nine array structure and foundation configurations described in Section 6 to form complete arrays. Consistent with the array configurations in Section 6, two panel sizes, 1.2 by 2.4 m (4 by 8 ft) and 2.4 by 4.8 m (8 by 16 ft), were designed. Three module sizes, 0.6 by 1.2 m (2 by 4 ft), 1.2 by 1.2 m (4 by 4 ft), and 1.2 by 2.4 m (4 by 8 ft), were used. In order to identify major cost drivers, designs were performed for uniform loadings of ±1.7 kPa (35 psf), ±2.4 kPa (50 psf), and ±3.6 kPa (75 psf). Nine array configurations, each consisting of foundations and primary support structure, were selected to determine major structural cost sensitivities of various structural support parameters such as slant height, foundation sharing, etc. With the variations in panel and array configurations, module and panel sizes, and loading, a total of 57 panels were designed and their costs estimated. An alpha-numeric numbering system was developed to assure that the proper panel type is associated with each of the array configurations described in Section 6.

5.1 DESIGN BASES

Bases and assumptions specific to the panel design efforts described herein are as follows:

- The panel material is lightweight steel sections in accordance with agreements with JPL.
- The steel has an allowable stress of 138 MPa (20,000 psi) and an elastic modulus of 2.02×10^5 MPa (29.3×10^6 psi).
- Deflections (d) are limited by $d \leq L/175 \leq 0.75''$, as specified by the American Metal Manufacturer's Association, where L is the length of the span. This is the normal specification for window frame design.
- The panels are designed to be simply supported with the upper end free to translate axially and to rotate.
- The panels are divided into two classes. Class 1 panels are designed to be end-supported. Class 2 panels are supported at that location where the moment at the upper support is equal to the moment between the supports and are referred to herein as intermediate supported panels.
- For estimating purposes, the steel members specified by the design vary from small angles to folded gage metal sections whose section modulii, areas, and weights are determined by usual engineering formulae and/or approximations.
- The method of fabrication specified for estimating purposes is flash butt welding with flush surface grinding of weld flash for surfaces that support modules.
- Corrosion protection is provided by hot dip galvanizing after panel fabrication.
- The applied loads are 1.7, 2.4, and 3.6 kPa (35, 50, and 75 psf) and are uniform. In accordance with agreements with JPL, loads are assumed to act in either of the directions normal to the module surfaces and are not differentiated into dead and live load fractions, relating to phenomenon which causes the loads.
- Panel ground connections are accomplished by a pair of quick-disconnect molded rubber connectors attached to

the panel steel by a short length of wire. The connectors are the same type as (but separate from) the module's power connectors and have the same ampere rating.

- Panel costs are estimated for the quantities needed for the 1.58 x 10^6 square meters of module surface area in a 200 MWp (nominal) central station power plant and normalized to terms of $/m².

- The estimated costs of installing the panels on the arrays is based on the results of two previous studies performed by Bechtel (Refs. 3-1 and 3-2).

- The estimated costs include materials, labor, shipping, and installation, but exclude distributables, engineering, and contingency costs. Thus, the costs presented are essentially direct field costs.

5.2 1.2 BY 2.4 METER (4 BY 8 FOOT) PANELS

Eight types of 1.2 by 2.4 m (4 by 8 ft) panels were evaluated. The labeling and configuration of these panels are shown in Figure 5-1. The class (end or intermediate supported) and associated array configuration case for each of the eight panels is presented in Table 5-1.

TABLE 5-1

PANEL TYPE, CLASS, AND ASSOCIATED ARRAY CONFIGURATION

Panel Class	End Supported			Intermediate Supported		
Array Configuration Case[1]	1,2,4,6			3		
Module Size (meters)	0.6x1.2	1.2x1.2	1.2x2.4	0.6x1.2	1.2x1.2	1.2x2.4
Module Size (feet)	2x4	4x4	4x8	2x4	4x4	4.8
Panel Type	A,E	Q	C	B,F	R	D

[1] See Section 6.2

END SUPPORTED PANELS

INTERMEDIATE SUPPORTED PANELS

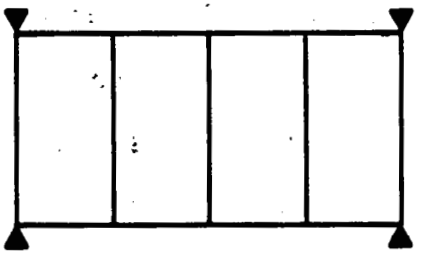

TYPE A PANEL (2'x4' MODULES)

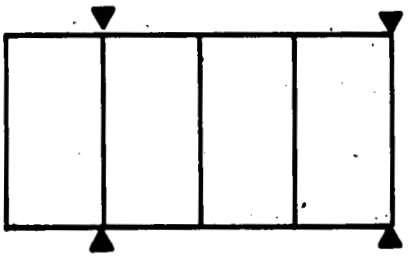

TYPE B PANEL (2'x4' MODULES)

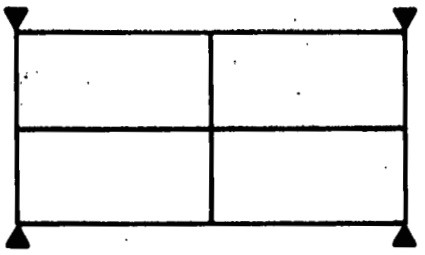

TYPE E PANEL (2'x4' MODULES)

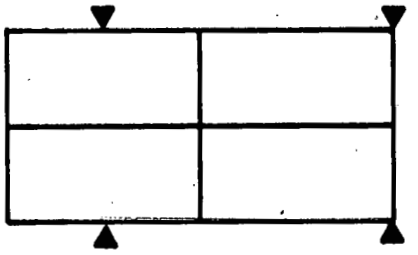

TYPE F PANEL (2'x4' MODULES)

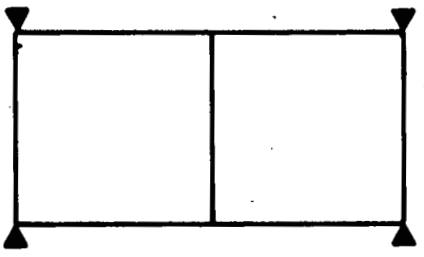

TYPE Q PANEL (4'x4' MODULES)

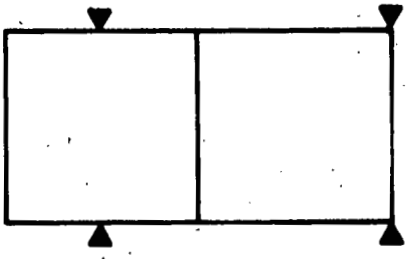

TYPE R PANEL (4'x4' MODULES)

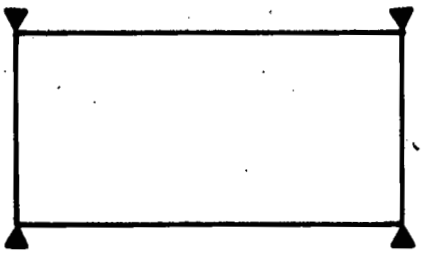

TYPE C PANEL (4'x8' MODULE)

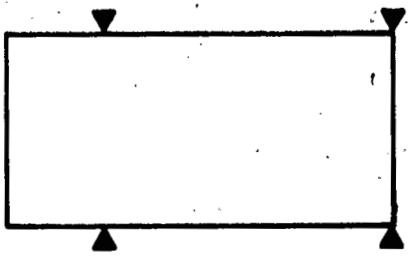

TYPE D PANEL (4'x8' MODULE)

NOTE
2'x4'=0.6x1.2M
4'x4'=1.2x1.2M
4'x8'=1.2x2.4M

▲ PANEL SUPPORT POINT

Figure 5-1 1.2 BY 2.4 METER (4 BY 8 FOOT) PANEL TYPES

The estimated costs of the eight 1.2 by 2.4 m (4 by 8 ft) panel types are presented in Tables 5-2 through 5-9 in terms of dollars per square meter (1975 $). The assembly labor cost consists of the cost to attach the module(s) to the steel frame (panel structure). The freight cost represents the cost ship assembled panel, including the module.

Intermediate supported panel types generally have lower costs than end supported panels. The lower costs are attributed to the smaller quantity of steel in those members which have intermediate supports.

Although the intermediate supported panel types have an apparent estimated cost advantage, they may also have disadvantages. One possible disadvantage is the rapid change in reverse bending of the panel side members that occurs at the panel upper supports. The reverse bending deviates from the simply supported assumptions used for sizing the module glass thicknesses (see Sections 4.1.1 and 4.5, and Appendix A) and could, conceivably, result in thicker glass for the modules. This is particularly true for type B panels, where the upper panel support point is close to the module corner location, the same location where reverse bending of the module would occur even if no beam bending occurred, as is assumed in selecting module thickness (see Figure 5-1 and Figure A-6 in Appendix A). For Type B panels, especially, it may be desirable to locate the support point at the location where an intermediate panel member attaches to the

TABLE 5-2

TYPE A PANEL COST ESTIMATE (1975 $/m²)
[end supported, 1.2m x 2.4m (4'x8') panel,
0.6m x 1.2m (2'x4') modules]

Item	Loading			
	1.7	2.4	3.6	kPa
	35	50	75	psf
Steel Frame				
Material	9.90	12.10	16.50	
Galvanizing	1.60	2.10	3.20	
Fabrication Labor	4.70	6.30	9.50	
Gasket	1.40	1.40	1.40	
Ground Connectors	1.20	1.20	1.20	
Assembly Labor	4.30	4.80	5.70	
Freight	0.80	0.90	1.20	
Installation, Direct Labor	2.00	2.00	2.00	
PANEL SUBTOTAL	25.90	30.80	40.70	
Modules	59.80	59.80	59.80	
PANEL TOTAL	85.70	90.60	100.50	

TABLE 5-3

TYPE B PANEL COST ESTIMATE (1975 $/m²)
[intermediate supported, 1.2m x 2.4m (4'x8') panel,
0.6m x 1.2m (2'x4') modules]

Item	Loading			
	1.7	2.4	3.6	kPa
	35	50	75	psf
Steel Frame				
Material	7.60	9.90	13.20	
Galvanizing	1.10	1.60	2.40	
Fabrication Labor	3.20	4.70	7.10	
Gasket	1.40	1.40	1.40	
Ground Connectors	1.20	1.20	1.20	
Assembly Labor	3.90	4.30	5.00	
Freight	0.70	0.80	1.00	
Installation, Direct Labor	2.00	2.00	2.00	
PANEL SUBTOTAL	21.10	25.90	33.30	
Modules	59.80	59.80	59.80	
PANEL TOTAL	80.90	85.70	93.10	

TABLE 5-4

TYPE C PANEL COST ESTIMATE (1975 $/m²)
[end supported, 1.2m x 2.4m (4'x8') panel,
1.2m x 2.4m (4'x8') module]

Item	Loading			
	1.7	2.4	3.6	kPa
	35	50	75	psf
Steel Frame				
Material	6.60	8.20	10.40	
Galvanizing	1.10	1.50	2.00	
Fabrication Labor	2.50	3.40	4.60	
Gasket	0.70	0.70	0.70	
Ground Connectors	1.20	1.20	1.20	
Assembly Labor	3.30	3.60	4.50	
Freight	0.60	0.70	0.90	
Installation, Direct Labor	2.00	2.00	2.00	
PANEL SUBTOTAL	18.00	21.30	26.30	
Module	60.30	60.30	60.60	
PANEL TOTAL	78.30	81.60	86.90	

TABLE 5-5

TYPE D PANEL COST ESTIMATE (1975 $/m²)
[intermediate supported, 1.2m x 2.4m (4'x8') panel,
1.2m x 2.4m (4'x8') module]

Item	Loading			
	1.7	2.4	3.6	kPa
	35	50	75	psf
Steel Frame				
Material	5.40	6.00	7.10	
Galvanizing	0.80	0.90	1.20	
Fabrication Labor	1.80	2.10	2.80	
Gasket	0.70	0.70	0.70	
Ground Connectors	1.20	1.20	1.20	
Assembly Labor	3.00	3.20	3.40	
Freight	0.50	0.60	0.70	
Installation, Direct Labor	2.00	2.00	2.00	
PANEL SUBTOTAL	15.40	16.70	19.10	
Module	60.30	60.30	60.60	
PANEL TOTAL	75.70	77.00	79.70	

TABLE 5-6

TYPE E PANEL COST ESTIMATE (1975 $/m²)
[end supported, 1.2m x 2.4m (4'x8') panel,
0.6m x 1.2m (2'x4') modules]

Item	Loading			
	1.7	2.4	3.6	kPa
	35	50	75	psf
Steel Frame				
Material	9.20	12.00	16.40	
Galvanizing	1.50	2.10	3.20	
Fabrication Labor	4.30	6.30	9.50	
Gasket	1.40	1.40	1.40	
Ground Connectors	1.20	1.20	1.20	
Assembly Labor	4.20	4.80	5.70	
Freight	0.70	0.90	1.20	
Installation, Direct Labor	2.00	2.00	2.00	
PANEL SUBTOTAL	24.50	30.70	40.60	
Modules	59.80	59.80	59.80	
PANEL TOTAL	84.30	90.50	100.40	

TABLE 5-7

TYPE F PANEL COST ESTIMATE (1975 $/m²)
[intermediate supported, 1.2m x 2.4m (4'x8') panel,
0.6m x 1.2m (2'x4') modules]

Item	Loading			
	1.7	2.4	3.6	kPa
	35	50	75	psf
Steel Frame				
Material	7.60	9.80	13.00	
Galvanizing	1.00	1.60	2.40	
Fabrication Labor	3.20	4.70	7.10	
Gasket	1.40	1.40	1.40	
Ground Connectors	1.20	1.20	1.20	
Assembly Labor	3.90	4.30	5.00	
Freight	0.60	0.80	1.00	
Installation, Direct Labor	2.00	2.00	2.00	
PANEL SUBTOTAL	20.90	25.80	33.10	
Modules	59.80	59.80	59.80	
PANEL TOTAL	80.70	85.60	92.90	

TABLE 5-8

TYPE Q PANEL COST ESTIMATE (1975 $/m²)
[end supported, 1.2m x 2.4m (4'x8') panel,
1.2m x 1.2m (4'x4') modules]

Item	Loading			
	1.7	2.4	3.6	kPa
	35	50	75	psf
Steel Frame				
Material	8.00	9.60	13.50	
Galvanizing	1.30	1.70	2.60	
Fabrication Labor	3.50	4.50	7.00	
Gasket	0.90	0.90	0.90	
Ground Connectors	1.20	1.20	1.20	
Assembly Labor	3.70	4.00	4.80	
Freight	0.70	0.80	1.00	
Installation, Direct Labor	2.00	2.00	2.00	
PANEL SUBTOTAL	21.30	24.70	33.00	
Modules	60.30	60.30	60.30	
PANEL TOTAL	81.60	85.00	93.30	

TABLE 5-9

TYPE R PANEL COST ESTIMATE (1975 $/m²)
[intermediate supported, 1.2m x 2.4m (4'x8') panel,
1.2m x 1.2m (4'x4') modules]

Item	Loading			
	1.7	2.4	3.6	kPa
	35	50	75	psf
Steel Frame				
Material	6.30	8.00	10.20	
Galvanizing	0.90	1.30	1.80	
Fabrication Labor	2.80	3.90	5.50	
Gasket	0.90	0.90	0.90	
Ground Connectors	1.20	1.20	1.20	
Assembly Labor	3.30	3.70	4.20	
Freight	0.60	0.70	0.80	
Installation, Direct Labor	2.00	2.00	2.00	
PANEL SUBTOTAL	18.00	21.70	26.60	
Modules	60.30	60.30	60.30	
PANEL TOTAL	78.30	82.00	86.90	

side member (the 25 percent point) rather than at the theoretically ideal (i.e., equal moment) location used throughout the course of this study.

Another potential disadvantage for intermediate supported panels results from a moving support point at the upper support location. When the load is applied, the array support structure and panel will deflect, resulting in a change in support location that varies with the applied load intensity. The change in support location results in a change in moment that is about 10 to 15 percent of that calculated for sizing the member. Of greater potential effect is the moving reverse bending "wave" that will occur in the module glass as the location of the panel point shifts, resulting in strain patterns different from those calculated by methods used in Appendix A.

The effect of preventing sliding of the panels at the upper support point was briefly considered. It was found that if sliding is prevented, then both the panel and module are subjected to both axial and bending forces. This results in a general increase in panel steel requirements and, (depending on the method of glass support) possibly module glass thickness.

The Type D panel has the lowest estimated costs for two reasons. One reason is that the module and panel are the same size and intermediate support members are not needed. Thus, the number of joints and linear feet of glass edge fastening is the smallest

possible for a 1.2 by 2.4 m (4 by 8 ft) panel. The second reason is that it is an intermediate supported panel, and the panel edge members are among the lightest possible for a 1.2 by 2.4 m (4 by 8 ft) panel. The disadvantages of intermediate supported panels were discussed in previous paragraphs. Changes in required glass thickness resulting from violation of the assumptions (e.g., simple support) discussed in Section 4.1.1 were not calculated in this study.

When compared with respect to magnitude of applied loads (1.7, 2.4, and 3.6 kPa (35, 50, and 75 psf)), there is an increase in cost with increase in load for all panel types, classes, and module sizes. There is as much as a 38 percent increase in panel cost in going from a 1.7 kPa (35 psf) to a 2.4 kPa (50 psf) load.

Further comparisons of panel types are made in Section 5.5.

5.3 2.4 BY 4.8 METER (8 BY 16 FOOT) PANELS

Ten types of 2.4 by 4.8 m (8 by 16 ft) panels were evaluated. The labeling and configuration of these panels are shown in Figure 5-2. The class (end or moment supported) and associated array configuration case for each of the ten panel types is presented in Table 5-10.

END SUPPORTED PANELS

INTERMEDIATE SUPPORTED PANELS

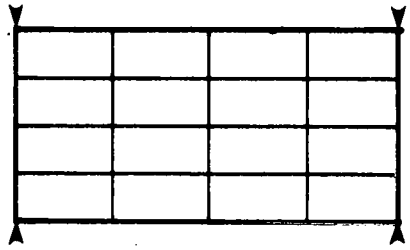

TYPE M PANEL (2'x4' MODULES)

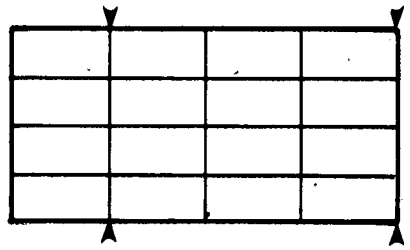

TYPE N PANEL (2'x4' MODULES)

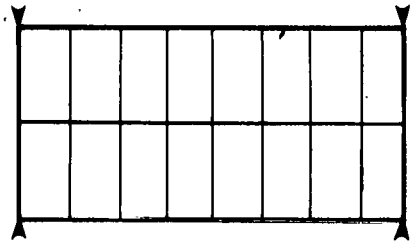

TYPE K PANEL (2'x4' MODULES)

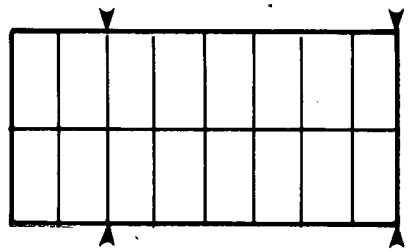

TYPE L PANEL (2'x4' MODULES)

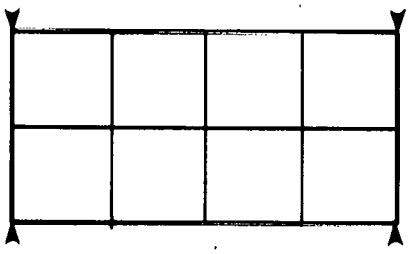

TYPE O PANEL (4'x4' MODULES)

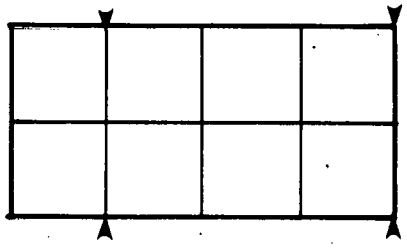

TYPE P PANEL (4'x4' MODULES)

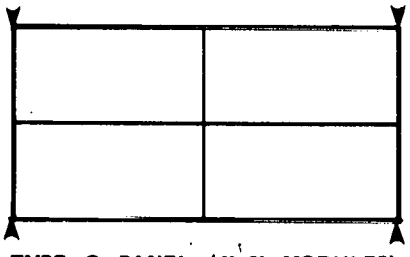

TYPE G PANEL (4'x8' MODULES)

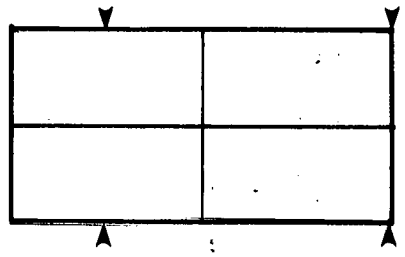

TYPE H PANEL (4'x8' MODULES)

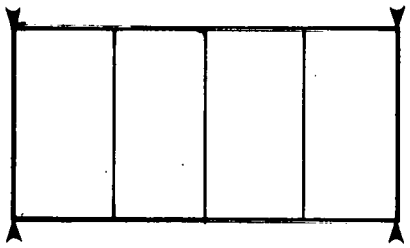

TYPE I PANEL (4'x8' MODULES)

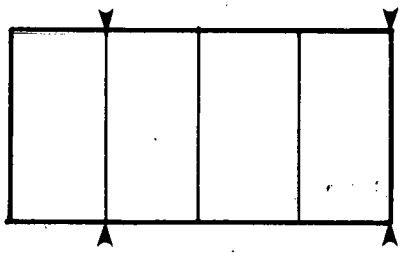

TYPE J PANEL (4'x8' MODULES)

NOTE
2'x4'=0.6x1.2M
4'x4'=1.2x1.2M
4'x8'=1.2x2.4M

▲ PANEL SUPPORT POINT

Figure 5-2 2.4 BY 4.8 METER (8 BY 16 FOOT) PANEL TYPES

TABLE 5-10

PANEL TYPE, CLASS, AND ASSOCIATED ARRAY CONFIGURATION

Panel Class	End Supported			Intermediate Supported		
Array Configuration Case[1]	5			7,8,9		
Module Size (meters)	0.6x1.2	1.2x1.2	1.2x2.4	0.6x1.2	1.2x1.2	1.2x2.
Module Size (feet)	2x4	4x4	4x8	2x4	4x4	4.8
Panel Type	K,M	O	G,I	L,N	P	H,J

[1] See Section 6.2

The estimated costs of the ten 2.4 by 4.8 m (8 by 16 ft) panel types are presented in Tables 5-11 through 5-20 in terms of dollars per square meter (1975 $).

Comparing the estimated costs for the 2.4 by 4.8 m (8 by 16 ft) panels shows that the pattern established for the smaller (1.2 by 2.4 m (4 by 8 ft)) panels is repeated for the large panel size. Applied load is a strong cost driver. Its effect is significant and relatively uniform for all of the panel types. A second cost driver is module size, with panel cost increasing for decreasing module size. Although a third cost driver could be considered to be the location of the upper support point on the panel (and it would be considered a cost driver if the study were restricted to 1.2 by 2.4 m (4 by 8 ft) modules), the effect of the estimated costs of added supports for the smaller modules reduces the relative effect of the panel support location. Thus, the panel support location effect is not considered a dominant cost driver.

TABLE 5-11

TYPE G PANEL COST ESTIMATE (1975 $/m²)
[end supported, 2.4m x 4.8m (8'x16') panel,
1.2m x 2.4m (4'x8') modules]

Item	Loading			
	1.7	2.4	3.6	kPa
	35	50	75	psf
Steel Frame				
Material	8.20	11.30	16.00	
Galvanizing	1.60	2.30	3.40	
Fabrication Labor	4.70	6.90	10.30	
Gasket	0.70	0.70	0.70	
Ground Connectors	0.30	0.30	0.30	
Assembly Labor	4.00	4.80	5.80	
Freight	0.80	0.90	1.20	
Installation, Direct Labor	1.10	1.10	1.10	
PANEL SUBTOTAL	21.40	28.30	38.80	
Modules	60.30	60.30	60.60	
PANEL TOTAL	81.70	88.60	99.40	

TABLE 5-12

TYPE H PANEL COST ESTIMATE (1975 $/m²)
[intermediate supported, 2.4m x 4.8m (8'x16') panel,
1.2m x 2.4m (4'x8') modules]

Item	Loading			
	1.7	2.4	3.6	kPa
	35	50	75	psf
Steel Frame				
Material	6.30	8.40	11.60	
Galvanizing	1.10	1.60	2.40	
Fabrication Labor	3.40	4.90	7.10	
Gasket	0.70	0.70	0.70	
Ground Connectors	0.30	0.30	0.30	
Assembly Labor	3.60	4.10	4.80	
Freight	0.70	0.80	0.90	
Installation, Direct Labor	1.10	1.10	1.10	
PANEL SUBTOTAL	17.20	21.90	28.90	
Modules	60.30	60.30	60.60	
PANEL TOTAL	77.50	82.20	89.50	

TABLE 5-13

TYPE I PANEL COST ESTIMATE (1975 $/m²)
[end supported, 2.4m x 4.8m (8'x16') panel,
1.2m x 2.4m (4'x8') modules]

Item	Loading			
	1.7	2.4	3.6	kPa
	35	50	75	psf
Steel Frame				
Material	8.00	10.00	15.00	
Galvanizing	1.50	2.10	3.20	
Fabrication Labor	4.50	6.30	9.50	
Gasket	0.70	0.70	0.70	
Ground Connectors	0.30	0.30	0.30	
Assembly Labor	4.00	5.00	6.00	
Freight	0.80	0.90	1.20	
Installation, Direct Labor	1.10	1.10	1.10	
PANEL SUBTOTAL	20.90	26.40	37.00	
Modules	60.30	60.30	60.60	
PANEL TOTAL	81.20	86.70	97.60	

TABLE 5-14

TYPE J PANEL COST ESTIMATE (1975 $/m²)
[intermediate supported, 2.4m x 4.8m (8'x16') panel,
1.2m x 2.4m (4'x8') modules]

Item	Loading			
	1.7	2.4	3.6	kPa
	35	50	75	psf
Steel Frame				
Material	5.00	8.00	10.00	
Galvanizing	1.00	1.50	2.10	
Fabrication Labor	3.00	4.00	6.00	
Gasket	0.70	0.70	0.70	
Ground Connectors	0.30	0.30	0.30	
Assembly Labor	3.00	4.00	5.00	
Freight	0.60	0.70	0.90	
Installation, Direct Labor	1.10	1.10	1.10	
PANEL SUBTOTAL	14.70	20.30	26.10	
Modules	60.30	60.30	60.60	
PANEL TOTAL	75.00	80.60	86.70	

TABLE 5-15

TYPE K PANEL COST ESTIMATE (1975 $/m²)
[end supported, 2.4m x 4.8m (8'x16') panel,
0.6m x 1.2m (2'x4') modules]

Item	Loading			
	1.7	2.4	3.6	kPa
	35	50	75	psf
Steel Frame				
Material	11.20	14.30	19.00	
Galvanizing	2.00	2.80	3.90	
Fabrication Labor	6.90	9.40	13.20	
Gasket	1.40	1.40	1.40	
Ground Connectors	0.30	0.30	0.30	
Assembly Labor	5.40	6.20	7.20	
Freight	0.90	1.10	1.40	
Installation, Direct Labor	1.10	1.10	1.10	
PANEL SUBTOTAL	29.20	36.60	47.50	
Modules	59.80	59.80	59.80	
PANEL TOTAL	89.00	96.40	107.30	

TABLE 5-16

TYPE L PANEL COST ESTIMATE (1975 $/m²)
[intermediate supported, 2.4m x 4.8m (8'x16') panel,
0.6m x 1.2m (2'x4') modules]

Item	Loading			
	1.7	2.4	3.6	kPa
	35	50	75	psf
Steel Frame				
Material	9.30	11.50	14.80	
Galvanizing	1.60	2.10	2.90	
Fabrication Labor	5.30	7.10	9.80	
Gasket	1.40	1.40	1.40	
Ground Connectors	0.30	0.30	0.30	
Assembly Labor	5.00	5.50	6.20	
Freight	0.80	0.90	1.10	
Installation, Direct Labor	1.10	1.10	1.10	
PANEL SUBTOTAL	24.80	29.90	37.60	
Modules	59.80	59.80	59.80	
PANEL TOTAL	84.60	89.70	97.40	

TABLE 5-17

TYPE M PANEL COST ESTIMATE (1975 $/m²)
[end supported, 2.4m x 4.8m (8'x16') panel,
0.6m x 1.2m (2'x4') modules]

Item	Loading			
	1.7	2.4	3.6	kPa
	35	50	75	psf
Steel Frame				
Material	11.00	13.70	17.90	
Galvanizing	2.00	2.60	3.60	
Fabrication Labor	6.70	8.90	12.30	
Gasket	1.40	1.40	1.40	
Ground Connectors	0.30	0.30	0.30	
Assembly Labor	5.40	6.00	7.00	
Freight	0.90	1.00	1.30	
Installation, Direct Labor	1.10	1.10	1.10	
PANEL SUBTOTAL	28.80	35.00	44.90	
Modules	59.80	59.80	59.80	
PANEL TOTAL	88.60	94.80	104.70	

TABLE 5-18

TYPE N PANEL COST ESTIMATE (1975 $/m²)
[intermediate supported, 2.4m x 4.8m (8'x16') panel,
0.6m x 1.2m (2'x4') modules]

Item	Loading			
	1.7	2.4	3.6	kPa
	35	50	75	psf
Steel Frame				
Material	9.00	10.70	13.70	
Galvanizing	1.50	1.90	2.60	
Fabrication Labor	5.00	6.50	8.90	
Gasket	1.40	1.40	1.40	
Ground Connectors	0.30	0.30	0.30	
Assembly Labor	5.00	5.30	6.00	
Freight	0.70	0.80	1.00	
Installation, Direct Labor	1.10	1.10	1.10	
PANEL SUBTOTAL	24.00	28.00	35.00	
Modules	59.80	59.80	59.80	
PANEL TOTAL	83.80	87.80	94.80	

TABLE 5-19

TYPE O PANEL COST ESTIMATE (1975 $/m²)
[end supported, 2.4m x 4.8m (8'x16') panel,
1.2m x 1.2m (4'x4') modules]

Item	Loading			
	1.7	2.4	3.6	kPa
	35	50	75	psf
Steel Frame				
Material	8.80	12.10	16.50	
Galvanizing	1.70	2.50	3.50	
Fabrication Labor	5.40	8.50	11.90	
Gasket	0.90	0.90	0.90	
Ground Connectors	0.30	0.30	0.30	
Assembly Labor	4.20	5.00	5.90	
Freight	0.80	1.00	1.10	
Installation, Direct Labor	1.10	1.10	1.10	
PANEL SUBTOTAL	23.20	31.40	41.20	
Modules	60.30	60.30	60.30	
PANEL TOTAL	83.50	91.70	101.50	

TABLE 5-20

TYPE P PANEL COST ESTIMATE (1975 $/m²)
[intermediate supported, 2.4m x 4.8m (8'x16') panel,
1.2m x 1.2m (4'x4') modules]

Item	Loading			
	1.7	2.4	3.6	kPa
	35	50	75	psf
Steel Frame				
Material	6.80	9.20	12.40	
Galvanizing	1.30	1.80	2.60	
Fabrication Labor	4.00	5.60	8.10	
Gasket	0.90	0.90	0.90	
Ground Connectors	0.30	0.30	0.30	
Assembly Labor	3.80	4.20	5.00	
Freight	0.70	0.80	1.00	
Installation, Direct Labor	1.10	1.10	1.10	
PANEL SUBTOTAL	18.90	23.90	31.40	
Modules	60.30	60.30	60.30	
PANEL TOTAL	79.20	84.20	91.70	

Concerns about the potential disadvantages of intermediate supported panels are the same as described in Section 5.2 for the 1.2 by 2.4 m (4 by 8 ft) panels. In particular, the choice of the panel support location should not ignore the effect of that location on the module glass. As has been previously stated, the function of the panel is to create module support conditions such that the module, as well as the panel, can survive the applied load conditions.

5.4 CASE 9 PANEL

Section 6.2.9 describes an array configuration (Case 9) in which there is no field-erected array structure per se. With this configuration, all of the array structure is included in the 2.4 by 4.8 m (8 by 16 ft) panel frame. This panel is similar to Type I but with a hinged back support strut added (at the factory) so that the panel and strut form an A-frame when erected in the field. The configuration of this array concept is shown in Figure 6-17, along with further details, in Section 6.2.9.

The estimated cost of this panel and, by virtue of its unique design, its integral array structure is presented in Table 5-21.

TABLE 5-21

CASE 9 PANEL/ARRAY STRUCTURE COST ESTIMATE (1975 $/m²)
(2.4m x 4.8m (8'x16') panel, 1.2m x 2.4m (4'x8') modules)

Item	Loading		
	1.7	2.4	3.6 kPa
	35	50	75 psf
Steel Frame			
Material	12.50	15.50	20.50
Galvanizing	2.20	2.90	4.10
Fabrication Labor	5.00	7.10	10.60
Gasket	0.70	0.70	0.70
Ground Connectors	0.30	0.30	0.30
Assembly Labor	4.30	5.50	6.70
Freight	0.90	1.10	1.40
Direct Installation Labor	1.00	1.00	1.00
PANEL SUBTOTAL	26.90	34.10	45.30
Modules	60.30	60.30	60.60
PANEL TOTAL	87.20	94.40	105.90

5.5 PANEL COMPARISONS

The estimated costs of the 57 panels are summarized in Table 5-22. To facilitate comparisons of panel design, only panel subtotal costs are presented. Adding the module costs would uniformly increase all of the costs by approximately $60/m² (i.e., $59.80 to $60.60/m²).

Inspection of the cost data in Table 5-22 leads to the following conclusions:

- Small module sizes lead to high panel costs.
- End supported panels are more costly than intermediate supported panels.
- Panel costs increase significantly with increases in loading (e.g., the panel cost, without the module,

increases 26 percent in going from a 1.7 kPa (35 psf) to a 2.4 kPa (50 psf) load.

TABLE 5-22

PANEL STRUCTURAL COST SUMMARY (1975 $/m²)

Panel Size (meters)	Module Size (meters)	End Supported Panel Type	Loading (kPa) 1.7	2.4	3.6	Intermediate Supported Panel Type	Loading (kPa) 1.7	2.4	3.6
1.2x2.4	0.6x1.2	A	25.90	30.80	40.70	B	21.10	25.90	33.30
1.2.2.4	0.6x1.2	E	24.50	30.70	40.60	F	20.90	25.80	33.10
1.2x2.4	1.2x1.2	Q	21.30	24.70	33.00	R	18.00	21.70	26.60
1.2x2.4	1.2x2.4	C	18.00	21.30	26.30	D	15.40	16.70	19.10
2.4x4.8	0.6x1.2	K	29.20	36.60	47.50	L	24.80	29.90	37.60
2.4x4.8	0.6x1.2	M	28.80	35.00	44.90	N	24.00	28.00	35.00
2.4x4.8	1.2x1.2	O	23.20	31.40	41.20	P	18.90	23.90	31.40
2.4x4.8	1.2x2.4	G	21.40	28.30	38.80	H	17.20	21.90	28.90
2.4x4.8	1.2x2.4	I	20.90	26.40	37.50	J	14.70	20.30	26.10
2.4x4.8	1.2x2.4	Case 9	26.90	34.10	45.30				

Panel Size (feet)	Module Size (feet)	End Supported Panel Type	Loading (psf) 35	50	75	Intermediate Supported Panel Type	Loading (psf) 35	50	75
4x8	2x4	A	25.90	30.80	40.70	B	21.10	25.90	33.30
4x8	2x4	E	24.50	30.70	40.60	F	20.90	25.80	33.10
4x8	4x4	Q	21.30	24.70	33.00	R	18.00	21.70	26.60
4x8	4x8	C	18.00	21.30	26.30	D	15.40	16.70	19.10
8x16	2x4	K	29.20	36.60	47.50	L	24.80	29.90	37.60
8x16	2x4	M	28.80	35.00	44.90	N	24.00	28.00	35.00
8x16	4x4	O	23.20	31.40	41.20	P	18.90	23.90	31.40
8x16	4x8	G	21.40	28.30	38.80	H	17.20	21.90	28.90
8x16	4x8	I	20.90	26.40	37.40	J	14.70	20.30	26.10
8x16	4x8	Case 9	26.90	34.10	45.30				

The effect of module size on panel costs is shown by Figure 5-3. In cases where there are two configurations for a panel and module size, the lowest cost is plotted (e.g., types G and I). For all of the panel designs, there is a decrease in panel cost with increasing module size for the size ranges evaluated. The

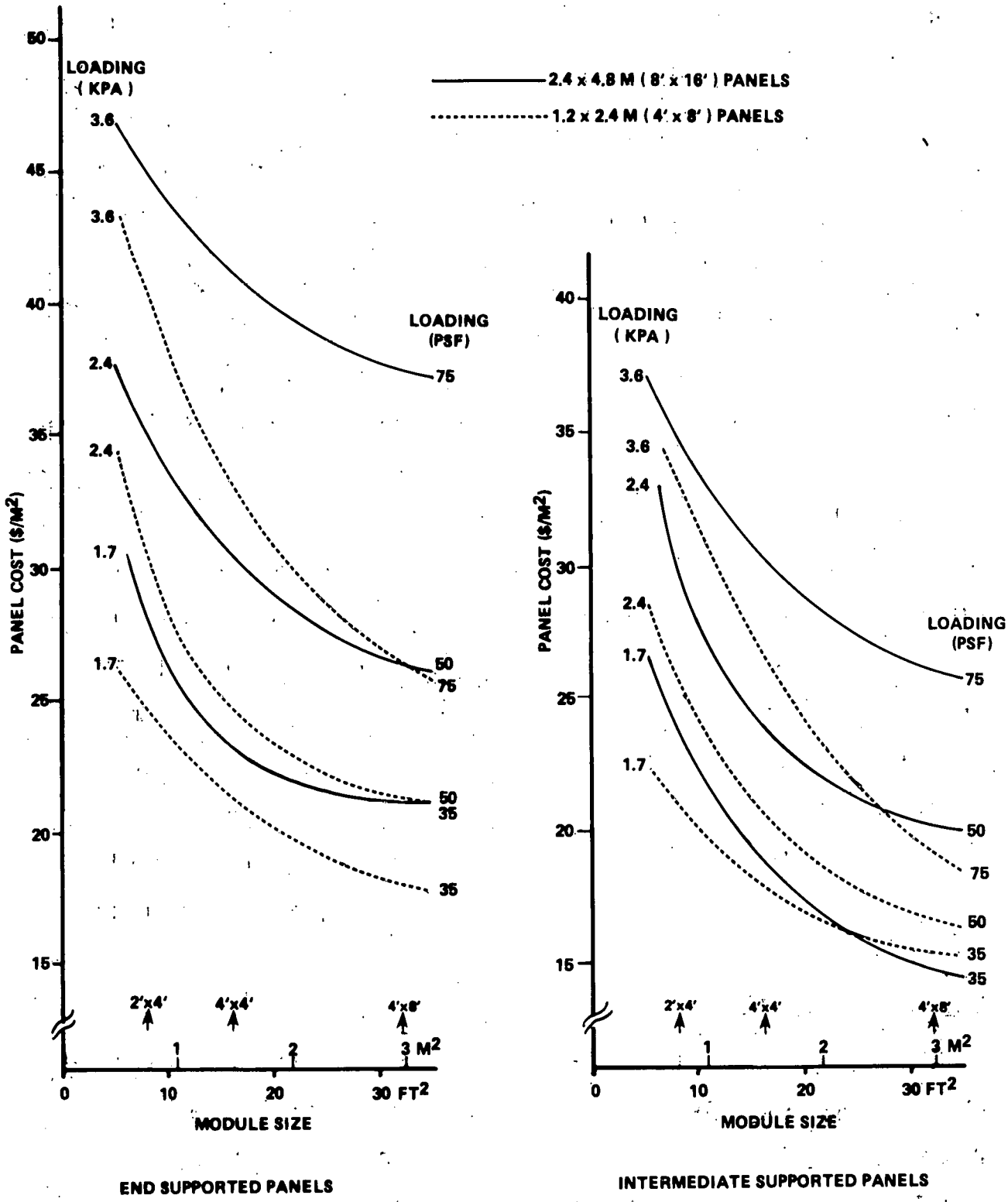

Figure 5-3 PANEL COST VERSUS MODULE SIZE

shapes of the curves indicate a leveling off in panel cost near the 1.2 by 2.4 m (4 by 8 ft) module size. A previous study by Bechtel (Ref. 3-1) indicated that the minimum cost 8 x 16 panel would utilize module sizes of approximately 1.2 by 2.4 m (4 by 8 ft). This trend is also evident in the present data. For module sizes above 1.2 by 2.4 m (4 by 8 ft), the thickness of the glass superstrate would have to be increased. This leads to higher light absorption losses in the glass (see Section 4.3.1), which in turn leads to higher life-cycle energy costs.

Panel cost decreases with increasing module size are attributable to fewer frame members and reduced fabrication labor associated with the panels for larger modules. The amount of assembly labor required per square meter of panel area increases rapidly with decreases in module size and the accompanying increases in the number of panel frame members and modules. With panel size constant, as the number of modules increases: the number of joints to fit and weld increases; the lineal feet of glass edges to fasten increases; and the number of modules to install increases. Further, the 1.2 meter (4 foot) long steel panel members for supporting 0.6 by 1.2 m (2 by 4 ft) modules are strongly affected by the need to provide a sufficiently wide bearing surface for the glass, and affected relatively strongly by the bending strength needed to span between support points. In effect, the intermediate members within a panel frame are a substitute (if needed) for the strength of the glass of the modules. If the glass strength is sufficient to span the longer

spans, then the panel costs can be lower and the converse is true. From the panel cost point of view, it is clear that it is cost effective to increase the glass spans to the maximum amount consistent with the glass strength. The cost effects of varying glass thicknesses and the selection of glass thicknesses for various module areas are discussed in Section 4.1.1.

Figure 5-3 also shows that intermediate supported panels are generally lower in cost than are end supported panels. The reason is that the intermediate support allows a reduction in moment which in turn allows a reduction in flange area of the support member and weight. This cost reduction is in the range of 15 to 25 percent. That range is sufficient to justify further consideration of the intermediate supported panels despite the disadvantages previously cited and some limitations in the modified equivalent flange method used for determining the required steel quantities.

Analyses of structural members with intermediate supports typically show that the analytical results vary widely with the assumptions as to type of loading and location of support. The analyses for these panels are no exception. One reason is that the moment peaks sharply at the intermediate support. If the load assumptions differ from the real condition, for example, with the changes in center of pressure due to wind and large module deflections, moments can be significantly different from those calculated assuming uniform panel loading. Typically,

building and bridge designers compensate for this uncertainty by pattern loading assumptions that determine the more adverse of various loading assumptions and, accordingly, size the member for those load conditions. That typical practice was not followed under the assumption of uniform loading used in this study. Later optimization of panel designs should take nonuniform loading into account. Further, to take advantage of the lower moments for intermediate supports, the support location must be selected independently from the module edge locations. The reversed bending of the module at the support location can differ from the simply supported assumptions made for determining module glass thickness requirements and as a result, premature corner breakage of modules is possible. Also, the equivalent flange area method, used for sizing panel structural members, assumes that the web areas of beams are a constant percentage of the flange areas. As the flange area decreases so does the web area. As a consequence, the lighter beams, if unstiffened, may have webs that are sensitive to web crippling (i.e., elastic instability of portions of the web at points of load or reaction concentration). Because of the above reasons, the relative costs of intermediate supported panels may increase, rather than decrease with further studies which consider more closely the effect of variations in loads, the effect of the reversed curvature of the member on the module, and web crippling of members where the member is not stiffened (at the support location) by the connections for cross-members used to support modules on the panel.

Figure 5-3 shows that, in general, the 1.2 by 2.4 m (4 by 8 ft) panels are less costly on a $/m² basis than the 2.4 by 4.8 m (8 by 16 ft) panels. However, the comparison of panels can not entirely neglect the costs of the associated arrays. As shown in Section 7.1, combining the panel and array costs tends to lessen cost differences. Results of another Bechtel study (Ref. 3-2) showed that use of 1.2 by 2.4 m (4 by 8 ft) panels actually lead to higher total array costs. However, that study compared 1.2 by 2.4 m (4 by 8 ft) and 2.4 by 4.8 m (8 by 16 ft) panel configurations in which each panel formed an array structure (this is similar to Case 9 (see Section 6.2.9), except that the long edges of the panels are horizontal). The 1.2 x 2.4 m (4 x 8 ft) panel configuration studied in Reference 3-2 considered mounting one such panel at a time on the array foundation. The net result was that labor costs involved resulted in the higher total installed cost for the smaller panel configuration. Combining the results of that study with the results of this study leads to the conclusion that cost effective use of the 1.2 by 2.4 m (4 by 8 ft) panels requires that several panels be mounted on each array structure (e.g., see Figure 6-7) as opposed to having one small panel per array as studied in Reference 3-2.

The designs for the panels could benefit from optimization. Fifty-seven panels were designed, and optimization of each design was considered outside the scope of this study, as well as ineffective until the major cost drivers were identified. The

panel designs were all made on a consistent basis, so that the relative differences between the designs are meaningful, unless they are so small as to be of the same order of accuracy as truncation effects on design calculations and the accuracy of cost estimation.

5.6 CURVED GLASS SUPERSTRATE PANEL

The results of the computer analysis of a curved glass superstrate module indicate this concept is a structurally viable design (see Section 4.3.2). The costs of the support clips and other items must be added to the cost of the module to form the panel cost. Further engineering efforts are still required to adequately specify the clip/gasket design. However, in order to allow a preliminary cost comparison to be made with the conventional designs that were evaluated in detail, a lightweight steel, roll-formed section is assumed for the clip. Gasket costs are estimated at the same cost per foot used for the other panels. A budgetary estimate from a glass supplier indicates that there will be a 30 to 35 percent premium for curving the glass (assumed to be 3.2 millimeters (0.125 inch) thick, tempered, 0.05 percent iron, drawn glass). Inspection of the module/panel configuration shown in Figure 4-21 shows that the 1.2 by 2.4 m (4 by 8 ft) glass superstrate holding the solar cells is supported at four points by clips fastened to an array structure. The need to provide individual ground connections for the four 0.3 meter (12 inch) steel clip segments bolted to a

grounded array structure is not clear, but in order to make comparisons equitable, the cost of a single pair of ground connectors is included. The base module cost is that shown in Table 4-1. Table 5-23 presents the estimated costs of a curved glass superstrate panel. Only one column of cost data is presented in this table because the design would be adequate for all loadings evaluated herein. It is assumed that the clips are purchased as a fabricated item; thus, there is no frame fabrication labor for this design. The cost of installing these clips on a module is shown as assembly labor. Extrapolation of the computer analyses of the annealed glass indicate that a 3.2 millimeter (0.125 inch) thick, tempered, curved sheet of glass will resist uniform loadings up to 3.6 kPa (75 psf). Calculations indicate that it may be possible to reduce costs by using annealed glass instead of tempered, but the glass supplier recommends against doing this.

TABLE 5-23

CURVED GLASS PANEL COST ESTIMATE (1975 $/m²)
(clip supported, 1.2m x 2.4m (4'x8') panel,
1.2m x 2.4m (4'x8') module)

Item	Cost (all loads)
Premium for Curved Glass	1.30
Steel Frame (i.e., Clips)	
Material	1.60
Galvanizing	0.40
Fabrication Labor	-
Gasket	0.10
Ground Connectors	1.20
Assembly Labor	1.10
Freight	0.40
Installation, Direct Labor	2.10
PANEL SUBTOTAL	8.20
Module	60.30
PANEL TOTAL	68.50

In comparison with the panel costs previously developed (see Table 5-22), it can be seen that the estimated cost of this "panel", without the module cost, is approximately half that of the lowest cost panel type at 1.7 kPa (35 psf) and a third the cost at 3.6 kPa (75 psf). Further, it is anticipated that manufacturing tolerances on glass dimensions would be less stringent than with conventional panel concepts where the glass plates must fit the panel frame. For the curved glass module, such dimensional errors could be accommodated in mounting the panel on the array. Thus, it is recommended that this concept be pursued further to determine whether the total cost of the panel and array structure, including foundations, is lower than the other cases fully evaluated in this study.

THIS PAGE

WAS INTENTIONALLY

LEFT BLANK

Section 6

ARRAY STRUCTURE AND FOUNDATION DESIGN

This section presents a discussion of array structure and foundation design. Section 6.1 lists the array design bases. Section 6.2 presents details and costs for the nine alternate array configurations evaluated. Results of the array structure and foundation design effort are compared and summarized in Section 6.3. The array configuration costs and panel structural costs (developed in Section 5) are combined in Section 7.

6.1 DESIGN BASES

This section lists the requirements, adopted conventions, and other bases pertinent to the design of the arrays and the estimation of their costs. General cost bases are discussed in Section 2.2.

6.1.1 Requirements

The following requirements are incorporated into the study:

- The nine array configurations evaluated herein were evolved through a collaborative effort between JPL and Bechtel. This number of configurations, permuted with the load range, appeared large enough to allow detection of major cost drivers.
- Loads are normal to the solar collector surfaces in both upward and downward directions.

- Three loads are considered: 1.7, 2.4, and 3.6 kPa (35, 50, and 75 psf). This required load range appeared sufficiently wide to assure that major load cost drivers would be identified by the study. The 3.6 kPa (75 psf) load is, most likely, outside of the range for actual array designs if the dominant load is wind. If translated solely to wind velocity, the 3.6 kPa (75 psf) load is a fastest mile of wind on the order of 72 to 76 meters per second (160 to 170 mph). It could also result from a lower velocity wind, where the air unit weight is higher than normal due to dirt, sand, or other airborne contaminants or from lower velocity winds with a large gusting factor.

- The loads are to be considered as combined live loads and dead loads with no differentiation between the two. This requirement, together with the load direction requirement, tends to overemphasize lift and drag forces. However, for these array designs, the superstructure weight per square foot is relatively small compared to the 1.7, 2.4, and 3.6 kPa (35, 50, and 75 psf) required load magnitudes. Consequently, major cost drivers are not likely to be obscured by this combined load requirement.

- Uniform Building Code (UBC) 1976 Edition, Class 3 site soil materials are to be assumed. Class 3 materials are characterized by the UBC as sandy gravel to gravel. The soil load resistance values specified by the UBC for the class are neither the highest nor the lowest that the UBC specifies. The values are: 96 kPa (2000 psf) bearing pressure downward, 9.6 kPa (200 psf) lateral bearing pressure, and a sliding resistance coefficient of 0.35. Increases in the values are permitted for increased depths below grade by step function statements. The values are considered reasonable for establishing consistency for study design work. As discussed later, a site soils investigation is considered advisable for final optimization.

- The vertical distance between grade and the panel's lower edge is required to be two feet in order to avoid rain splatter of soil onto the modules.

- A 35° latitude array tilt angle was used for this study and is implied in further discussions unless otherwise stated.

- The construction materials are to be concrete for foundations and steel for the superstructure.

6.1.2 Assumptions And Conventions

- The foundation design methods and equations are those specified and permitted by the UBC. This convention was adopted to assure consistency between the UBC "allowables" and the methods for predicting values for comparison with the allowables.

- Commercially available steel shapes were selected. This convention was adopted to assure the greater cost estimating reliability usually possible with a wide base pricing system. As described later, the convention was departed from when it was obvious that the selection of a commercially available steel shape most closely satisfying the need would significantly influence the results of intercase comparisons. Since this study was intended as a screen to determine major cost drivers, it was assumed that any later optimization of the arrays would include detailed calculations to refine the specific member dimensions.

- Simply supported end conditions are assumed for connections between members. Later optimizations may show that moment connections are more cost effective. However, moment connections are usually cost effective only when the connection costs are a small part of the total cost (e.g., the material cost for long steel members with a large weight per foot is much higher than the cost of connecting such members).

- The panel strength is not relied on to brace the array on the basis that array structure and panels are erected and installed during two different time periods. An exception is Case 9 whose concept requires a structure, complete with attached panels, to be erected on preprepared foundations. All required bracing is included, although not shown specifically on the array sketches in this section.

- Allowable stresses, design methods, and equations specified by the American Institute of Steel Construction (AISC) code are adopted. An exception is the adoption of the American Metal Manufacturers Association (AMMA) specified deflection for metal members that directly support glass. Implicit in this experimental and experience based specification is the assumption that the glass is supported by an elastomer and does not bear directly on the metal support member. The adoption of these conventions was made for consistency throughout the study and with accepted practices for the materials used. One exception, of a judgmental nature, was a restriction of the slenderness

ratio (L/r) to less than or equal to 120 for cantilevered posts whose free ends are not guided.

- As a convention, American Concrete Institute Code requirements were adopted for concrete foundation members.

6.1.3 Cost Bases

The array structure and foundation costs are presented in 1975 dollars and are normalized to dollars per square meter of total module surface area.

These costs include shipping and installation. Also, the steel costs include the cost of galvanizing to protect the steel and the foundation costs include the cost of excavating and backfilling trenches for the foundations. Costs for clearing and grading the site are excluded. Also excluded are the costs of distributables, engineering, and contingency. Thus, these costs are essentially direct field costs.

6.2 ARRAY CONFIGURATIONS

This section presents design details and cost data for nine array configuration cases. A design for each of the cases was developed for ±1.7 kPa (35 psf), ±2.4 kPa (50 psf), and ±3.6 kPa (75 psf) loading. The cost data presented are for the foundation and, except for Case 9, the support structure; panel and module costs are excluded. Array structure, foundation, and panel costs are combined in Section 7.

As has been discussed previously, there are several sources of inaccuracies that arise in a comparison study such as this one. These include: inaccuracies due to engineering approximations and subsequent utilization of available non-optimized structural shapes, and cost estimation inaccuracies due to the unavailability of data on similar construction projects and their historical costs. These inaccuracies are inherent in the cost data presented in the following sections.

In the figures for each case, the proportions of the foundations are shown for the ±2.4 kPa (50 psf) load.

6.2.1 Case 1 Design

The configuration of the Case 1 array design is illustrated by Figure 6-1. This case is one of three having an 2.4 meter (8 foot) slant height and one of five having 1.2 by 2.4 m (4 by 8 ft) panels.

The simply supported back girders (i.e., the horizontal array structure element) are all specially designed steel members using folded gage metal plate. Commercially available steel shapes are generally designed for larger loads than were calculated for the 4.8 meter (16 foot) span in this study. The commercially available shapes had either greater than needed shear strength (and consequently greater than needed weight per foot) or an adequate shear and moment strength but large calculated

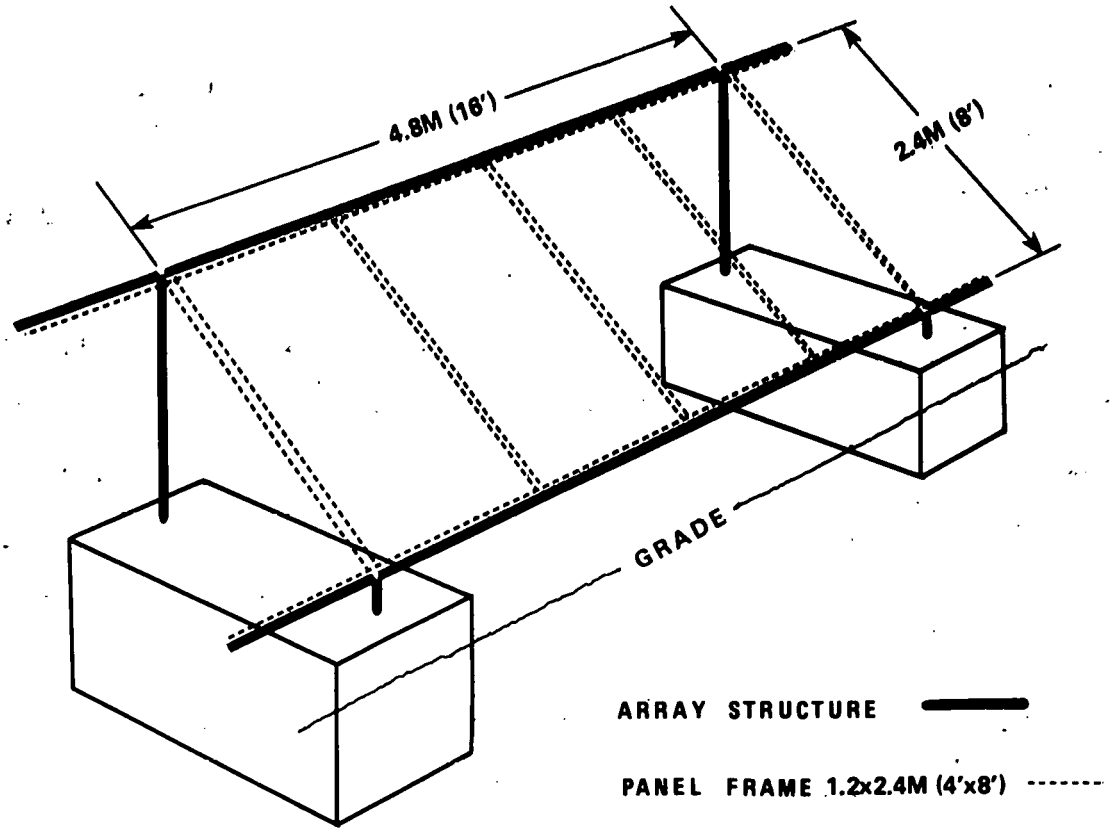

Figure 6-1 CASE 1 ARRAY CONFIGURATION

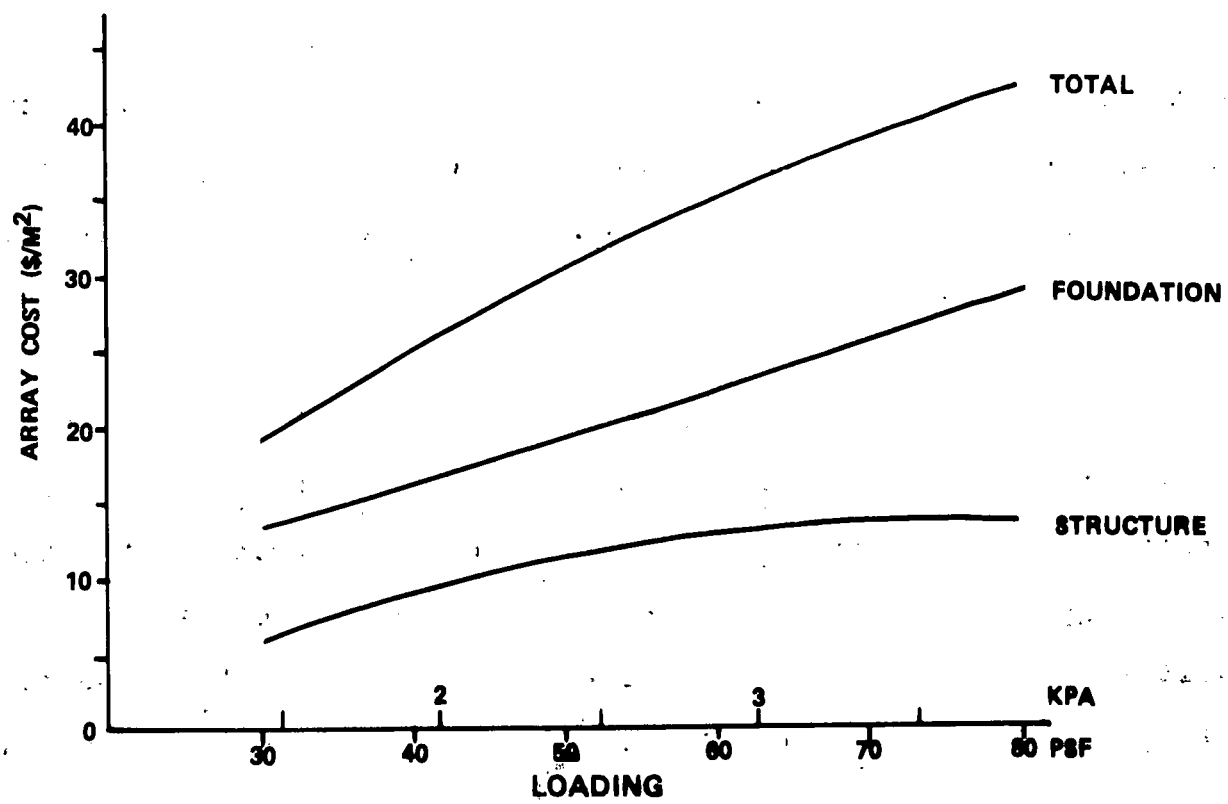

Figure 6-2 CASE 1 ARRAY COST VERSUS LOADING

deflections. The specifically designed shapes are not considered optimum but do have a better balance for these loads between shear and moment resistance than do commercially available shapes. Shapes considered include wide flanges, bar joists, structural tube, pipe, and gage metal joists. As a class, bar joists and gage metal studs have a moment of inertia (I) about the minor axis that is quite small compared to the I about the major axis. Further, the major axis cannot be efficiently located vertically, since the load is applied to the backbeam in a direction that is 35° from vertical. The bar joists and gage metal joists with the minor axis 35° from vertical tend to sag in the vertical direction due to out of plane loads. To correct this, the special sections designed were rectangular tubes, with perforated webs, whose ratio of major to minor moments of inertia was closer to one as is normally required for structural members with loads in three directions. (This ratio is not provided by commercially available joists.) The back and front posts for this case are both lightweight wide flange commercially available shapes and are suitable for the ±1.7 kPa (35 psf), ±2.4 kPa (50 psf), and ±3.6 kPa (75 psf) loadings evaluated.

The general configuration of foundations for this case are shown in Figure 6-1. The foundation size changes with loading. The location and orientation of the foundations with respect to the major applied loads maximize the foundation resistance to overturning moments, especially for the cantilevered back posts. Attempts to design separate foundations for the back posts and

front posts, with the long foundation dimension perpendicular to the north-south direction, resulted in the addition of more concrete than needed for the foundations shown, and was not considered further.

Figure 6-2 shows the installed costs for the array superstructure and foundations for the Case 1 design as a function of loading. As discussed in Section 6.1.3, these costs are in terms of 1975 dollars and are normalized to dollars per square meter.

6.2.2 Case 2 Design

The array superstructure and foundation configuration for the Case 2 design is illustrated in Figure 6-3. This case includes a 2.4 meter (8 foot) slant height, 1.2 by 2.4 m (4 by 8 ft) panel, and a 2.4 meter (8 foot) span between the posts. The cantilivered girder sections are not connected to adjacent array structures.

The problem of finding a suitable commercially available steel back (horizontal) girder shape for this case were greater than for Case 1 due primarily to the smaller total load imposed on the shorter spans which results in both smaller moments and shears. The steel superstructure costs for Case 2 dropped, primarily due to the lower tonnage of steel for the back and front girders as compared to Case 1. The number of back and front posts increased for this case, as compared to Case 1, in the ratio of $2n/(n+1)$,

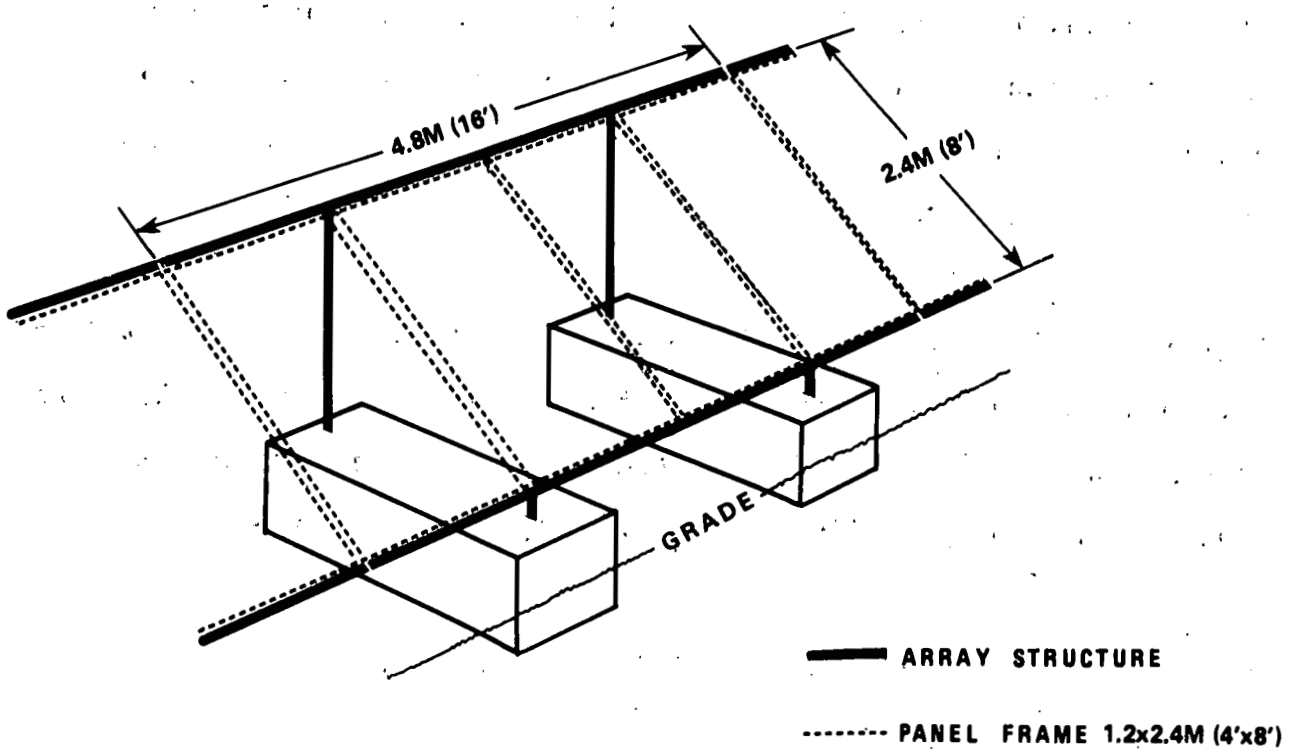

Figure 6-3 CASE 2 ARRAY CONFIGURATION

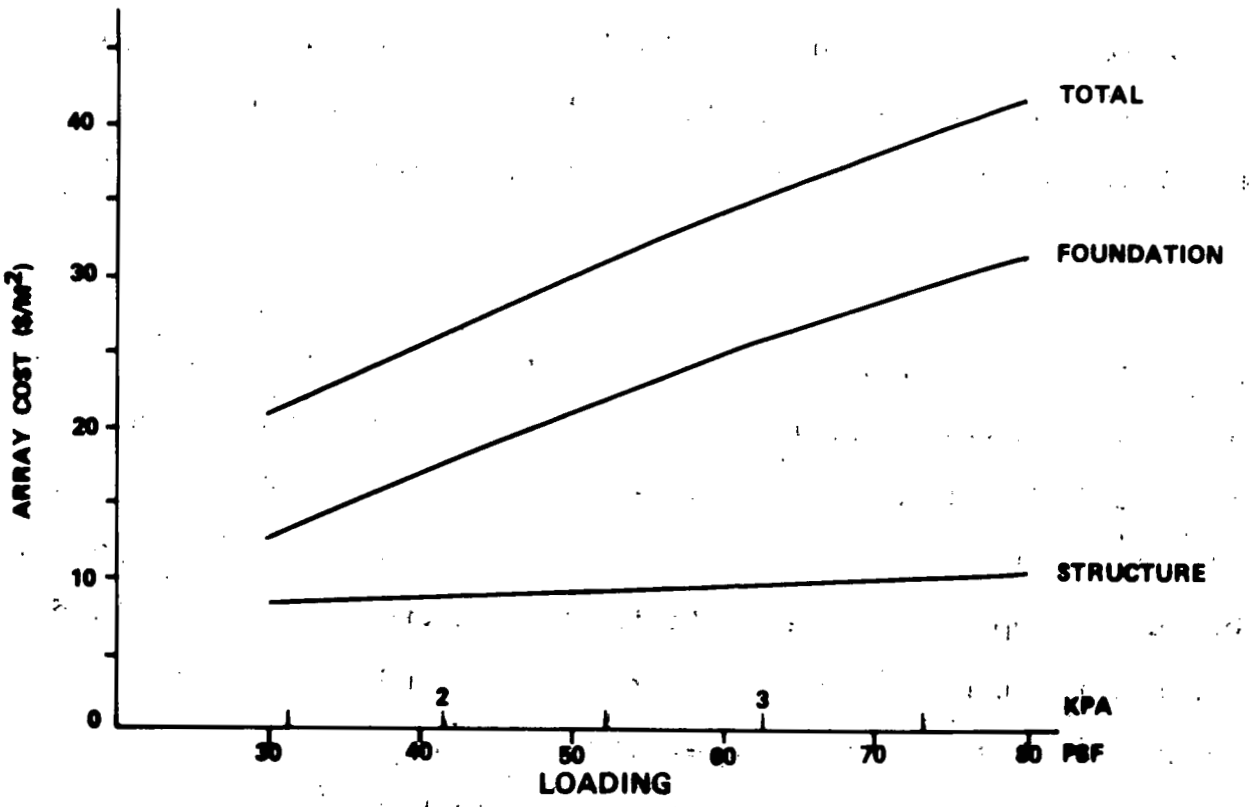

Figure 6-4 CASE 2 ARRAY COST VERSUS LOADING

where n is the number of side-by-side panels in a row (60 in this case). The back and front posts tend to use steel less efficiently than does Case 1 because although the axial and bending loads are smaller for Case 2, the slenderness ratio requirements are the same for both cases.

The number of foundations for Case 2 is greater than for Case 1 by the ratio of 2n/(n+1). However, the total weight and cubic yards of concrete are almost the same, since the product of load times array area is the same for both cases. Differences in estimated foundation quantities between Cases 1 and 2 result primarily from small differences in resistance to lateral movement provided by lateral bearing of the soil for the smaller foundations.

One item noted for Case 2 is that the ratio of steel surface area to steel weight is larger than for Case 1 due, generally, to the thinner material required for members of the same depth. This increases both the need for corrosion protection for this case (because of the thinner steel) and increases the relative surface area to be protected by the galvanized coating selected.

The estimated costs for the Case 2 design are presented in Figure 6-4.

6.2.3 Case 3 Design

The configuration of the Case 3 array superstructure and foundations is presented in Figure 6-5. As for Cases 1 and 2, this design is for a 2.4 meter (8 foot) slant height and 1.2 by 2.4 m (4 by 8 ft) foot panels.

The superstructure back posts are shorter and more efficient, when rated by force/area ratio, than for either Cases 1 or 2. Girder spans for Case 3 are identical to those for Case 1 but the loads on the span are greater. Although the tonnage of steel for the back beams is larger for Case 3 than for Case 1, the increase is compensated for by a decrease in the tonnage for the back posts. As a consequence, the estimated costs for the Case 3 superstructure is close to, but about midway between, those for Cases 1 and 2. At 2.4 kPa (50 psf) loading, the differences between superstructure costs for Cases 1, 2, and 3 are about ±10 percent of the average estimated costs for the three cases. Some of the cost differences between the cases may be due to calculational inaccuracies rather than a difference due to changes in the superstructures.

Differences in foundation costs between Cases 1, 2, and 3 are only about ±5 percent of the average at 2.4 kPa (50 psf). As for the superstructure, Case 3 costs are between Case 1 and Case 2 but closer to Case 1. Case 1 and Case 3 foundation costs are virtually identical, being within 3 percent of each other. Since

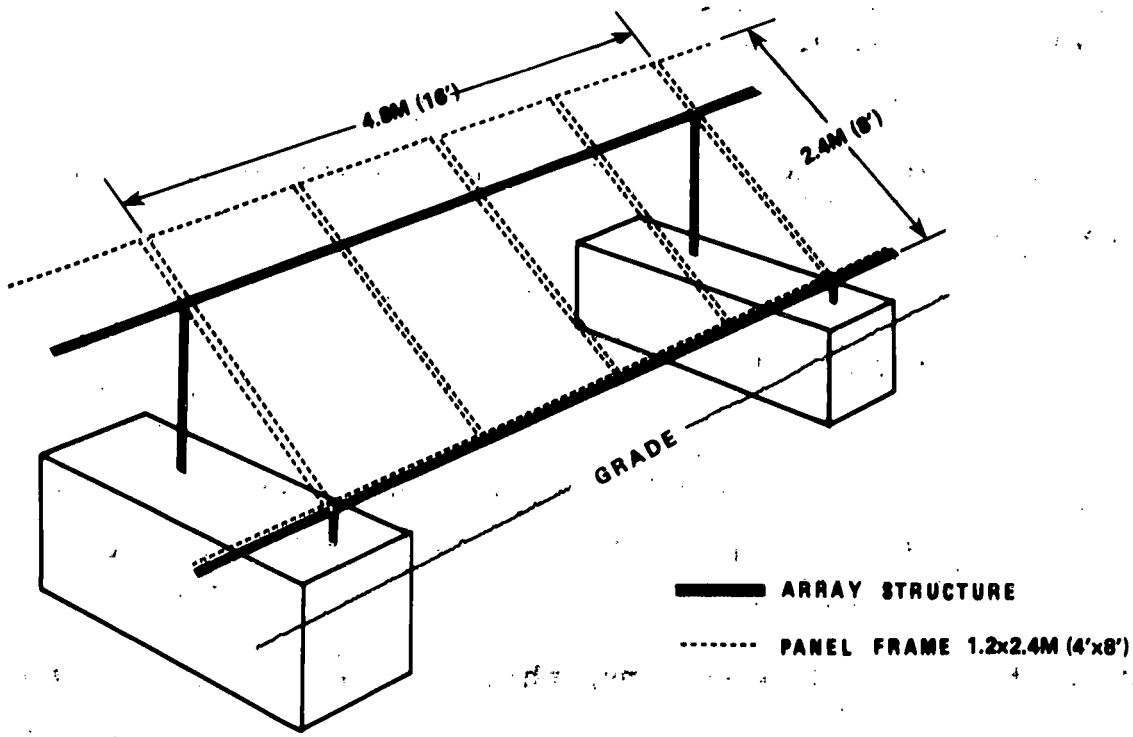

Figure 6-5 CASE 3 ARRAY CONFIGURATION

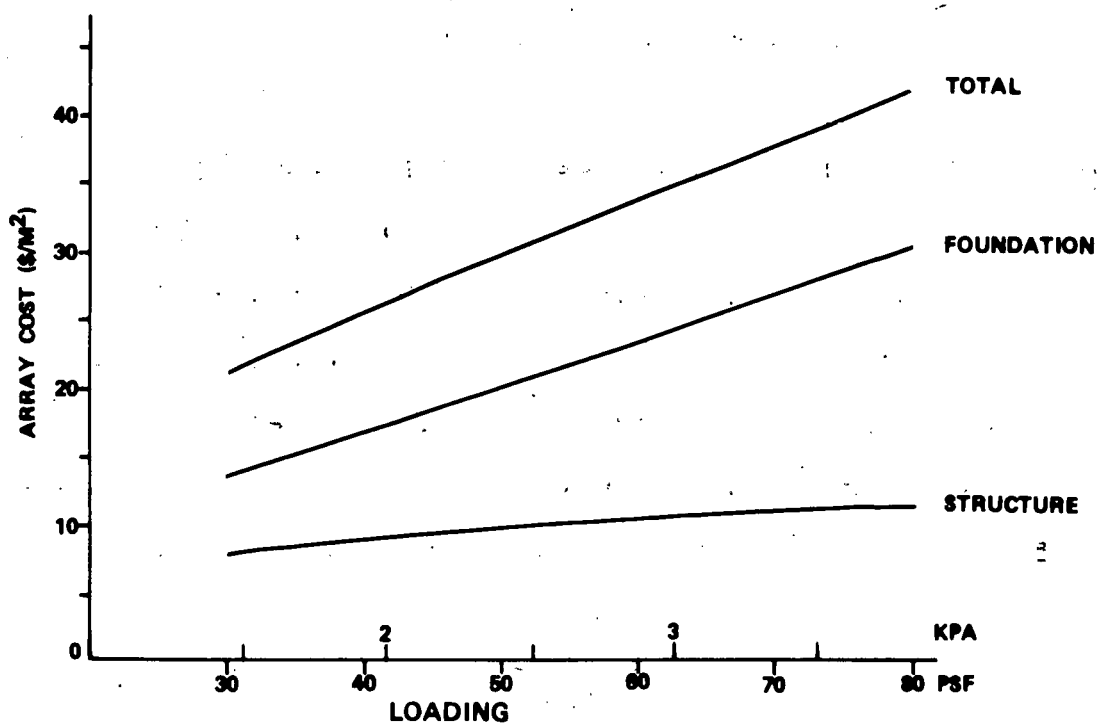

Figure 6-6 CASE 3 ARRAY COST VERSUS LOADING

the total foundation loads and number of foundations for Case 3 are the same as for Case 1, the closely equivalent foundation costs are to be expected.

The estimated costs for the Case 3 array design are presented in Figure 6-6.

6.2.4 Case 4 Design

Case 4 is comprised of 1.2 by 2.4 m (4 by 8 ft) panels and a 4.8 meter (16 foot) slant height as illustrated in Figure 6-7.

From a total load viewpoint, this case is identical to Case 1 because the loaded areas per superstructure frame are identical. The siderails (beams) for Case 4 are the equivalent of the front and back girders of Case 1 except that the siderails (beams) are subjected to both flexural and axial loads.

Estimated steel costs for Case 4 are virtually identical to Case 1 at 2.4 kPa (50 psf) and 3.6 kPa (75 psf). Since the back legs are longer than for Case 1 and the siderails (beams) would brace the backposts in the north-south direction, the back posts were designed as pin ended columns with added east-west bracing. The permissible value of slenderness ratio was, accordingly, larger for Case 4 than for the cantilevered posts of Case 1.

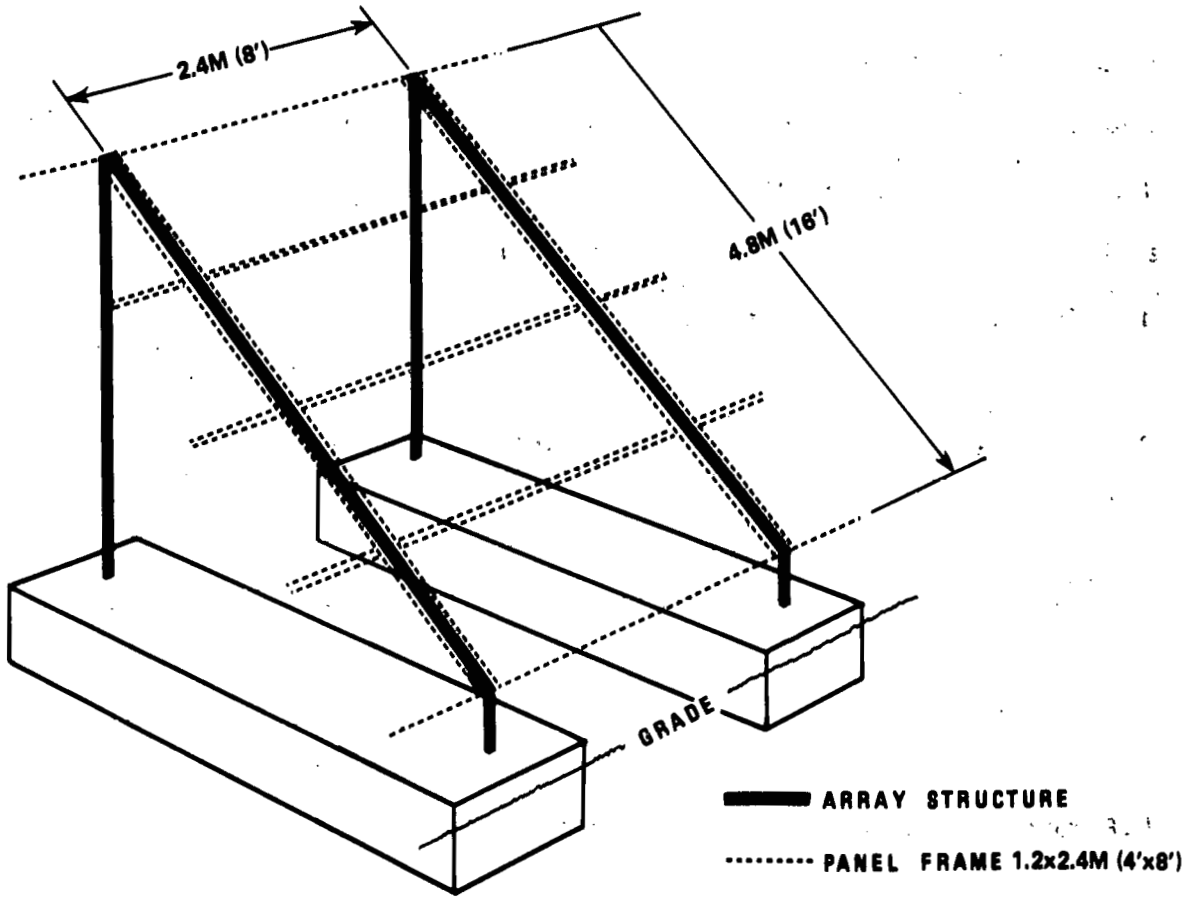

Figure 6-7 CASE 4 ARRAY CONFIGURATION

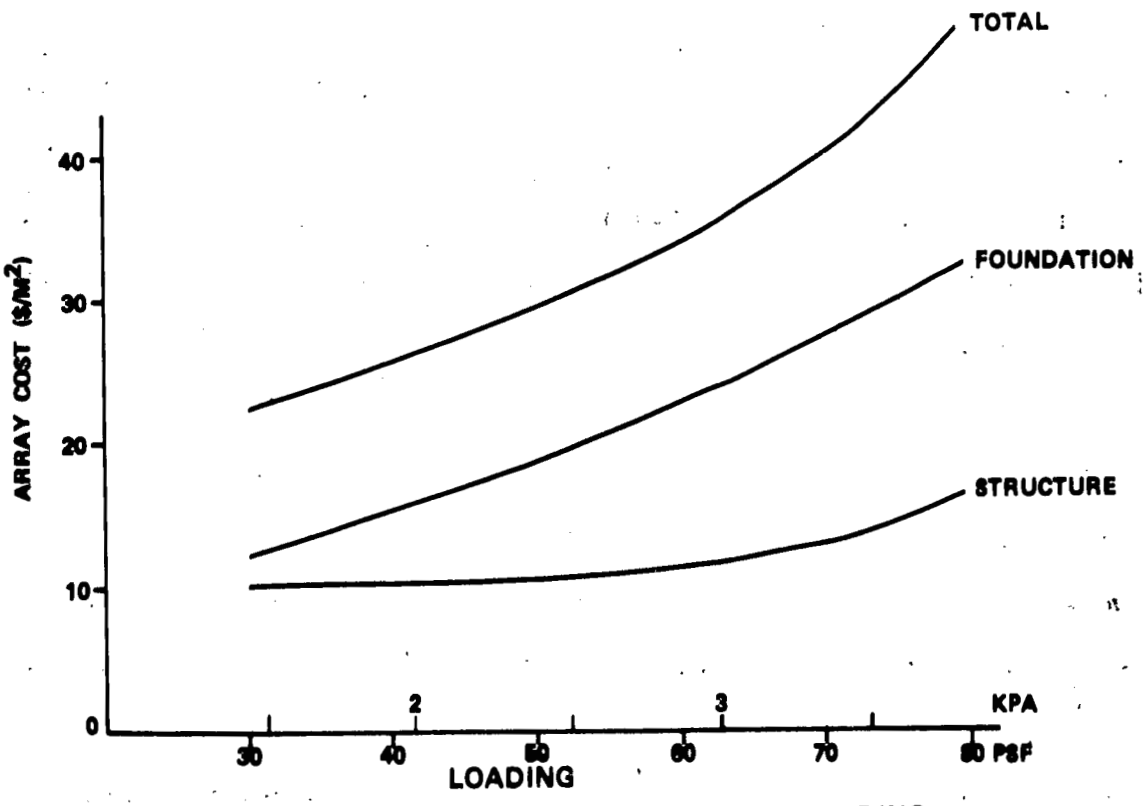

Figure 6-8 CASE 4 ARRAY COST VERSUS LOADING

Foundation costs for Case 4 are estimated to be virtually identical to those for Case 1, showing that common parameters dominated their costs. Those common parameters were load, area, and the need to provide sufficient concrete mass to prevent uplift and side motion of the array.

Case 4 estimated costs are presented in Figure 6-8.

6.2.5 Case 5 Design

The configuration of the Case 5 design is shown in Figure 6-9. This design is for 2.4 by 4.8 m (8 by 16 ft) panels and a 4.8 meter (16 foot) slant height.

Cases 4 and 5 are similar from a loaded area viewpoint. However, Case 5 superstructure costs are lower than for Case 4. The reason for this is that the siderails (beams) equivalent for Case 4 are, for Case 5, a part of the panel costs instead of the superstructure costs. The major design difference is that the posts for Case 4 are designed as upright cantilevers rather than pin ended braced columns.

Foundation costs for Case 5 are about 10 percent higher than for Case 4, partly because of the greater moment created by the cantilivered posts of Case 5 which does not have a siderail (beam) and the panel connection at the top of the posts is assumed to be a sliding connection.

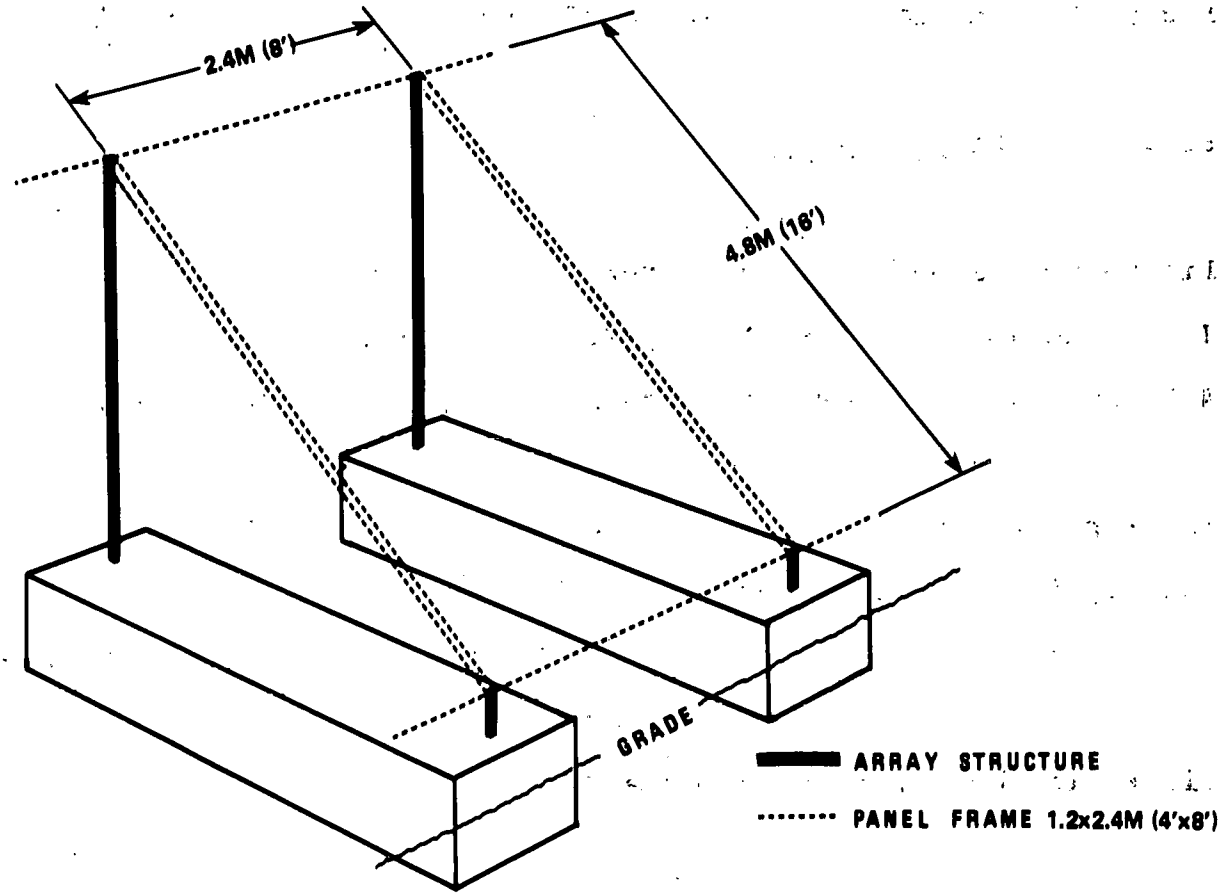

Figure 6-9 CASE 5 ARRAY CONFIGURATION

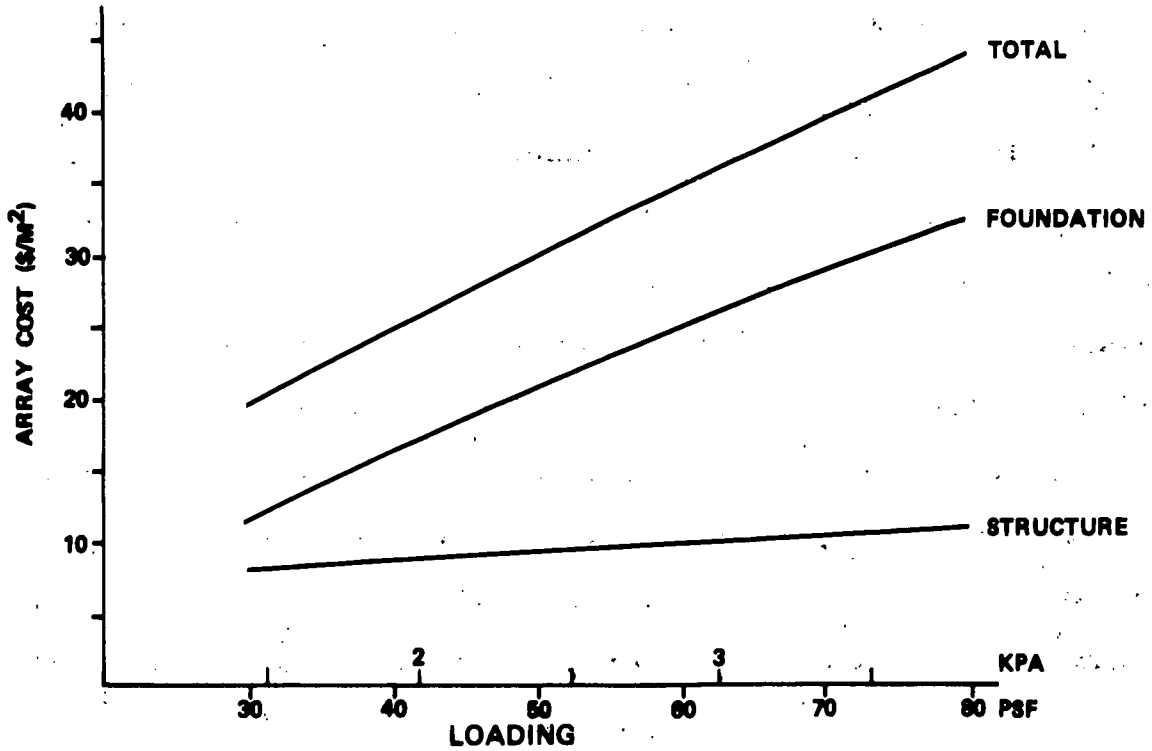

Figure 6-10 CASE 5 ARRAY COST VERSUS LOADING

Figure 6-10 presents the estimated costs for the Case 5 design.

6.2.6 Case 6 Design

Figure 6-11 shows the configuration of the Case 6 array design. This design is for 1.2 by 2.4 m (4 by 8 ft) panels and a 4.8 meter (16 foot) slant height. Case 6 is similar to Case 4.

The superstructue costs for Case 6 are lower than those for Case 4, its nearest equivalent. The cost reduction is attributed partly to a reduction in length of the back posts, shorter siderail (beam) spans, and smaller flexural loads on the siderails (beams) than for Case 4.

The foundations for Case 6 are shorter and deeper than for Case 4 in order to increase the resistance to lateral motion afforded by the soil. However, foundation costs for Case 6 are higher than for Case 4 at ±1.7 kPa (35 psf) and ±2.4 kPa (50 psf) loadings. This is attributed to the smaller distances between posts for Case 6, and the consequent greater importance of overturning moment compared to lateral motion. At 3.6 kPa (75 psf), foundation costs for Case 4 are higher than for Case 6. Lower foundation costs may result from optimization of the plan dimensions of the Case 6 foundations (i.e., for the constant foundation weight needed to resist uplift forces, select the dimensions that maximize the resistance of the soil to lateral movement while retaining sufficient resistance to overturning).

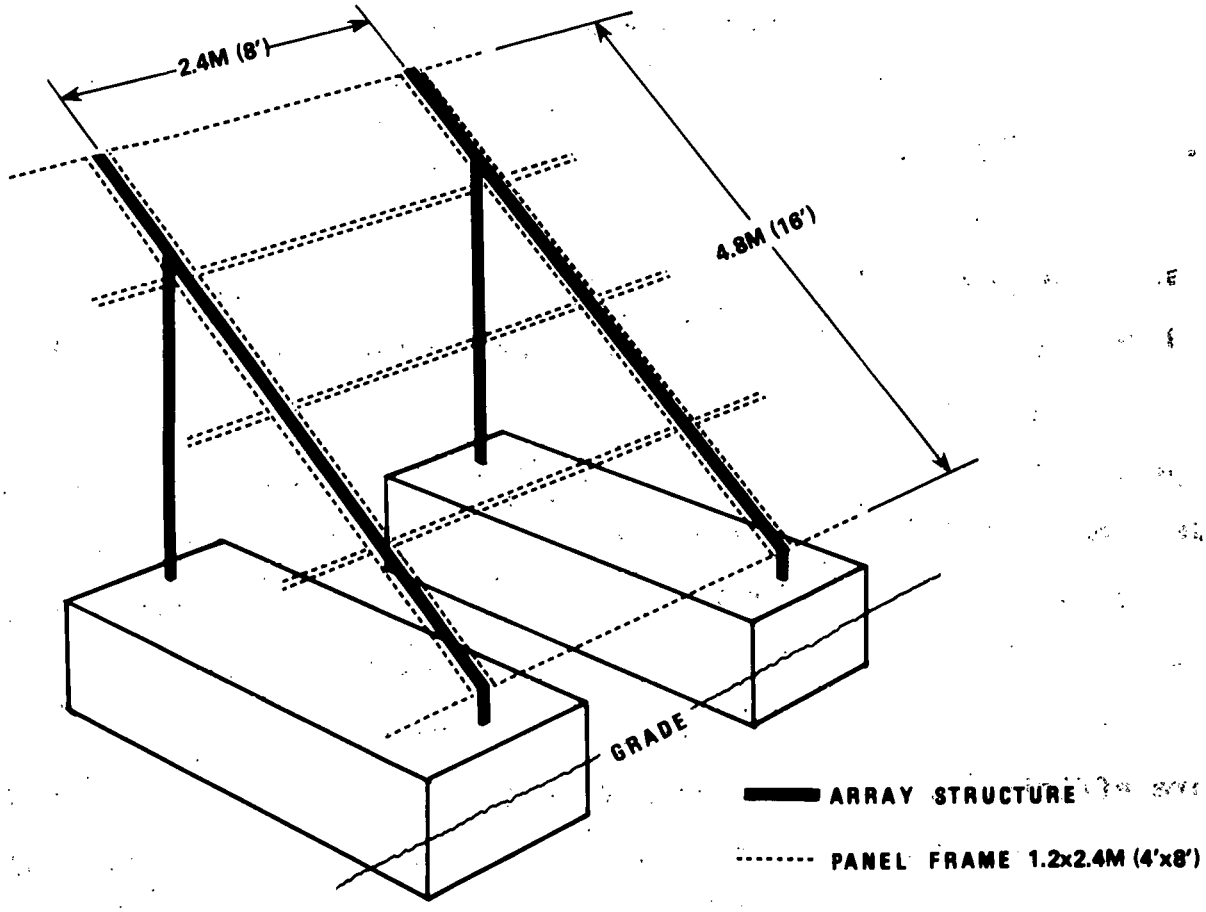

Figure 6-11 CASE 6 ARRAY CONFIGURATION

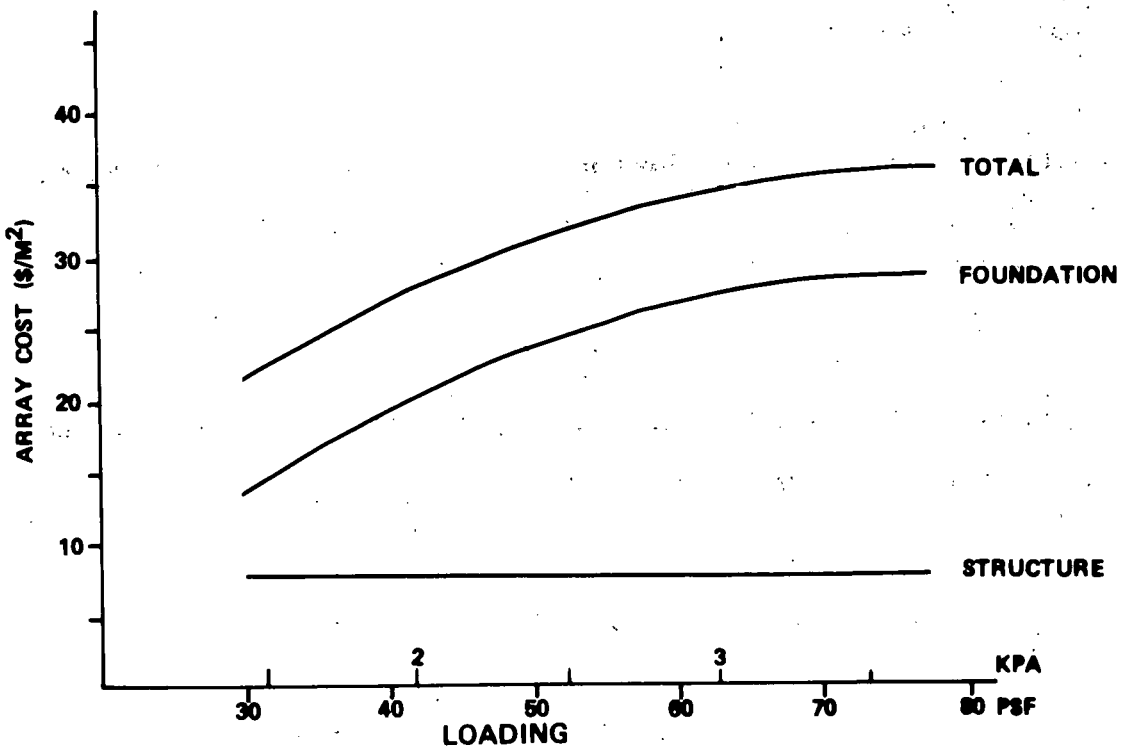

Figure 6-12 CASE 6 ARRAY COST VERSUS LOADING

Case 6 costs are presented in Figure 6-12.

6.2.7 Case 7 Design

Case 7 utilizes 2.4 by 4.8 m (8 by 16 ft) foot panels and a 4.9 meter (16 foot) slant height as illustrated in Figure 6-13.

Case 7 is similar to Case 5 and Case 8 (Section 6.2.8), which also have 4.9 meter (16 foot) slant heights and utilize 2.4 by 4.8 m (8 by 16 ft) foot panels. Case 7 results in slightly lower superstructure costs than Case 5. The reduction is attributed primarily to fewer, shorter back posts that are more efficiently used than for Case 5. Also, back and front girders are required for Case 7 but not for Case 5. However, the girder supported loads for Case 7 are relatively small and the added beam (panel member) steel for Case 5 was not as great as the reduction in post steel.

As for Cases 1 to 6, the foundation "long" dimension is located parallel to the load direction so as to make overturning not a critical concern. Consequently, the foundation cost driver is the need to provide resistance to lateral (horizontal) motion as well as uplift. The foundation costs for Case 7 are very close to the average for all cases and to those for Case 5.

Costs for the Case 7 design are presented in Figure 6-14.

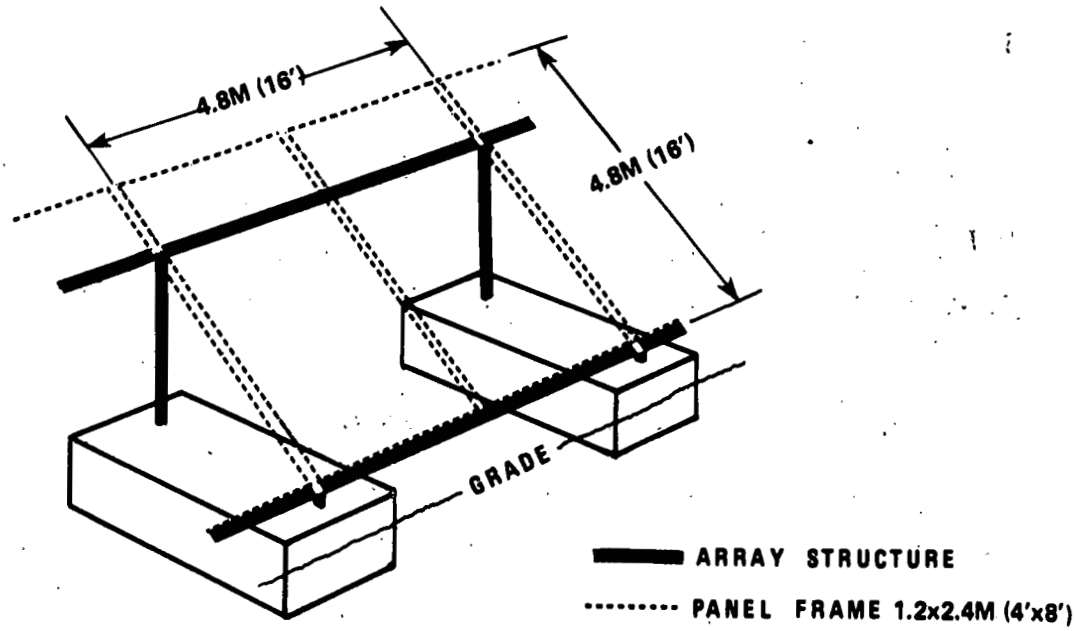

Figure 6-13 CASE 7 ARRAY CONFIGURATION

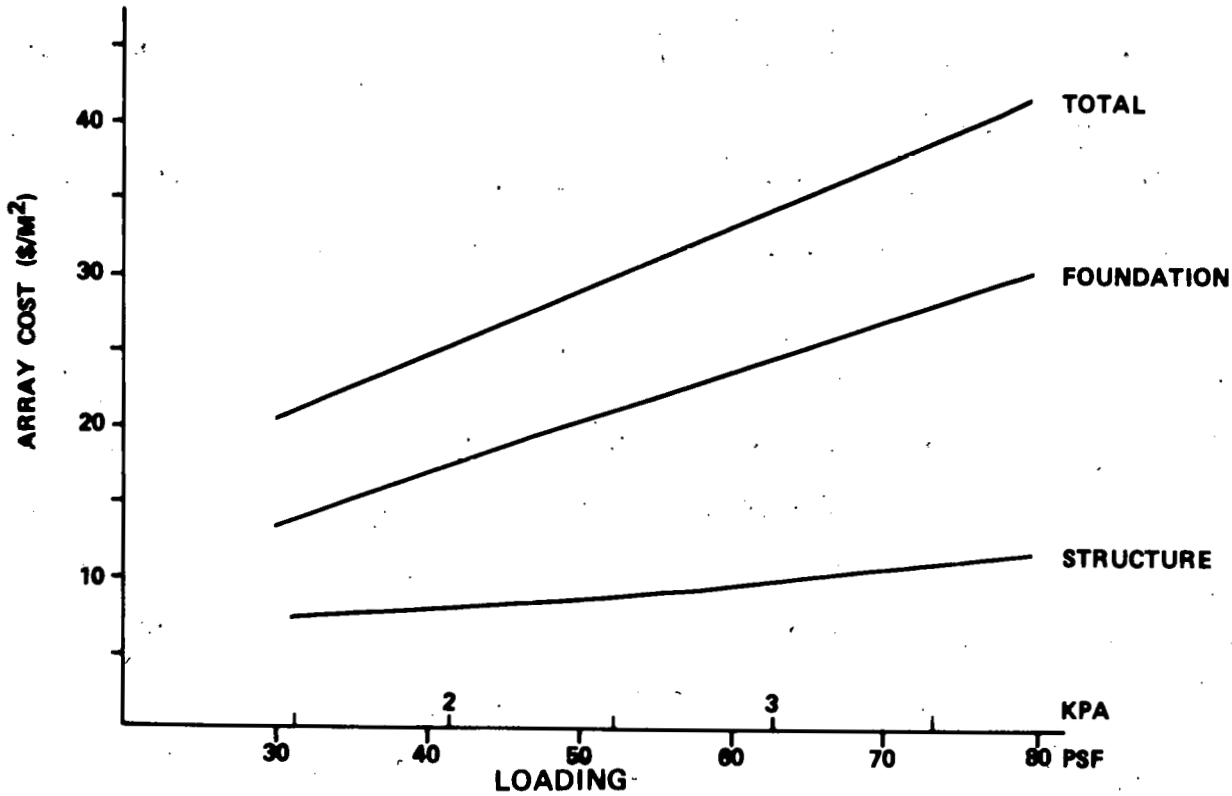

Figure 6-14 CASE 7 ARRAY COST VERSUS LOADING

6.2.8 Case 8 Design

Figure 6-15 shows the configuration of the Case 8 array superstructure and foundation. A 4.8 meter (16 foot) slant height and 2.4 by 4.8 m (8 by 16 ft) panels are used.

The general configuration of this case is the same as for Case 7 except that the girder span is increased to 9.8 meters (32 feet). The amount of steel required for posts decreased for Case 8 as compared to Case 7 because of a lower number of more efficiently utilized posts for Case 7. The weight is controlled by the slenderness ratio of the posts for Case 7 rather than maximum stress. However, the weight per foot of girders for Case 8 increased due to the increase in span length to 9.8 meters (32 feet) from 4.8 meters (16 feet). Optimization may result in some decrease in Case 8 girder steel by design of steel sections that have a similar section modulus but lower adequate shear strength compared to those estimated in this study.

There are fewer, but larger, foundations in Case 8 as compared to Case 7. However, the total weight of concrete is the same within ±10 percent for both cases.

Figure 6-16 shows the estimated costs for the Case 8 design.

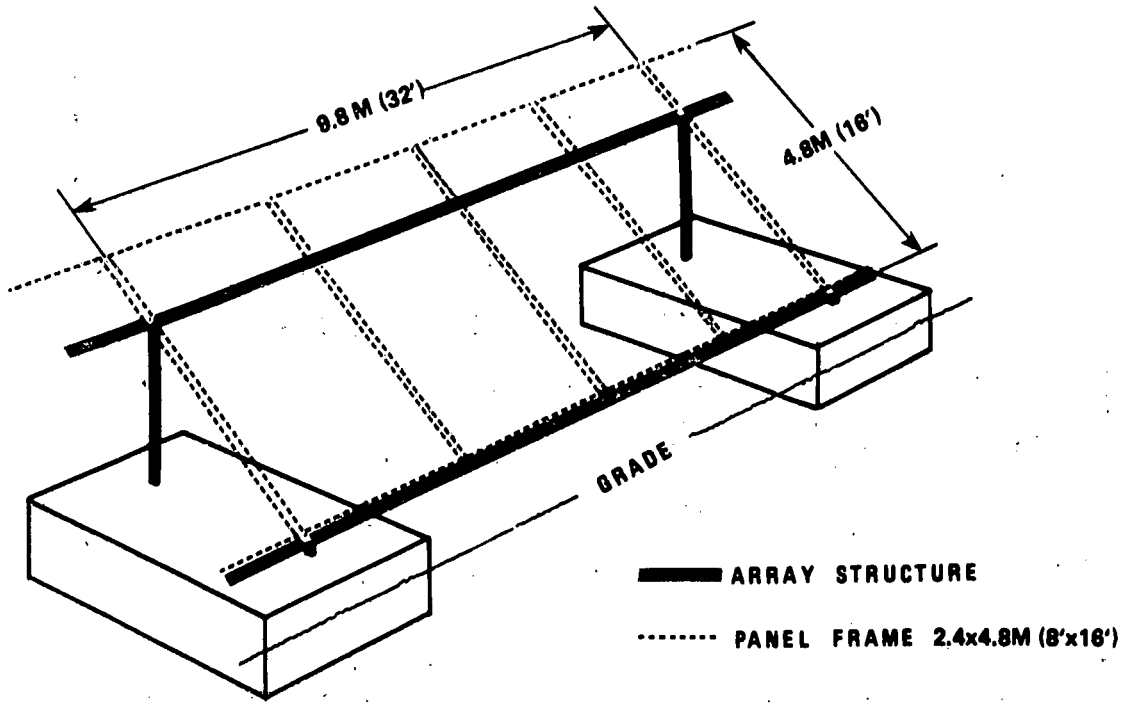

Figure 6-15 CASE 8 ARRAY CONFIGURATION

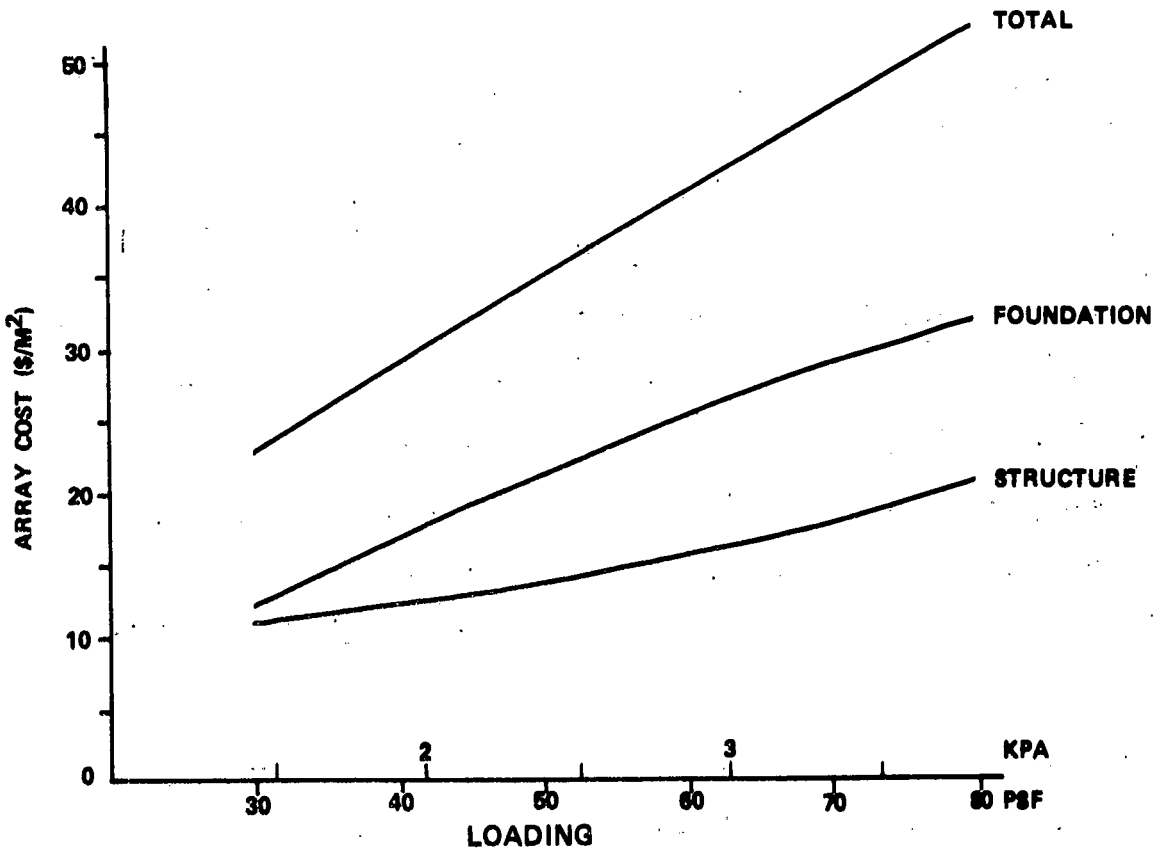

Figure 6-16 CASE 8 ARRAY COST VERSUS LOADING

6.2.9 Case 9 Design

The configuration of the Case 9 array design is shown in Figure 6-17. This design uses 2.4 by 4.8 m (8 by 16 ft) panels with a 4.8 meter (16 foot) slant height and is generally similar to Case 5. However, Case 9 differs from all of the preceding cases in several major respects. There is no separate, field-erected array structure per se. All of the structural functions are incorporated into the panels. The back posts (part of the panels in this case) are inclined, forming an A-frame with the panel. Also, the back posts share foundations with adjacent array panels, as illustrated in Figure 6-17. The foundations run in an east-west direction as opposed to north-south in the other cases.

The objective in including the Case 9 design was to evaluate the effect of combining panel and array superstructure structural functions into a single unit (i.e., the panel) and the effect of sharing foundations. The Case 9 concept assumes that the superstructure, complete with glass modules, will be shipped with the back leg folded. Field installation requires unfolding the legs, fastening the entire structure to the foundation, and completing the fastening of the legs at the fold point.

The reduction in Case 9 foundation costs compared to the other eight cases occurs because of:

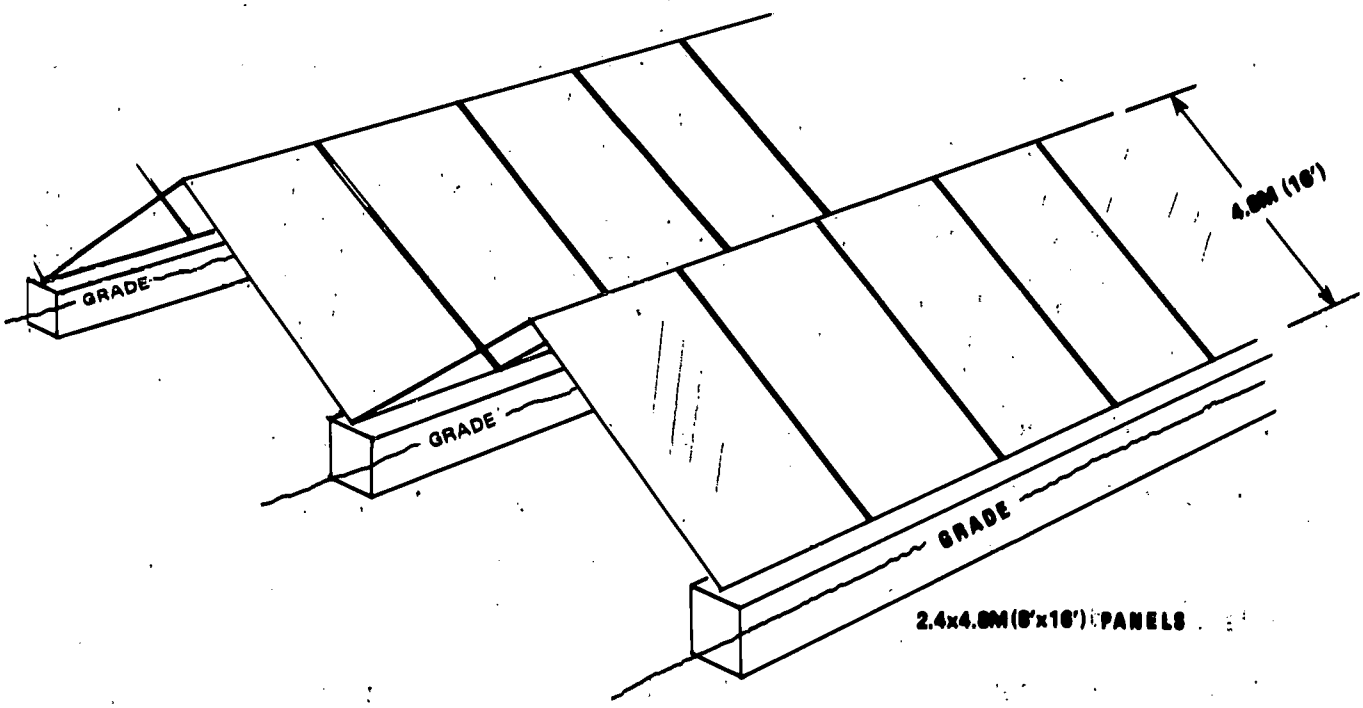

Figure 6-17 CASE 9 ARRAY CONFIGURATION

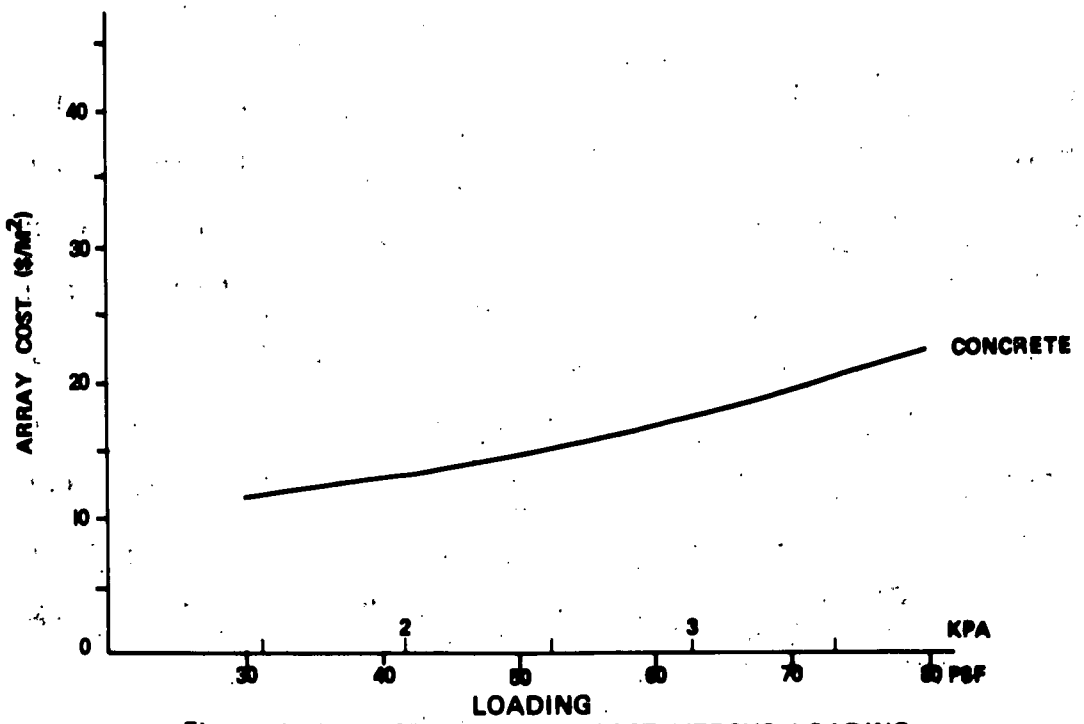

Figure 6-18 CASE 9 ARRAY COST VERSUS LOADING

- Fewer foundations (the front leg of one panel structure A-frame shares a foundation with the back leg of another).

- An increase in the distance between support points relative to the loaded area, which reduces the relative importance of the overturning moments created by the loads.

- Placing the long dimension of the foundations perpendicular to major load directions. This is made possible by the reduction in relative importance of overturning moment. This orientation of the foundation allowed maximizing the amount of soil lateral bearing resistance per cubic yard of concrete.

The reduction in weight of Case 9 foundations also reduced the sliding component of resistance to lateral motion (i.e., the UBC coefficient of sliding resistance times the weight). However, the Case 9 gain in foundation area for soil lateral bearing resistance compensated for the loss in sliding resistance with an increase in that fraction of the resistance to lateral motion attributed to the lateral bearing resistance of the soil.

Since the scope of this study permitted only a relatively superficial consideration of the cost tradeoffs for foundations considered for Case 9, later optimizations should examine the cost tradeoffs in more detail. However, any later optimizations of this sort may not be cost effective unless the load magnitudes and directions are better identified and the site soil values are more accurately determined. In particular, cost optimizations for foundations of this type are sensitive to the lift to drag ratio for winds from the north since winds from this direction

produce the maximum uplift force and govern foundation weight requirements.

The foundation costs for the Case 9 design are shown in Figure 6-18 while structure costs (i.e., panel costs) are presented in Table 5-21. The structure cost for Case 9 is actually a panel cost and should not be compared with the structure costs in the preceding eight cases. Case 9 structural steel costs include the 2.4 meter (8 foot) long members that directly support glass modules and span from leg to leg of the A-frame and which are only partly included in some other cases as front and back beams. As expected, the Case 9 superstructure costs are higher than for other cases even without inclusion of the 2.4 meter (8 foot) member mentioned. This is due to the longer back leg compared to Case 4, for example. Case 9 total costs are presented in the summary in Section 7.1.

6.3 ARRAY COMPARISONS

6.3.1 Cost Comparisons

Estimated array structure and foundation costs for the nine array configurations presented in Section 6.2 are summarized in Table 6-1. A comparison between the Case 9 foundation cost and corresponding costs for the other cases shows Case 9 foundation cost to be 15 to 25 percent lower (depending on loading) than the next lowest case.

TABLE 6-1

ARRAY STRUCTURE AND FOUNDATION COST ESTIMATE SUMMARY (1975 $/m^2)

ARRAY CASE	1.7 KPA (35 PSF) LOADING			2.4 KPA (50 PSF) LOADING			3.6 KPA (75 PSF) LOADING		
	STRUCTURE	FOUNDATION	TOTAL	STRUCTURE	FOUNDATION	TOTAL	STRUCTURE	FOUNDATION	TOTAL
1	7.50	14.60	22.10	11.20	19.10	30.30	13.50	27.00	40.50
2	8.30	14.80	23.10	9.00	20.70	29.70	9.90	29.80	39.70
3	8.30	15.10	23.40	9.80	20.00	29.80	11.10	28.70	39.80
4	10.50	13.80	24.30	10.70	19.00	29.70	14.40	30.40	44.80
5	8.30	13.80	22.10	9.20	20.70	29.90	10.80	31.00	41.80
6	7.40	16.50	23.90	7.40	23.30	30.70	7.40	28.20	35.60
7	7.40	14.90	22.30	8.70	20.10	28.80	11.00	28.60	39.60
8	11.50	14.40	25.90	13.70	21.30	35.00	19.00	30.40	49.40
9	–(1)	12.10	12.10	–(1)	14.40	14.40	–(1)	20.70	20.70

(1) All Case 9 structural costs are associated with the panel costs.

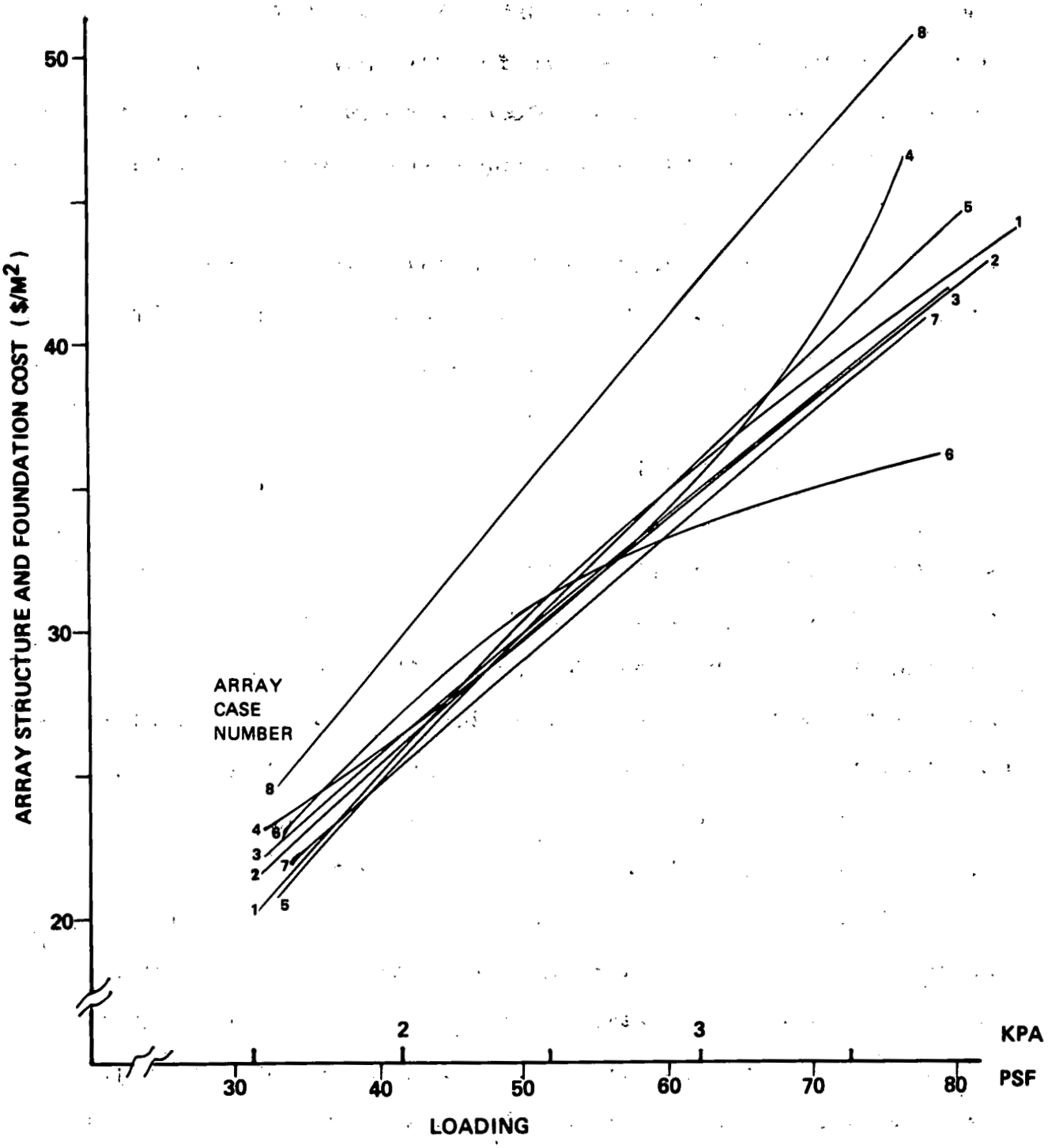

Figure 6-19 ARRAY STRUCTURE AND FOUNDATION COST VERSUS LOADING

Array superstructure and foundation costs for eight of the nine array design cases evaluated are shown graphically in Figure 6-19. This figure presents costs, normalized to 1975 dollars per square meter of total module surface area, as a function of loading. As with the other cost data presented herein, the curves represent the best fit for data points at 1.7, 2.4, and 3.6 kPa (35, 50, and 75 psf). Costs for Case 9 are not included since that case does not have a superstructure cost per se.

As can be seen from Figure 6-19, array structure and foundation costs are highly dependent on loading and, for the eight cases shown, depend on design to a much lesser extent.

6.3.2 Array Tilt Angle

Some consideration was given to tilt angles other than 35°. Conclusions were possible only if it was assumed that the load magnitude was unchanged by the angle. This is unlikely to be true for wind loads. The lowest cost foundations and superstructure will result from horizontal arrays. This is because the foundation costs are largely attributed to the necessity to resist lateral motion concurrent with uplift. In the idealized limiting case of a horizontal array, there are only uplift or downward forces and the concrete needed is only that necessary to preclude upward motion. Also for the horizontal array, superstructure costs are minimum since the lengths of loaded members are shortest. Horizontal arrays, their energy

output, and their life-cycle energy costs are discussed further in Reference 3-2.

It is expected that, if loads remain constant, inclined array structures in locations with latitude angles less than 35° would be less costly than for those considered in this study. For locations with latitude angles greater than 35°, the converse is true. The uplift force component will decrease with an increasing angle of inclination relative to horizontal. However, the lateral force component will at the same time increase. The foundation weight opposes uplift forces on a one-to-one basis. However, for lateral forces and with a sliding coefficient of 0.35, only 35 percent of the foundation weight in excess of the amount needed to resist uplift, is effective in creating sliding resistance. Consequently, an additional 1.4 kilograms (3 pounds) of foundation are needed to resist each additional 0.45 kilogram (pound) of lateral force component, while a decrease in the upward force component of 0.45 kg (1 pound) results in a decrease in needed foundation weight of 0.45 kg (1 pound). The above observation is based on the assumptions that the lateral bearing resistance to lateral motion and the applied loads remain constant while angle of inclination varies. Further, the observations are based on the design requirements and conventions for this study.

If, however, the plant site has a south facing natural slope, then the relative costs attributable to array inclination

relative to the horizontal would be different than those considered in this study. For such sites, superstructure material costs would tend to decrease. However, it is not known how many potential sites with this characteristic exist. Further, construction costs would tend to increase with the increasing difficulty of working on steeper slopes.

6.3.3 Array Structure and Foundation Design Summary

Foundations. When considering only the foundation and superstructure costs, the major cost fraction is the foundation cost. The ratio of foundation to superstructure costs is approximately two or more for all cases and loads. Later optimizations could well reduce foundation costs. However, the ratio found here is so large that it is highly unlikely that foundation costs will be insignificant in comparison with other costs.

The major driver for foundation costs was found to be the load in the upward direction and normal to the panel surface for all load magnitudes and the one set of soil conditions used. In effect, this load direction creates an uplift and sideward force requiring enough foundation weight to not only resist uplift alone but to create frictional resistance to horizontal motion.

Several optimization routes were found in an evaluation of the study results. At least one requires considering the array

foundations and superstructure in combination rather than separately and is discussed later under the subheading Array Structure.

Two types of foundations were considered for this application--a shallow based spread footing and a pole (caisson). The shallow based spread footing, where the entire top surface of the footing is exposed above grade, was considered since it typically has a relatively high overturning resistance compared to the concrete weight required. The other foundation type, the pole or caisson type, was considered as an alternative because it can be more suitable for some types of soil (e.g., cohesive type soils, such as rock ledges). A brief investigation was made of the applicability of these two foundation types for the study. For the pole type foundation, the investigation indicated that the UBC equations governing the use of pole type foundations (i.e., that equation found in Section 2907(f)1 of the 1976 edition of the UBC) may not have considered concurrent in its derivation uplift and lateral forces, required by this application. Further, the gravel-type soils (UBC, class 3) specified for this study, often require that the larger diameter holes be cased. For a study such as this, where no specific site is specified, there is insufficient data available to determine the largest required diameter of uncased hole for a pole type foundation. Spread footing foundations are more generally applicable for the UBC class 3 soils specified for this study and, accordingly, were chosen for use in this study. Pole-type foundations may be more

cost effective for sites with a more cohesive soil. When specific site soil conditions are known, optimizations can more closely consider foundation design alternatives.

One disadvantage of a shallow based, trenched-in spread footing is that the soil cannot be counted on to resist uplift, a factor that should be closely considered during any later optimization. In effect, the tradeoff to be considered is the higher costs for improved lateral force resistance of deeper spread footings against the lower unit costs for the shallow based footings with, at times, superior overturning moment resistance.

Foundation Sharing. Cases 1, 2, and 9 share foundations to various degrees. The costs of these foundations as a function of loading are presented in Figure 6-20.

The difference in foundation costs between Case 1 and 2 is not considered as significant as the difference between the average for Cases 1 and 2 and Case 9. Calculational inaccuracies could be the reason for the differences between Cases 1 and 2 but are less likely to be the reason for the difference between Case 9 and the average for Cases 1 and 2.

Two variables separate the three different foundations. One common variable is the degree to which foundations are shared, with Case 9 representing the greatest sharing and Case 2 the least. Case 9 has a different force resistance mechanism from

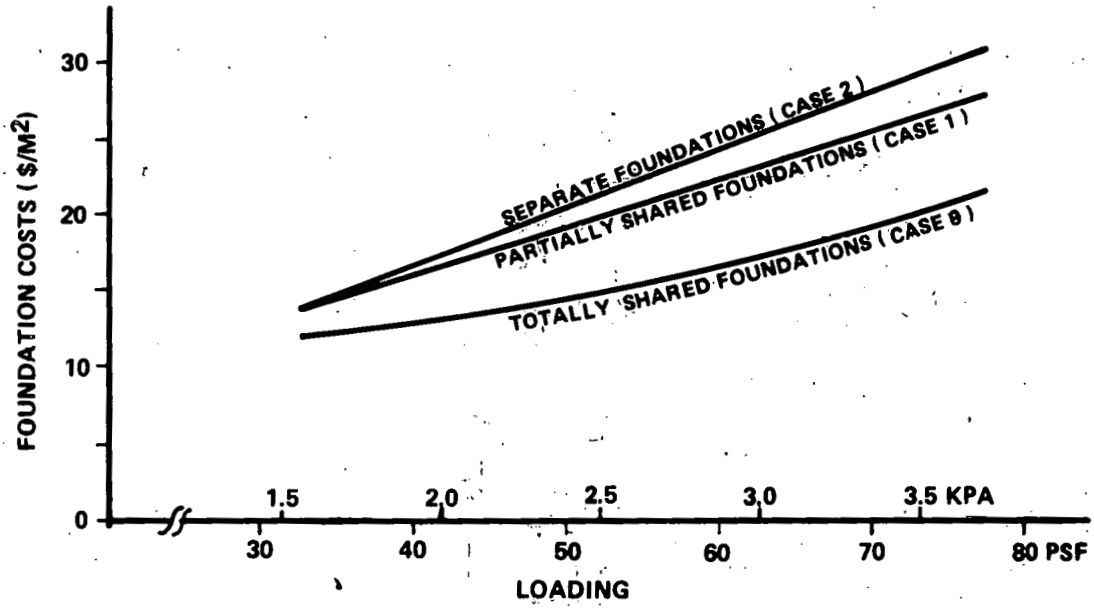

Figure 6-20 COST IMPACT OF SHARING FOUNDATIONS

the others in that the long axis of the foundation is perpendicular to the direction of applied load. For Case 9 the force resistance from lateral bearing on the soil is consequently larger than for Cases 1 and 2 collectively. Cases 1 and 2 have the short dimension of the foundations perpendicular to the direction of the applied load (in order to develop suitable overturning resistance). As a consequence, Cases 1 and 2 require more mass since they depend more on friction between the soil and foundation for resistance to horizontal motion than does Case 9.

One conclusion from this comparison is that Case 9 could benefit from a reduction in the requirement that the bottom end of the panel be located at least 0.61 meter (2 feet) above grade in order to prevent rain backsplash from puddles onto the modules.

Since Case 9 has a 0.4 meter (1.35 ft) wide concrete surface (i.e., the top of the foundation) under the entire length of the front lower edge of the panels, collection of dirt on the panels from backsplashes would be less likely than would be the case for Cases 1 and 2. Consequently, the 0.61 meter (2 foot) height above grade requirement should be reviewed for Case 9 because of the potential savings in structural (back strut) and foundation costs.

Foundation Conclusions. Several conclusions result from a review of the foundation work. One concern is the dependency of the foundation design upon the uplift force due to wind. Although uniform loading was used in the study to determine cost drivers, actual wind loading is random and, as a consequence, imposes more stringent design conditions on the structures. An investigation of building codes and other germane literature has revealed a lack of pertinent design information relative to wind loading on both structures analogous to photovoltaic module support structures and, more particularly, to large installations of sawtooth structures (i.e., an array field). Further work is needed to more accurately define the wind load environment. Wind tunnel testing can, for a given array configuration, wind velocity, and angle with respect to the array, more accurately define the load magnitudes, particularly in the upward direction. Close consideration of the aerodynamic shape is likely to be the quickest way to more accurately define foundation costs, since the cost data show that wind loads play the strongest single role

in controlling array costs. A further discussion on wind loading is presented in Section 7.3.

Another conclusion is that the final array designs should be based on soil values determined by site investigations which give special consideration to lateral bearing and sliding resistance coefficient values. Due to the variable nature of soils, it is not possible to make a simple table, such as provided by the UBC, that accurately describes the site soil values. Further, it is essential to know whether the actual values are higher or lower than those tabulated by the UBC. If the actual values are lower than UBC value, premature array failure could result. However, if the actual values are higher than UBC values, then array costs would be higher than otherwise necessary. A brief analysis estimated that array failures could result with upward loads of about 1.3, 1.9, and 2.9 kPa (28, 40, and 60 psf) instead of the 1.7, 2.4, and 3.6 kPa (35, 50, and 75 psf) loads considered, if the foundations were designed for UBC Class 3 soil and constructed on Class 4 soil instead. Damage would most likely be expected for the glass modules and silicon cells rather than the array structures. Array foundation costs could be 20 to 30 percent higher than necessary if the foundations were designed for Class 4 soil and constructed on Class 3 soil instead.

Another conclusion and recommendation is that later foundation optimization should attempt to devise foundations that more fully utilize the lateral bearing resistance of the soil. A comparison

of Case 9 with all other cases shows the improved lateral motion resistance possible for foundations parallel with the east-west axis instead of the north-south axis. Attempts were made in this study to parallel the east-west axis with foundations for other cases. However, this tended to increase the amount of concrete required to resist overturning because the relatively short dimension of the foundations is then perpendicular to the major load direction. Also, as mentioned, caisson-type foundations should be evaluated for sites with soils that are more cohesive than UBC Class 3.

Other conclusions and recommendations concerning foundations are discussed under the general topic of superstructure since, for completeness, they cannot be discussed separately.

Array Structure. The superstructure costs are lower than foundation costs by a relatively wide margin. However, this fact should not obscure the important role the superstructure plays in determining foundation costs.

In more normal structures, the wind uplift and horizontal forces are of less critical importance than is the case for these array designs. Usually every pound of building weight reduction results in a reduction in foundation costs.

For these array designs, the design intent was to minimize array superstructure steel costs by keeping superstructure weights low.

As a consequence, every pound of superstructure weight reduction would result in the need to increase foundation weights by a like amount. This study did not attempt optimizations of this kind, since no differentiation was made between live loads, and dead loads and consequently the superstructure dead load was not subtracted from the live load uplift. A tradeoff of a pound of steel for a pound of concrete would likely be cost effective. However, later optimizations may find it cost effective to utilize the foundation concrete more effectively by using concrete instead of steel in the superstructure. In doing so, however, it would be prudent to consider materials other than steel for the superstructure.

As mentioned under foundation discussions, the load magnitude has the most important effect on costs. Since the aerodynamic shape of the superstructure, rather than the foundation, controls the lift and drag, the effect of load upon cost is repeated here under the assumption that wind forces are those that predominate in the 1.7, 2.4, and 3.6 kPa (35, 50, and 75 psf) loads specified for this study. Wind tunnel testing is discussed in Section 7.3.

Unlike the foundations, the superstructure costs are determined by the downward, instead of upward, loads. For a more accurate determination of costs for wind loads, the downward loads should be accurately determined for use in superstructure design and the upward loads for foundation design.

A review of the superstructure costs shows that, in general, there is a greater variability than for foundation costs. This is attributable to the use of commercially available steel members and in estimating of costs.

Although some special sections were designed for this study, an optimized design for every case and load combination was not considered in the study scope. However, in later optimizations of particular cases, specially designed sections should be considered for quantities as large as needed for a 200 MWp plant. Those optimizations should closely consider shop fabrication cost variables.

The requirement for module surfaces to be 0.61 meters (2 feet) above grade should be reviewed. One reason is that the selection of many of the array back posts was strongly influenced by the slenderness ratio restrictions of the AISC, and, as a consequence, the calculated steel axial stresses were significantly lower than normally considered allowable and the steel used inefficiently. If the posts were concrete instead, the situation might be reversed. For either concrete or steel, however, costs will be reduced by minimizing the length of axially loaded members. That length could be minimized by reducing the 0.61 meter (2 foot) minimum height above ground requirement, particularly for Case 9 where the concrete sill formed by the foundation under the front lower edges of the panels will minimize dirt transported by backsplashing water.

Array Structure Conclusions. Conclusions concerning the superstructures, as a class, include:

- Aerodynamic shape should be more closely considered in later optimizations.
- Optimizations should consider the superstructure weight in conjunction with foundation weight.
- Dead loads and live loads should be considered separately as well as combined since, in foundation design, the dead load will reduce foundation weight requirements.
- Specially designed structural members should be considered more closely since a number of the case-load combinations resulted in a calculated section modulus need almost midway between the next higher and next lower available modulus. Further the differences between the next higher and next lower moduli were large compared to that calculated as required.

Section 7

ARRAY DESIGN SUMMARY

This section presents a summary, combining all the elements of the total array (i.e., modules, panels, array structures and foundations) discussed in the preceding section. The effects of wind forces, a major cost driver, is also discussed.

7.1 TOTAL ARRAY COSTS

Inspection of the panel cost estimate tables in Sections 5.2 and 5.3 show that glass superstrate module costs vary between $59.80 and $60.60 per square meter for all of the module sizes, panel sizes, and variations in loading considered in this study. The module costs uniformly bias the cost of the total array costs upwards by approximately $60/m². Thus, the module cost is not included in the array cost summary.

Table 7-1 summarizes the estimated total structural costs at 1.7, 2.4, and 3.6 kPa (35, 50, and 75 psf) for the nine array design cases evaluated. The lowest-cost panel type (see Table 5-22) appropriate for each of the array cases is added to the array structure and foundation costs to form the total array cost.

At 1.7 kPa (35 psf) loading, the array costs range between +6 and -8 percent of their average. At 3.6 kPa (75 psf) loading, the cost range widens to +17 and -13 percent of the average. Further

TABLE 7-1

ARRAY COST ESTIMATE SUMMARY (1975 $/m^2)

ARRAY CASE	PANEL TYPE	1.7 KPA (35 PSF) LOADING				2.4 KPA (50 PSF) LOADING				3.6 KPA (75 PSF) LOADING			
		ARRAY		PANEL FRAME	TOTAL (1)	ARRAY		PANEL FRAME	TOTAL (1)	ARRAY		PANEL FRAME	TOTAL (1)
		STRUCTURE	FOUNDATION			STRUCTURE	FOUNDATION			STRUCTURE	FOUNDATION		
1	C	7.50	14.60	18.00	40.10	11.20	19.10	21.30	51.60	13.50	27.00	26.30	66.80
2	C	8.30	14.80	18.00	41.10	9.00	20.70	21.30	51.00	9.90	29.80	26.30	66.00
3	D	8.30	15.10	15.40	38.80	9.80	20.00	16.70	46.50	11.10	28.70	19.10	58.90
4	C	10.50	13.80	18.00	42.30	10.70	19.00	21.30	51.00	14.40	30.40	26.30	71.10
5	I	8.30	13.80	20.90	43.00	9.20	20.70	26.40	56.30	10.80	31.00	37.00	78.80
6	C	7.40	16.50	18.00	41.90	7.40	23.30	21.30	52.00	7.40	28.20	26.30	61.90
7	J	7.40	14.90	14.70	37.00	8.70	20.10	20.30	49.10	11.00	28.60	26.10	65.70
8	J	11.50	14.40	14.70	40.60	13.70	21.30	20.30	55.30	19.00	30.40	26.10	75.50
9	—	—	12.10	26.90	39.00	—	14.40	34.10	48.50	—	20.70	45.30	66.00

(1) Module costs increase this total by approximately $60/m^2.

inspection of the table shows that foundation and panel costs are approximately equal and either is approximately twice the array structure cost. It is felt that the given assumption of uniform loading results in foundation costs that are higher than would be calculated for resolving the loading into its dead and live components since the dead load (e.g., panel weight) would be subtracted from uplift forces and thereby reduce foundation weight and cost.

Total array costs less the costs of the modules as a function of loading are presented graphically in Figure 7-1. This figure illustrates the strong dependence of costs on loading and the relatively narrow cost range for the nine designs, particularly at lower loadings. The Case 3 array design (1.2 by 2.4 meter (1.2 by 2.4 m (4 by 8 ft) foot)) intermediate supported panels with a 2.4 meter (8 foot) array slant height and 4.8 meter (16 foot) span is generally the lowest cost design at the higher loadings. Within the accuracy of the designs and cost estimates, it is difficult to select the lowest cost design at 1.7 kPa (35 psf) loadings.

7.2 COMBINED ARRAY AND PANEL DESIGN COMPARISONS

In this section, selected comparisons of the combined array and panel costs presented in Figure 7-1 are made in an attempt to determine structural cost drivers and sensitivities. As in Section 7.1, the costs are for array structures and foundations,

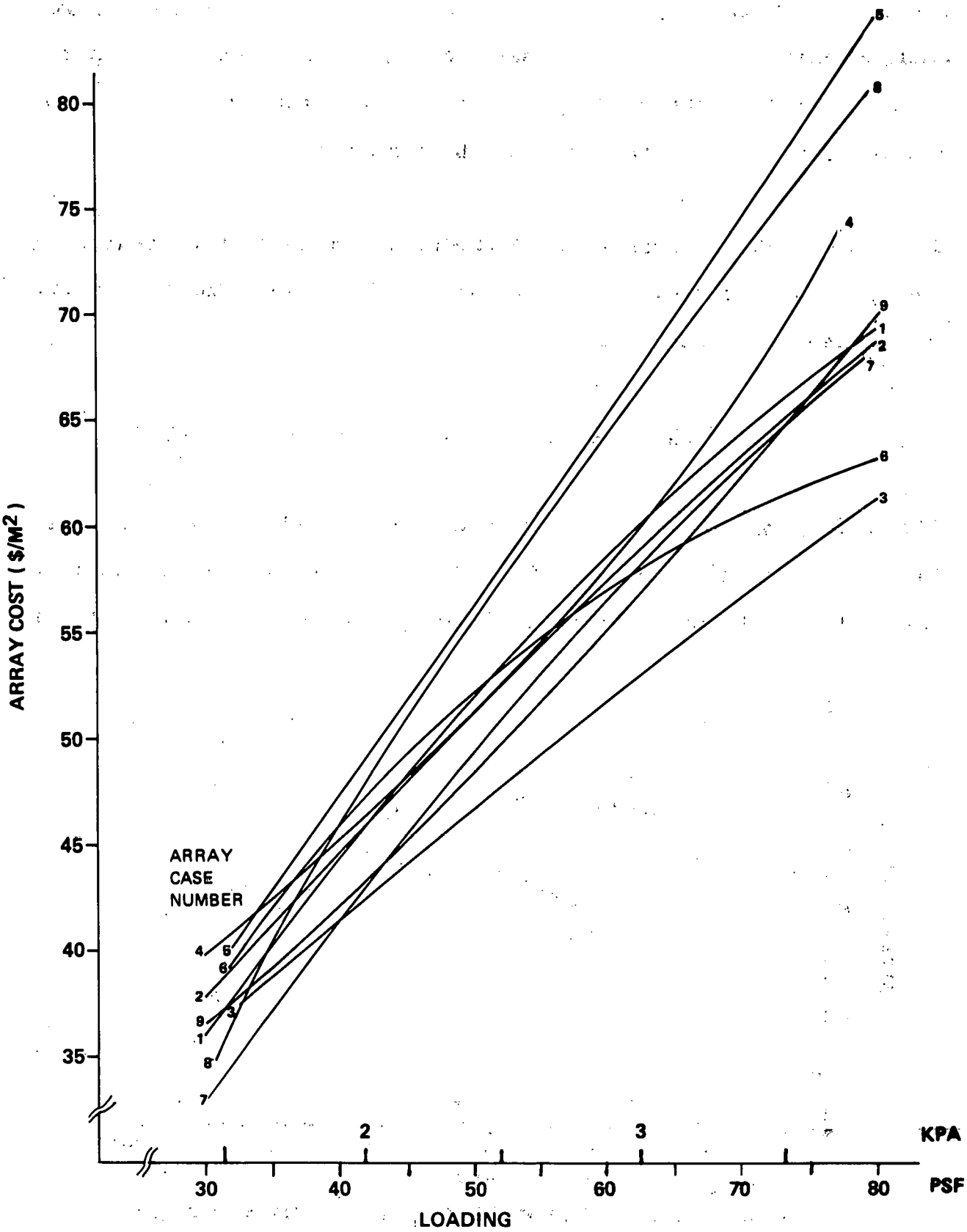

Figure 7-1 ARRAY COST VERSUS LOADING

and for the lowest cost panel suitable for each particular array configuration. Since the cost of the modules would uniformly bias all of the cost data upward by approximately $60/m^2$, the module costs are not included in the comparisons.

Each comparison is presented in order, building on the results of previous comparisons. The results of these comparisons are summarized in Section 7.2.6.

7.2.1 Beam Versus Post Support (Case 4 Versus Case 5)

Figure 7-2 compares the structural costs of a beam support configuration (Case 4) with that of a post support configuration (Case 5). At higher loadings, the beam support configuration is

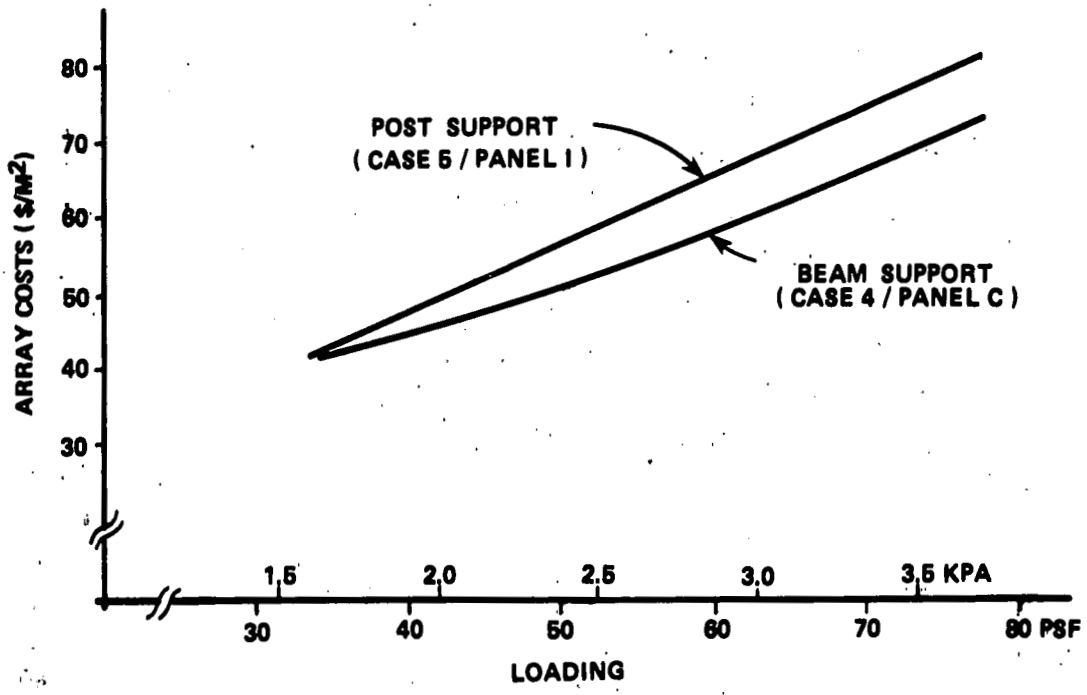

Figure 7-2 COST COMPARISON OF POST VERSUS BEAM SUPPORT

approximately 12 percent less costly than the post support configuration, while at 1.7 kPa (35 psf), the costs are approximately equal. Because of its lower cost at higher loads and its ability to accept a variety of panel types, the beam support configuration is considered advantageous.

The cost differences are due to the distinctly different designs for the two configurations.

The beam support configuration (Case 4 with panel Type C) features beams (siderails), mounted in the north-south direction, on which 1.2 by 2.4 meter (4 by 8 foot) panels are mounted. The beams (siderails) offer support for adjacent panels (i.e., sharing), and are designed for both axial and bending loads. The backposts are designed for axial loads only.

The post support configuration (Case 5 with panel Type I) allows no beam (siderail) sharing. Each 2.4 by 4.8 meter (8 by 16 foot) panel is connected to the cantilevered backposts by means of a sliding connection. As a result, the backposts, which are subjected both axial and bending loads, have greater strength and weight requirements than those for the beam support case. The long panel members (the closest analogy to the beams (siderails) of the beam support configuration) are designed for bending only. Consequently, these panel members were designed using higher allowable stresses than permitted for the beams (siderails) of the beam supported configuration.

7.2.2 Best Beam Support (Case 4 Versus Case 6)

As seen in Section 7.2.1, beam support is less costly than post support. Figure 7-3 compares the costs of supporting the beam (siderail) configuration in an intermediate location (Case 6) with that of an end location (Case 4). Since both of these arrays support the same number of Type C panels, the comparison is essentially between the two types of support locations. The costs seem to be virtually identical in the 1.4 kPa (30 psf) to 2.9 kPa (60 psf) load range and differ by approximately 13 percent at a 3.6 kPa (75 psf) load, although inaccuracies could have caused Case 6 costs to be higher than Case 4. The comparison between end and intermediate support of 2.4 meter (8 foot) slant height configurations (Case 1 versus Case 3),

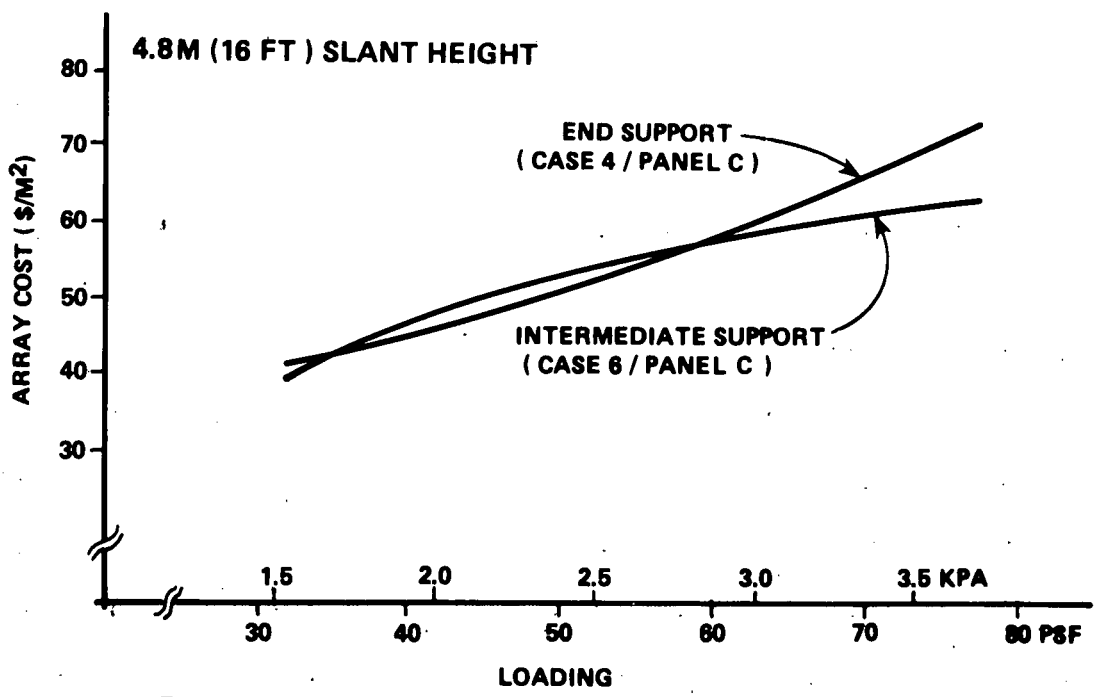

Figure 7-3 COST COMPARISON OF BEAM SUPPORT, INTERMEDIATE VERSUS END SUPPORT

Section 7.2.3, indicates an advantage to intermediate support. Intermediate support appears to have an advantage over end support assuming that the module design is not significantly affected by the differences in module support conditions.

If no axial loads were imposed on the siderails, the siderail for Case 6 would be expected to be of lighter weight than for Case 4 due to the reduced bending stresses. However, the siderails for both Case 4 and 6 must also resist axial forces and the axial forces for Case 6 are larger than for Case 4, resulting in an increase of the steel requirements for Case 6.

The backposts for Case 4 are longer and more lightly loaded than for Case 6. Unless optimized members are designed for the backposts for both cases, it would be difficult to assess the changes in cost due on one hand to a reduction in length (and L/r ratio) and on the other hand to an increase in axial load.

The fact that the costs differ more at the 3.6 kPa (75 psf) load condition could be attributed to use of commercially available members which are more efficient in the 1.7 to 2.4 kPa (35 to 50 psf) load range than was the case at a 3.6 kPa (75 psf) load condition, where the commercially available members were less suitable.

7.2.3 Best Girder Support

The effect of sharing foundations was discussed in Section 6.3.3 and, as was illustrated by Figure 6-20, there is a trend for foundation costs to decrease with increases in the degree of foundation sharing. With foundation costs a significant fraction of total support structure cost, as seen in Table 7-1, increasing the distance between foundations (and decreasing the number of foundations) through use of long spanning girders is one possible way of reducing costs. Three comparisons are made in this section: the best span--4.8 or 9.8 meter (16 or 32 foot)--for 4.8 meter (16 foot) slant height configurations, the best span--2.4 or 4.8 meter (8 or 16 foot)--for 2.4 meter slant height configurations, and the best support (intermediate or end) for 2.4 meter (8 foot) slant height configurations.

4.8 meter (16 foot) Slant Height--Best Span. Figure 7-4 compares the costs for a 4.8 meter (16 foot) girder span (Case 7) with a corresponding design for a 9.8 meter (32 foot) girder span (Case 8). There is a consistently lower cost shown for Case 7 as compared to Case 8. The difference is of the order of 10 percent with Case 8 as the base.

Further studies should consider 4.8 meter (16 foot) slant height girder configurations with spans in the range of 2.4 to 4.8 meters (8 to 16 feet) to determine if there is any advantage

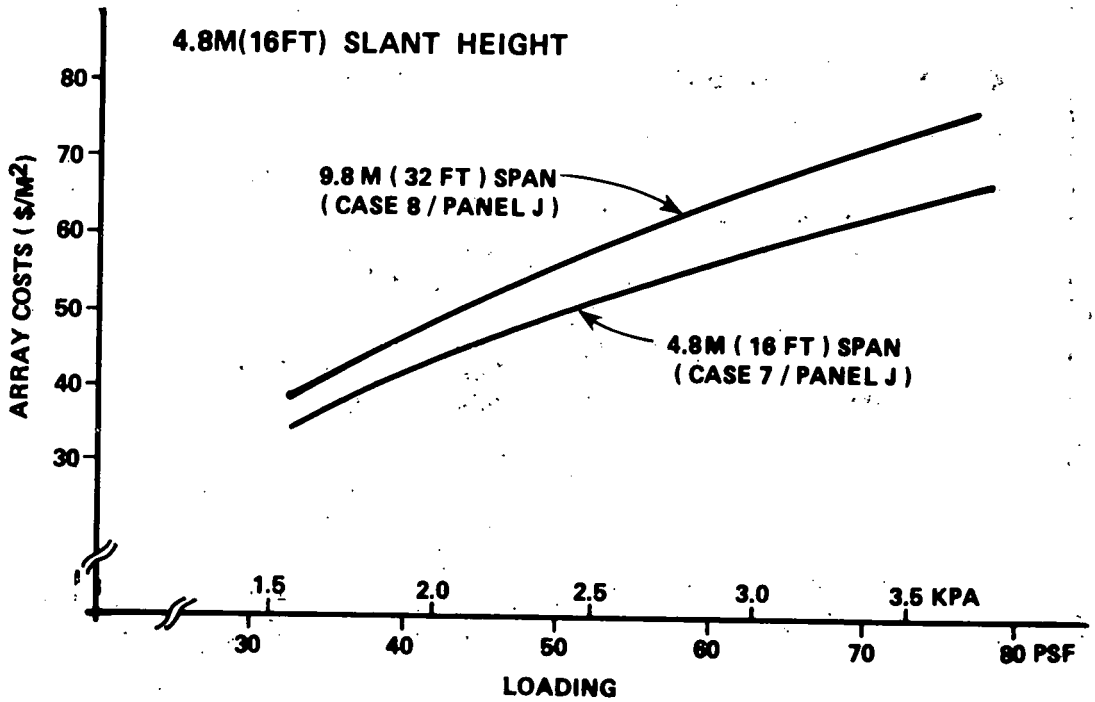

Figure 7-4 COST COMPARISON OF GIRDER SPAN

to spans less than 4.8 meters (16 feet) unless the soil conditions are not as good as assumed.

<u>2.4 meter(8 foot) Slant Height--Best Span</u>. As seen in Table 7-1, the costs for a 2.4 meter (8 foot) girder span (Case 2) and a 4.8 meter (16 foot) girder span (Case 1) configurations utilizing end supported 2.4 meter (8 foot) panels are equal.

<u>2.4 meter (8 foot) Slant Height--Best Support (Intermediate or End)</u>. Figure 7-5 compares the costs of end support (Case 1) with intermediate support (Case 3) for 4.8 meter (16 foot) girder spans. Case 3 is consistently lower cost than Case 1 (i.e., 10 percent) for 2.4 kPa to 3.6 kPa (50 to 75 psf) loading; Case 3

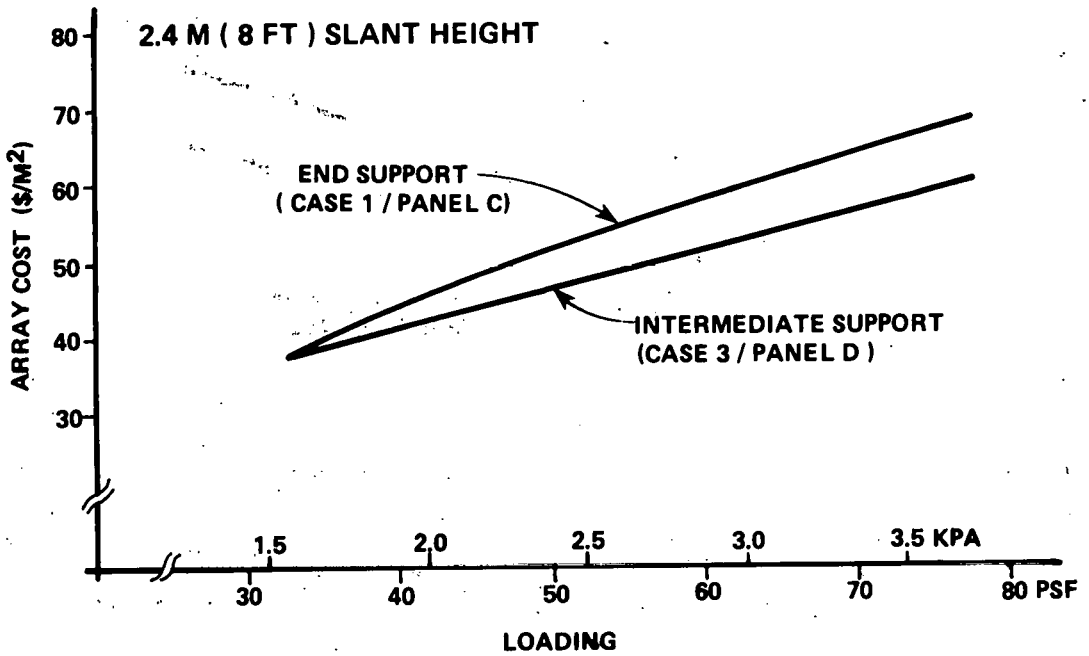

Figure 7-5 COST COMPARISON OF GIRDER SUPPORT

is nearly equal in cost to Case 1 at 1.7 kPa (35 psf), being within 3 percent.

Summary. On the basis of the above comparisons, a 4.8 meter (16 foot) girder span for 4.8 meter (16 foot) slant height configurations appears advantageous although additional studies should determine whether there is any advantage in girder spans less than 4.8 meters (16 feet). For 2.4 meter (8 foot) slant height configurations, there is no apparent advantage to decreasing the girder span. However, there is an advantage to using intermediate support rather than end support with girder span configurations.

7.2.4 Best Beam Support Versus Best Girder Support (Case 6 Versus Case 7)

The previous sections have indicated that for beam support configurations, intermediate beam support is advantageous (Section 7.2.2); for girder support configurations, 4.8 meter (16 foot) girder spans and intermediate panel support are advantageous (Section 7.2.3). The costs of these two configurations, Case 6/panel type C and Case 7/panel type J, respectively, are compared in Figure 7-6. At 1.7 kPa (35 psf), Case 7 is 12 percent less costly than Case 6. At 2.4 kPa (50 psf), Case 7 is 6 percent less costly than Case 7. However, with loads greater than 2.9 kPa (60 psf), Case 6 becomes less costly than Case 7; at 3.6 kPa (75 psf) Case 6 is less costly than Case 7. Load level, therefore, dictates the best configuration. At lower loads, the girder support configuration with intermediate panel support is advantageous. Whereas, at higher loads, the beam support configuration with intermediate beam support is advantageous.

7.2.5 Best Slant Height (Case 3 Versus Case 7)

Girder support, as was described in Section 7.2.4, is advantageous for lower loads, whereas beam support is advantageous for higher loads. One remaining question concerns optimum slant height. Figure 7-7 compares the cost of two similar girder support configurations, the only difference being slant height--a 2.4 meter (8 foot) slant height (Case 3 with panel

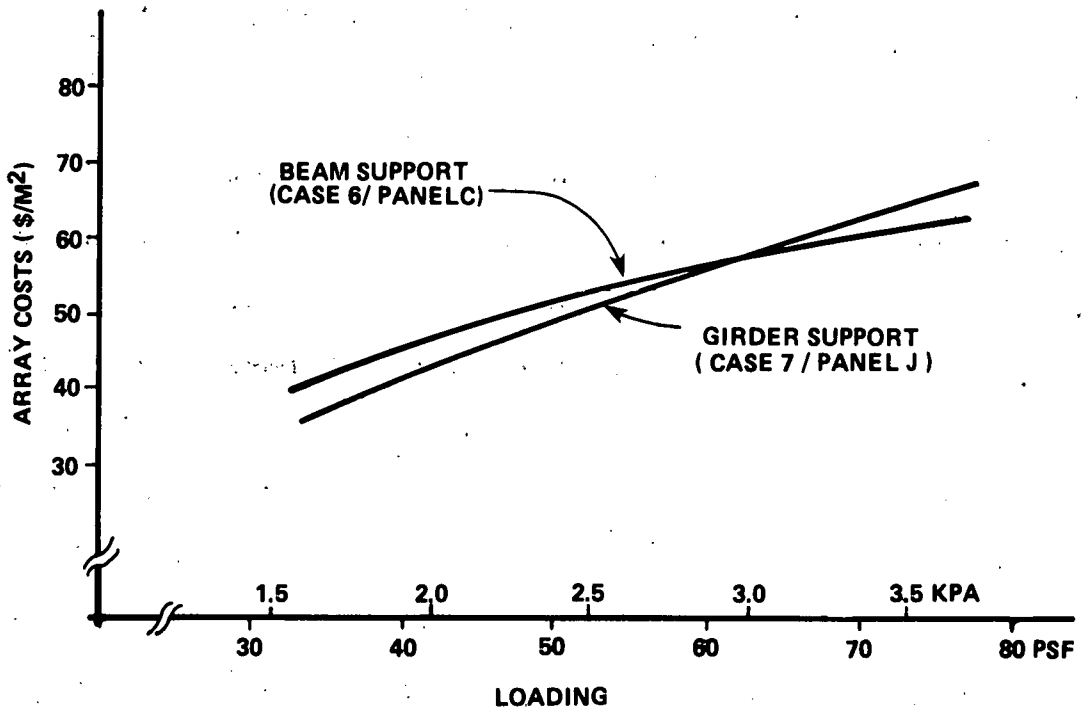

Figure 7-6 COST COMPARISON OF BEAM VERSUS BEST GIRDER SUPPORT

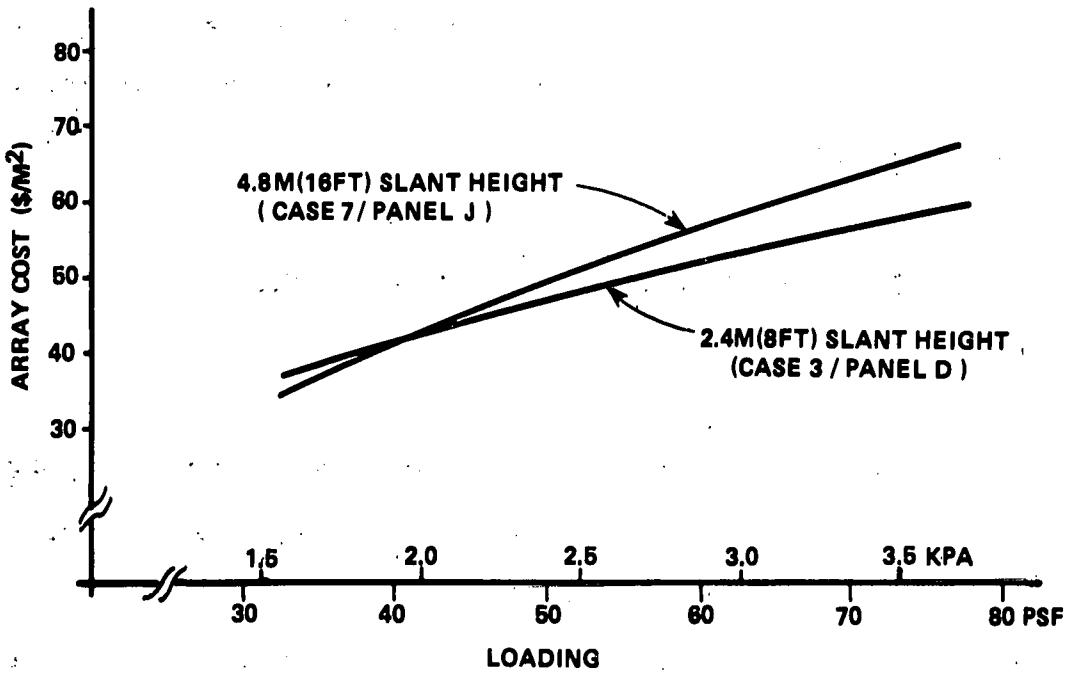

Figure 7-7 COST COMPARISON OF SLANT HEIGHTS

type D) versus a 4.8 meter (16 foot) slant height (Case 7 with panel type J). At 1.7 kPa (35 psf), Case 7 is 5 percent less costly than Case 3. However, with loads greater than 1.9 kPa (40 psf), Case 3 becomes less costly than Case 7; at 2.4 kPa (50 psf) Case 3 is 5 percent less costly than Case 7, and at 3.6 kPa (75 psf), Case 3 is 10 percent less costly than Case 7. Here, again, load level dictates the best slant height. At low loads, a 4.8 meter (16 foot) slant height is advantageous. Whereas, at high loads, a 2.4 meter (8 foot) slant height is advantageous.

7.2.6 Comparison Summary

From the cost comparisons made in the preceding portion of Section 7.2, it can be concluded that:

- Foundation sharing leads to lower costs
- Intermediate support designs are less expensive than end support designs
- Girder support configurations with 4.8 meter (16 foot) slant heights and 4.8 meter (16 foot) girder spans are less costly than those with the same slant height but with 9.8 meter (32 foot) girder spans
- The best support configuration is load dependent
  - At low loading preferred support features are: 4.8 meter (16 foot) slant height, girder support configuration with 4.8 meter (16 foot) girder span, intermediate panel support, and 2.4 by 4.8 meter (8 by 16 foot) panels.
  - At high loading preferred support features are: 2.4 meter (8 foot) slant height, beam (siderail) support configuration with intermediate beam

(siderail) support, and 1.2 by 2.4 meter (4 by 8 foot) end supported panels.

- For loading levels less than 1.7 kPa (35 psf), there is great difficulty in drawing conclusions. Should wind loading studies indicate loading levels less than 1.7 kPa (35 psf) are possible, additional optimization studies would be needed because of the uncertainty in the lower loading regions.

Also, it should be pointed out that arriving at several of the above conclusions borders the bounds of accuracy for the design and cost estimates.

7.3 WIND FORCES

The study has shown that structural loads are a major cost driver for the panels, array structures and foundations. As discussed earlier, the loads in this study were assumed to be uniform and act in both directions normal to the panel surface. The loads were not separated into components (e.g., dead loads, wind, etc.), although wind forces are implicit in the upward loads.

The study has shown that the lateral (horizontal) forces concurrent with uplift forces are the major determinant for foundation costs and therefore are a major cost driver (see Section 6.3.3). For naturally occurring loads, only wind and earthquake can create concurrent upward and sideward forces. Consequently, the wind loads must be accurately estimated, otherwise excessive array costs or structure failures may result.

For the arrays studied, there are two major, interrelated uncertainties related to wind.

One uncertainty is the estimate of true wind velocity variation with height above grade. Typically, designs are based on velocities 10 meters or more above grade because of inadequate knowledge of wind speed variation at lower elevations. That velocity basis is considered conservative because of the observed phenomenon that wind shear reduces velocity with decreasing height. Figure 7-8 shows design wind loads specified by ANSI (Ref. 7-1) for a wind velocity of 4.47 meters per second at a height of 9.1 meters (100 mph at a height of 30 feet) above ground. As can be seen on the figure, the code makes no allowance for decreases in wind velocity for heights below 9.1 meters (30 feet). This is due to uncertainty in wind behavior below this height.

Also included on the figure is the pressure calculated from the classical equation in which pressure varies with height to the 0.232 power. Logically, the lower height arrays would be impinged by lower velocity winds, a factor not within the scope of this study. Further, the local wind velocity is considered to be affected by the terrain roughness, with the greater roughness generally resulting in lower velocities. The plant studied is so large (about 3.6×10^6 square meters (1.4 square miles)) as to produce an equivalent velocity reduction due to natural terrain roughness if wind channeling effects are avoided. Wind tunnel

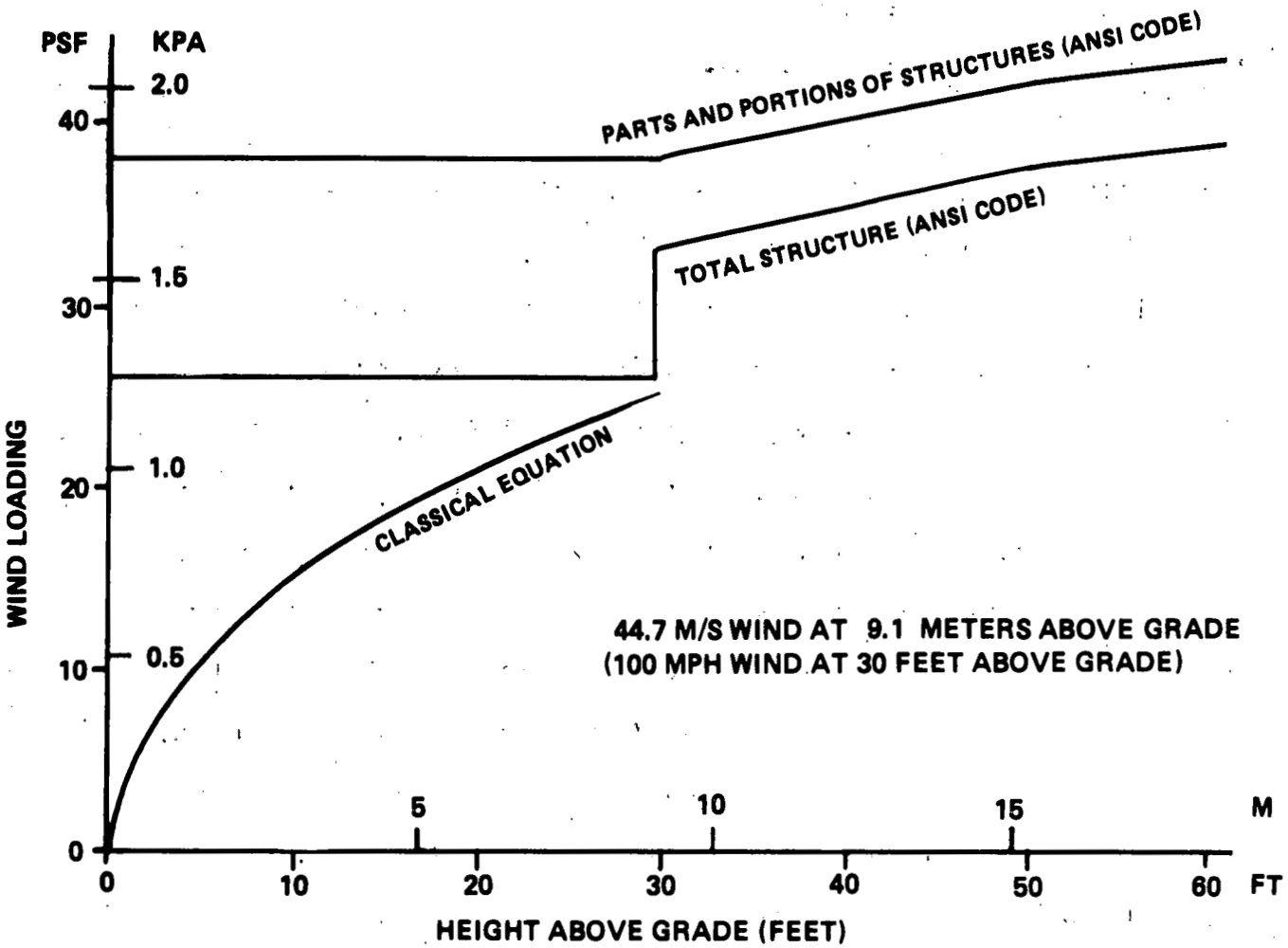

Figure 7-8 WIND LOADING VERSUS HEIGHT ABOVE GRADE

testing varies the roughness of surfaces upwind of the model under test when this parameter is considered significant. In this case, it is recommended that the roughness effect of the array on wind velocity within the array be investigated.

Further, it is recommended that the testing provide a better estimate of the velocity of the wind (that approaching the

array), at heights closer to array heights than the 30 foot (10 meter) standard.

Uplift, combined with drag, was found to be the major determinant of array foundaton cost for whatever wind velocities assumed in establishing the 1.7, 2.4, and 3.6 kPa (35, 50, and 75 psf) loads for this study. Typically, lift and drag vary with the aerodynamic shape as well as wind angle of attack and velocity. Often, the use of spoilers on airfoils is an effective way of reducing drag or lift as desired. Spoiling can be effected by one of several means that involve creating local wind pressure and velocity areas favorable for either minimizing or maximizing either lift or drag. For example, an array with slots as wind channels between panels or modules will react differently to a given wind velocity than one which presents a solid front even though the total solid areas are identical. This is particularly true for fluttering induced by turbulences. Further, the separation angle, between a surface and the wind stream lines leaving the surface is almost as an important determinant of lift and drag as the undisturbed wind relative velocity and small detail changes can result in significant force changes.

As an example of changes that can significantly alter wind forces on a structure, consider the Case 9 array configuration (see Section 6.2.9). If an inexpensive cover for the sloping back legs were designed, then wind from the north would impinge on it and create a downward force which would tend to counterbalance

uplift on the leeward (south) side of the structure. As a result, net lift may decrease and thereby decrease foundation costs. The tradeoff would be an increase in superstructure costs because of the added cover, and the decrease in foundation costs because of the decreased lift. This cover could also be a reflector panel and its addition would increase the energy generated by the solar panels. Reflector augmented designs have been evaluated in several studies (Refs. 3-2 and 7-2).

Because of the cost sensitivity and common mode failure of the array structure to wind forces, wind tunnel testing is recommended for optimizing aerodynamic shape and array costs, as well as specifying forces to be considered in design.

THIS PAGE

WAS INTENTIONALLY

LEFT BLANK

Section 8

CONCLUSIONS

This section presents major conclusions derived from the conduct of this study.

8.1 MAJOR COST DRIVERS

Design loading is found to be the most significant cost driver in the ±1.7 kPa (35 psf) to ±3.6 kPa (75 psf) range considered. Depending on the design, panel and array structure, and foundation costs increase by \$20 (50%) to \$36/m² (85%) in going from 1.7 kPa (35 psf) to 3.6 kPa (75 psf). The percent cost changes are based on 1.7 kPa (35 psf) loads.

Increasing module size from 0.6 by 1.2 m (2 by 4 ft) to 1.2 by 2.4 m (4 by 8 ft) decreases the panel's estimated cost by \$5 to \$15/m², depending on panel size and loading. The cost change is an increase of about 15 to 75 percent, with the 1.2 by 2.4 m (4 by 8 ft) module panels cost as a base.

Panel frames supported at intermediate points along their long edge are estimated to cost \$3 to \$11/m², approximately 15 to 45 percent, less than panel frames supported at their ends. The cost benefit depends on loading, panel size and module size. However, the panels designed for these conditions are generally subject to more complicated bending moment variations and so may

be more likely to fail when service conditions deviate from those assumed in the design.

Generally, 1.2 by 2.4 m (4 by 8 ft) panels are less costly on a normalized basis (i.e., $/m²) than 2.4 by 4.8 m (8 by 16 ft) panels. The cost benefit ranges from -$1 to $12/m², depending on panel configuration and loading.

A preliminary estimate indicates that the cost of a curved glass superstrate panel configuration would be about one half to one third that of the lowest-cost conventional panel configuration evaluated, depending on loading. Further study is needed to determine if the total structural cost (array foundation, array structure, and panel structure) would be less than the cases studied herein.

8.2 MODULES

The brief analysis conducted in this study indicates that a glass superstrate module would be slightly less expensive than a metal substrate configuration. Concluding which module type is least costly requires a detailed study, such as those being conducted as a part of JPL's Automated Array Assembly Task.

Unlike the panel and array, the cost of the glass superstrate module evaluated in this study is virtually unaffected by loading. This is because the glass was constrained to be thicker

than 3.2 millimeter (0.125 inch) for reasons of hail resistance and the size of commercially available tempered glass.

Several methods exist for calculating the thickness of glass needed to resist a uniform loading. Linear methods generally overspecify the required thickness. Nonlinear computer analyses lead to more accurate specification of thickness, but are very expensive to run. Thickness versus loading data derived from glazing industry experience varies among manufacturers. The results depend on the method used and indicate a need for a more consistent methodology.

Consideration of the economics of light absorption in glass superstrates leads to the selection of tempered glass over lower priced but thicker annealed glass. Further, 0.05 percent iron drawn glass is more economic than 0.01 percent iron, rolled glass for present glass pricing, cell costs of $\$40/m^2$, and projected balance-of-plant costs (reduced to 1975 $). With present (1978) cell costs, the 0.01 percent iron glass should be used.

Experience in the cable industry indicates that some module encapsulating materials may have to be thicker than required for weatherability in order to provide long-term electrical insulation at the voltage levels estimated as being economic for central station power plants (e.g., 1,500 volts). Material thicknesses postulated by most panel fabricators appear to be

adequate for voltage levels currently being used (e.g., less than 500 volts).

8.3 PANELS

Panel costs increase significantly with increases in loading.

Panels supported at intermediate points along their long edge are less costly than equivalent panels supported at their ends. However, further analysis is required to assure that the lower cost of intermediate supported panels is not offset by the effects of reverse bending on glass thickness selection, the movement of the support location with applied loading, and nonuniform loading.

A 1.2 by 2.4 m (4 by 8 ft) module size appears to result in minimum panel cost. Smaller sizes are more costly because of more panel steel framing. Much larger sizes require thicker glass which results in more light lost to absorption and thereby, higher costs for a fixed level of power output.

For the designs evaluated, the cost ($/m) of 1.2 by 2.4 m (4 by 8 ft) panels is generally less than for the 2.4 by 4.8 m (8 by 16 ft) panels. The opposite was found in a study by Bechtel (Ref. 3-2) for 1.2 by 2.4 m (4 by 8 ft) foot panels installed on single panel array structures (as opposed to the four panel array structures evaluated in this study). A

composite conclusion drawn from the two studies is that in order to be economical, several small panels must be installed on large array structures and not as single panel array structures.

The curved superstrate glass module has a potential for greatly reducing panel costs. The small amount of curvature required does not reduce panel conversion efficiency.

8.4 ARRAY STRUCTURES AND FOUNDATIONS

Array structure and foundation costs are a strong function of loading, increasing at an average rate of $0.5/m² per psf of loading.

In general, there is little difference in the array structure/foundation costs for the arrays evaluated.

Foundation costs are approximately double the cost of the array structures. Foundation costs could be reduced by resolving the loading into its component parts (e.g., subtract the dead load from the live load uplift); finding other methods to prevent rain spashback (e.g., plastic shields) so that foundations can be set deeper and utilize soil resistance more effectively (particularly for the foundations in Case 9); and performing wind tunnel tests to more accurately define wind forces on structures close to the ground.

Although caisson foundations wre not evaluated in detail (because they generally are not as suitable as spread footing foundations in gravel-type UBC Class 3 soils specified for purposes of this study), caissons may prove cost effective for sites with a more cohesive type of soil.

8.5 COMBINED ARRAY AND PANEL

It was found that lower costs may result from sharing foundations and using 4.8 meter (16 foot) girder spans as opposed to 9.8 meter (32 foot) span (for 4.8 meter (16 foot) slant heights). The optimum support conditions was found to be dependent on loading. Also, clear conclusions cannot be drawn for loadings of 1.7 kPa (35 psf), or lower, because of the similarity in costs for the cases studied.

Section 9

RECOMMENDATIONS

In view of the relative costs of foundations, a study should be made to find ways of reducing their cost. The study should include array structures, trade-offs between structure and foundation costs, a reduction in the two foot minimum height specification, and the effect of postulated nonuniform wind loading for low height structures.

In view of the low foundation cost for Case 9, this concept should be pursued by parametrically evaluating 1.2 by 2.4 m (4 by 8 ft) and 2.4 by 4.8 m (8 by 16 ft) panels with the short and long edge horizontal and with end and intermediate support. Further, since this array concept has a concrete sill under the lower edge of the panel, the 0.61 meter (two foot) minimum height to prevent rain splashback should be reevaluated and possibly reduced. Also, the effect of adding a reflector panel to (or instead of) the back leg should be evaluated with respect to increasing energy output for little additional cost and possibly reducing wind forces transmitted to the foundations.

The lowest cost, intermediate supported panel designs should be reevaluated assuming a postulated, nonuniform wind loading.

The lowest cost panel designs should be evaluated for frame materials other than steel. When evaluating other panel

materials, care must be taken to assure compatibility with the array structure (e.g., galvanic corrosion between aluminum panel members and steel array members could increase maintenance costs).

The curved glass superstrate concept should be pursued further with respect to manufacturability, array design and installation requirements, and evaluation of the clip design, location and size using a finer finite-element mesh in the vicinity of the clips.

Long term electrical insulation requirements for high voltage arrays should be investigated further to establish module costs versus system voltage and facilitate setting optimum system voltage for large plants.

Since actual performance data will be a large factor in the ultimate determination of module insulation requirements, performance tests should be initiated as soon as possible. To accomplish this, one or more modules (either existing or special designs) could be mounted outdoors, biased to about 1000 volts dc with respect to ground, and operated to simulate the actual conditions to which full scale power plant modules will be subjected. Periodic injection of transient overvoltage pulses, followed by measurement of insulation resistance and other significant parameters, would provide valuable data as to the

long-term performance of module insulation systems under central station photovoltaic power plant conditions.

Wind loading should be looked at in depth. When the available design options and tradeoffs are better understood, wind tunnel tests should be conducted to better establish the forces acting on structures close to the ground, the force distributions resulting from the nonuniform wind distribution, the forces on panels at the edge and center of a large array field, and the effects of terrain roughness discussed in Section 7.3. It is anticipated that the results of such testing would allow lower design loads to be used and thereby reduce costs.

Criteria for hail resistance should be established to allow comparison of various module designs on a uniform basis. Such comparisons might include assessing a hail damage cost penalty based on the risk of hail damage in conjunction with panel replacment costs and/or insurance costs.

THIS PAGE

WAS INTENTIONALLY

LEFT BLANK

Section 10

NEW TECHNOLOGY

During the conduct of this work, Bechtel found that applying the principles of the arch to photovoltaic glass superstrate module designs has potential to significantly reduce panel costs. Preliminary calculations indicate that the resulting curved glass module design's conversion efficiency would be virtually identical to that of corresponding flat plate designs now being used.

THIS PAGE

WAS INTENTIONALLY

LEFT BLANK

COMPUTER ANALYSES

This appendix presents details of the nonlinear structural analyses summarized in Section 4.5. The presentation in this appendix assumes that the reader has some knowledge of structural design, its terminology, and finite element analyses. The three support concepts for a 1.2 by 2.4 m (4 by 8 ft) glass superstrate module analyzed are:

- Case I - a flat glass plate, continuously supported along the edges as in a picture frame.
- Case II - a flat glass plate supported at four points on the long sides by 0.3 meter (12 inch) long clips.
- Case III - a curved glass plate supported at four points on the long sides by 0.3 meter (12 inch) long clips.

For all three cases, the plate was a 1.2 by 2.4 m (4 by 8 ft), 4.7 millimeter (0.187 inch) thick, annealed glass sheet. For convenience, the figure showing the configurations of these three module support concepts is shown in Figure A-1.

At the loadings specified for this study (1.7, 2.4, and 3.6 kPa (35, 50, and 75 psf)), the deflections of the flat plates are much larger than the thickness of the plate and therefore require nonlinear analyses to indicate their true behavior. Because of the large deflections, significant membrane action occurs along with the bending of the glass.

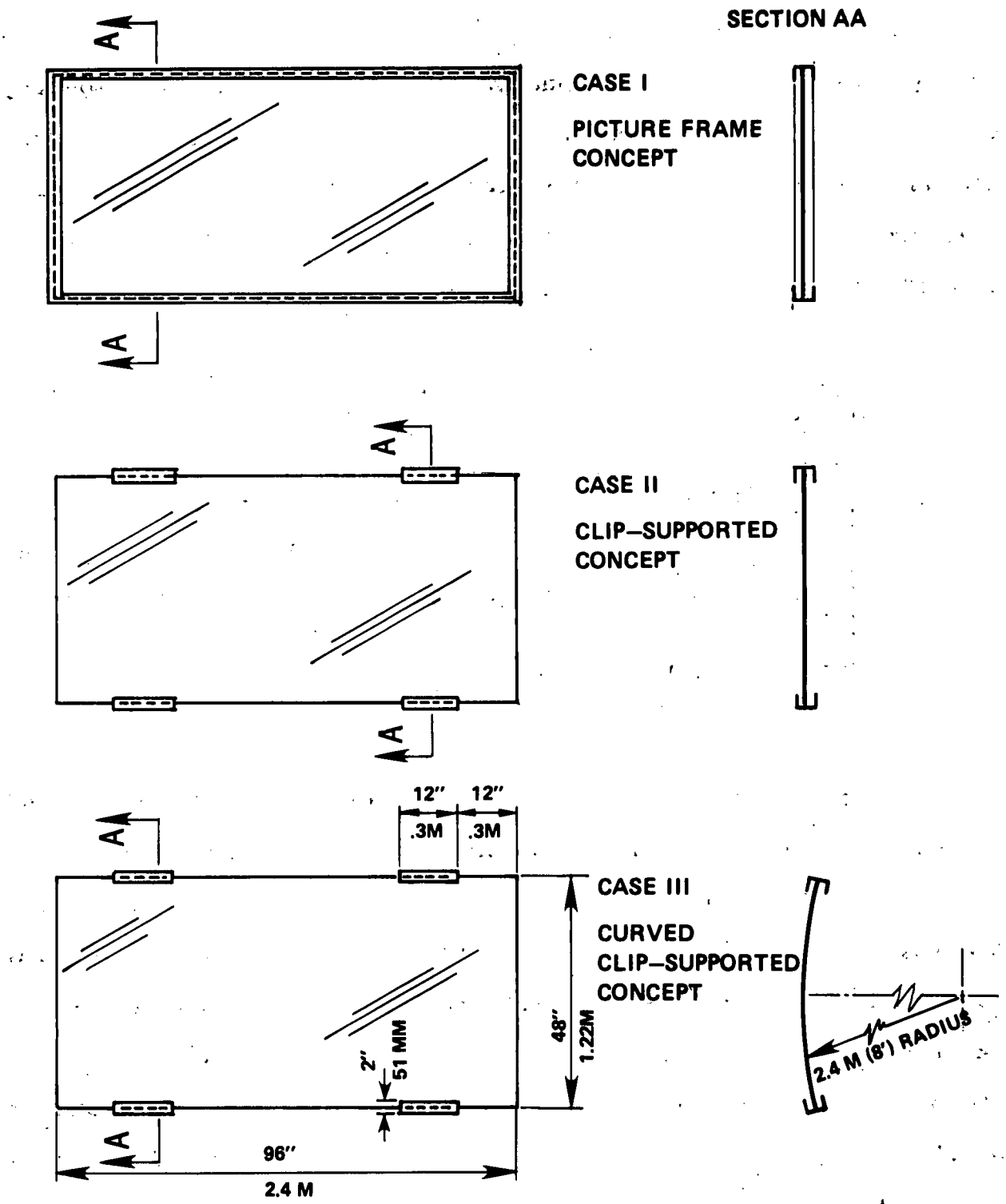

Figure A-1 GLASS SUPERSTRATE MODULE CONCEPTS

The ANSYS computer program was selected for the structural analyses. This program is commercially available and has had extensive use throughout industry. However, care was taken to verify the results of the analyses. This was done by comparing Case I results with available experimental results. After discussions with ANSYS consultants, the STIF53 element was selected for the model. Development of the model (or finite element mesh) was based on the following criteria:

- The mesh should be applicable for all three cases analyzed.
- The mesh regions should be fine enough to accurately model behavior around stress concentrations.
- There should be no large aspect ratios for the elements.
- There should be no abrupt or discontinuous changes in mesh.
- Symmetry should be used so that only one quarter of the plate is analyzed.

The nonlinear analysis uses a combination incremental and iterative approach for the solution. The ANSYS program compiles the stiffness matrix for each loading for the structure being analyzed, solves, through matrix methods, for the displacements and then uses these displacements to calculate and compile a new stiffness matrix for the next iteration or load increment. These steps are repeated for either a specified number of iterations or until a deflection tolerance is met. The analyst usually limits the number of iterations in order to control costs. The degree of convergence of the solution with increasing numbers of

iterations can be judged by checking equilibrium and changes in the reported displacements. Perfect convergence would generally require a very large number of solutions of the structural system and become very costly. The results reported here represent a solution estimated to be within 10 percent of perfectly converged values.

The stresses reported and plotted herein are principal stresses. In the stress plots, an "X" indicates maximum tensile stresses and an "O" indicates maximum compressive stresses. Similarly, for displacement plots, an "X" indicates maximum positive displacement and an "O" indicates maximum negative displacement. Dashed lines indicate a zero stress or change in the sign of the field being plotted. For Case I, the center stress plotted is that calculated from interpolated moments and loads ("tractions") which are reported at the element centroids.

A.1 CASE I - PICTURE FRAME CONCEPT

A 1.2 by 2.4 m (4 by 8 ft) glass superstrate module was selected for the analysis because it was one of the sizes being evaluated in the study and because experimental data was available for this size (Ref. 4-22). The 4.7 millimeter (0.187 inch) thick, annealed glass was selected to allow comparisons to be made with the experimental data.

The experimental data indicated that high stress concentrations will be present near the corner of the plate (e.g., coordinates X=5", Y=5"). Similarly, high stresses can reasonably be expected to occur near the clip supports for Cases II and III. Thus, a fine mesh is required in these regions. To reduce computer run times, a coarser mesh was used for the interior regions of the plate where lower, less rapid changes in stress levels are expected to occur. The finite element mesh used for Case I is shown in Figure A-2.

The model was verified in two ways. Comparisons were made with a closed form solution (Ref. 4-19) and with experimental data (Ref. 4-22). Figure A-3 shows experimental and computer calculated stress levels as a function of applied load. Computer calculated stress levels are shown for both the center (mesh element 260, Figure A-2) and the "corner" (mesh element 53) of the plate. As can be seen from the figure, the point of highest stress changes from the center of the plate to the corner of the plate as loading is increased. Also evident is the good agreement with actual stress levels measured in PPG's experiments.

Figure A-4 shows displacements versus loading as calculated by linear methods, the nonlinear ANSYS program, and from experimental data. As with the stress levels, there is good agreement between the ANSYS calculated displacements and those measured by PPG. The stresses for the top and bottom surface are calculated in these analyses and are also resolved into principal

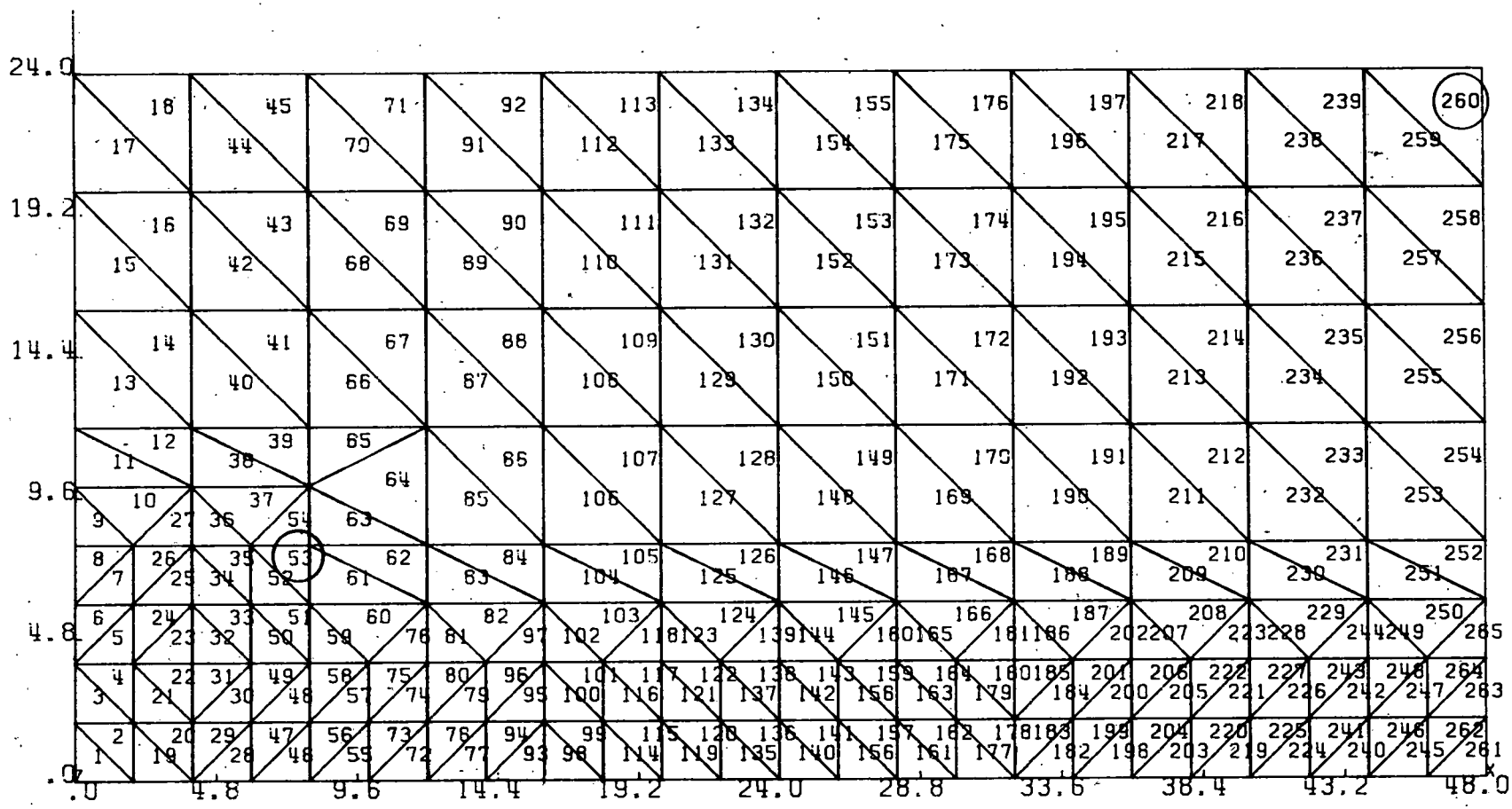

Figure A-2 FINITE ELEMENT LAYOUT FOR CASE I

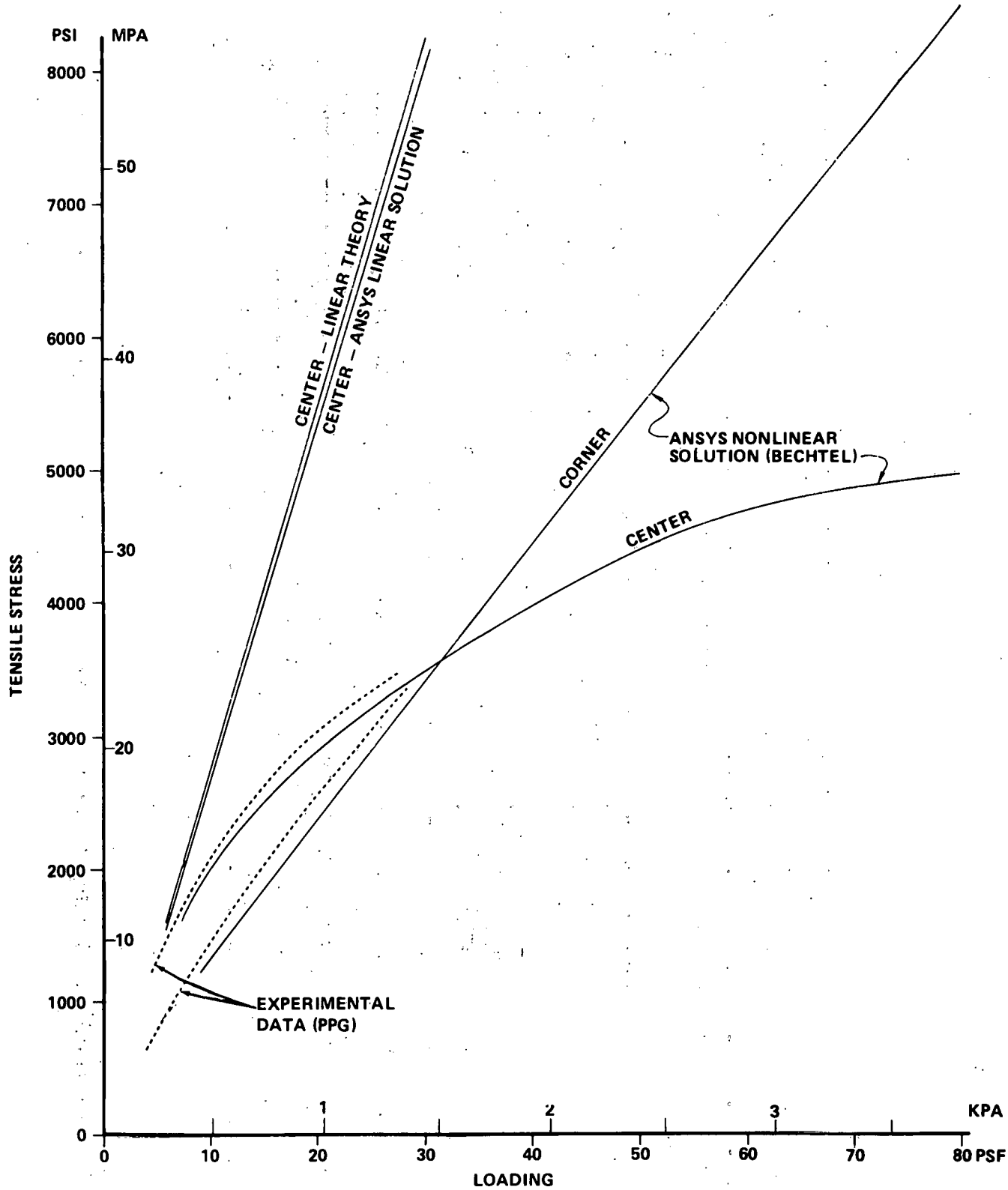

Figure A-3 CASE I TENSILE STRESS VERSUS LOADING

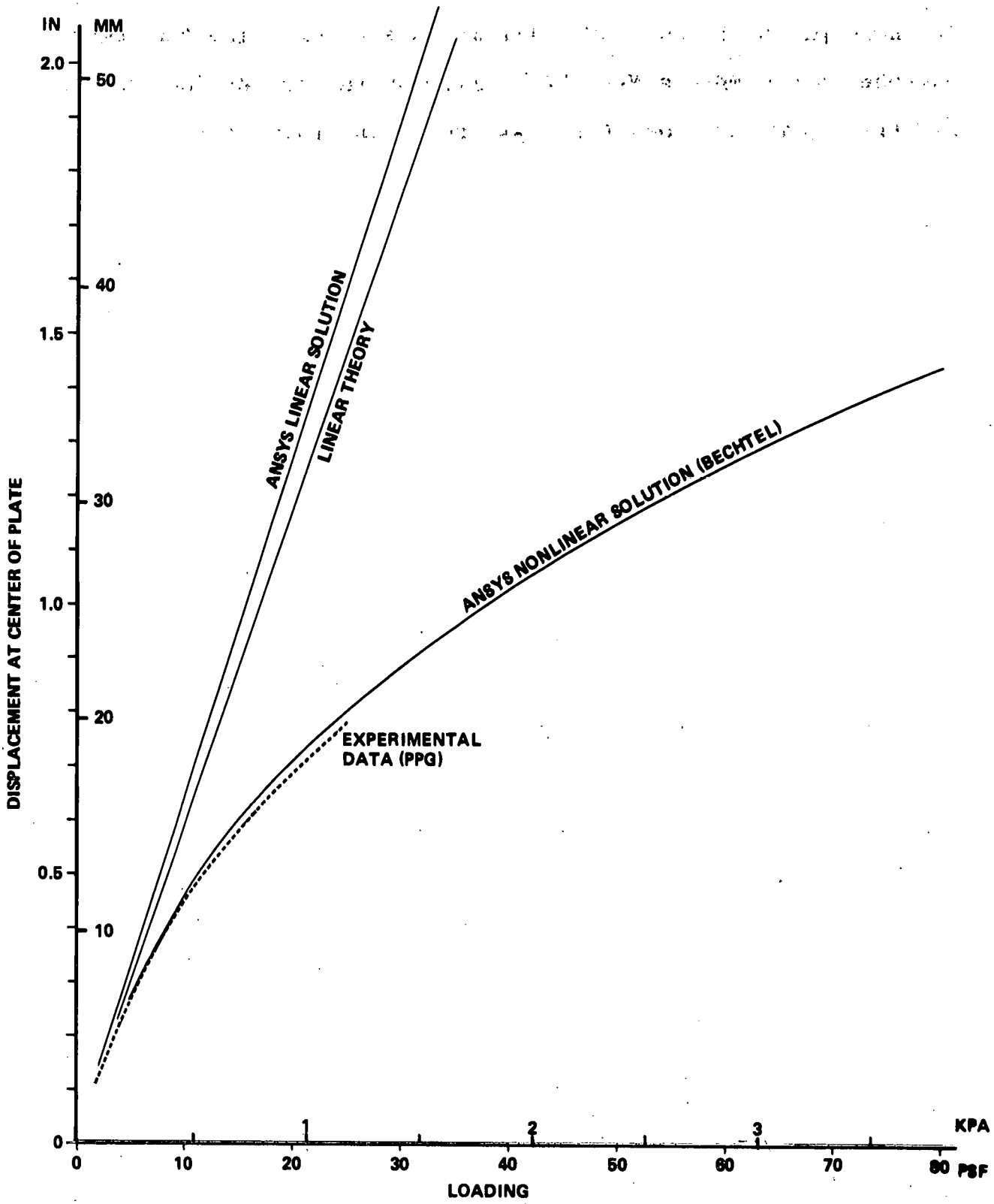

Figure A–4 CASE I DISPLACEMENT VERSUS LOADING

stresses. The contours of maximum and minimum principal stresses are shown in Figure A-5 to A-8 for the top and bottom surfaces. In these plots the positive stresses are tensile and the negative stresses are compressive. The corresponding deflection contours for the successive load steps are shown in Figure A-9.

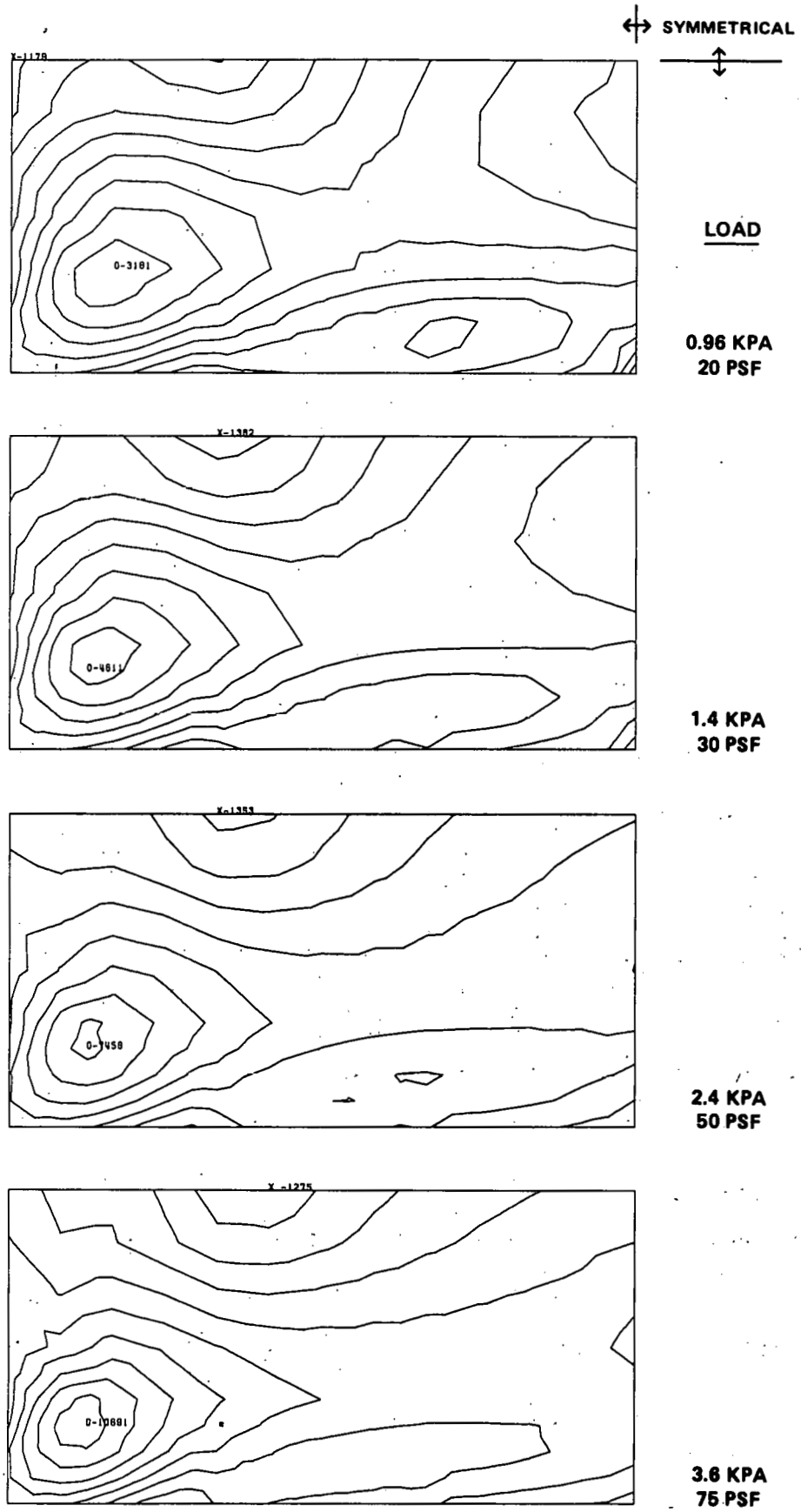

Figure A-5 CASE I – MINIMUM PRINCIPAL STRESS, TOP OF PLATE

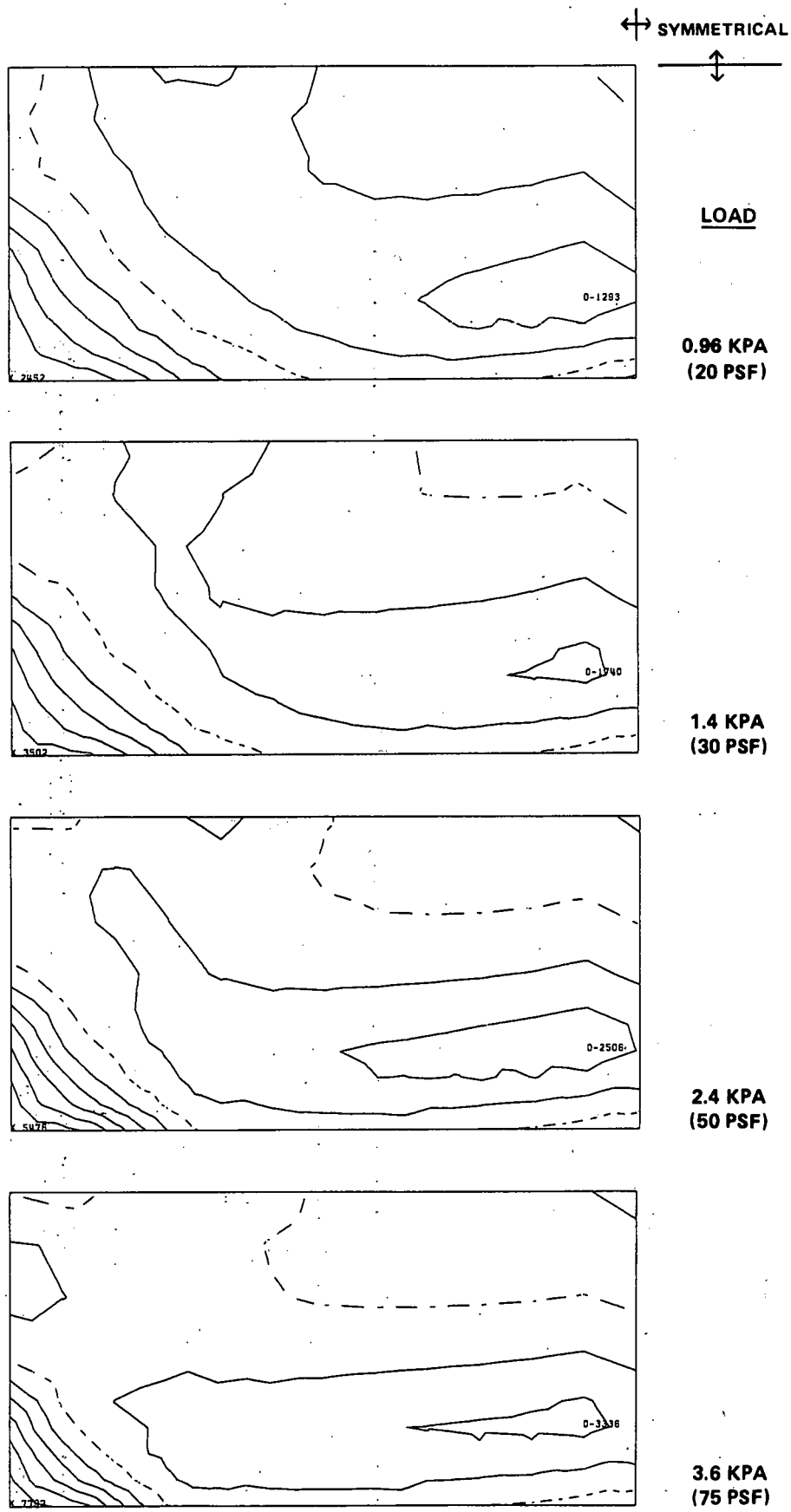

Figure A-6 CASE I – MAXIMUM PRINCIPAL STRESS, TOP OF PLATE

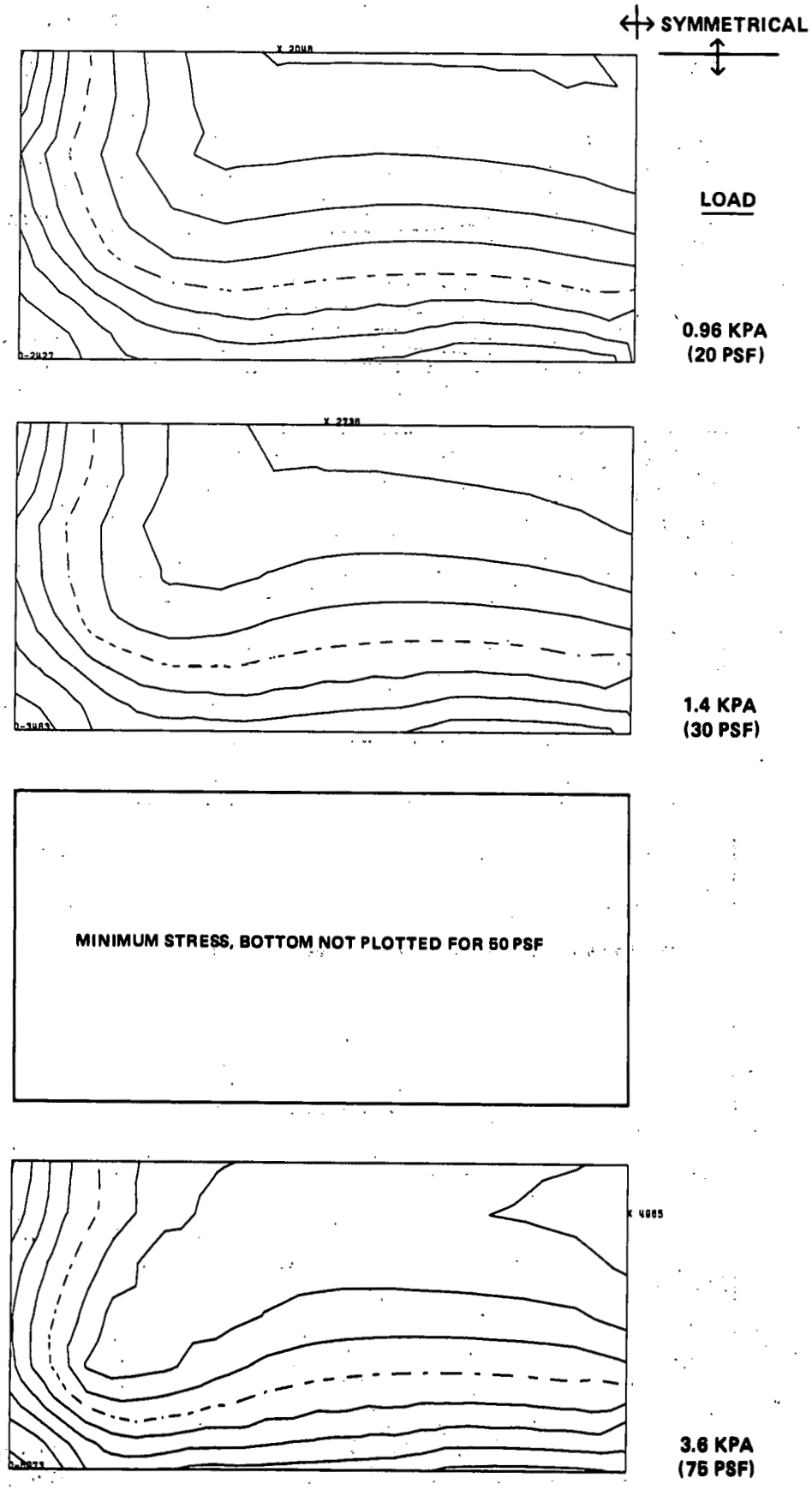

Figure A-7 CASE I – MINIMUM PRINCIPAL STRESS, BOTTOM OF PLATE

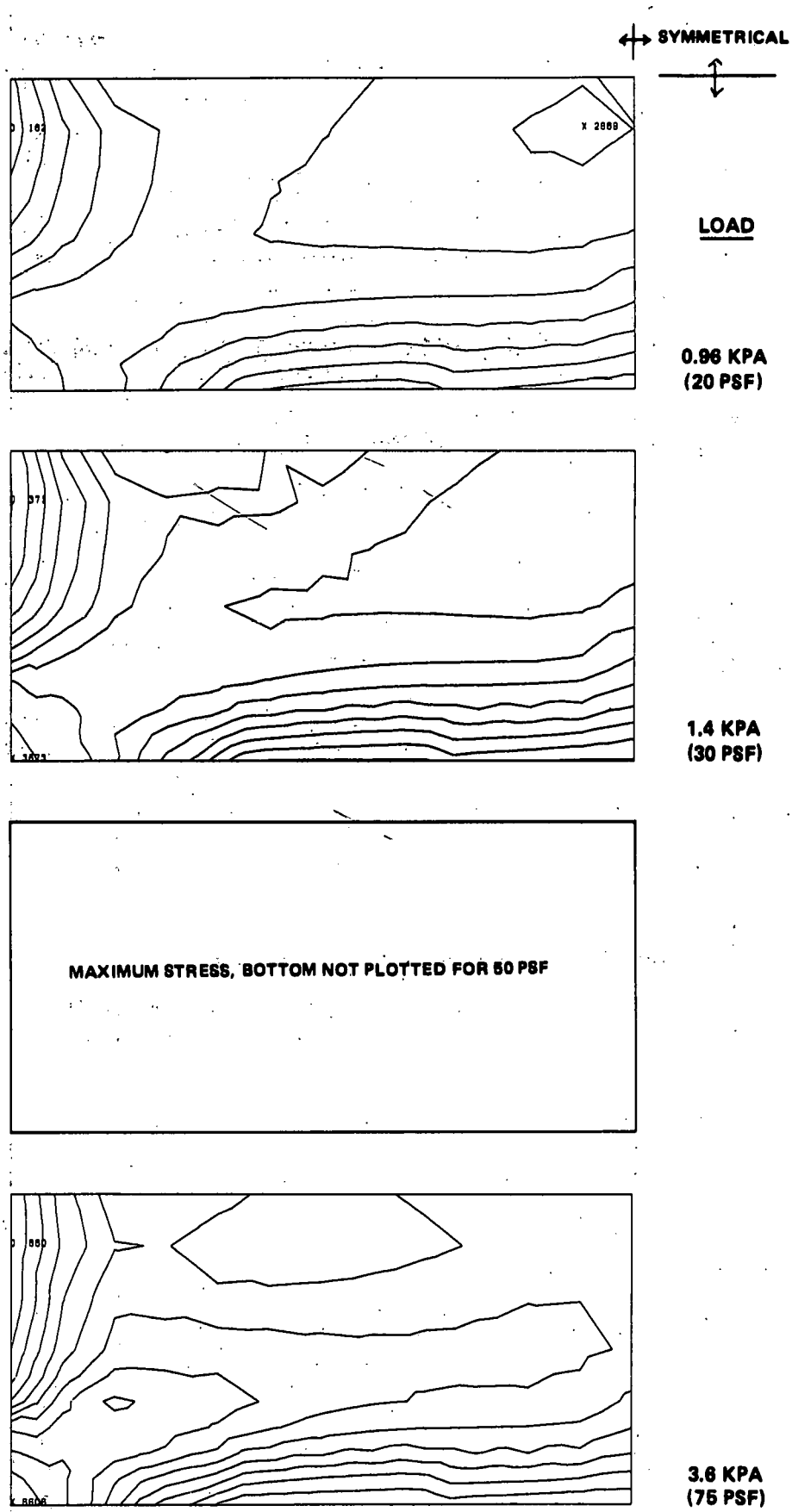

Figure A-8 CASE I – MAXIMUM PRINCIPAL STRESS, BOTTOM OF PLATE

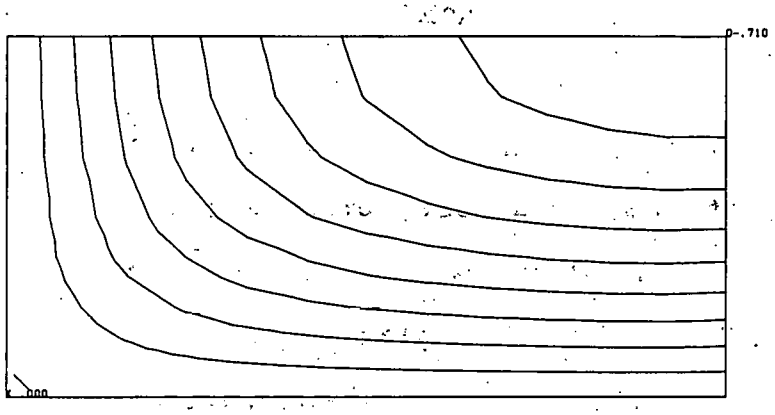

LOAD

0.96 KPA
(20 PSF)

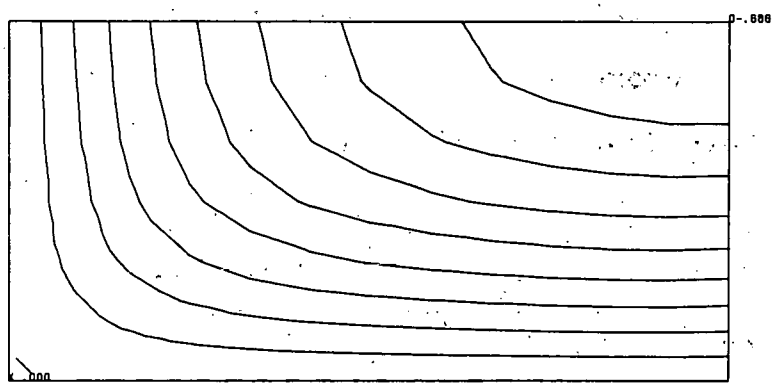

1.4 KPA
(30 PSF)

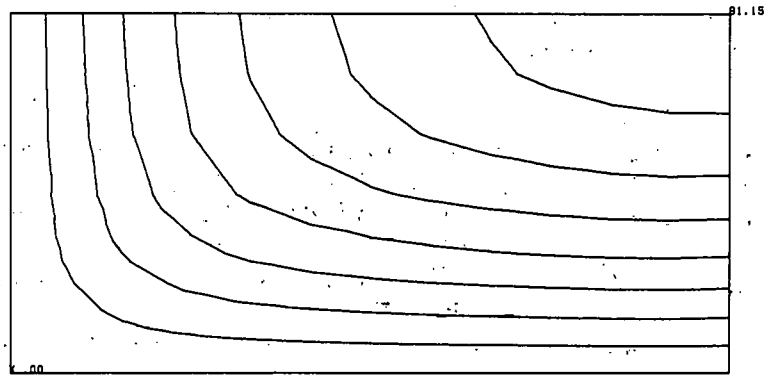

2.4 KPA
(50 PSF)

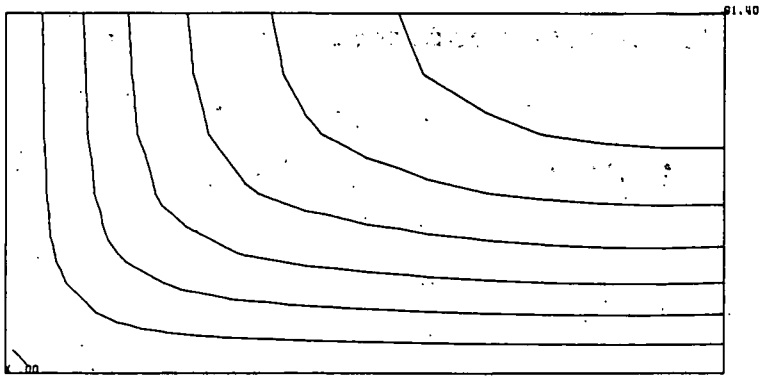

3.6 KPA
(75 PSF)

Figure A-9 CASE I – PERPENDICULAR DISPLACEMENT

A.2 CASE II - CLIP SUPPORTED CONCEPT

Putting the flat plate on four clip supports instead of on the continuous support causes a more severe stress state. Reaction forces become concentrated at the clips and this gives local stress concentrations in the plate. Hence, even at 0.48 kPa (10 psf) loading this plate had stress levels that were not reached in Case I until loads had reached 0.96 kPa (20 psf) to 2.4 kPa (50 psf). Accordingly the analyses were not extended to loadings higher than 0.48 kPa (10 psf).

The principal stress contours are shown in Figure A-10 for 0.48 kPa (10 psf).

A.3 CASE III - CURVED, CLIP SUPPORTED CONCEPT

A modified mesh was used in the analysis of the curved clip supported plate. The mesh and model behavior was verified by modeling the plate analyzed as part of an infinitely long cylindrical shell rigidly supported along the long edge. The reactions compared very closely to those calculated by hand. Since other calculations had indicated that the results would be sensitive to the kind of edge support, a design was developed which provided fair rigidity tangent to the plane of curvature at the edge.

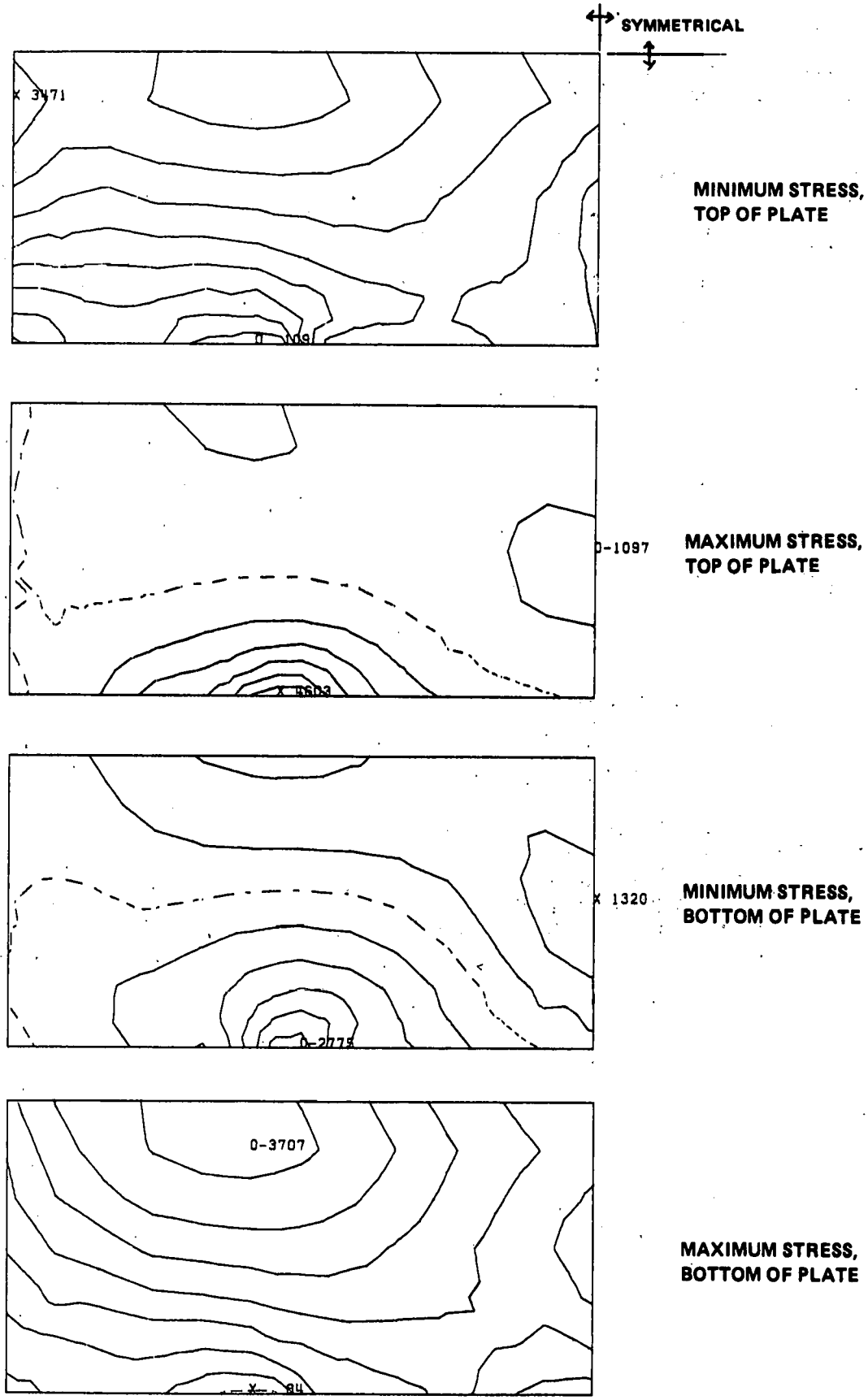

Figure A-10 CASE II – PRINCIPAL STRESSES AT 0.48 KPA (10 PSF)

A study of the linear elastic analysis done for verification of this model revealed in plane tensile reaction forces. Since the clip design wouldn't support this type of loading, the nodes at the edges of elements 80, 85, 101, and 106 (see Figure A-11) were released in the in-plane direction. This results in nodes connecting elements 59 and 64 and 122 and 127 carrying all the in-plane thrust. Since the response of the plate might be sensitive to flexibility in the supports, all clip nodes have spring supports normal to the shell's surface along with springs restraining motion parallel to the long edge. The springs represent a 60-durometer gasket material. The finite element mesh of the curved plate is shown in Figure A-11.

Providing some curvature to the otherwise flat plate increases the structural stiffness. This is because compressive membrane stresses are induced by arching under downward loads. The results show the increased stiffness due to the expected arch action. The reduction in stress and displacements compared to the flat plate are shown in Figures A-12 and A-13, respectively. This also infers a reduction in the nonlinear action. The analyses calculated the stresses at both surfaces and then resolved these into principal stresses. The contours of maximum and minimum principal stresses are shown in Figures A-14 to A-17. The contours of displacements for each load step are given in Figure A-18.

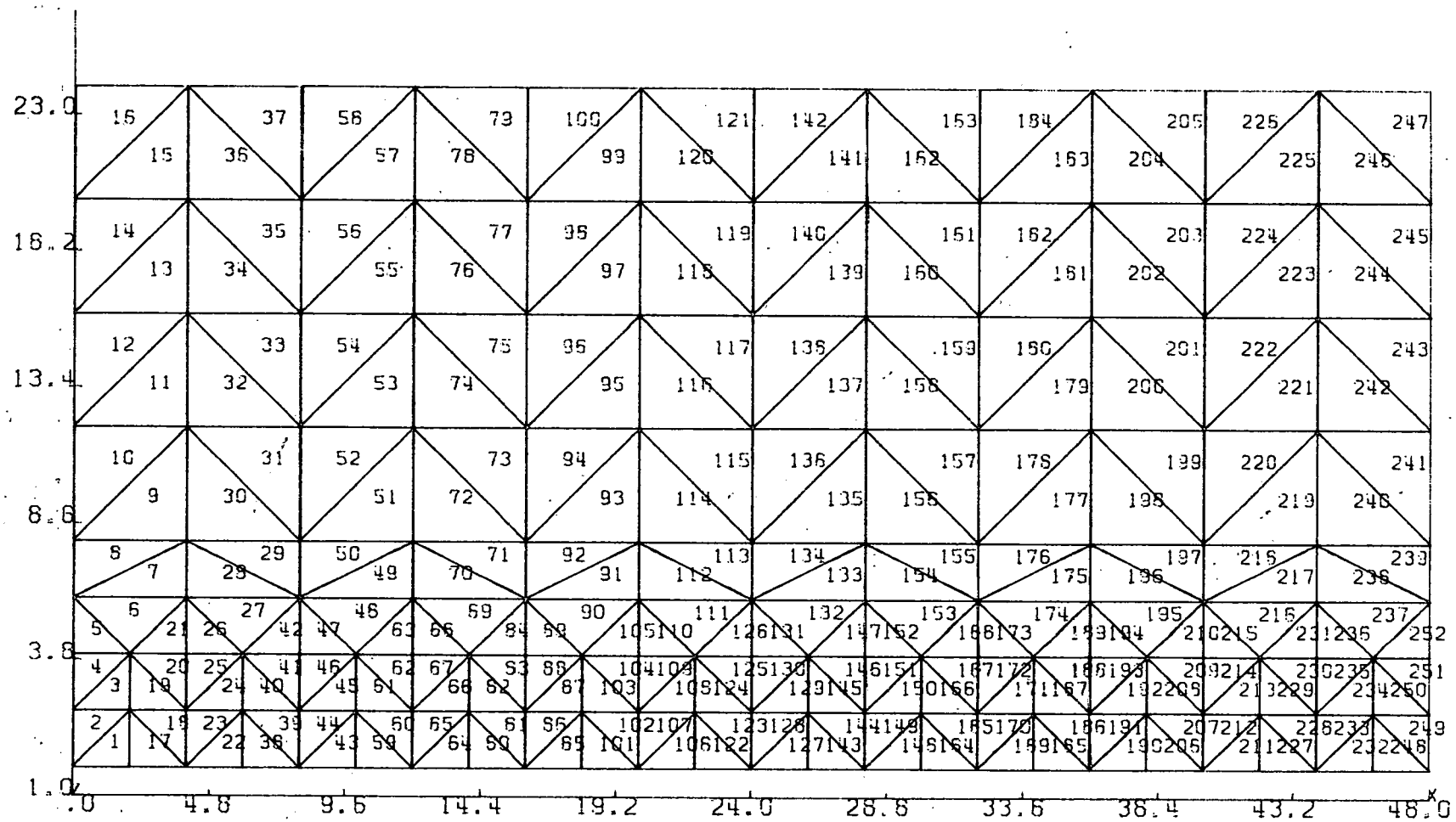

Figure A-11 FINITE ELEMENT LAYOUT FOR CASE III

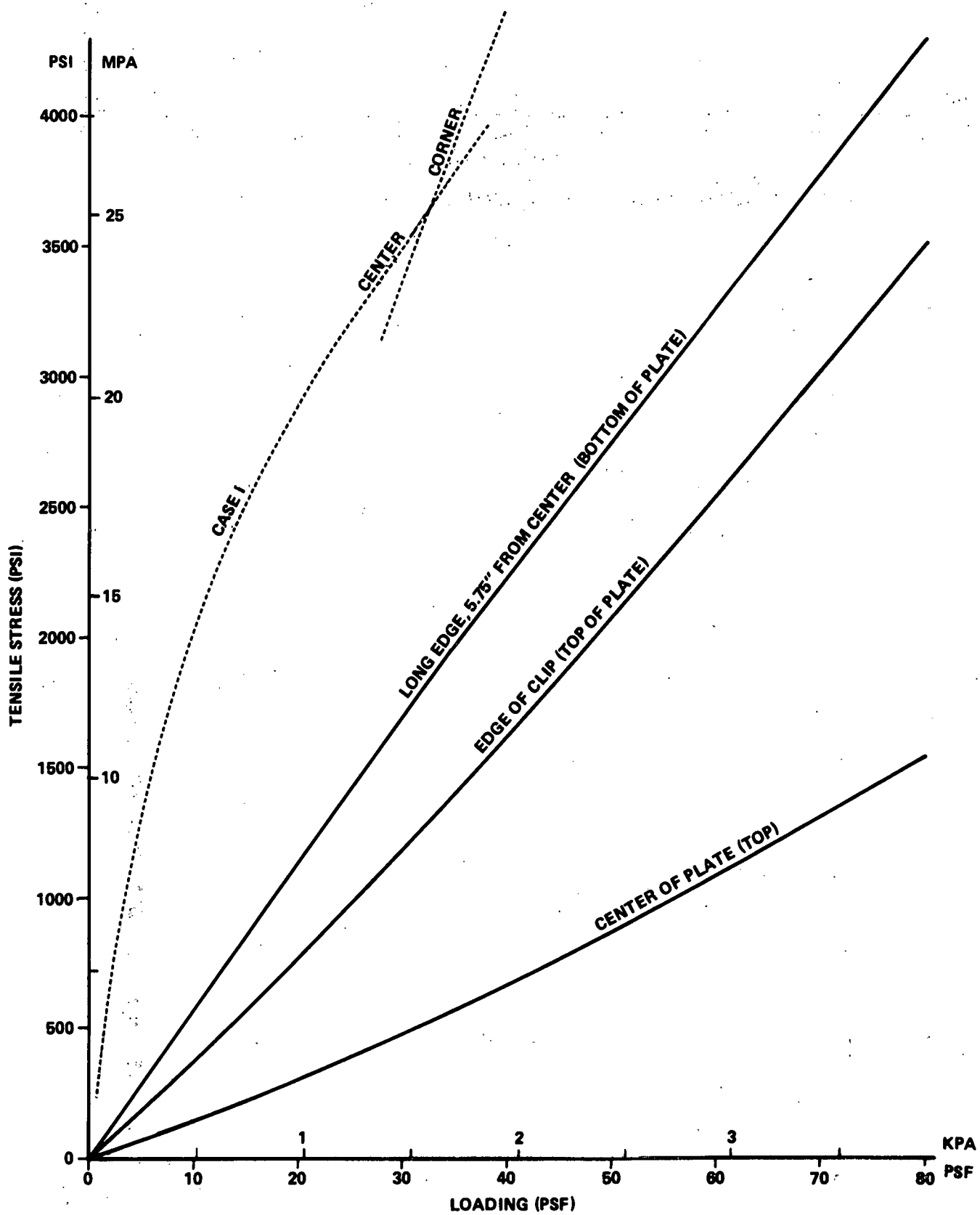

Figure A–12 CASE III TENSILE STRESS VERSUS LOADING

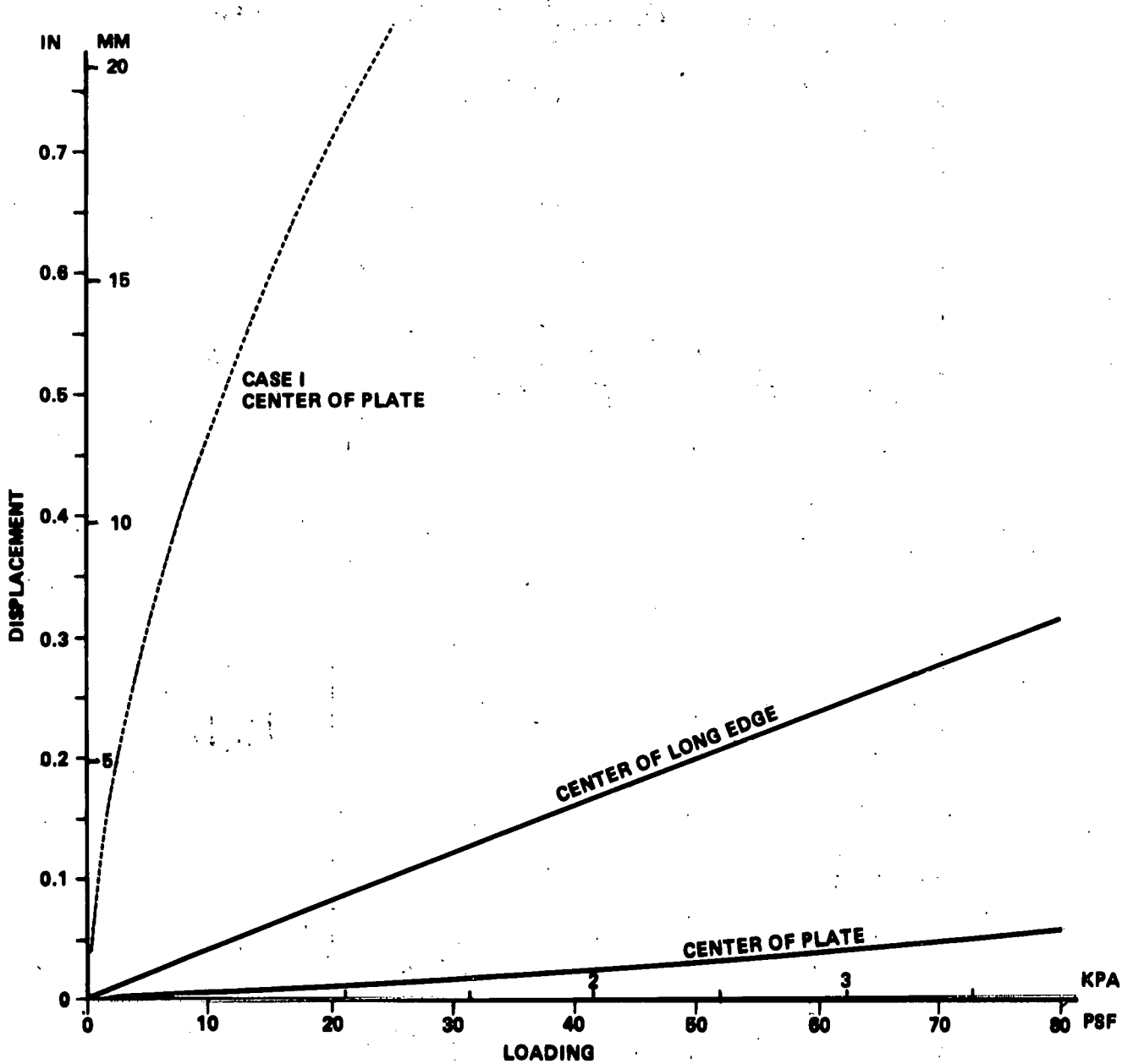

Figure A–13 CASE III DISPLACEMENT VERSUS LOADING

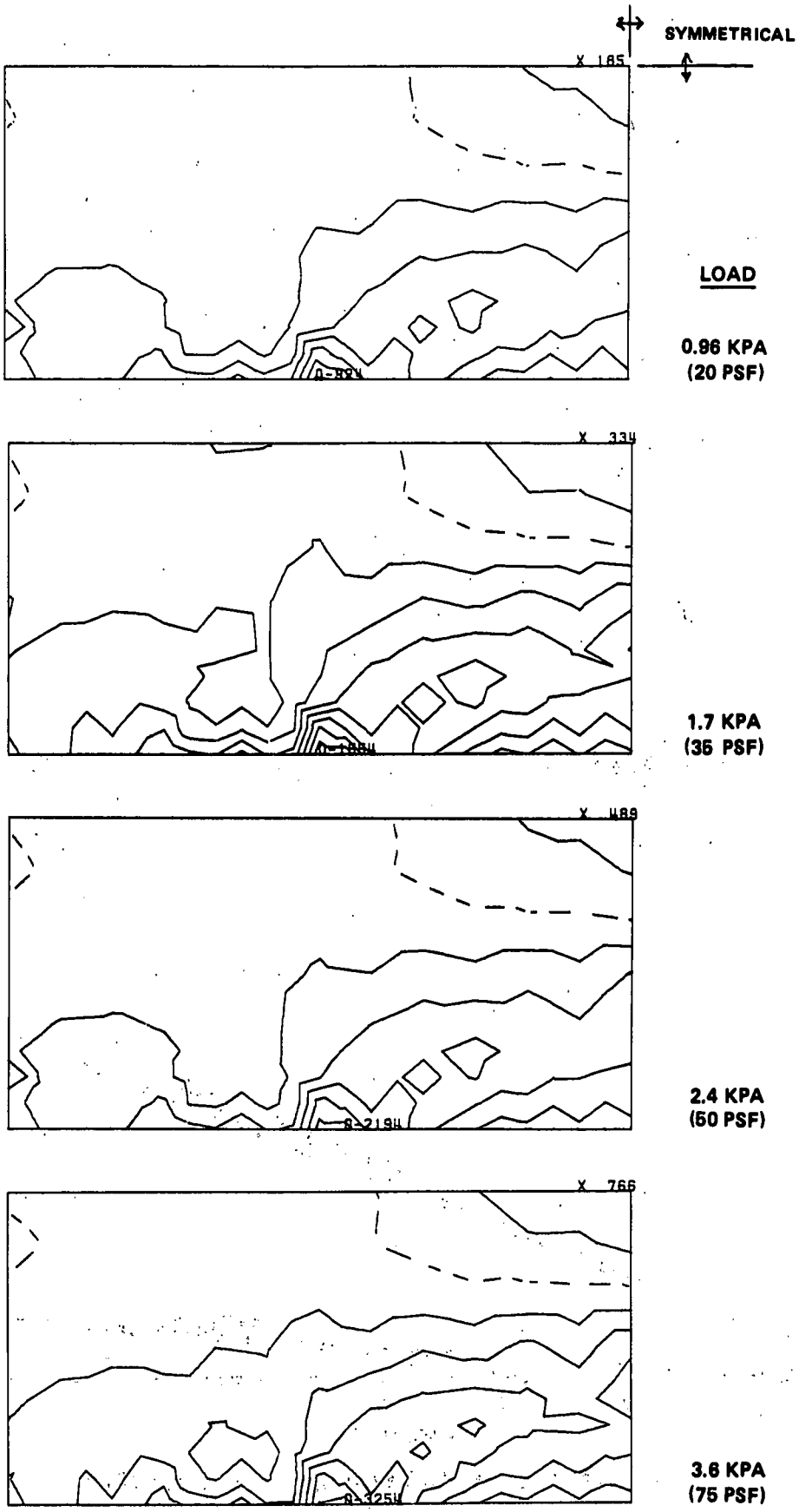

Figure A-14 CASE III – MINIMUM PRINCIPAL STRESS, TOP OF PLATE

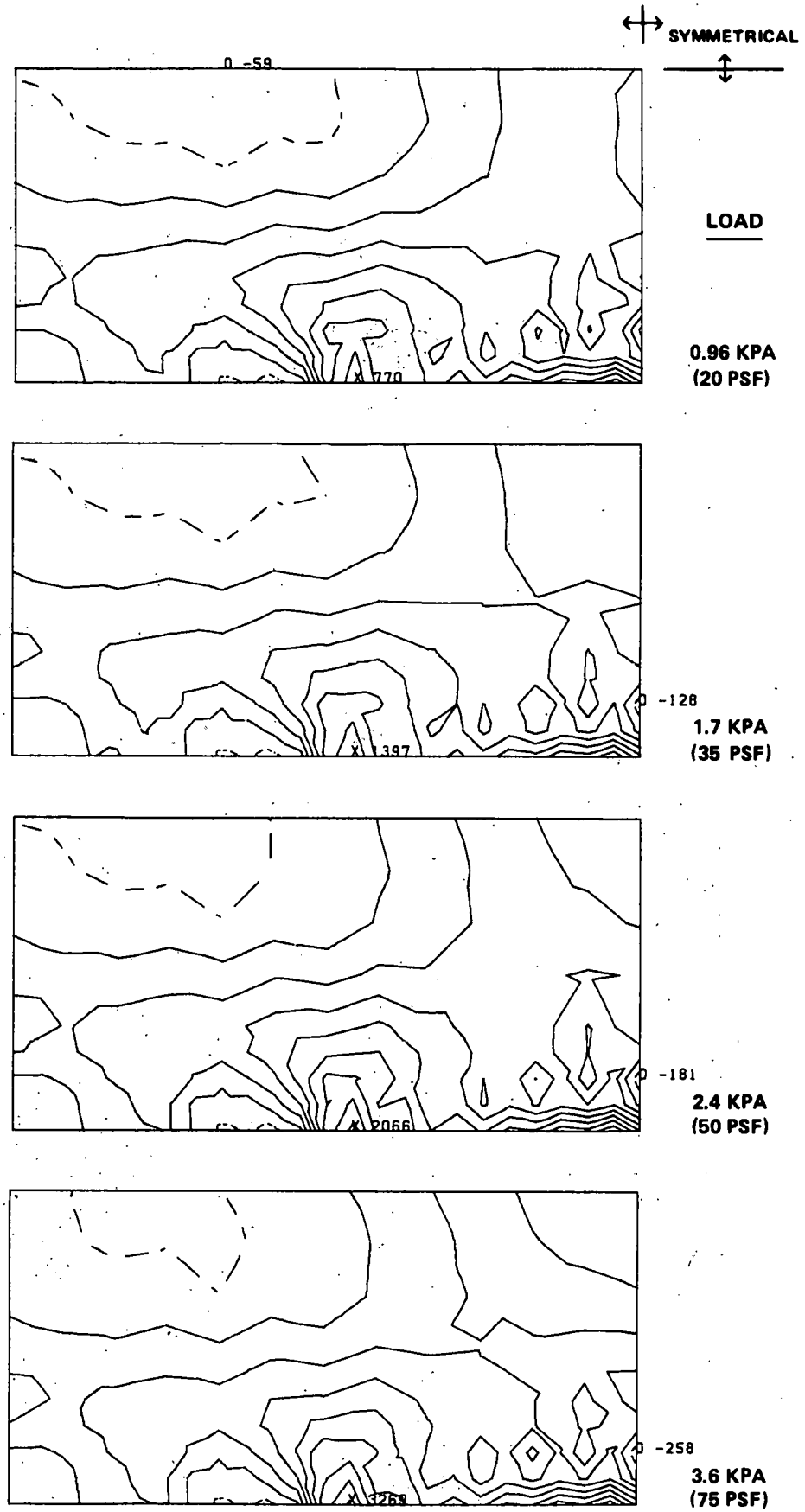

Figure A-15 CASE III – MAXIMUM PRINCIPAL STRESS, TOP OF PLATE

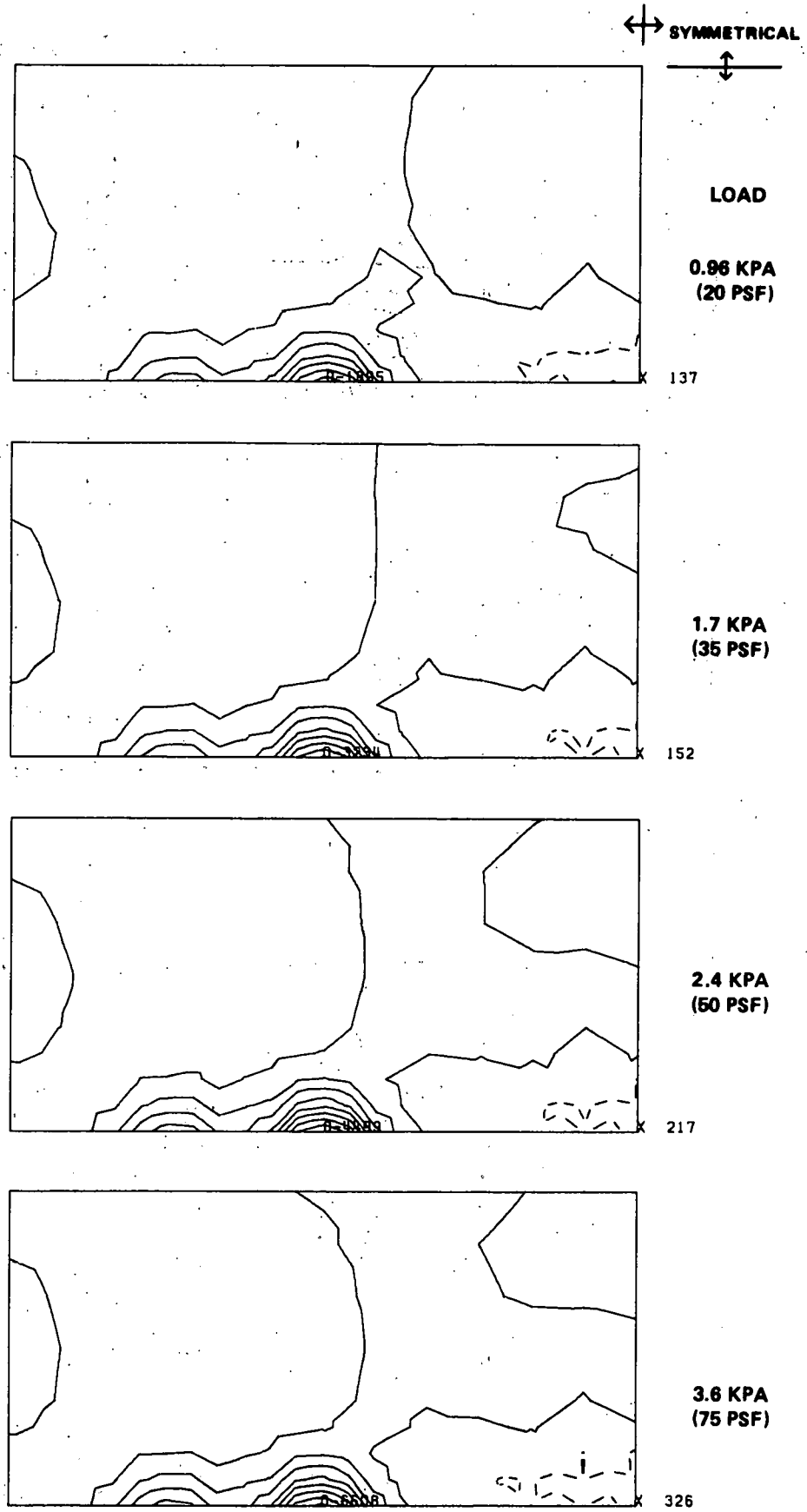

Figure A-16 CASE III – MINIMUM PRINCIPAL STRESS, BOTTOM OF PLATE

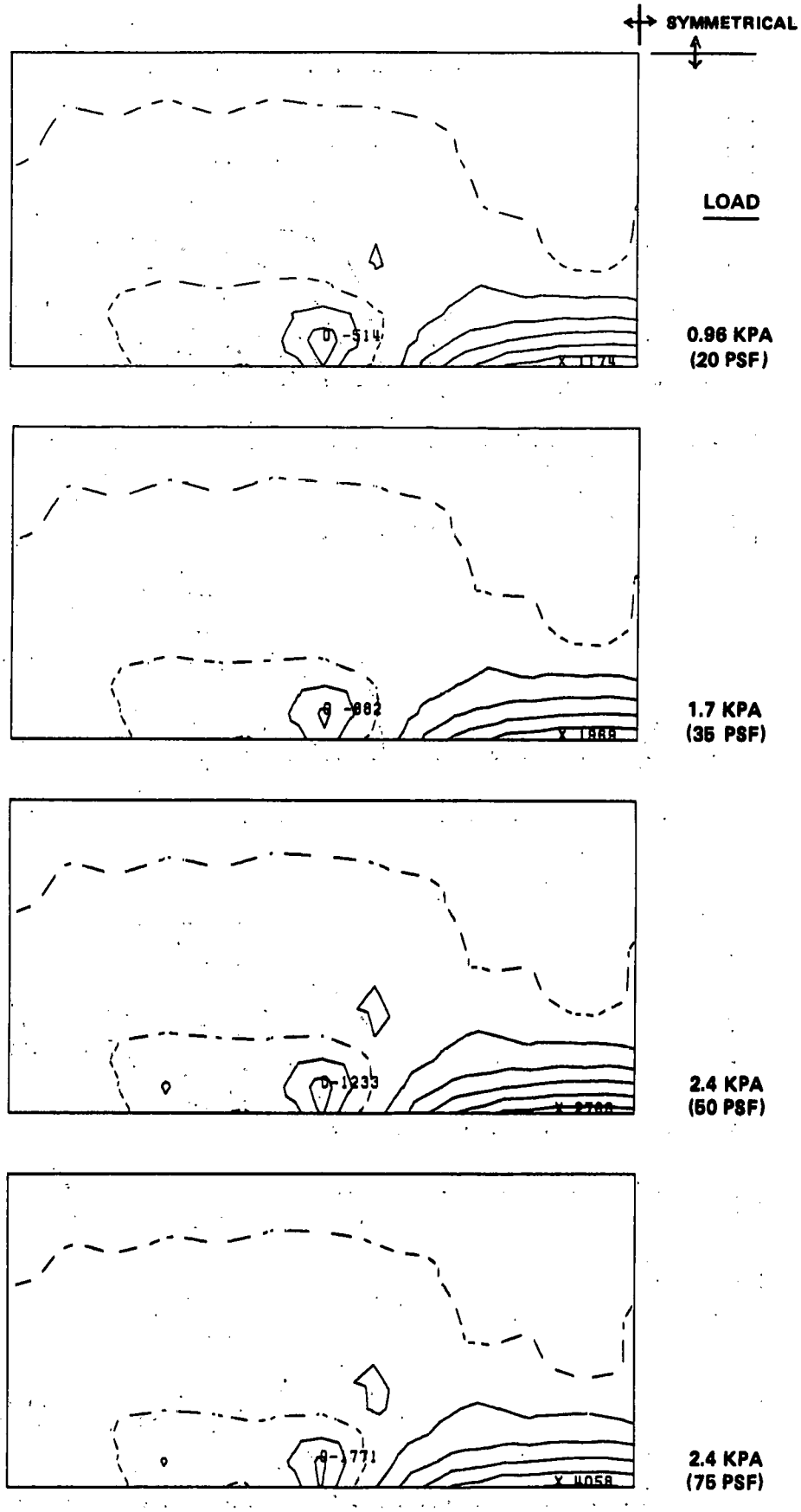

Figure A-17 CASE III – MAXIMUM PRINCIPAL STRESS, BOTTOM OF PLATE

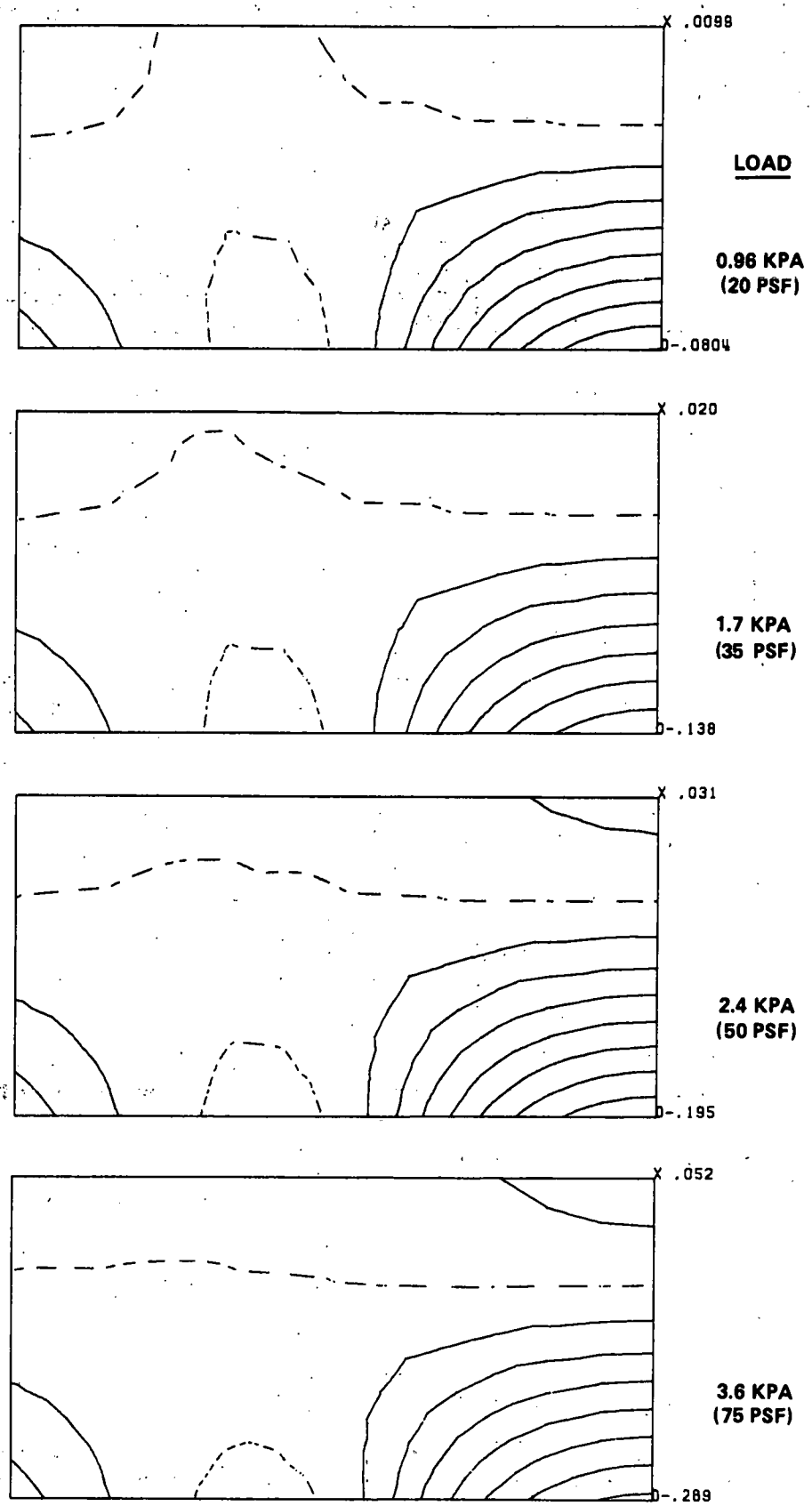

Figure A-18 CASE III – RADIAL DISPLACEMENT

THIS PAGE

WAS INTENTIONALLY

LEFT BLANK

REFERENCES

2-1 J.W. Doane, LSSA Price Deflator Update, Jet Propulsion Laboratory Interoffice Memo, October 24, 1977

3-1 Bechtel Corporation, Engineerng Study of the Module/Array Interface for Large Terrestrial Photovoltaic Arrays, Final Report prepared for the Jet Propulsion Laboratory under contract number 954698, June 1977

3-2 Bechtel National, Inc., Terrestrial Central Station Life-Cycle Analysis Support Study, Final Report prepared for the Jet Propulsion Laboratory under contract number 954848, August 1978

3-3 Bechtel Corporation, A Conceptual Design of a Photovoltaic Central Station Power Plant, Final Report prepared for Spectrolab, Inc. under subcontract number 66725, July 1976

4-1 "Severe Local Storm Occurrences, 1955-1967," Technical Memorandum WBTM FCST 12, USCOM, ESSA, USWB, September 1969

4-2 S.A. Changnon, Jr., "Examples of Economic Losses from Hail in the United States," Journal of Applied Meteorology, Vol. 11, October 1972

4-3 B.B. Hull, "Hail Size and Distribution," Technical Report EP-83, U.S. Army Quartermaster Research and Engineering Center, Environmental Protection Research Division, Natick, Massachusetts, February 1958

4-4 D.S. Roos, "A Giant Hailstone from Kansas in Free Fall," Journal of Applied Meteorology, Vol. II, Sept. 1972

4-5 H.C.S. Thom, "Tornado Probabilities," Monthly Weather Review, October-December 1963

4-6 J.O. Roads, "A Study of Hailswaths by Means of Airborne Infrared Radiometry," Journal of Applied Meteorology, Vol. 12, No. 5, August 1973

4-7 C. Gonzalez, "Environmental Hail Model For Assessing Risk To Solar Collectors," Jet Propulsion Laboratory, LSSA Project, December 6, 1977, LSSA Project Internal Document No. 5101-45

4-8 Solar Cell Array Design Handbook, Jet Propulsion Laboratory, Volume 2, October 1976, p. 3.1-4

4-9 ASG Industries Inc., News Bulletin, 1974

4-10 ASHRAE Handbook of Fundamentals, Chapter 22

4-11 H. B. Y. Mar, et al., "Optical Coatings For Flat Plate Solar Collectors," Systems Research Center, Honeywell Inc., Final Report on ERDA contract number NSF-C-957, September 1975

4-12 Encyclopedia of Chemical Technology, Second revised edition, Volume 21, John Wiley and Sons, Inc.

4-13 "Underground Power Transmission," A Study Prepared by Arthur D. Little, Inc. for the Electric Research Council, ERC Publication No. 1-72, October 1972

4-14 Standard Handbook For Electrical Engineers, McGraw Hill, 1969

4-15 Review of World Experience and Properties of Materials for Encapsulation of Terrestrial Photovoltaic Arrays, Final Report, work performed by Battelle Columbus Laboratories, Columbus, Ohio, for ERDA, under Contract No. NAS-7-100-954328, July 21, 1976

4-16 Investigation of Test Methods, Material Properties, and Processes for Solar Cell Encapsulants, Annual Report, work performed for ERDA, by Springborn Laboratories, Inc., Enfield, Connecticut, under Contract No. NAS-7-100-954527, September, 1977

4-17 G. J. DeSalvo and J. A. Swanson, ANSYS, Engineering Analysis System, User's Manual, Swanson Analysis Systems, Inc., Elizabeth, Pennsylvania, March 1975, with updates to No. 4 dated 11/5/77

4-18 P. C. Kohnke, ANSYS, Engineering Analysis System, Theoretical Manual, Swanson Analysis Systems, Inc., Elizabeth, Pennsylvania, Nov. 1, 1977

4-19 S. Levy, "Bending of Rectangular Plates with Large Deflections," Technical Note 846, National Advisory Committee for Aeronautics

4-20 R. J. Roark, Formulas for Stress and Strain, 4th Edition, McGraw-Hill, 1965

4-21 S. P. Timoshenko and D. H. Young, Theory of Structure, 2nd Edition, McGraw-Hill, 1965

4-22 C. R. Tsai and R. A. Stewart, "Stress Analysis of Large Deflection of Glass Plates by the Finite Element Method," Journal of the American Ceramic Society, Vol. 59, No. 9-10, Sept.-Oct. 1976, pp. 445-448

7-1 American National Standards Institute, Building Code Requirements for Minimum Design Loads in Buildings and Other Structures, A58.1-1972

7-2 Spectrolab, Inc., Photovoltaic Systems Concept Study, Final Report prepared for ERDA under Contract Number E(11-1)-2748, April 1977

☆U.S. GOVERNMENT PRINTING OFFICE: 1979-640-014/4006 REGION NO. 4